Evolutionary biogeography of catfishes (Siluriformes, Actinopterygii): The influence of habitat and landscape on gene flow and genetic diversification

By: Francesco H. Janzen

Supervisor: Dr. Gabriel Blouin-Demers
Committee Members: Dr. Julian R. Starr, Dr. Steven J. Cooke
Examiners: Dr. Stéphane Aris-Brosou (Internal), Dr. Jonathan W. Armbruster (External)

Thesis submitted in partial fulfillment of the requirements
for the Doctorate in Philosophy degree in the
Ottawa-Carleton Institute of Biology

Department of Biology
Faculty of Science
University of Ottawa

Abstract

A fundamental goal of evolutionary biology is to understand what processes have led to the great diversity of organisms we see today. An important factor of diversification is an organism's environment. Abiotic factors can shape the evolutionary trajectory of species by affecting fundamental mechanisms of evolution, including mutation, gene flow, genetic drift, and natural selection. In my thesis, I investigated how abiotic factors, such as habitat and landscape, have influenced the genetic diversification of catfishes (Siluriformes). More specifically, I compared genetic data within and between species to understand how natural barriers have shaped the origins and evolutionary trajectory of species.

In Chapter 1, I investigated whether habitat preferences and segregation of breeding populations in lacustrine-like and fluvial habitats affected the genetic structure of a sympatric population of channel catfish (*Ictalurus punctatus*). In Chapter 2, I elucidated the origins of cave species within North American catfishes (Ictaluridae), determining whether they shared a common ancestor or evolved in parallel from surface-dwelling ancestors. In Chapter 3, I tested whether impermeable and semi-permeable boundaries between South American river basins have restricted gene flow and resulted in potentially new species within the widespread ornate pim catfish (*Pimelodus ornatus*). In Chapter 4, I determined whether orogenesis and river capture corresponded with speciation events and cladogenesis within Neotropical long-whiskered catfishes (Pimelodidae).

Throughout my thesis, I observed evolutionary patterns related to gene flow, vicariance, and dispersal. Physical barriers imposed on populations often coincided with genetic diversification and allopatric speciation. These barriers reduced gene flow, allowing populations to genetically diverge in response to unique selective pressures. As these barriers changed over

time, dispersal opportunities may have further promoted diversification as species radiated into new areas. I also observed that ecological gradients, such as water chemistry, may have facilitated parapatric speciation; however, differences between habitats do not always restrict gene flow. Given that patterns of genetic diversification and speciation are not uniform across the tree of life, it is important for evolutionary biologists to document trends among different taxa to elucidate macroevolutionary patterns.

Résumé

Un objectif fondamental de la biologie évolutive est de comprendre quels processus ont produit la grande diversité d'organismes que nous voyons aujourd'hui. Un facteur important à considérer est l'environnement d'un organisme. Les facteurs abiotiques peuvent influencer la trajectoire évolutive des espèces en affectant les mécanismes fondamentaux de l'évolution, notamment la mutation, le flux génétique, la dérive génétique et la sélection naturelle. Dans ma thèse, j'ai étudié comment les facteurs abiotiques, tels que l'habitat et la géographie, ont influencé la diversification génétique des poissons-chats (Siluriformes). Plus précisément, j'ai comparé des données génétiques au sein et entre les espèces pour comprendre comment les barrières naturelles ont influencé les origines et la trajectoire évolutive des espèces.

Dans le chapitre 1, j'ai étudié si les préférences d'habitat et la ségrégation des populations reproductrices dans des habitats de type lacustre et fluvial affectaient la structure génétique d'une population sympatrique de barbue de rivière (*Ictalurus punctatus*). Dans le chapitre 2, j'ai élucidé les origines des espèces cavernicoles chez les poissons-chats nord-américains (Ictaluridae), en observant s'ils partageaient un ancêtre commun ou s'ils avaient évolué en parallèle à partir d'ancêtres vivant en surface. Dans le chapitre 3, j'ai testé si les frontières imperméables et semi-perméables entre les bassins fluviaux sud-américains ont restreint le flux génétique et ont entraîné la création de nouvelles espèces potentielles au sein du poisson-chat orné (*Pimelodus ornatus*). Dans le chapitre 4, j'ai déterminé si l'orogenèse et la capture en rivière correspondaient aux événements de spéciation et à la cladogenèse chez les poissons-chats antennes (Pimelodidae).

Tout au long de ma thèse, j'ai observé des motifs évolutifs liés au flux génétique, à la vicariance et à la dispersion. Les barrières physiques imposées aux populations coïncidaient souvent avec la diversification génétique et la spéciation allopatrique. Ces barrières ont réduit le flux de gènes, permettant aux populations de diverger génétiquement en réponse à des pressions sélectives uniques. Au fur et à mesure que ces barrières ont changé au fil du temps, les possibilités de dispersion ont peut-être favorisé la diversification à mesure que les espèces rayonnaient dans de nouvelles zones. J'ai également observé que des gradients écologiques, tels que la chimie de l'eau, peuvent avoir facilité la spéciation parapatrique; cependant, les différences entre les habitats ne restreignent pas toujours le flux de gènes. Étant donné que les modèles de diversification génétique et de spéciation ne sont pas uniformes dans l'arbre de la vie, il est important que les biologistes de l'évolution documentent les tendances entre les différents taxons pour élucider les modèles macro-évolutifs.

Preface

My thesis is composed of four independent manuscripts that have either been published in peer-reviewed journals, or are in preparation for submission to peer-reviewed journals. I provided publication details on the title page of each accepted and/or published chapter. I conceptualized each study, performed all experimental methodologies and statistical analyses, analyzed and interpreted results, and created each table and figure included within this thesis. For most chapters, I collaborated with other researchers who provided materials for analyses and personal expertise, meriting co-authorship in the associated publications. Therefore, I use the pronoun "we" instead of "I" in each chapter, acknowledging the important contributions of my co-authors. Differences between journal formatting, however, have been standardized throughout this thesis.

Acknowledgements

I would like to thank all the people who supported me and contributed to my development as a scientific researcher throughout my PhD. First and foremost, I thank my supervisor Dr. Gabriel Blouin-Demers for his invaluable guidance and support in developing and refining the studies that comprise this thesis. More importantly, Gabriel taught me valuable lessons necessary for any researcher, such as critical thinking, independence, and never losing sight of the big picture. For these reasons, I am eternally grateful. I also thank my committee members, Dr. Julian Starr and Dr. Steven Cooke for their valuable feedback that helped shape and refine my thesis. I am also thankful for the opportunity to have collaborated with several research scientists who shared my enthusiasm for catfishes and systematics, including Dr. Mark Sabaj (ANSP), Dr. Dean Hendrickson (UT Austin), Dr. Omar Domínguez-Domínguez (UMSNH), and Rodolfo Pérez-Rodríguez (UMSNH). Special thanks to Mark for his enthusiastic contributions to several chapters of this thesis.

I thank my dedicated field assistants, Allison Drake and Spencer Karau, for helping me wrangle channel catfish. I also thank Peter Janzen, Sheena Fry, and Stéphanie Tessier for volunteering their time in the field. Thank you to Roger Bull and the Canadian Museum of Nature for allowing me to use the Laboratory of Molecular Biodiversity and National Biodiversity Cryobank of Canada. Roger's help optimizing molecular laboratory protocols was invaluable when generating genetic data for this thesis. Thank you to Stéphanie Tessier at the Canadian Museum of Nature for her help with museum loans, madtom identifications, and rescuing our stranded boat. Special thanks to Noel Alfonso at the Canadian Museum of Nature for encouraging my love of fishes from the very beginning of my scientific career and teaching

me invaluable lessons involving field collections, fish identifications, and recognizing that all fishes are marvelous creatures, even minnows.

Thank you to all of the museum curators and researchers who generously provided tissue samples used to conduct phylogenetic analyses in this thesis: Mark Sabaj (ANSP), Jonathan Armbruster and David Werneke (AUM), Andrew Simons (JFBM), Robert Ellwanger (MMNS), Larry Page and Robert Robins (UF), Gregory Watkins-Colwell (YPM), Caleb McMahan (FMNH), Christopher Taylor (INHS), Lily Hughes and Gabriela Hogue (NCSM), Erling Holm (ROM), Adam Cohen (TNHC), and Benjamin Keck and Jennifer Brummett (UTEIC).

Thank you to the funding agencies and institutions who financially supported my thesis research. This included an Ontario Graduate Scholarship from the Government of Ontario, a Postgraduate Scholarship-Doctoral award from the Natural Sciences and Engineering Research Council of Canada (NSERC), an Ottawa Field-Naturalists' Club research grant, graduate student stipends and excellence scholarships from the University of Ottawa, and an NSERC discovery grant held by my supervisor, Gabriel Blouin-Demers.

Thank you to all the people who have made my time as a doctoral student memorable and exciting, including fellow graduate students from the University of Ottawa and my network of wonderful friends. Special thanks to Sheena Fry, Garreth Murphy, and Emma Lehmberg for their patience and emotional support throughout this experience. Finally, I am deeply grateful for my supportive family that have been cheering me on throughout my PhD. Ti amo ora e per sempre.

Table of Contents

List of Tables

List of Figures

List of Abbreviations

AICc…...…….. Corrected Akaike Information Criterion

AMOVA…….. analysis of molecular variance

BI…… Bayesian Inference

BOLD…. Barcode of Life Data

BS……...……... bootstrap support

CI…… confidence interval

co1……...……... cytochrome oxidase subunit 1

cyt b……. cytochrome b

dNTPs…….. deoxynucleotides

ddNTPs...……... dideoxynucleotides

DMSO…..……...……. dimethyl sulfoxide

egr1……..…….. early growth response protein 1

enc1…….……. ectoderm-neural cortex protein 1

ESS……..…… effective sample size

glyt……...……... glycosyltransferase

MCMC……. Markov chain Monte Carlo

ML……...…… maximum likelihood

MP……...…… maximum parsimony

Mya……..…….. million years ago

OCP clade…….. "*Pimelodus*" *ornatus* – *Calophysus* – *Pimelodus* clade

PCR……..…… polymerase chain reaction

PP……. posterior probability

RADseq...…… restriction-site-associated DNA sequencing

rag1……..……... recombination activating gene 1

rag2……..……recombination activating gene 2

rh1……...……...rhodopsin

sreb2……. super conserved receptor expressed in brain 2

zic1……..…….. zinc finger protein of cerebellum 1

General Introduction

Within an ecosystem, both biotic and abiotic factors are intrinsically linked by the flow of energy and matter (Tansley, 1935; Willis, 1997; Chapin III et al., 2011). An animal, for example, must obtain these resources from other organisms and its physical environment, which includes light, water, oxygen availability, heat, soil/water chemistry, weather, etc. (Herberstein & Fleisch, 2003; Bornette & Puijalon, 2011). These immediate environmental factors are in turn dependent on large scale geographic features, such as topography, latitude, and climate (Thomas et al., 1998; Klausmeyer & Shaw, 2009; Liu et al., 2014). Consequently, where an animal chooses to live directly influences its survival and reproductive success (Rosenzweig, 1981; Huey, 1991; Pulliam & Danielson, 1991; Camacho et al., 2015). A habitat provides an animal with basic life necessities, such as shelter, food, and potential mates (Hutto, 1985; Morris, 2003; Hernández Cordero & Seitz, 2014). Animals should select habitats that maximize their fitness, balancing survival with reproductive needs (Rosensweig, 1981; Pulliam & Danielson, 1991).

The interaction between animals and the physical environment, however, not only impacts survivability, but also shapes their evolutionary trajectory. This is made possible when abiotic factors directly affect the fundamental mechanisms of evolution. First, some abiotic factors act as mutagens when they come into contact with animals (Chen & White, 2004; Bolognesi & Hayashi, 2011). For example, solar radiation can cause cellular damage in exposed organisms, resulting in DNA replication errors (Cleaver & Crowley, 2002; Cadet et al., 2005; Hessen, 2008). Environmental metals, such as lead found in soil and water, may cause DNA replication errors as well, reducing the accuracy of DNA polymerases (Johnson, 1998; Woźniak & Blasiak, 2003). Naturally occurring arsenic is also known to cause chromosomal instability, resulting in replication errors (Banerjee et al., 2008; Bustaffa et al., 2014). Thus, abiotic factors

acting as mutagens directly facilitate evolution by introducing novel genetic material within populations of animals.

Second, abiotic factors can act as driving forces of genetic drift. Stochastic events, such as destructive weather and geological processes may remove great numbers of individuals from a given population (Howe, 1976; Brante et al., 2019). By chance, certain alleles disappear from the gene pool, drastically reducing the genetic variability of the population, creating a bottleneck effect (Menotti-Raymond & O'Brien, 1993; Peery et al., 2012). Pujolar et al. (2011) found evidence of the direct link between abiotic factors and genetic drift while studying marble trout (*Salmo marmoratus*) in river tributaries of the Adriatic Sea near Slovenia. The study area had been experiencing an increase in rainfall, which was attributed to climate change. These intense rains caused intermittent flash flooding events, which resulted in high mortality rates (56.4-77.6%) for several trout populations. Using fin clippings collected between 2004-2008, Pujolar et al. (2011) conducted microsatellite analyses, comparing the genetic structure of four sampled trout populations before and after major flooding events resulting in mass mortalities. What they found was that each of the four populations showed a moderate decrease in genetic diversity, and a loss of nine rare alleles. Heterozygosity and allelic richness were also found to be low in each population, with a mean of two alleles per microsatellite locus. Dramatic decreases in marble trout population numbers may exacerbate further genetic variability loss; smaller populations are statistically more likely to experience genetic fixation in response to additional stochastic events, such as continued flash-flooding. As such, abiotic factors function as potent facilitators of genetic drift.

Third, abiotic factors act as barriers that impede gene flow, facilitating genetic divergence between populations of organisms (Barton, 1986; Steeves et al., 2003). In the absence of barriers,

gene flow acts as a homogenizing force that prevents genetic divergence of panmictic populations (Lande, 1980; Slatkin, 1985; Crispo et al., 2006). Barriers, such as mountain ranges and rivers, may restrict or eliminate reproductive opportunities between demes of a population (Lande, 1980; Steeves et al., 2003; Weir & Price, 2011). As a result, the genetic composition of isolated demes diverges over successive generations, caused by independent mutations, stochastic phenomena, and selective pressures (Lande, 1980; Hoskin et al., 2005). For example, Ni et al. (2011) investigated the genetic composition of Chinese surf clams (*Mactra chinensis*) in Northern China. Using microsatellites from eight localities within the Bohai and Yellow Seas, the researchers found significant genetic differences between clusters of sampled populations. Some of these clusters correlated with physical barriers, such as ocean currents limiting larval dispersal, and the Shandong Peninsula separating northern and southern populations. By restricting or preventing gene flow between demes of Chinese surf clams, abiotic factors have facilitated genetic variability within the species.

Finally, abiotic factors can function as selective pressures in the process of natural selection. Factors including temperature, water availability, weather, water/soil chemistry, and oxygen availability place demands upon animals that favour some individuals, owing to the variability of heritable traits within a given population (Tauber & Tauber, 1981; Soares et al., 2006; Bidau et al., 2012). For example, seasonal change in temperature places demands upon animals, in which some are unable to cope and die as a result. Schultz et al. (1998) exposed Atlantic silversides (*Menidia menidia*) collected from Nova Scotia, New York, and South Carolina to a range of mild to low winter temperatures in the absence and presence of regular feeding. They found that survivability was primarily linked with body size, but also intraspecific differences in metabolic kinetics. Larger fish were more likely to survive as they possessed

larger energy reserves to offset the impact of reduced food availability in the winter. Cold temperatures, they concluded, favour both larger individuals and those with faster growth rates prior to winter weather.

Over time, genetic diversification of animal populations may result in speciation. Abiotic factors feature as an essential component of speciation models; geography is used to differentiate between sympatric, parapatric, and allopatric speciation (Templeton, 1980; Fitzpatrick et al., 2009). Briefly, sympatric speciation occurs when populations differentiate from a common ancestor within the same geographic area (Smith, 1966; Fitzpatrick et al., 2009). Allopatric speciation, in contrast, occurs when populations that are geographically isolated from one another differentiate from a common ancestor (Lande, 1980; Hoskin et al., 2005). Finally, parapatric speciation occurs when populations differentiate from a common ancestor over a geographic range that may have incomplete barriers, restricting gene flow (Gavrilets et al., 2000; Yamaguchi & Iwasa, 2017). These modes of speciation will be discussed in greater detail throughout this thesis.

Although the diversity we see is a product of habitat and geography among other factors, it is ultimately controlled by genetics (Hughes et al., 2008). Variations in genotype resulting from mutation and genetic recombination produce new phenotypes, which are in turn subject to natural selection (Hughes et al., 2008). This includes pressures from the physical environment and biotic interactions (Park & Lloyd, 1955; Van den Berghe & Gross, 1989; Hughes et al., 2008). Therefore, it is of interest to understand how habitat and geography influence genetic diversification of animals. The general purpose of this thesis is to investigate how landscape and geography have influenced the genetic diversification and speciation of animals by altering gene

flow within and between populations. This thesis seeks to address this question using catfishes (Siluriformes, Actinopterygii) as a study system.

The order Siluriformes is highly speciose, containing 4,000+ described species divided into 36 families (Sullivan et al., 2006; Kappas et al., 2016). Catfishes are found on all continents, including fossils discovered in Antarctica (Sullivan et al., 2006; Kappas et al., 2016). Catfishes also inhabit a diversity of habitats, including both marine and freshwater: lakes, rivers, streams, estuaries, and caves (Lundberg et al., 2011; Arce- et al., 2016; Nelson, 2016). Siluriformes have previously been used to study biogeographical patterns and speciation, and therefore present an excellent system for studying the interaction of landscape, gene flow, and genetic diversification within this thesis (Sullivan et al., 2006; Kappas et al., 2016).

This thesis is composed of four chapters addressing how habitat and landscape have facilitated the genetic diversification of catfishes. More specifically, how have the physical environment and geological phenomena affected gene flow within Siluriformes, promoting diversification and speciation? My four thesis chapters will each address one of the following questions:

1. Does habitat segregation associated with breeding habitat preference affect the genetic structure of a sympatric population of channel catfish (*Ictalurus punctatus*)?
2. Is cave specialization in North American catfishes (family Ictaluridae) a result of shared ancestry, or independent parallel speciation?
3. How have impermeable and semi-permeable geographical barriers shaped the genetic composition of the widespread Neotropical ornate pim catfish (*Pimelodus ornatus*)?
4. Have Andean uplift and subsequent river capture influenced cladogenesis and speciation in Neotropical long-whiskered catfishes (family Pimelodidae)?

The thesis chapters were ordered using two criteria: 1) continent (North and South America) and 2) geographical scale. With respect to North American catfishes, the first chapter focused on one sympatric population of channel catfish and the second chapter focused on the family Ictaluridae. Shifting to South America, the third chapter focused on one widespread species across its entire distribution and the fourth chapter focused on the family Pimelodidae. The chapters were meant to provide complementary evidence for evolutionary patterns at both local and continental scales.

In the first chapter, I tested the hypothesis that habitat segregation potentially linked with breeding site preferences has reduced gene flow and promoted genetic differentiation between fluvial and lacustrine-like subpopulations in a sympatric population of channel catfish. I predicted that channel catfish from the Ottawa River (lacustrine-like) would be genetically distinct from individuals within its tributaries (fluvial). I collected genetic material from channel catfish in Lac des Chats, and genotyped them using microsatellites. I then performed population genetics analyses to characterize the genetic structure of the sampled population with and without *a priori* assumptions.

In the second chapter, I tested the hypothesis that ictalurid cave species have evolved in parallel from repeated invasions of subterranean habitats. I predicted that the troglobitic ictalurids are not monophyletic and are each sister to surface-dwelling taxa. To test my hypothesis, I created a multi-gene phylogeny of Ictaluridae including all but one species to assess whether or not this clade was monophyletic. I also time-calibrated the phylogeny using fossil data to provide historical context for the evolution of these species.

In the third chapter, I tested the hypothesis that both permanent and intermittent barriers between major South American river basins have reduced or eliminated gene flow between subpopulations of *P. ornatus*, resulting in distinct lineages that may represent new species. I

predicted the presence of at least three distinct lineages corresponding with the Essequibo, Orinoco, and Amazon-Paraná rivers, as observed in previous studies. To test this hypothesis, I created a multi-gene phylogeny of *Pimelodus ornatus* and calculated uncorrected *p*-distances between observed lineages within the phylogeny using cytochrome oxidase subunit 1 (*co1* or *cox1*) sequences, a commonly used gene for DNA barcoding (Herbert et al., 2004).

In the fourth chapter, I tested the hypothesis that speciation events within Pimelodidae increased following vicariance caused by Andean uplift and river capture events. Furthermore, I hypothesized that dispersal into new river basins via river capture also promoted speciation within the family as pimelodids colonized new habitats. I tested these hypotheses by constructing a time-calibrated phylogeny of Pimelodidae using the largest molecular dataset and most comprehensive taxon-sampling of any study to date. I used first-occurrence fossil data to estimate divergence times within the family. I then compared the timing of speciation events between allopatrically distributed species pairs with the timing of known orogenic and river capture events.

Chapter 1

Estimating the genetic diversity and potential influence of habitat segregation in channel catfish (*Ictalurus punctatus*)

This chapter formed the basis of the following publication:

Janzen, F.H., & Blouin-Demers, G. 2023. Estimating the genetic diversity and potential influence of habitat segregation in Channel Catfish, *Ictalurus punctatus*. *Transactions of the American Fisheries Society*, in press.

Abstract

Animals select habitats that maximize their fitness. Individual habitat preference can reduce intraspecific competition for resources, and may differ between age groups, sexes, and adult phenotypes. The channel catfish *Ictalurus punctatus* is a widespread species occurring in a diversity of freshwater habitats. This species displays breeding philopatry, returning to nesting sites occupied in previous years. Larger catfish tend to nest in the main channels of large rivers, whereas smaller catfish tend to prefer smaller tributaries. The purpose of our study was to determine whether this habitat segregation potentially associated with habitat preference affects the genetic structure of a sympatric population. We hypothesized that spatial segregation of breeding sites in the Ottawa River and its smaller tributaries at Lac des Chats reduced gene flow within the population, resulting in genetically differentiated demes associated with lacustrine-like and fluvial habitats. Using microsatellite data for 162 channel catfish, we found little genetic variation between the Ottawa, Mississippi, and Madawaska rivers. Furthermore, our analyses suggested the sampled specimens comprised one panmictic population. Fish from one site in the Ottawa River, however, were significantly differentiated from fish from a nearby site also in the Ottawa River as well as from fish from the Mississippi River tributary. Given that fish from sites further up the Ottawa River were not differentiated from fish from these sites, it is unlikely that geography can account for the differences observed; rather, assortative mating may explain the differentiation. We propose that panmixia within the population is caused by ontogenetic changes in habitat selection, straying individuals, or sex-biased dispersal and philopatry.

Introduction

Where animals choose to live influences their survival and reproductive success (Rosenzweig, 1981; Huey, 1991; Pulliam & Danielson, 1991; Camacho et al., 2015). A habitat provides an animal with basic life necessities, such as shelter, food, and potential mates (Hutto, 1985; Morris, 2003; Hernández Cordero & Seitz, 2014). Animals should select habitats that maximize their fitness, balancing survival with reproductive needs (Rosensweig, 1981; Pulliam & Danielson, 1991). Resources can vary spatially and temporally, demonstrating patchy distribution over a given area or seasonal variation (Cahn, 1925; Beyer et al., 2010; Bowlin et al., 2010; Zúñiga et al., 2017). Animals often display preferences for certain habitats, increasing their fitness by using some available areas disproportionately more than others (Johnson, 1980; Beyer et al., 2010; McGarigal et al., 2016; Fieberg et al., 2021).

Intraspecific variation in habitat preference can occur within populations where individuals differ in the habitats they select (Robinson et al., 1996; Violle et al., 2012; Dehnhard et al., 2019). Individual habitat preference and specialization is a strategy that reduces intraspecific competition for resources (Svanbäck et al., 2008; Violle et al., 2012; Dehnhard et al., 2019). This habitat variation can occur between age groups, sexes, and polymorphic adult phenotypes (Robinson et al., 1996; Marra & Holmes, 2001; Ward et al., 2006; Violle et al., 2012; Mills et al., 2021). For example, Antarctic fur seals (*Arctocephalus gazella*) display sexual segregation of foraging sites (Kernaléguen et al., 2016; Jones et al., 2020). Females forage closer to pupping sites because they are constrained by parental care, whereas males travel further from pupping sites, potentially seeking areas of high food density to support their larger body sizes (Kernaléguen et al., 2016; Jones et al., 2020). Another example is the link between habitat specialization and polymorphic adult morphology of Arctic charr (*Salvelinus alpinus*) (Snorrason

et al., 1994; Kapralova et al., 2015). Arctic charr display four adult morphs partially determined by genetics and environmental conditions (Snorrason et al., 1994; Kapralova et al., 2015). Benthic and limnetic morphs differ in cranial, fin, and gill raker morphology, as well as coloration linked with differences in diet and habitat use (Snorrason et al., 1994; Kapralova et al., 2015).

Differences in intraspecific habitat preference can lead to habitat segregation and subsequently influence the genetic structure of a population. If reproduction is restricted to individuals occupying the same preferred habitats, gene flow will be constrained between different habitats (Rausher, 1984; Hellberg, 1994; Stepien et al., 2009). These subpopulations, also known as demes, may genetically diverge over time, thus increasing genetic diversity within the population, further reinforced by selection for different traits between habitats (Rausher, 1984; Jaenike & Holt, 1991; Hellberg, 1994; Berner & Thibert-Plante, 2015). Genetically distinct demes have been observed in many species that demonstrate intraspecific habitat preference variation, such as American bullfrogs (*Lithobates catesbeianus*) (Cloyed & Eason, 2017), flour beetles (*Tribolium castaneum*) (Agashe & Bolnick, 2010), Arctic charr (*Salvelinus alpinus*) (Adams et al., 2006), and great white sharks (*Carcharodon carcharias*) (Jorgensen et al., 2010). As demes accrue genetic differences over time due to assortative mating, reproductive isolation and speciation may occur within a population (Markert et al., 1999; Via, 2001; Berner & Thibert-Plante, 2015; Igarashi et al., 2018).

Another example of a widespread species that occurs in a diversity of habitats is the channel catfish, *Ictalurus punctatus* (Ictaluridae, Siluriformes). An economically important food and sport fish, channel catfish are distributed throughout North America, occupying streams, rivers, and lakes (Wellborn, 1988; Dames & Coon, 1989; Pellett et al., 1998; Hubert, 1999;

Sotola et al., 2017). Channel catfish migrate between protective overwintering deep-water habitats and shallow-water spawning sites with abundant food in the summer (Dames & Coon, 1989; Pellett et al., 1998; Hubert, 1999). These migrations are prompted by water temperature; autumnal migrations coincide with water temperatures dropping between 10°C and 13°C (Pellett et al., 1998). Temperatures associated with spring migrations are still unknown. On average, channel catfish migrate ~8-16 km, but can migrate up to 100-500 km (Pellett et al., 1998; Sotola et al., 2017). Channel catfish display breeding philopatry, an annual return to previously occupied nesting sites (Greenwood, 1980; Pellett et al., 1998; Pearce, 2007; Hastings et al., 2017; Sotola et al., 2017; Winger et al., 2019). During the summer, channel catfish return to previously occupied territories, and rarely travel further than 5.7 km from this location (Pellett et al., 1998; Sotola et al., 2017). About 30-40% of the population, however, strays throughout the river and its tributaries (Pellett et al., 1998).

Site fidelity is related to fish size; fish of intermediate size (~280-380 mm) tend to roam throughout tributaries of large rivers (Dames & Coon, 1989; Pellett et al., 1998). Both smaller (<250 mm) and larger (>380 mm) fish tend to remain within 2-5.7 km of their nesting sites throughout the summer, preferring large river channels (Dames & Coon, 1989; Pellett et al., 1998; Sotola et al., 2017). Pellett et al. (1998) proposed that larger fish are better able to defend high quality territories and thus have more incentive to return to those sites in following years. Furthermore, they propose that smaller fish unable to establish territories due to competition are forced into less desirable habitats, resulting in little incentive to return to those sites (Pellett et al., 1998). Therefore, a smaller roaming fish that reaches a large size should eventually establish a territory and return to that site annually. This hypothesis, however, has not yet been formally tested. Conversely, breeding site fidelity and habitat preference may be influenced by

intraspecific variation in habitat preference and genetics, reinforced by lower migration and the separation of breeding populations between different spawning habitats (fluvial and lacustrine) (Bolnick et al., 2009). Channel catfish as short as 170 mm and weighing 0.34 kg can spawn (Wellborn, 1988; Hubert, 1999), indicating the possibility of a smaller adult subpopulation that may prefer smaller tributaries to large lakes and rivers. These smaller fish can reproduce within the tributaries, separated and protected from the larger fish in lakes and the main channels of rivers. Genetic sub-structuring of populations has been observed between fluvial and lacustrine habitats in freshwater fishes, such as three-spine sticklebacks (*Gasterosteus aculeatus*) (Bolnick et al., 2009). Furthermore, the migratory Neotropical dorado or dourada (*Brachyplatystoma rousseauxii*) exhibits differences between habitat-associated subpopulations within ~300 km (Carvajal-Vallejos et al., 2014). Genetically distinct demes potentially linked with philopatry occur within the Western Amazon River and the Upper Madeira, a tributary of the Amazon River (Carvajal-Vallejos et al., 2014).

To date, few studies have investigated the potential influence of habitat preference and segregation on the genetic structure of channel catfish populations. Understanding the link between habitat preference and genetic diversity of this economically important food and sport fish may prove useful in predicting how habitat fragmentation, for instance through hydroelectric dam building, might impact the survival of the species. As genetic diversity decreases within a species, the likelihood of extinction increases in response to changing environmental conditions due to the species' reduced adaptive potential (Parmesan, 2006; Exposito-Alonso et al., 2022). Therefore, determining whether habitat segregation in channel catfish promotes genetic isolation is useful for the protection and management of the species in response to climate change and anthropogenic activities.

The purpose of our study was to investigate whether breeding habitat preferences in channel catfish translates into genetic differentiation within a population of the Ottawa River and its tributaries. We hypothesized that habitat segregation potentially linked with breeding site preferences has reduced gene flow and promoted genetic differentiation between shallow river subpopulations and deep lake-like subpopulations in Lac des Chats. We predicted that channel catfish from the Ottawa River would be genetically distinct from individuals within its tributaries. Conversely, if segregation of breeding populations is not caused by habitat preference, the population should not demonstrate genetic sub-structuring associated with habitat type/river. To test this hypothesis, we collected channel catfish from Lac des Chats of the Ottawa River and from the Mississippi, Madawaska, and Bonnechere rivers. Using microsatellite allelic data, we estimated the relative genetic differentiation of each subpopulation sampled.

Materials and Methods

We collected channel catfish from Lac des Chats, an ~40 km reach of the Ottawa River between Portage-du-Fort, Québec, and Chats Falls Generating Station during summer 2018 (Figure 1-1). Two hydroelectric dams delineate this portion of the river and prevent upriver fish movements. This reach of the Ottawa River has become a reservoir lake due to the presence of both dams. Three major tributaries meet the Ottawa River between the dams: the Mississippi River, the Madawaska River, and the Bonnechere River. These smaller rivers, and the shallow banks of the Ottawa River, offer ideal summer nesting sites for channel catfish that provide cover, such as wood debris, large rocks, and undercut river banks (Hubert, 1999; Haxton & Chubbuck, 2002). Throughout their distribution, channel catfish spawn as early as March and as late as August, exhibiting latitudinal differences in exact spawning months (Hubert, 1999). Northern American populations from South Dakota and Wyoming typically spawn from mid-

June to July (June, 1977; Hubert & O'Shea, 1991; Hubert, 1999). Given the more northern latitude of Ottawa, we collected catfish between June and August from five sites along the Ottawa River and from one site in each tributary using a combination of angling and hoop nets. We selected these sites based on two criteria: 1) even distribution throughout Lac des Chats and its tributary rivers, and 2) empirically determined sites of high channel catfish abundance. We measured total body length with a measuring board and weight with a spring scale. We collected muscle tissue samples from each individual and stored them in 95% ethanol.

We extracted DNA from the muscle tissue samples with a homemade animal extraction kit and a modified protocol from Ivanova et al. (2006). We used the resulting extractions to amplify 16 microsatellite loci (Table 1-S1) chosen from a pool of 30 available loci for channel catfish (Vieira et al., 2016). We chose our loci based on successful amplification and allelic length variation (Waldbieser & Bosworth, 1997; Waldbieser & Wolters, 1999; Tatarenkov et al., 2006; Waldbieser & Bosworth, 2013). We used the following PCR recipe to amplify all microsatellite loci: 1X Dream buffer containing 2 mM $MgCl_2$ (ThermoFisher Scientific), 0.2 mM of deoxynucleotides (dNTPs), 0.05 μM of forward primer labelled with 5'-M13 or 5'-CAG tag (Table 1-S1), 0.2 μM of reverse primer, 0.2 μM 5'-labelled tag primers with fluorescent dye (FAM, VIC, NED, or PET; Table 1-S1), 0.75 U of Dream Taq, ca. 20-30 ng of template DNA, and nuclease-free water to adjust the final reaction volume to 15 μL. Using a Mastercycler pro S (Eppendorf Canada), we amplified our PCR products with the following heat cycling conditions: initial heating to 95°C for 3 minutes, 35 cycles of denaturation (95°C for 30 seconds), primer annealing (55°C for 30 seconds), and extension (72°C for 1 minute and 30 seconds) phases, and a final extension phase at 72°C for 10 minutes. Samples that could not be amplified on the first attempt were reamplified using an annealing temperature of 59°C.

Once we amplified all 16 microsatellite loci, we combined the PCR products into two pools per individual for genotyping. Each pool contained eight loci: two loci of non-overlapping allelic size ranges for each of the four fluorescent tags listed above. The first pool for each individual comprised BM1-37, IpCG18, IpCG11, IpCG14, IpCG01, IpCG54, IpCG08, and IpCG195. The second pool for each individual comprised IpCG12, POMC, 71-59, IpCG71, GY047K03, IpCG07, IpCG273, and BM1-33. Each genotyping reaction contained 8 μL of PCR product (1 μL per locus), 0.4 μL of fluorescent size standard ladder (LIZ), and 9.6 μL of HIDI formamide. We genotyped each individual using a 3500 xL Genetic Analyzer (ThermoFisher Scientific). Finally, we visualized and scored alleles using GeneMarker v2.6.4 (Hulce et al., 2011).

Using Micro-Checker v2.2.3 (Van Oosterhout et al., 2004), we corrected allelic scoring errors in our microsatellite dataset and assessed each locus for the presence of null alleles and large allele dropout. Then, we used Arlequin v3.5.2.2 (Excoffier & Lischer, 2010) to estimate basic indices of genetic diversity within the sampled subpopulations (the number of alleles per locus (A), expected heterozygosity (H_E), and observed heterozygosity (H_O)), to test for Hardy-Weinberg equilibrium (using a Bonferroni correction), and to test for linkage disequilibrium between loci (Holm, 1979; Benjamini & Yekutieli, 2001; Excoffier & Lischer, 2010). We also estimated allelic richness (A_R) and the inbreeding coefficient (F_{IS}) per locus for each collection site using HP-Rare v1.1 (Kalinowski, 2005) and FSTAT (Goudet, 1995; Goudet, 2002), respectively. To test our hypothesis, we used Arlequin to calculate pairwise subpopulation differentiation (F_{ST}) using the sum of squared differences for 16,000 permutations and a hierarchical analysis of molecular variance (AMOVA) using the sum of squared differences for 16,000 permutations. We performed the pairwise subpopulation differentiation and AMOVA

analyses after excluding loci with evidence of null alleles and linkage. For these analyses, we used nine loci: IpCG01, IpCG54, IpCG195, IpCG11, IpCG14, GY047K03, IpCG07, 71-59, and IpCG71. We assessed the statistical power of our differentiation analyses with NeEstimator (Do et al., 2014) and POWSIM (Ryman & Palm, 2006) using the effective population size (Ne), number of proposed subpopulations (two (fluvial vs lacustrine), three (Ottawa, Mississippi, and Madawaska rivers), and seven (collection sites)), subpopulation size, number of microsatellite loci, and allele frequencies per locus. Finally, we inferred the number of distinct genetic populations (*K*) free of *a priori* assumptions using STRUCTURE (Pritchard et al., 2000; Falush et al., 2003). We ran seven independent runs for each value of K = 1-8, each run for 100,000 replicates (10,000 burn-in replicates) using an admixture ancestry model and a correlated allele frequencies model (Pritchard et al., 2000; Falush et al., 2003). Using STRUCTURE HARVESTER (Earl & VonHoldt, 2012), we compared the probability of K = 1-8, identifying the most supported value with the highest natural logarithm of the probability of K ($\ln \Pr(x|K)$ as the number of genetic populations. We then plotted results for K = 2 and K = 3 using STRUCTURE PLOT (Ramasamy et al., 2014).

Results

We collected 162 channel catfish: 100 individuals from five sites on the Ottawa River (~20 individuals per site), 40 individuals from the Mississippi River, and 22 individuals from the Madawaska River (Table 1-1). We were unable to collect any channel catfish from the Bonnechere River, possibly because it is too narrow and shallow between its mouth and the Bonnechere Falls. Total body length ranged from 232-594 mm; sampled individuals comprised small (<280 mm, n = 12), intermediate (~280-380 mm, n = 96), and large (>380 mm, n = 54)

channel catfish as defined in previous migratory studies of the species (Dames & Coon, 1989; Pellett et al., 1998; Table 1-S2).

Within the corrected allele dataset, the total number of alleles per locus ranged from 5-29 (Table 1-S3), averaging between 7.4-9.0 per sampling site over all loci (Table 1-1). Mean allelic richness of all loci per sampling site ranged from 5.7-6.1, mean expected heterozygosity ranged from 0.76-0.79, mean observed heterozygosity ranged from 0.72-0.77, and mean inbreeding coefficient ranged from 0.001-0.058 (Table 1-1). We detected null alleles at two loci (IpCG08 and BM1-33), but we did not detect large allele dropout. Our sampled population was at Hardy-Weinberg equilibrium: only four of 112 tests (per locus per sampling site) significantly deviated from Hardy-Weinberg equilibrium after Bonferroni correction. In each of the four cases, observed heterozygosity was significantly lower than expected heterozygosity for locus IpCG08 at the Mississippi River, Madawaska River, and two Ottawa River sites. We also found evidence of linkage disequilibrium between some loci (Table 1-S4).

Pairwise differentiation tests revealed that catfish from most sites were not significantly differentiated (Table 1-2). We detected minor, however statistically significant, differentiation between catfish from: 1) Ottawa River site 1 and Ottawa River site 5 (F_{ST} = 0.042, P <0.04), and 2) Ottawa River site 1 and Mississippi River (F_{ST} = 0.033, P <0.02) (Table 1-2). When we grouped catfish from our five Ottawa River sites and repeated the analysis, the catfish from the Ottawa and Madawaska rivers showed no significant differentiation (F_{ST} = 0.000, P >0.45), nor did the catfish from the Ottawa and Mississippi rivers display significant differentiation (F_{ST} = 0.012, P >0.06). When comparing the tributaries, we did not detect any significant differentiation between the subpopulations (F_{ST} = 0.004, P >0.22). Finally, when we grouped all Ottawa River sites as the lacustrine-like subpopulation and the Madawaska and Mississippi sites as the fluvial

subpopulation, we did not detect significant differentiation (F_{ST} = 0.006, P >0.09). The statistical power calculated for each of these comparisons is as follows: 1) lacustrine-like versus fluvial χ^2 = 0.802, Fisher = 0.795, 2) three rivers χ^2 = 0.678, Fisher = 0.642, and 3) each sample site χ^2= 0.610, Fisher = 0.585. The hierarchical AMOVA revealed that 99.3% of the variance was attributed to differences within individuals, whereas only 0.7% of the variance was due to differences between subpopulations collected from different rivers (Table 1-3). Finally, our *a priori* STRUCTURE analysis identified K = 1 as the best supported K value, indicating the 162 sampled channel catfish form one panmictic population (Figure 1-S1). Bar plots for K = 2 and K = 3 provide visual depiction of population clustering (Figure 1-S2).

Discussion

Genetic structure of channel catfish subpopulations

Using channel catfish collected from the Ottawa River and its major tributaries at Lac des Chats, our goal was to determine whether habitat segregation potentially facilitated by breeding philopatry was linked with genetic differentiation within a population. We show that habitat type (large river and tributaries) is not associated with distinct demes within the sampled population. Therefore, we reject our hypothesis that spatial segregation of main river channel (lacustrine-like) and smaller tributary (fluvial) breeding subpopulations has contributed to genetic differentiation within the population. Our pairwise differentiation tests with microsatellite data revealed that catfish from the Ottawa River subpopulation were not significantly different from catfish from either the Madawaska River or the Mississippi River subpopulations. Fish from the Ottawa River subpopulation, however, showed minor yet significant differentiation from fish from the Mississippi River subpopulation. When observing differences between sampling sites, it appears that significant differentiation occurred between catfish from both the Ottawa River site

1 and Ottawa River site 5, and catfish from the Ottawa River site 1 and the Mississippi River. Catfish from the Mississippi River subpopulation, however, were not significantly differentiated from catfish from other Ottawa River collection sites further upriver, indicating that differentiation is not strictly associated with each river subpopulation. Furthermore, our hierarchical AMOVA indicated that almost all genetic variation within the sampled population occurred within individuals, whereas little variation occurred between river subpopulations. Finally, our STRUCTURE analysis indicated that a panmictic population was the most supported scenario within the Ottawa, Mississippi, and Madawaska rivers.

Our study is one of few to investigate how habitat preference affects the genetic structure of a population of channel catfish. Sotola et al. (2017) determined whether isolation by distance facilitated by long-distance migration and breeding site preference and philopatry was associated with genetic differentiation within a population of channel catfish from the Ohio and Wabash rivers. They sampled catfish from five sites across ~380 km of uninterrupted river, as well as from two sites separated by dams, and found evidence for isolation by distance. We did not find evidence of differentiation between catfish from our eastern-most and western-most collection sites, separated by ~25 km. The minimum distance between collection sites in Sotola et al. (2017) was 53 km, more than double the distance in our study. The relatively short distance encompassing all our sampling sites may account for the lack of differentiation between catfish from our furthest collection sites. Our results also differ from those of Carvajal-Vallejos et al. (2014) on the genetic structure of the Dorado, a migratory catfish from the Amazon River basin. Within catfish collected from the Western Amazon River and Upper Madeira River, ~300 km in distance, Carvajal-Vallejos et al. (2014) found three genetic clusters. They proposed that the co-

occurrence of these distinct demes may be due to spatial segregation of breeding populations associated with breeding site fidelity or temporal segregation of breeding populations.

One possible explanation for the observed panmixia within our sampled population is that habitat selection changes over a channel catfish's lifespan. As a catfish becomes larger with age, it may be better able to establish and defend a high-quality summer territory (Pellett et al., 1998). This suggests that fish of intermediate and larger sizes have similar habitat preferences for summer breeding sites; differences in the competitive capability for these sites may explain why each size category of channel catfish appears to select different habitats. We could test this hypothesis by conducting a multi-year telemetry study, tagging individuals of various sizes to characterize their seasonal movements and determine whether these movements and habitat preferences change as the catfish grow. Ontogenetic shifts in habitat preference have been observed in several animals, such as bluegills (*Lepomis macrochirus*) (Werner & Hall, 1988), loggerhead sea turtles (*Caretta caretta*) (Turner Tomaszewicz et al., 2017), red and blue damsels (*Xanthagrion erythroneurum*) (Khan & Herberstein, 2020), and common chameleons (*Chamaeleo chamaeleon*) (Keren-Rotem et al., 2006). Changes in habitat preference over an animal's lifespan can occur due to reduced intraspecific competition, predator avoidance, food availability, dispersal capability, etc. (Dahlgren & Eggleston, 2000; Keren-Rotem et al., 2006; Nakazawa, 2015).

Another possible explanation for the observed panmixia within our sampled population of channel catfish is that straying individuals may increase gene flow between catfish from different breeding sites, effectively weakening possible genetic reinforcement of habitat preferences (Dionne et al., 2008; Chen et al., 2020). Given that a significant proportion (~30-40%) of channel catfish stray from previously occupied summer habitats (Pellett et al., 1998),

subsequent gene flow may reduce the genetic isolation of breeding sites within the main river channel and its tributary rivers (Homola et al., 2010; Chen et al., 2020). It is also possible that philopatry might be sex-biased, as has been observed in blacktip sharks (*Carcharhinus limbatus*) (Keeney et al., 2005), lesser kestrels (*Falco naumanni*) (Alcaide et al., 2009), ringed salamanders (*Ambystoma annulatum*) (Williams et al., 2021), and several other animals. If one sex does not display philopatry, sufficient gene flow may be maintained between breeding habitats by the non-philopatric sex, genetically homogenizing the population (Blundell et al., 2002; Portnoy et al., 2015). Channel catfish may display male-biased philopatry because males build nests alone, mate monogamously, and provide uniparental care after driving off the female (Tatarenkov et al., 2006). These conditions favour dispersal in females, potentially reducing breeding site fidelity and habitat segregation (Greenwood, 1980; Portnoy et al., 2015). To test for sex-biased habitat preferences, we could estimate the genetic structure of channel catfish populations using sex-linked gene markers or observe differences between mitochondrial DNA (uniparental inheritance) and nuclear DNA (biparental inheritance) (Lawson Handley & Perrin, 2007; Portnoy et al., 2015).

Although we had strong statistical power when comparing lacustrine-like and fluvial subpopulations, increased sampling at each site could increase the statistical power when comparing each river and each individual site. Future studies should increase the number of fishes collected at each site and could expand their scope to include several lakes and rivers throughout the distribution of channel catfish. Furthermore, we used microsatellites to assess fine-scale genetic differences within the sampled population. Although microsatellites can detect fine-scale intrapopulation genetic differences (Coates et al., 2009; Lemopoulos et al., 2019; Sunde et al., 2020), contemporary technologies assessing genome-wide single nucleotide

polymorphisms, such as restriction-site-associated DNA sequencing (RADseq), can provide added resolution for subtle sub-structuring within a population due to the increased number of loci (Andrews et al., 2016; Lemopoulos et al., 2019; Sunde et al., 2020).

Genetic diversity indices

Genetic diversity within a population may be a useful predictor of the adaptive potential and survival of a species when faced with climate change and habitat fragmentation due to anthropogenic activities, such as dam construction (Reed & Frankham, 2003; Parmesan, 2006; Exposito-Alonso et al., 2022). By assessing the genetic diversity across the distribution of channel catfish, biologists can identify areas of lower diversity that may indicate a need for conservation efforts (Reed & Frankham, 2003; DeWoody et al., 2021). We quantified the genetic diversity of channel catfish at Lac des Chats and its tributaries, the northernmost population assessed to date. Allelic richness of channel catfish from the Ottawa, Mississippi, and Madawaska rivers (5.7-6.1) was higher than that from Alabama hatchery populations (2.8-4.1, Lamkom et al., 2008), and within the range of American Midwestern wild populations (5.4-6.5, Sotola et al., 2017). Hatchery populations (10.6-10.9) and wild populations (8.2-16.3) from Tamaulipas, Mexico, however, were considerably more diverse than our study population (Parra-Bracamonte et al., 2011; Lara-Rivera et al., 2019). This is unsurprising given that population differentiation and speciation rates generally increase towards the equator (Mittelbach et al., 2007; Freeman & Pennell, 2021).

The Hardy-Weinberg equilibrium is a useful metric when examining population genetics. When a population has departed from this equilibrium, it may indicate non-random mating, inbreeding, or genotyping error (Wittke-Thompson et al., 2005; Mayo, 2008; Chen et al., 2017). In our study, expected and observed heterozygosity were similar at each sampling site. All four

failed tests of Hardy-Weinberg equilibrium occurred at locus IpCG08. Thus, it is possible that these deviations are related to the presence of null alleles detected at this locus, indicating genotyping error rather than assortative mating (Van Oosterhout et al., 2006; De Meeûs, 2018). The mean observed heterozygosity at each sampling site was also within the range of those observed in both American and Mexican populations (De La Rosa-Reyna et al., 2014; Sotola et al., 2017). Our study population, however, had higher observed heterozygosity than some Mexican farm populations (Perales-Flores et al., 2007; Parra-Bracamonte et al., 2011) and both wild and domestic Alabama populations (Mickett et al., 2003; Simmons et al., 2006).

Channel catfish sampled from Lac des Chats and its tributaries displayed low levels of inbreeding, as evidenced by low F_{IS} values between 0.001-0.058, comparable to wild channel catfish from the Ohio and Wabash rivers (0.008-0.115, Sotola et al., 2017) and rivers throughout Mexico (0.006-0.065, Lara-Rivera et al., 2019). These low inbreeding levels indicate that the installation of both dams bordering Lac des Chats have not yet negatively impacted the genetic diversity of this population, even though they clearly prevent upriver movement. In contrast, higher F_{IS} values have been documented for Alabama hatchery populations (-0.012-0.370, Lamkom et al., 2008) and Tamaulipas hatchery populations (0.140-0.320, De La Rosa-Reyna et al., 2014). Inbreeding tends to increase in domesticated populations due to the few available mates constrained over generations by hatchery space limitations (Waters et al., 2020). This inbreeding leads to an increase in homozygosity within the population, consequently reducing allelic diversity (Busack & Currens, 1995; Frost et al., 2006). Furthermore, selection for specific traits that improve fitness in captivity may also homogenize farmed populations (Christie et al., 2014).

Conclusion

The purpose of our study was to investigate whether habitat segregation previously observed in channel catfish was associated with genetic differentiation within a population. We hypothesized that habitat preferences linked to breeding philopatry for the lacustrine-like Lac des Chats and its fluvial tributary rivers would result in spatial isolation of breeding populations and genetic differentiation of each habitat type subpopulation. Microsatellite genotyping of 162 channel catfish from the Ottawa, Mississippi, and Madawaska rivers revealed a panmictic population, with little differentiation between river subpopulations. Further study is required to determine whether habitat preference changes over a fish's lifespan resulting from improved ability to establish and defend high-quality nesting sites, or if sex-biased philopatry could explain the observed gene flow. The logical next steps include estimating population structure with sex-specific genetic markers and telemetry to observe potential differences between the sexes or changes in movements over time, respectively.

Tables

Table 1-1 Collection site information and basic genetic diversity indices for 162 channel catfish captured from Lac des Chats. Site information includes river, site code, GPS coordinates, and the number of individuals collected. Genetic diversity indices presented for each collection site are averaged over 16 microsatellite loci. Diversity indices include number of alleles (A), allelic richness (A_R), expected heterozygosity (H_E), observed heterozygosity (H_O), and inbreeding coefficient (F_{IS}).

River	Site code	GPS coordinates	Number of individuals	A	A_R	H_E	H_O	F_{IS}
Ottawa	Ot1	N45°27'46.4" W076°23'13.0"	21	7.44	5.65	0.768	0.736	0.043
Ottawa	Ot2	N45°30'47.6" W076°30'17.2"	19	7.44	5.71	0.764	0.760	0.006
Ottawa	Ot3	N45°29'48.0" W076°26'47.0"	20	7.88	5.95	0.763	0.720	0.058
Ottawa	Ot4	N45°31'08.0" W076°32'22.0"	20	7.50	5.65	0.766	0.750	0.022
Ottawa	Ot5	N45°26'51.0" W076°19'04.2"	20	7.69	5.80	0.761	0.760	0.001
Mississippi	Mis	N45°25'47.0" W076°15'40.0"	40	9.00	5.87	0.773	0.763	0.013
Madawaska	Mad	N45°26'32.9" W076°20'54.9"	22	8.63	6.12	0.791	0.770	0.027

Table 1-2 Pairwise differentiation tests (sum of squared differences) between channel catfish collection sites along the Ottawa, Mississippi, and Madawaska rivers using data from 9 microsatellites after excluding linked loci and loci with null alleles. F_{ST} values calculated between each collection site are presented above the diagonal and *P*-values presented below. Significant differences are indicated with an asterisk (*). Collection sites are labelled as follows: Ottawa River = Ot1-Ot5, Mississippi River = Mis, and Madawaska River = Mad.

Collection site	Ot1	Ot2	Ot3	Ot4	Ot5	Mis	Mad
Ot1		0.0000	0.0000	0.0000	0.0418*	0.0330*	0.0000
Ot2	0.6985		0.0000	0.0000	0.0151	0.0191	0.0000
Ot3	0.3248	0.6091		0.0000	0.0069	0.0066	0.0000
Ot4	0.4167	0.5661	0.6578		0.0331	0.0303	0.0026
Ot5	0.0316*	0.2007	0.1882	0.1180		0.0000	0.0077
Mis	0.0154*	0.0984	0.1371	0.0547	0.8446		0.0040
Mad	0.4425	0.5765	0.4293	0.3446	0.2254	0.2165	

Table 1-3 Analysis of molecular variance (AMOVA) results using a sum of squared differences in Arlequin v3.5.2.2 between three subpopulations of channel catfish (n = 162) collected from the Ottawa, Mississippi, and Madawaska rivers.

Source of variation	Sum of squares	Variance components	Percentage variation (%)
Among rivers	3,363.17	7.31	0.68
Among individuals within rivers	165,844.53	0.00	0.00
Within individuals	179,058.00	1,105.30	99.32
Total	348,265.70	1,112.61	100.00

Figures

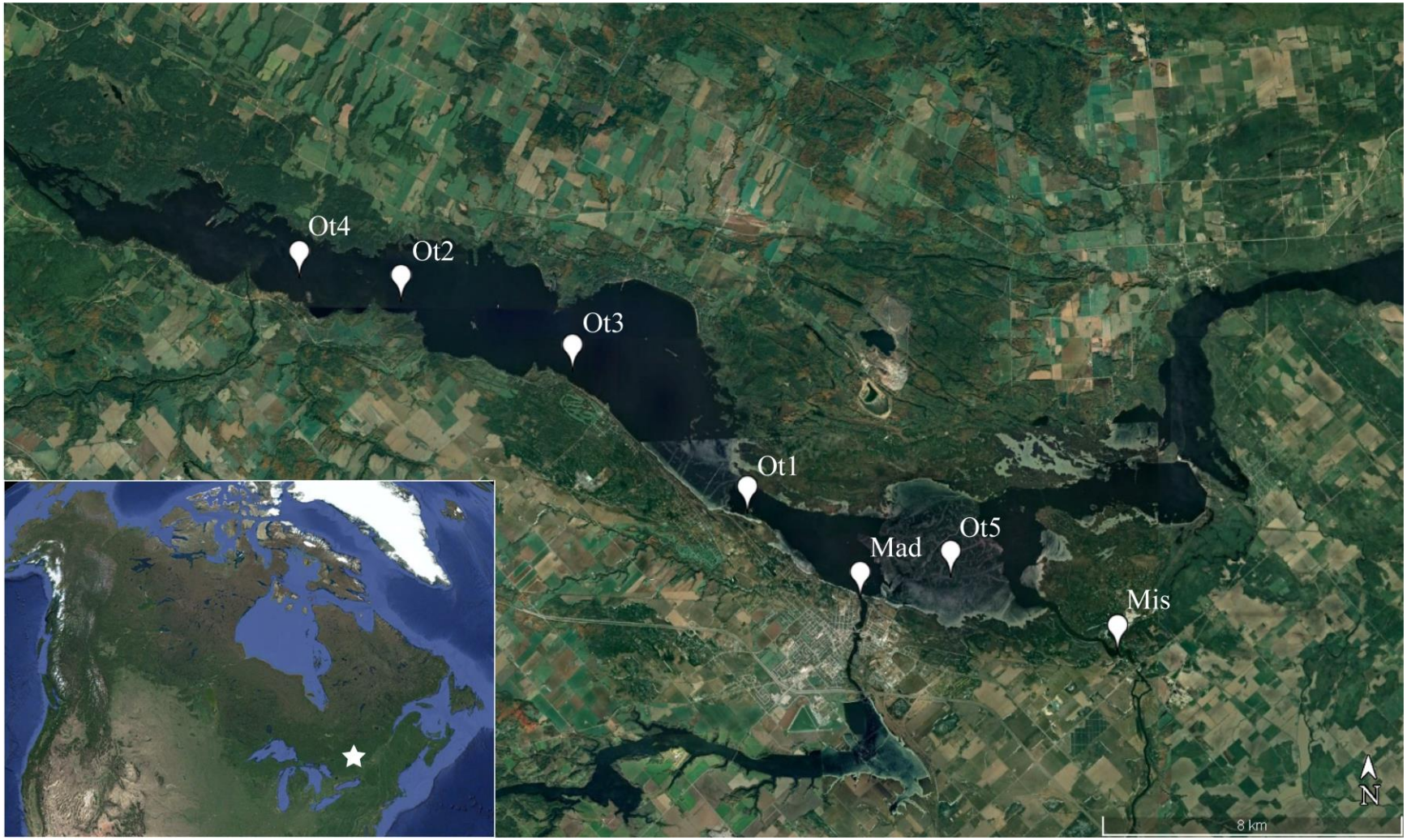

Figure 1-1 Aerial view of the ~40 km Ottawa River reach known as Lac des Chats, between Portage-du-Fort and Chats Falls Generating Station at the border between Québec and Ontario, Canada. Bottom-left image depicts study location in Canada with a white star. Collecting sites are indicated by white markers. Ottawa River collection sites are labelled Ot1-Ot5, Mississippi River

collection site is labelled Mis, and Madawaska River collection site labelled as Mad. Map data: Google Earth Pro, Maxar, CNES/Airbus.

Supplemental Material for Chapter 1

Table 1-S1 Primer sequences used for PCR amplification and genotyping reactions of microsatellite loci for 162 channel catfish captured from Lac des Chats. Forward primers denoted with M13 are preceded by 5'TGTAAAACGACGGCCAGT3' and forward primers denoted with CAG are preceded by 5'CAGTCGGGCGTCATCA3'.

Locus	Primer name	Primer sequence (5'-3')	Fluorescent tag	Reference
BM1-37	BM1-37F-M13	GTCCGGACATGCCTACAGAATA	FAM	Tatarenkov, 2006
	BM1-37R	CATTTCACAGCAACCTCCC		
IpCG18	IpCG18F-M13	GATCTTGTTACAAGAGATAATA	FAM	Waldbieser, 1999
	IpCG18R	GGGTTCGGCAACTTCAAG		
IpCG01	IpCG01F-CAG	GTACCACTGGTCAGTATCTCC	NED	Waldbieser, 1999
	IpCG01R	GTTTCACCATCACCAGAGTCCAGG		
IpCG54	IpCG54F-M13	CAAGGTCCAGGAGCTGTCAC	NED	Waldbieser, 2013
	IpCG54R	GTTTGTCCTGGGAACGCTCTGTGT		
IpCG08	IpCG08F-M13	GTAGGGATGATATTGGTGG	PET	Waldbieser, 1999
	IpCG08R	TGGCCTCTCTGTTGTTCTC		
IpCG195	IpCG195F-M13	AACTGTCATTTACACACATTCATCTA	PET	Waldbieser, 2013
	IpCG195R	GCAGGTCTGTCGTCATCTAC		
IpCG11	IpCG11F-M13	CACAGAGTTGGGACAGCA	VIC	Waldbieser, 1997
	IpCG11R	GATCTCTGAGTGATTTGTGTC		
IpCG14	IpCG14F-CAG	GGCCAGGATAAAGCAGTT	VIC	Waldbieser, 1997
	IpCG14R	GATCCACATATCAGGCCA		
IpCG12	IpCG12F-CAG	GGAGTTGATGTGTTTACTGG	FAM	Waldbieser, 1997
	IpCG12R	TCTGCTGACAAATTTGGG		
POMC	POMCF-M13	TGCTTTTACCACATCAGAAGACC	FAM	Waldbieser, 2013
	POMCR	GTTTGGTGGAGAATACAGGTAGC		
GY047K03	GY047K03F-M13	CCCTCTATGCCTGTGATTGTTTATG	NED	Waldbieser, 2013
	GY047K03R	GTTTGTCCACCAAGTCCCTGTGTAAC		
IpCG07	IpCG07F-M13	CCTCTGCAGAACCATCTCTA	NED	Waldbieser, 1999
	IpCG07R	GCATAAACGTCTGTAGCTC		
IpCG273	IpCG273F-CAG	CGTTTTACTTCCTCATACAGCAC	PET	Waldbieser, 2013
	IpCG273R	GTTTCAAGAGACCTGTGACATCGC		

BM1-33	BM1-33F-CAG	TCAGGTTCGTCTTCAGACTTGAG	PET	Tatarenkov, 2006
	BM1-33R	AGTGCAGCTCCAGTCAACATCA		
71-59	71-59F-M13	TGCTTAGGGTAAGTCAGTTATAGATTC	VIC	Waldbieser, 2013
	71-59R	GTTTCCATATTCACCAGGGTGTG		
IpCG71	IpCG71F-CAG	CGAAGGTTTATAACTAAGGAGCAGG	VIC	Waldbieser, 2013
	IpCG71R	GTTTGTACCTGGCTGTGAAGACAC		

Table 1-S2 Specimen data for 162 channel catfish collected from Lac des Chats and its tributaries. Specimen data includes river name, collection site code, GPS coordinates, collection date, and body measurements taken using a spring scale and measuring board.

Fish #	River	Site Code	GPS Coordinate		Date	Length (mm)	Weight (g)
			N	W			
1	Mississippi	Mis	45°25'47.0"	76º15'40.0"	07-06-2018	495	900
2	Mississippi	Mis	45°25'47.0"	76º15'40.0"	07-06-2018	360	150
3	Mississippi	Mis	45°25'47.0"	76º15'40.0"	07-06-2018	350	360
4	Mississippi	Mis	45°25'47.0"	76º15'40.0"	08-06-2018	332	270
5	Ottawa	Ot1	45º27'46.4"	76º23'12.9"	12-06-2018	292	180
6	Ottawa	Ot1	45º27'46.4"	76º23'12.9"	12-06-2018	444	400
7	Ottawa	Ot1	45º27'46.4"	76º23'12.9"	12-06-2018	376	355
8	Ottawa	Ot1	45º27'46.4"	76º23'12.9"	12-06-2018	413	490
9	Ottawa	Ot1	45º27'46.4"	76º23'12.9"	12-06-2018	380	390
10	Mississippi	Mis	45º25'47.0"	76º15'40.0"	04-07-2018	306	180
11	Mississippi	Mis	45º25'47.0"	76º15'40.0"	04-07-2018	309	210
12	Mississippi	Mis	45º25'47.0"	76º15'40.0"	04-07-2018	347	200
13	Mississippi	Mis	45º25'47.0"	76º15'40.0"	04-07-2018	307	190
14	Mississippi	Mis	45º25'47.0"	76º15'40.0"	05-07-2018	400	550
15	Mississippi	Mis	45º25'47.0"	76º15'40.0"	05-07-2018	308	230
16	Mississippi	Mis	45º25'47.0"	76º15'40.0"	05-07-2018	331	280
17	Mississippi	Mis	45º25'47.0"	76º15'40.0"	05-07-2018	380	430
18	Mississippi	Mis	45º25'47.0"	76º15'40.0"	05-07-2018	311	220
19	Mississippi	Mis	45º25'47.0"	76º15'40.0"	05-07-2018	309	190
20	Mississippi	Mis	45º25'47.0"	76º15'40.0"	09-07-2018	515	1300
21	Mississippi	Mis	45º25'47.0"	76º15'40.0"	09-07-2018	426	700
22	Mississippi	Mis	45º25'47.0"	76º15'40.0"	09-07-2018	464	780
23	Mississippi	Mis	45º25'47.0"	76º15'40.0"	09-07-2018	439	890

24	Mississippi	Mis	45º25'47.0"	76º15'40.0"	09-07-2018	430	690
25	Mississippi	Mis	45º25'47.0"	76º15'40.0"	09-07-2018	428	600
26	Mississippi	Mis	45º25'47.0"	76º15'40.0"	10-07-2018	343	295
27	Mississippi	Mis	45º25'47.0"	76º15'40.0"	10-07-2018	327	265
28	Mississippi	Mis	45º25'47.0"	76º15'40.0"	10-07-2018	350	335
29	Mississippi	Mis	45º25'47.0"	76º15'40.0"	10-07-2018	333	255
30	Mississippi	Mis	45º25'47.0"	76º15'40.0"	11-07-2018	358	320
31	Mississippi	Mis	45º25'47.0"	76º15'40.0"	11-07-2018	310	225
32	Mississippi	Mis	45º25'47.0"	76º15'40.0"	11-07-2018	297	185
33	Mississippi	Mis	45º25'47.0"	76º15'40.0"	11-07-2018	320	265
34	Mississippi	Mis	45º25'47.0"	76º15'40.0"	11-07-2018	357	347
35	Mississippi	Mis	45º25'47.0"	76º15'40.0"	11-07-2018	350	330
36	Mississippi	Mis	45º25'47.0"	76º15'40.0"	11-07-2018	341	298
37	Mississippi	Mis	45º25'47.0"	76º15'40.0"	11-07-2018	331	280
38	Mississippi	Mis	45º25'47.0"	76º15'40.0"	11-07-2018	321	240
39	Mississippi	Mis	45º25'47.0"	76º15'40.0"	11-07-2018	321	220
40	Mississippi	Mis	45º25'47.0"	76º15'40.0"	11-07-2018	305	215
41	Mississippi	Mis	45º25'47.0"	76º15'40.0"	12-07-2018	344	285
42	Mississippi	Mis	45º25'47.0"	76º15'40.0"	12-07-2018	300	190
43	Mississippi	Mis	45º25'47.0"	76º15'40.0"	12-07-2018	532	1100
44	Mississippi	Mis	45º25'47.0"	76º15'40.0"	12-07-2018	332	260
45	Mississippi	Mis	45º25'47.0"	76º15'40.0"	12-07-2018	377	400
46	Ottawa	Ot1	45º27'46.4"	76º23'12.9"	12-07-2018	505	950
47	Ottawa	Ot1	45º27'46.4"	76º23'12.9"	12-07-2018	422	600
48	Ottawa	Ot1	45º27'46.4"	76º23'12.9"	12-07-2018	397	215
49	Ottawa	Ot1	45º27'46.4"	76º23'12.9"	12-07-2018	320	205
50	Ottawa	Ot1	45º27'46.4"	76º23'12.9"	12-07-2018	309	200

51	Ottawa	Ot1	45º27'46.4"	76º23'12.9"	12-07-2018	301	200
52	Ottawa	Ot1	45º27'46.4"	76º23'12.9"	12-07-2018	358	345
53	Ottawa	Ot1	45º27'46.4"	76º23'12.9"	12-07-2018	299	195
54	Ottawa	Ot1	45º27'46.4"	76º23'12.9"	16-07-2018	421	660
55	Ottawa	Ot1	45º27'46.4"	76º23'12.9"	16-07-2018	287	190
56	Ottawa	Ot1	45º27'46.4"	76º23'12.9"	16-07-2018	475	860
57	Ottawa	Ot1	45º27'46.4"	76º23'12.9"	16-07-2018	411	520
58	Ottawa	Ot1	45º27'46.4"	76º23'12.9"	16-07-2018	420	635
59	Ottawa	Ot1	45º27'46.4"	76º23'12.9"	18-07-2018	372	385
60	Ottawa	Ot1	45º27'46.4"	76º23'12.9"	18-07-2018	445	785
61	Ottawa	Ot1	45º27'46.4"	76º23'12.9"	18-07-2018	445	690
62	Ottawa	Ot2	45º30'47.6"	76º30'17.2"	18-07-2018	450	700
63	Ottawa	Ot2	45º30'47.6"	76º30'17.2"	18-07-2018	369	370
64	Ottawa	Ot2	45º30'47.6"	76º30'17.2"	18-07-2018	380	415
65	Ottawa	Ot2	45º30'47.6"	76º30'17.2"	18-07-2018	375	440
66	Ottawa	Ot2	45º30'47.6"	76º30'17.2"	18-07-2018	358	350
67	Ottawa	Ot2	45º30'47.6"	76º30'17.2"	18-07-2018	382	450
68	Ottawa	Ot2	45º30'47.6"	76º30'17.2"	18-07-2018	336	305
69	Ottawa	Ot2	45º30'47.6"	76º30'17.2"	18-07-2018	394	490
70	Ottawa	Ot2	45º30'47.6"	76º30'17.2"	18-07-2018	464	750
71	Ottawa	Ot2	45º30'47.6"	76º30'17.2"	18-07-2018	276	150
72	Ottawa	Ot2	45º30'47.6"	76º30'17.2"	18-07-2018	389	490
73	Ottawa	Ot2	45º30'47.6"	76º30'17.2"	19-07-2018	442	625
74	Ottawa	Ot2	45º30'47.6"	76º30'17.2"	19-07-2018	451	790
75	Ottawa	Ot2	45º30'47.6"	76º30'17.2"	19-07-2018	397	490
76	Ottawa	Ot4	45º31'08.0"	76º32'22.0"	19-07-2018	356	310
77	Ottawa	Ot2	45º30'47.6"	76º30'17.2"	24-07-2018	361	360

78	Ottawa	Ot2	45º30'47.6"	76º30'17.2"	24-07-2018	373	400
79	Ottawa	Ot2	45º30'47.6"	76º30'17.2"	24-07-2018	388	500
80	Ottawa	Ot2	45º30'47.6"	76º30'17.2"	24-07-2018	280	150
81	Ottawa	Ot2	45º30'47.6"	76º30'17.2"	24-07-2018	259	120
82	Ottawa	Ot3	45º29'48.0"	76º26'47.0"	26-07-2018	402	470
83	Ottawa	Ot3	45º29'48.0"	76º26'47.0"	26-07-2018	305	200
84	Ottawa	Ot3	45º29'48.0"	76º26'47.0"	26-07-2018	370	405
85	Ottawa	Ot3	45º29'48.0"	76º26'47.0"	26-07-2018	280	160
86	Ottawa	Ot3	45º29'48.0"	76º26'47.0"	26-07-2018	340	295
87	Ottawa	Ot3	45º29'48.0"	76º26'47.0"	26-07-2018	401	500
88	Ottawa	Ot3	45º29'48.0"	76º26'47.0"	26-07-2018	311	230
89	Ottawa	Ot3	45º29'48.0"	76º26'47.0"	26-07-2018	313	250
90	Ottawa	Ot3	45º29'48.0"	76º26'47.0"	26-07-2018	305	210
91	Ottawa	Ot3	45º29'48.0"	76º26'47.0"	26-07-2018	335	260
92	Ottawa	Ot3	45º29'48.0"	76º26'47.0"	26-07-2018	277	155
93	Ottawa	Ot3	45º29'48.0"	76º26'47.0"	26-07-2018	349	350
94	Ottawa	Ot3	45º29'48.0"	76º26'47.0"	26-07-2018	302	200
95	Ottawa	Ot3	45º29'48.0"	76º26'47.0"	26-07-2018	484	900
96	Ottawa	Ot4	45º31'08.0"	76º32'22.0"	30-07-2018	246	105
97	Ottawa	Ot4	45º31'08.0"	76º32'22.0"	30-07-2018	300	215
98	Ottawa	Ot4	45º31'08.0"	76º32'22.0"	30-07-2018	262	120
99	Ottawa	Ot4	45º31'08.0"	76º32'22.0"	30-07-2018	339	300
100	Ottawa	Ot4	45º31'08.0"	76º32'22.0"	30-07-2018	311	210
101	Ottawa	Ot4	45º31'08.0"	76º32'22.0"	30-07-2018	240	100
102	Ottawa	Ot4	45º31'08.0"	76º32'22.0"	30-07-2018	358	340
103	Ottawa	Ot4	45º31'08.0"	76º32'22.0"	30-07-2018	267	170
104	Ottawa	Ot4	45º31'08.0"	76º32'22.0"	30-07-2018	290	195

105	Ottawa	Ot4	45º31'08.0"	76º32'22.0"	30-07-2018	279	155
106	Ottawa	Ot4	45º31'08.0"	76º32'22.0"	30-07-2018	265	145
107	Ottawa	Ot4	45º31'08.0"	76º32'22.0"	30-07-2018	355	340
108	Ottawa	Ot4	45º31'08.0"	76º32'22.0"	30-07-2018	521	1175
109	Ottawa	Ot3	45º29'48.0"	76º26'47.0"	02-08-2018	404	510
110	Ottawa	Ot3	45º29'48.0"	76º26'47.0"	02-08-2018	458	830
111	Ottawa	Ot3	45º29'48.0"	76º26'47.0"	02-08-2018	432	605
112	Ottawa	Ot3	45º29'48.0"	76º26'47.0"	02-08-2018	449	740
113	Ottawa	Ot3	45º29'48.0"	76º26'47.0"	02-08-2018	495	1030
114	Ottawa	Ot3	45º29'48.0"	76º26'47.0"	02-08-2018	423	625
115	Ottawa	Ot5	45º26'51.0"	76º19'04.2"	02-08-2018	321	245
116	Ottawa	Ot4	45º31'08.0"	76º32'22.0"	03-08-2018	519	1050
117	Ottawa	Ot4	45º31'08.0"	76º32'22.0"	03-08-2018	435	720
118	Ottawa	Ot4	45º31'08.0"	76º32'22.0"	03-08-2018	386	435
119	Ottawa	Ot4	45º31'08.0"	76º32'22.0"	03-08-2018	594	1900
120	Ottawa	Ot4	45º31'08.0"	76º32'22.0"	03-08-2018	450	890
121	Ottawa	Ot4	45º31'08.0"	76º32'22.0"	03-08-2018	417	615
122	Ottawa	Ot4	45º31'08.0"	76º32'22.0"	03-08-2018	387	515
123	Ottawa	Ot5	45º26'51.0"	76º19'04.2"	09-08-2018	232	95
124	Ottawa	Ot5	45º26'51.0"	76º19'04.2"	09-08-2018	320	250
125	Ottawa	Ot5	45º26'51.0"	76º19'04.2"	09-08-2018	302	205
126	Ottawa	Ot5	45º26'51.0"	76º19'04.2"	09-08-2018	317	240
127	Ottawa	Ot5	45º26'51.0"	76º19'04.2"	09-08-2018	339	260
128	Ottawa	Ot5	45º26'51.0"	76º19'04.2"	09-08-2018	377	335
129	Ottawa	Ot5	45º26'51.0"	76º19'04.2"	09-08-2018	323	270
130	Ottawa	Ot5	45º26'51.0"	76º19'04.2"	09-08-2018	298	190
131	Ottawa	Ot5	45º26'51.0"	76º19'04.2"	09-08-2018	290	190

132	Ottawa	Ot5	45º26'51.0"	76º19'04.2"	09-08-2018	358	345
133	Ottawa	Ot5	45º26'51.0"	76º19'04.2"	09-08-2018	368	370
134	Ottawa	Ot5	45º26'51.0"	76º19'04.2"	10-08-2018	378	400
135	Ottawa	Ot5	45º26'51.0"	76º19'04.2"	10-08-2018	417	535
136	Madawaska	Mad	45º26'32.9"	76º20'54.9"	13-08-2018	299	170
137	Madawaska	Mad	45º26'32.9"	76º20'54.9"	13-08-2018	336	250
138	Madawaska	Mad	45º26'32.9"	76º20'54.9"	13-08-2018	308	200
139	Madawaska	Mad	45º26'32.9"	76º20'54.9"	13-08-2018	339	270
140	Ottawa	Ot5	45º26'51.0"	76º19'04.2"	14-08-2018	408	565
141	Ottawa	Ot5	45º26'51.0"	76º19'04.2"	14-08-2018	410	600
142	Madawaska	Mad	45º26'32.9"	76º20'54.9"	15-08-2018	297	185
143	Madawaska	Mad	45º26'32.9"	76º20'54.9"	16-08-2018	295	170
144	Madawaska	Mad	45º26'32.9"	76º20'54.9"	16-08-2018	344	295
145	Madawaska	Mad	45º26'32.9"	76º20'54.9"	16-08-2018	381	430
146	Madawaska	Mad	45º26'32.9"	76º20'54.9"	16-08-2018	310	215
147	Madawaska	Mad	45º26'32.9"	76º20'54.9"	20-08-2018	344	265
148	Madawaska	Mad	45º26'32.9"	76º20'54.9"	20-08-2018	275	145
149	Madawaska	Mad	45º26'32.9"	76º20'54.9"	20-08-2018	397	445
150	Madawaska	Mad	45º26'32.9"	76º20'54.9"	20-08-2018	311	200
151	Madawaska	Mad	45º26'32.9"	76º20'54.9"	20-08-2018	319	240
152	Madawaska	Mad	45º26'32.9"	76º20'54.9"	20-08-2018	264	125
153	Madawaska	Mad	45º26'32.9"	76º20'54.9"	20-08-2018	305	230
154	Madawaska	Mad	45º26'32.9"	76º20'54.9"	23-08-2018	303	170
155	Madawaska	Mad	45º26'32.9"	76º20'54.9"	23-08-2018	307	210
156	Madawaska	Mad	45º26'32.9"	76º20'54.9"	23-08-2018	309	210
157	Madawaska	Mad	45º26'32.9"	76º20'54.9"	23-08-2018	325	225
158	Madawaska	Mad	45º26'32.9"	76º20'54.9"	23-08-2018	356	315

159	Ottawa	Ot5	45º26'51.0"	76º19'04.2"	24-08-2018	410	480
160	Ottawa	Ot5	45º26'51.0"	76º19'04.2"	24-08-2018	524	1000
161	Ottawa	Ot5	45º26'51.0"	76º19'04.2"	24-08-2018	500	1050
162	Madawaska	Mad	45º26'32.9"	76º20'54.9"	18-09-2018	345	295

Table 1-S3 Number of alleles per microsatellite locus of 162 channel catfish collected at Ottawa River, Mississippi River, and Madawaska River sampling sites. Site labels are as follows: Ottawa River = Ot1-Ot5, Mississippi River = Mis, and Madawaska River = Mad.

Locus	Ot1	Ot2	Ot3	Ot4	Ot5	Mis	Mad	Total
BM1-37	10	9	11	9	11	13	11	13
IpCG18	8	9	10	6	10	11	10	12
IpCG01	6	8	8	8	5	9	8	9
IpCG54	15	18	17	14	15	23	19	29
IpCG08	6	4	6	7	5	6	5	7
IpCG195	8	7	7	7	8	7	7	9
IpCG11	6	6	6	5	6	6	6	6
IpCG14	6	6	9	8	8	10	8	13
IpCG12	8	6	4	6	7	8	8	9
POMC	6	6	8	6	8	8	9	9
GY047K03	7	8	6	8	7	7	6	9
IpCG07	5	5	5	5	5	5	5	5
IpCG273	7	7	8	6	5	6	8	8
BM1-33	9	9	9	12	10	12	13	17
71-59	6	6	6	6	6	7	7	8
IpCG71	6	5	6	7	7	6	8	9

Table 1-S4 Significant linkage disequilibrium between microsatellite loci (P <0.05). Locus numbers are: 1) BM1-37, 2) IpCG18, 3) IpCG01, 4) IpCG54, 5) IpCG08, 6) IpCG195, 7) IpCG11, 8) IpCG14, 9) IpCG12, 10) POMC, 11) GY047K03, 12) IpCG07, 13) IpCG273, 14) BM1-33, 15) 71-59, and 16) IpCG71. Linked loci are designated by an asterisk (*).

Locus	1	2	3	4	5	6	7	8	9	10	11	12	13	14	15	16
1		-	-	-	-	-	-	-	-	-	-	-	*	*	-	-
2	-		-	*	-	-	-	*	-	*	-	-	-	-	-	-
3	-	-		-	-	-	-	-	-	-	-	-	-	-	-	-
4	-	*	-		-	-	-	-	-	-	-	-	-	-	-	-
5	-	-	-	-		-	-	-	-	-	-	-	-	-	-	-
6	-	-	-	-	-		-	-	-	-	-	-	-	-	-	-
7	-	-	-	-	-	-		-	*	-	-	-	*	-	-	-
8	-	*	-	-	-	-	-		-	-	-	-	-	-	-	-
9	-	-	-	-	-	-	*	-		*	-	-	-	-	-	-
10	-	*	-	-	-	-	-	-	*		*	*	-	-	-	-
11	-	-	-	-	-	-	-	-	-	*		-	-	-	-	-
12	-	-	-	-	-	-	-	-	-	*	-		-	-	-	-
13	*	-	-	-	-	-	*	-	-	-	-	-		-	*	-
14	*	-	-	-	-	-	-	-	-	-	-	-	-		-	*
15	-	-	-	-	-	-	-	-	-	-	-	-	*	-		-
16	-	-	-	-	-	-	-	-	-	-	-	-	-	*	-	

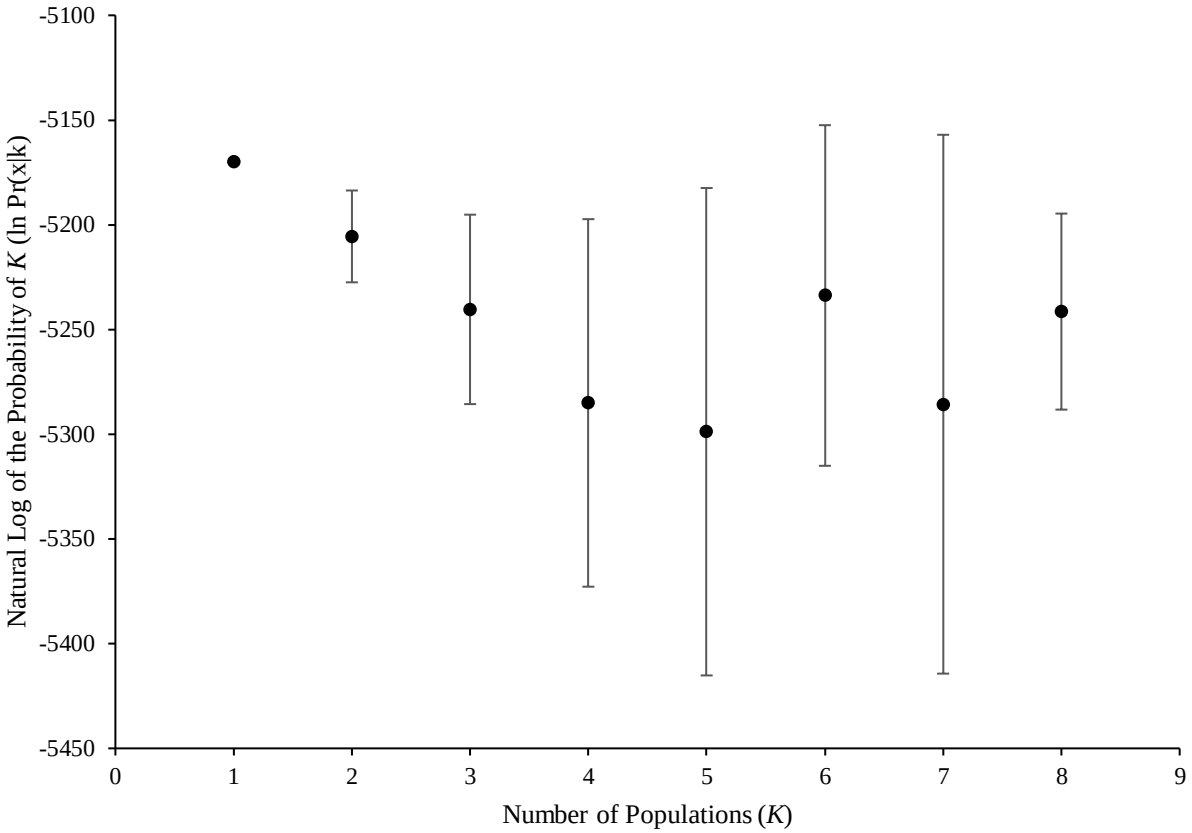

Figure 1-S1 Mean estimates of the natural log of the probability of *K* (ln Pr(x|k)) for the number of distinct populations (*K*) of 162 channel catfish collected from the Ottawa, Mississippi, and Madawaska rivers. Seven independent runs were averaged for each value of *K*. Standard deviation bars are presented above and below each data point. Data summarized from all independent runs using STRUCTURE HARVESTER (Earl & VonHoldt, 2012).

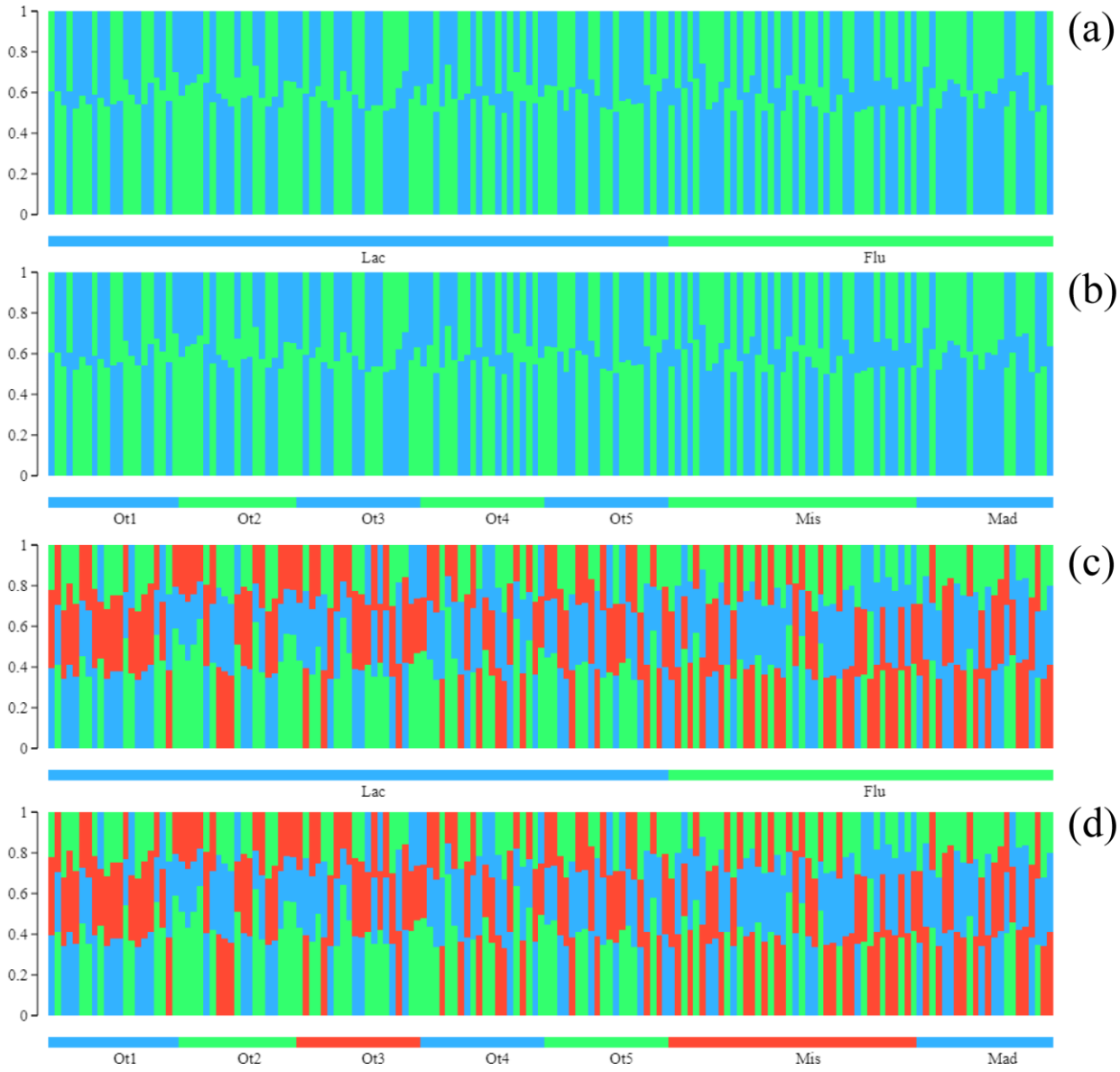

Figure 1-S2 Bar plots of Q estimate values from STRUCTURE analysis of 162 Channel Catfish from Lac des Chats. Panels depict results for: a) *K*= 2 with the population grouped by habitat type (Lac = lacustrine-like, Flu = fluvial), b) *K* = 2 with the population grouped by collection site (Ot1-Ot5 = Ottawa River, Mis = Mississippi River, Mad = Madawaska River), c) *K* = 3 with populations grouped by habitat type, and d) *K* = 3 with the population grouped by collection site. Bar plots created using STRUCTURE PLOT (Ramasamy et al., 2014).

Chapter 2

Phylogenetic relationships of the North American catfishes (Ictaluridae, Siluriformes): investigating the origins and parallel evolution of the troglobitic species

This chapter formed the basis of the following publication:

Janzen, F.H., Pérez-Rodríguez, R., Domínguez-Domínguez, O., Hendrickson, D.A., Sabaj, M.H., & Blouin-Demers, G. 2023. Phylogenetic relationships of the North American catfishes (Ictaluridae, Siluriformes): Investigating the origins and parallel evolution of the troglobitic species. *Molecular Phylogenetics and Evolution* 182: 107746.

Abstract

Insular habitats have played an important role in developing evolutionary theory, including natural selection and island biogeography. Caves are insular habitats that place extreme selective pressures on organisms due to the absence of light and food scarcity. Therefore, cave organisms present an excellent opportunity for studying colonization and speciation in response to the unique abiotic conditions that require extreme adaptations. One vertebrate family, the North American catfishes (Ictaluridae), includes four troglodytic species that inhabit the karst region bordering the western Gulf of Mexico. The phylogenetic relationships of these species have been contentious, and conflicting hypotheses have been proposed to explain their origins. The purpose of our study was to construct a time-calibrated phylogeny of Ictaluridae using first-occurrence fossil data and the largest molecular dataset on the group to date. We test the hypothesis that troglodytic ictalurids have evolved in parallel, thus resulting from repeated cave colonization events. We found that *Prietella lundbergi* is sister to surface-dwelling *Ictalurus* and that *Prietella phreatophila* + *Trogloglanis pattersoni* are sister to surface-dwelling *Ameiurus*, suggesting that ictalurids colonized subterranean habitats at least twice in evolutionary history. The sister relationship between *Prietella phreatophila* and *Trogloglanis pattersoni* may indicate that these two species diverged from a common ancestor following a subterranean dispersal event between Texas and Coahuila aquifers. We recovered *Prietella* as a polyphyletic genus and recommend *P. lundbergi* be removed from this genus. With respect to *Ameiurus*, we found evidence for a potentially undescribed species sister to *A. platycephalus*, which warrants further investigation of Atlantic and Gulf slope *Ameiurus* species. In *Ictalurus*, we identified shallow divergence between *I. dugesii* and *I. ochoterenai*, *I. australis* and *I. mexicanus*, and *I. furcatus* and *I. meridionalis*, indicating a need to reexamine the validity

of each species. Lastly, we propose minor revisions to the intrageneric classification of *Noturus* including the restriction of subgenus *Schilbeodes* to *N. gyrinus* (type species), *N. lachneri*, *N. leptacanthus*, and *N. nocturnus*.

Introduction

Insular habitats have played an important role in advancing our understanding of evolutionary processes (Darwin, 1859; Brown, 1978; Schluter, 1988; Losos & Ricklefs, 2009; Lescak et al., 2015). Insular habitats are suitable for the persistence of adapted organisms, but are surrounded by habitat that is unsuitable for those organisms (Brown, 1978; Acosta, 1999). Using oceanic islands as an example of insular habitats, MacArthur and Wilson (1967) developed one of the most influential theories in evolutionary biology, *The Theory of Island Biogeography* (Whittaker et al., 2008; Patiño et al., 2017). They proposed that species richness on oceanic islands is a function of island area and distance from the continent through their effects on rates of immigration and extinction (MacArthur & Wilson, 1963; MacArthur & Wilson, 1967). Owing to the central role of islands in the development of the theory of island biogeography, insular habitats have proven invaluable for better understanding how processes including colonization, habitat complexity, habitat connectivity, and extinction influence species diversity (MacArthur & Wilson, 1967; Whittaker et al., 2008).

Islands are not the only example of insular habitats. Mountain peaks, ponds, lakes, caves, and natural habitats fragmented by anthropogenic activities may also function as insular habitats (Brown, 1971; Whittaker et al., 2008). Caves differ markedly from other insular habitats because their abiotic conditions are unique, relatively uniform among cave systems, and temporally stable (Culver, 1970; Salin et al., 2010; Ferreira & Pellegrini, 2019). For example, cave temperature, light availability, and humidity exhibit low variation in comparison with surface habitats (Salin et al., 2010; Ferreira & Pellegrini, 2019). Similar abiotic conditions in different cave systems have resulted in convergent evolution of troglobitic species spanning the kingdom Animalia (Barr & Holsinger, 1985; Mammola & Isaia, 2017). These animals possess similar traits, such as

unpigmented skin and non-functional eyes (Christman et al., 2005; Culver & Pipan, 2015). Dispersal into caves and selection for traits required to live in these extreme environments are driving forces of speciation, ecologically isolating these populations from their surface-dwelling relatives (Christiansen, 1961; Barr & Holsinger, 1985; Strecker et al., 2012). Owing to their insular nature and to the relative uniformity of selective pressures, caves provide an excellent opportunity to improve our understanding of colonization, convergent and parallel evolution, and speciation (Culver, 1970; Culver, 1976; Culver & Pipan, 2010).

One vertebrate family containing several troglobitic species is the North American catfishes, Ictaluridae (Lundberg, 1970; Lundberg, 1992; Walsh & Gilbert, 1995; Burr et al., 2020). This monophyletic family occurs from Southern Canada to Guatemala (Figure 2-1), inhabiting a wide diversity of lentic and lotic habitats, such as creek riffles, large river channels, lakes, and subterranean pools (Arce H. et al., 2016; Nelson et al., 2016; Burr et al., 2020). Fossils extend the historical distribution of ictalurids to the Pacific Northwest of the United States (Lundberg, 1992). Ictaluridae comprises seven genera, including four surface genera (*Ameiurus*, *Ictalurus*, *Noturus*, and *Pylodictis*) and three cave genera (*Prietella*, *Satan*, and *Trogloglanis*) (Figure 2-1; Walsh & Gilbert, 1995; Wilcox et al., 2004). There are currently 50 recognized extant species in the family, of which four are troglobitic: *Prietella lundbergi*, *Prietella phreatophila*, *Satan eurystomus*, and *Trogloglanis pattersoni* (Wilcox et al., 2004; Arce H. et al., 2016; Nelson et al., 2016; Burr et al., 2020). These four troglobitic species exhibit similar morphological adaptations to subterranean life observed in other aquatic cave fauna, such as non-functional eyes, achromatism, reduced swim bladder size, and fragmented lateral-line systems (Walsh & Gilbert, 1995; Arce H. et al., 2016).

Troglobitic ictalurids are found in the karst region surrounding the Gulf of Mexico, from southern Texas, USA, to southern Tamaulipas, Mexico (Figure 2-1; Wilcox et al., 2004; Sharp et al., 2019; Burr et al., 2020). *Satan eurystomus* and *Trogloglanis pattersoni* co-occur in the San Antonio Pool of the Edwards Aquifer to depths of at least 300 m below sea level (Langecker & Longley, 1993; Walsh & Gilbert, 1995). *Prietella phreatophila* occurs in underground streams in deep caves in northern Coahuila, Mexico, as well as in two caves in Amistad National Recreation Area north of the Rio Grande (Walsh & Gilbert, 1995; Hendrickson et al., 2001; Hendrickson et al., 2017; Krejca & Reddell, 2019; GBIF.org, 2022). There are hydrological connections between some of these localities, but the extent of connectivity between collection sites is still largely unknown (Hendrickson et al., 2001). *Prietella lundbergi* occurs further south than other troglobitic ictalurids, specifically in two subterranean springs in the Tamesí River drainage in southern Tamaulipas (Walsh & Gilbert, 1995; Hendrickson et al., 2001). The cave systems that *P. phreatophila* and *P. lundbergi* inhabit are separated by approximately 600 km and extensive mountain ranges (Hendrickson et al., 2001; Wilcox et al., 2004). These cave systems are in two karst regions, the Coahuila and Sierra Madre Oriental karsts, respectively (Espinasa-Pereña, 2007). As such, it is highly unlikely that there are hydrological connections between them (Hendrickson et al., 2001; Wilcox et al., 2004). *Prietella phreatophila*, *S. eurystomus* and *T. pattersoni*, however, all occur in aquifers developed in the Edwards Formation that underlies much of southwestern Texas and northern Coahuila (Sanchez et al., 2016; Sanchez et al., 2018a). That parts of this broad complex of variably interconnected aquifers, all recharged by runoff from the Edwards Plateau, are international is now well demonstrated, as are subterranean aquifer interconnections that extend far west of the ranges of *S. eurystomus* and *T. pattersoni* (under San Antonio) to very near the Texas *P. phreatophila*

localities (Boghici et al., 2004; Sanchez et al., 2016; Lundberg et al., 2017; Sanchez et al., 2018a; Sanchez et al., 2018b).

The phylogenetic positions of the four troglobitic ictalurids have always been contentious. Despite their convergent cave adaptations, *Prietella*, *Satan*, and *Trogloglanis* share traits with surface-dwelling genera (Hubbs & Bailey, 1947; Langecker & Longley, 1993; Wilcox et al., 2004). This caused confusion in early morphological classifications, which disagree with respect to intergeneric relationships. *Prietella* was often considered to be most closely related to *Noturus* (Taylor, 1969; Lundberg, 1970; Lundberg, 1982; Walsh & Gilbert, 1995); however, Suttkus (1961) proposed that *Ictalurus* + *Ameiurus* were close relatives of *Prietella*. The phylogenetic position of *Trogloglanis* varied widely between studies. Upon its description, Eigenmann (1919) proposed *T. pattersoni* shared a common ancestor with *Noturus*. As additional morphological and anatomical data were collected, the phylogenetic position of *Trogloglanis* changed, being grouped with *Ameiurus* (Hubbs & Bailey, 1947) or *Ictalurus* (Taylor, 1969), placed sister to all ictalurids except *Ictalurus* (Lundberg, 1970; Lundberg, 1982), or placement uncertain (Lundberg, 1970). Unlike *Prietella* and *Trogloglanis*, morphological studies consistently agreed that *S. eurystomus* and *Pylodictis olivaris* formed a sister pair (Hubbs & Bailey, 1947; Taylor, 1969; Lundberg, 1982; Lundberg, 1992; Lundberg et al., 2017) due to several shared internal and external traits, such as a flattened head, flaring adipose fin, and a broadly-forked mesethmoid (Hubbs & Bailey, 1947; Suttkus, 1961; Taylor, 1969; Lundberg, 1970; Lundberg, 1982; Lundberg et al., 2017).

More recent studies have included molecular data for phylogenetic analyses of Ictaluridae (e.g., Hardman & Hardman, 2008); however, to date, only *P. phreatophila* and *P. lundbergi* have been included in molecular phylogenies (Wilcox et al., 2004; Egge & Simons, 2009; Arce H. et

al. 2016). Similar to morphological studies, molecular analyses disagree on the phylogenetic position of both *Prietella* species. Maximum Parsimony (MP) analyses of molecular sequence data support *Prietella* as monophyletic (Wilcox et al., 2004; Arce H. et al., 2016), whereas Bayesian Inference (BI) and Maximum Likelihood (ML) analyses place each species of *Prietella* sister to a surface-dwelling genus (Wilcox et al., 2004). Arce H. et al. (2016) combined fossil, morphological, and genetic data (one nuclear and four mitochondrial genes). This time-calibrated MP phylogeny included representatives of all extant and extinct ictalurids, except for three *Ictalurus* species (Arce H. et al., 2016). Genetic data were analyzed for the two *Prietella* species, but *Satan eurystomus* and *Trogloglanis pattersoni* were included in the phylogeny based only on morphological characters. In contrast to previous phylogenies, Arce H. et al. (2016) found that the four cave species comprised a monophyletic Troglobites clade, sister to all other ictalurids; this placement was further supported by Lundberg et al. (2017) with morphological characters. This unexpected result implied that these four species descended from a common ancestor, despite their allopatric distribution (*Satan* and *Trogloglanis* excepted). Arce H. et al. (2016) mention that the putative dispersal events require further investigation, given that hydrological connections are largely unknown between cave locations.

Due to the phylogenetic contradictions concerning troglobitic ictalurids in previous studies, we aimed to determine the evolutionary origins of these species. We elucidated the evolutionary history of Ictaluridae by creating a species-level molecular phylogeny using the largest molecular dataset of any study to date, as well as the first inclusion of genetic data for *Trogloglanis pattersoni*. We then time-calibrated the phylogeny using the earliest fossil occurrence data of ictalurid and siluriform outgroups to determine when cave colonization events may have occurred. Using our time-calibrated phylogeny, we tested the hypothesis that ictalurid

cave species have evolved in parallel from repeated invasions of subterranean habitats. We predicted that the troglobitic ictalurids are not monophyletic and are each sister to surface-dwelling taxa, as observed in other troglobitic fishes (Wilkens, 2001). Given the distance and geological barriers between their known locations, we also predicted that *P. phreatophila* is sister to *Ameiurus* and *P. lundbergi* is sister to *Ictalurus*, as observed in previous molecular-only phylogenies (Wilcox et al., 2004; Egge & Simons, 2009).

Materials and methods

Taxon sampling and gene selection

To construct our species-level phylogeny of Ictaluridae, we used muscle and fin tissue samples from museum-deposited and field-collected specimens. When possible, we included two voucher specimens per ingroup species from different localities. We obtained all nominal extant species except *Satan eurystomus*. *Satan eurystomus* is a rare species that has not been collected since 1984 and no useable tissue samples are available from formalin-fixed specimens (Wilcox et al., 2004; Lundberg et al., 2017). We selected 17 outgroup species from closely-related families within Siluriformes (infraclass Teleostei, class Actinopterygii) to root the tree, representing Austroglanididae, Bagridae, Clariidae, Claroteidae, Cranoglanididae, Mochokidae, Pangasiidae, and Sisoridae (Betancur-R et al., 2017; Schedel et al., 2022). Lastly, we included eight potentially undescribed ictalurid species in our phylogeny. We used at total of 118 specimens (Table 2-S1).

We selected nine protein-coding genes to construct our phylogeny, including two mitochondrial genes and seven nuclear genes. We also downloaded mitochondrial sequences from GenBank (Clark et al., 2016) composed of 12S ribosomal RNA, tRNA-Val, and 16S ribosomal RNA for as many available catfish species as possible. These genes were chosen

based on three criteria: (1) inclusion of a combination of quickly-evolving and slowly-evolving genes to provide phylogenetic resolution for both interspecific and intergeneric relationships (Lovejoy, 2000; Le et al., 2006), (2) single-copy genes to prevent biases associated with sequencing gene paralogs (Lovejoy & Collette, 2001; Li et al., 2007; Chen et al., 2008; Hughes et al., 2018), and (3) inclusion of previously published sequences from rare species when genetic tissue samples were unavailable. The two mitochondrial genes we selected for phylogenetic analyses were cytochrome c oxidase subunit 1 (*co1*) and cytochrome b (*cyt b*). The seven nuclear genes we selected for phylogenetic analyses were early growth response protein 1 (*egr1*), ectoderm-neural cortex protein 1 (*enc1*), glycosyltransferase (*glyt*), recombination activating gene 1 (*rag1*), recombination activating gene 2 (*rag2*), rhodopsin (*rh1*), and zinc finger protein of cerebellum 1 (*zic1*).

DNA sequencing and alignment

We extracted DNA from muscle and fin tissues stored in 95% ethanol at -20°C using a homemade kit for animal extractions following a protocol adapted from Ivanova et al. (2006). Each extraction was amplified for nine of the selected genes (as described above) using the polymerase chain reaction (PCR). We used previously published primers to amplify *co1* (Ward et al., 2009) and *cyt b* (Palumbi et al., 1991), and designed primers to amplify each nuclear gene. For *co1* and *cyt b*, we used the same primers for amplification and sequencing. For all nuclear genes, we designed internal primers for sequencing to avoid non-specific PCR products amplification (Table 2-S2).

To amplify *cyt b*, *enc1*, *rag2*, and *zic1*, we used the following PCR recipe for each reaction: 1X Dream buffer containing 2 mM $MgCl_2$, 0.2 mM of dNTPs, 0.25 μM of forward and reverse primers, 0.75 U of Dream *Taq*, ca. 20-30 ng of template DNA, and nuclease-free water to

adjust to the final reaction volume of 15 µL. We used a Mastercycler pro S (Eppendorf Canada) to amplify our PCR products with the following heat cycling conditions: initial heating to 95°C for 3 minutes, 35 cycles of denaturation (95°C for 30 seconds), primer annealing (55°C for 30 seconds), and extension (72°C for 1 minute and 30 seconds) phases, and a final extension phase at 72°C for 10 minutes. For *co1*, *egr1*, *glyt*, *rag1*, and *rh1*, we used the following PCR recipe: 1X Q5 buffer containing 2 mM $MgCl_2$, 0.2 mM of dNTPs, 0.5 µM of forward and reverse primers, 0.45 µL of dimethyl sulfoxide (DMSO), 0.3 U of Q5 polymerase, ca. 20-30 ng of template DNA, and nuclease-free water to adjust to the final reaction volume of 15 µL. Cycling conditions for amplification were as follows: initial heating to 98°C for 30 seconds, 34 cycles of denaturation (98°C for 10 seconds), primer annealing (56°C for 30 seconds), and extension (72°C for 30 seconds) phases, and a final extension phase at 72°C for 5 minutes.

PCR products were visualized using gel electrophoresis and products were subsequently diluted with a volume of nuclease-free water dependent on the strength of the band. Strong bands were diluted with 60 µL of water, medium bands were diluted with 30 µL of water, and weak bands were diluted with 15 µL of water. Diluted products were then used in sequencing reactions, each containing 0.9X ABI buffer, 0.5 µM of primer, 0.5 µL of BigDye containing dideoxynucleotides (ddNTPs), 1 µL of diluted PCR products, and nuclease-free water to adjust to the final reaction volume of 10 µL. Sequencing reactions were then run through the Mastercycler pro S using the following cycling conditions: initial heating to 95°C for 3 minutes, 25 cycles of denaturation (96°C for 30 seconds), primer annealing (50°C for 20 seconds), and extension (60°C for 4 minutes) phases. Sequencing reactions were then purified using an EDTA-NaOH-ethanol precipitation protocol provided by the manufacturer. DNA pellets were resuspended using HIDI formamide and sequenced using a 3500 xL Genetic Analyzer (ThermoFisher

Scientific). Each individual gene was aligned with the Clustal Omega plugin 1.2.2 (Sievers et al., 2011) in Geneious Prime 2022.0.2. Gene alignments were then concatenated using SequenceMatrix 1.8 (Vaidya et al., 2011).

Phylogenetic analyses

We constructed a species-level phylogeny of Ictaluridae using a ML analysis. We first partitioned the concatenated alignment by gene and codon position, resulting in 30 partitions. Using PartitionFinder2 2.1.1 (Lanfear et al., 2017) on the CIPRES Science Gateway (Miller et al., 2011), we selected the best substitution model for each partition with the Corrected Akaike Information Criterion (AICc). Unlinked substitution models that best fit each partition were selected from those available for IQ-TREE (Nguyen et al., 2015; Table 2-S3). Using the substitution models of best fit, we then performed a ML analysis to construct our phylogeny using the IQ-TREE web server (Trifinopoulos et al., 2016). The analysis was run for 100 likelihood searches and branch support was calculated using the ultrafast bootstrap (BS) approximation for 1000 replicates (Minh et al., 2013). Finally, we used FigTree 1.4.4 to visualize the output tree file (Rambaut, 2009).

Fossil-based divergence-time estimation of Ictaluridae

To construct a time-calibrated phylogeny of Ictaluridae, we performed a BI analysis using the CladeAge package (Matschiner et al., 2017) in BEAST2 2.6.3 (Bouckaert et al., 2019). First, we created the necessary XML file in BEAUti2 2.6.3 (Bouckaert et al., 2019) to time-calibrate our phylogeny using fossil-record information available for ingroup ictalurids and outgroup siluriforms. The concatenated gene matrix was partitioned by gene and codon position, resulting in 30 partitions. The substitution models that best fit each partition were determined with the bModelTest package (Bouckaert & Drummond, 2017) in BEAST2 using a reversible

jump Markov chain Monte Carlo (MCMC). For the clock models, we selected an uncorrelated lognormal relaxed molecular clock model (Drummond et al., 2006) for the mitochondrial genes and for the nuclear genes separately. We used a birth-death process model for the tree prior (Kendall, 1948), specifying teleost-specific net diversification rate parameters (λ-μ; 0.041-0.081), turnover rate parameters ($\mu\lambda^{-1}$; 0.0011-0.37), and fossil sampling rate parameters (ψ; 0.0066-0.01806) based on previous studies (Foote & Miller, 2007; Santini et al., 2009; Matschiner et al., 2017); our ML phylogeny was used as a starting tree prior for the analysis. CladeAge accounts for clade age estimation uncertainty by inferring the optimal shape of calibration densities of each clade, combining sampling rates, diversification rates, and first-occurrence fossil ages (Matschiner et al., 2017).

We included 17 first-occurrence catfish fossils to time-calibrate clades using their minimum and maximum age estimations. Ictalurid fossils from Arce H. et al. (2016) were used to calibrate ingroup clades and first-occurrence outgroup fossils were selected using Database of Vertebrates: Fossil Fishes, Amphibians, Reptiles, and Birds database (Böhme & Ilg, 2003), the Paleobiology Database (Paleobiology Database, 2018), and original species descriptions. We calibrated *Ameiurus* using the oldest known fossil species belonging to the genus, †*Ameiurus pectinatus* from the Late Eocene, 34-34.2 million years ago (mya) (Lundberg, 1975; Lundberg, 1992; Hardman & Hardman, 2008; Arce H. et al., 2016). This fossil lineage is considered a member of *Ameiurus* given its synapomorphies, including an anteroventral crest of the dentary, broad snout, and broad premaxillae (Lundberg, 1975). We calibrated *Ictalurus* using the oldest fossil species, †*Ictalurus rhaeas* from putatively Late Eocene deposits 30-37 mya of the Cypress Hills Formation (Cope, 1891; Lundberg, 1975; Hardman & Hardman, 2008; Arce H. et al., 2016). This species is classified as *Ictalurus* based on shared pectoral spine anatomy with other

Ictalurus species (Lundberg, 1975), although Divay & Murray (2015) could not confirm the presence of *Ictalurus* in Eocene deposits of the Cypress Hills Formation. Fossil *Ictalurus* also have been identified from the Brule Formation of South Dakota, which is similar in age, 30-32 mya (J.G. Lundberg pers. comm. 2022). Fossil records of all extant *Ameiurus* species (except *Ameiurus platycephalus*), *Ictalurus dugesii*, *Ictalurus furcatus*, *Ictalurus punctatus*, and *Pylodictis olivaris* were used to calibrate each respective species. These fossils were listed in Lundberg (1975, 1992) and used by Arce H. et al. (2016) to construct their phylogeny.

According to Murray & Holmes (2021), †*Eomacrones wilsoni*, from Late Paleocene deposits (56.0-59.2 mya) in Africa, represents the oldest species belonging to Bagridae based on cranial ornamentation, which we used to calibrate our bagrid outgroups: *Bagrus ubangensis* and *Hemibagrus wyckioides*. Older fossils (59.2-66 mya) from China have been assigned to Bagridae (e.g., Wang et al., 1981), but have not been critically evaluated. To calibrate our outgroup representatives of Clariidae, *Clarias batrachus* and *Channallabes apus*, we used the oldest record of Clariidae fossils found in Africa in the Lower Eocene (Gayet & Meunier, 2003; Jansen et al., 2006; Kappas et al., 2016). The Eocene fossil species †*Chrysichthys mahengeensis* was used to calibrate *Chrysichthys cranchii*. This is the oldest fossil species known of Claroteidae, and was assigned to *Chrysichthys* based on shared dorsal- and pectoral-spine morphology with extant congeners (Murray & Budney, 2003; Sullivan et al., 2008; Murray & Holmes, 2021). We calibrated our outgroup representatives of Mochokidae, *Chiloglanis occidentalis* and *Microsynodontis batesii*, using fossilized *Synodontis* remains dating from the Miocene (Priem, 1920; Pinton et al., 2011). The morphology of the supraoccipital collected from Egypt closely resembles those of living *Synodontis* species (Priem, 1920; Pinton et al., 2011). Lastly, we used †*Pangasius indicus* from the Eocene Sangkarewang Formation, 33.7–54.8 mya (*sensu* Fatimah

& Ward 2009, Zonneveld et al., 2012; Murray, 2019) to calibrate our four representatives of Pangasiidae: *Helicophagus waandersii*, *Pangasianodon hypophthalmus*, *Pangasius larnaudii*, and *Pseudolais pleurotaenia*. Specific fossil information, including age and references, are in Table 2-1.

To construct our time-calibrated phylogeny, we performed two MCMC analyses for 250 million generations. In both analyses, trees were sampled every 10,000 generations. We assessed the effective sample size (ESS) and convergence for both analyses using Tracer 1.7.1 (Rambaut et al., 2018). We discarded the first 10% of trees as burn-in and summarized the remaining trees using TreeAnnotator 2.6.3 (Bouckaert et al., 2019). Lastly, we visualized our time-calibrated phylogeny using FigTree 1.4.4.

Results

We constructed a ML phylogeny (Figure 2-2) using a concatenated DNA sequence alignment of 24,470 nucleotide base pairs. The family Ictaluridae was strongly supported as monophyletic with a 100 BS value. Within Ictaluridae, non-monotypic genera *Ameiurus*, *Ictalurus* and *Noturus* were also strongly supported as monophyletic (100 BS for *Ameiurus* and *Noturus*, 99 BS for *Ictalurus*). *Noturus* was sister to all other genera followed by *Pylodictis* as sister to a clade composed of *Ameiurus*, *Ictalurus*, *Prietella*, and *Trogloglanis* (98 BS). Within that clade (94 BS), we found two strongly supported subclades: (1) *Ameiurus* (*P. phreatophila* + *Trogloglanis pattersoni*) (100 BS) and (2) *Ictalurus* + *P. lundbergi* (95 BS). Within the first subclade, *P. phreatophila* was strongly supported as sister to *T. pattersoni* (100 BS); these hypogean species were sister to the epigean genus *Ameiurus* (100 BS). In the second clade, the hypogean *P. lundbergi* was sister to the epigean genus *Ictalurus* (95 BS). Thus, *Prietella* was polyphyletic with *P. phreatophila* and *P. lundbergi* descending from different common ancestors

shared with the surface-dwelling relatives *Ameiurus* and *Ictalurus*, respectively. Furthermore, the polyphyletic status of *Prietella* indicated that troglobitic ictalurids do not form a monophyletic clade.

Both independent MCMC runs of our fossil-calibrated phylogeny (Figure 2-3) achieved convergence with strong ESS likelihood scores >200. The topology of our fossil-calibrated phylogeny was consistent with our ML phylogeny, placing *Noturus* as sister to all other genera (1.0 posterior probability (PP)), followed by *Pylodictis* as sister to a clade composed of *Ameiurus*, *Ictalurus*, *Prietella*, and *Trogloglanis* (1.0 PP). The placement of the three cave species was also consistent with our ML phylogeny: (1) *P. phreatophila* formed a sister pair with *T. pattersoni* (1.0 PP), which was sister to *Ameiurus* (1.0 PP), and (2) *P. lundbergi* was sister to *Ictalurus* (0.99 PP).

With respect to our fossil-calibration analysis, we estimated the origin of crown group Ictaluridae to ~60 mya, with a 95% confidence interval (CI) of 47-74 mya. Thus, ictalurids originated sometime between the Late Cretaceous and the Eocene. Within Ictaluridae, the ancestor of *Noturus* began to diversify ~32 mya (24-39 mya 95% CI). Between the Paleocene and the Eocene, *Pylodictis* diverged from the ancestor of *Ameiurus* + *Ictalurus* + *Prietella* + *Trogloglanis* ~54 mya (43-65 mya 95% CI). The ancestor of these remaining genera began to diversify shortly afterwards, ~52 mya (42-62 mya 95% CI). During the Eocene ~40 mya (34-48 mya 95% CI), the common ancestor of *P. phreatophila* and *T. pattersoni* diverged from the ancestor of *Ameiurus*; *P. phreatophila* split from *T. pattersoni* ~28 mya (19-37 mya 95% CI). The ancestor of *Ameiurus* began to diversify ~23 mya (17-30 mya 95% CI). *Prietella lundbergi* split from the ancestor of *Ictalurus* ~43 mya (33-54 mya 95% CI), between the Eocene and Oligocene. Lastly, the ancestor of *Ictalurus* began to diversify ~28 mya (23-36 mya 95% CI).

Discussion

Evolutionary relationships of cave ictalurids

We constructed both a ML phylogeny and a fossil-calibrated phylogeny of Ictaluridae using the largest molecular dataset of any study to date, as well as the first inclusion of molecular data from *Trogloglanis pattersoni*. The topologies of our two phylogenies were consistent, and the positions of each cave species and of the surface-dwelling genera were strongly supported. We found that the hypogean taxa *Prietella lundbergi*, *P. phreatophila*, and *T. pattersoni* did not form a monophyletic clade. Moreover, *P. phreatophila* and *T. pattersoni* were recovered as sister taxa, and this relationship was observed in each gene tree with the exception of that of *co1*. Thus, these two species may have diverged as a result of a subterranean dispersal event, which we discuss below. Branches were long in the ML phylogeny. This is likely due to the more numerous point mutations observed in the sequenced genes than in those from surface-dwelling relatives. Alternatively, missing data for these species could explain these long branches; however, other surface-dwelling relatives represented by 2-3 genes did not display long branches. The polyphyletic nature of the Troglobites clade proposed by Arce H. et al. (2016) supports our hypothesis that the troglobitic ictalurids have evolved in parallel, resulting from a minimum of two cave colonization events by surface-dwelling ancestors. Furthermore, the placement of *P. lundbergi* as sister to *Ictalurus*, and *P. phreatophila* + *T. pattersoni* as sister to *Ameiurus*, indicates that *Prietella* is a polyphyletic genus. This supports our prediction: *Prietella* should be restricted to *P. phreatophila* (type species) and *P. lundbergi* requires generic reclassification.

The phylogenetic placement of the three cave species included in our analyses was congruent with previous molecular phylogenies of Ictaluridae. Egge & Simons (2009) observed a

sister relationship between *Ameiurus melas* and *P. phreatophila* in their MP and BI molecular-only and BI molecular + morphological phylogenies of *Noturus*. Our results are related to those of Egge & Simons (2009) because we used the same *cyt b* and *rag2* sequences downloaded from GenBank. Our addition of *co1* did not affect the previously observed relationship between *Ameiurus* and *Prietella phreatophila*. Egge & Simons (2009) alternatively found a sister-group relationship between *P. phreatophila* and *Noturus* in their MP phylogeny combining morphological and molecular data. Wilcox et al. (2004) observed sister relationships between *P. lundbergi* + *Ictalurus* and *P. phreatophila* + *Ameiurus* in their BI and ML analyses, consistent with our results, which again was expected because we used the same mitochondrial genes for *P. lundbergi* and *P. phreatophila* downloaded from GenBank. We included additional genes for *P. phreatophila* in our analysis, and these genes in combination supported the same relationship. Arce H. et al. (2016), however, found the four troglobitic species to be monophyletic in their MP phylogeny combining molecular and morphological data. These results may be due to a combination of using convergent morphological characters as well as long-branch attraction of the highly divergent troglobites, as suggested by Wilcox et al. (2004). Long-branch attraction occurs when two distantly-related lineages are erroneously grouped together based on convergent similarities, such as identical amino acids acquired independently due to finite combinations of nucleotides (Bergsten, 2005; Susko & Roger, 2021). The more differences that accrue in long-branch lineages, the higher the likelihood of sharing similarities with distantly related lineages (Bergsten, 2005). MP phylogenetic analyses are the most susceptible to long-branch attraction (Wilcox et al., 2004; Bergsten, 2005) and they were the only phylogenetic analyses to recover the troglobitic species as monophyletic (Wilcox et al., 2004; Arce H. et al., 2016).

Some early morphological studies also support the placement of the cave species included in our study. Hubbs & Bailey (1947) suggested that *T. pattersoni* most likely diverged from *Ameiurus*, which was its closest relative at the time given that *P. phreatophila* had not yet been described. Also, Suttkus (1961) proposed *P. phreatophila* to be closely related to *Ictalurus*, which at the time also included *Ameiurus* as a subgenus. Furthermore, caudal fin morphology supports our placements of both *Prietella* species. The emarginate caudal fin observed in *P. lundbergi* more closely resembles *Ictalurus*, whereas the more truncated and rounded caudal fin observed in *P. phreatophila* more closely resembles *Ameiurus* (Walsh & Gilbert, 1995; Wilcox et al., 2004).

Topology of Ictaluridae

Of the many phylogenies of Ictaluridae, we are the first to recover *Noturus* as the sister clade to all other ictalurids. Previous studies have placed *Ameiurus* (Hardman & Hardman, 2008), *Ictalurus* (Taylor, 1969; Lundberg, 1992; Egge & Simons, 2009), and the Troglobites clade (Arce H. et al., 2016) as sister to all remaining genera. Prior to Arce H. et al. (2016), taxonomic coverage in phylogenetic studies was incomplete; the cave species as well as most Mexican *Ictalurus* species were often missing. With respect to Arce H. et al. (2016), the inclusion of potentially convergent morphological characters available for *Prietella*, *Satan*, and *Trogloglanis*, as well as long-branch attraction may have contributed to the unique placement of the troglobitic ictalurid genera within the family. We believe our novel findings more accurately reflect relationships among extant Ictaluridae given the near-complete taxon sampling and the use of the largest molecular-only dataset of any study to date. This applies to the discrepancies between our phylogeny and previous work for each of the genera discussed below.

Topology of Noturus

Within *Noturus*, the most species-rich ictalurid genus, Taylor (1969) grouped species into three subgenera (Table 2-2) based on morphological similarities: monotypic *Noturus* (*N. flavus*), *Rabida* (containing the *elegans*, *furiosus*, *hildebrandi*, and *miurus* species groups), and *Schilbeodes* (containing the *funebris* species group). *Noturus* phylogenies by Hardman (2004), Near & Hardman (2006), Hardman & Hardman (2008), and Egge & Simons (2009) supported *Rabida* as monophyletic, but not *Schilbeodes*. Egge & Simons (2009) considered Taylor's subgenera to be untenable and proposed seven phylogenetic clades unassigned to Linnean rank: *albater*, *elegans*, *funebris*, *furiosus*, *gyrinus*, *hildebrandi*, and *rabida*, the last one comprising the *albater*, *elegans*, *furiosus*, and *hildebrandi* subclades (Table 2-2).

Our phylogenetic analyses similarly supported the monophyly of Taylor's (1969) subgenus *Rabida*, but not his *Schilbeodes*. The subgenus *Schilbeodes* is therefore restricted here to four species: *N. gyrinus* (type species), *N. lachneri*, *N. leptacanthus* and *N. nocturnus*. With respect to the groups and subclades proposed by Taylor (1969) and Egge & Simons (2009), respectively, our results were largely consistent. For example, our analysis supported Egge & Simons' *furiosus* subclade which consolidated the *furious* and *miurus* groups of Taylor, as well as their *elegans* subclade which combined Taylor's *elegans* and *hildebrandi* groups.

Discrepancies between our tree and previous ones include the placements of *N. leptacanthus* and *N. phaeus*. Our analyses did not support a sister group relationship between *N. leptacanthus* and *N. funebris*, the only two members of the *funebris* clade proposed by Egge & Simons (2009) and likewise supported by Hardman & Hardman (2008). Instead, our analyses placed *N. leptacanthus* sister to a clade composed of *N. gyrinus*, *N. lachneri*, and *N. nocturnus* with all four species comprising the subgenus *Schilbeodes* as restricted herein. Regarding *N. phaeus*, our analyses placed this species in a clade with *N. funebris* and two potentially

undescribed species. Taylor (1969) likewise proposed a close relationship between *N. funebris* and *N. phaeus*, the only two members of his *funebris* group of *Schilbeodes*. Our results support his group, but not its placement in subgenus *Schilbeodes* as restricted here. The placement of *N. phaeus* varied among phylogenetic analyses by Egge & Simons (2009). Their MP and BI analyses of morphological data supported a sister group relationship between *N. phaeus* and *N. funebris* (Egge & Simons, 2009), consistent with Taylor (1969) and our study. Their MP analyses of molecular data and combined molecular and morphological data placed *N. phaeus* sister to *N. funebris* + *N. leptacanthus* (Egge & Simons, 2009). Finally, their BI analyses of molecular data and combined data upheld *N. funebris* + *N. leptacanthus*, but did not support its close relationship with *N. phaeus* (Egge & Simons, 2009).

Among the 29 valid species of *Noturus*, only five remain here unassignable to nominal subgenera: *N. exilis*, *N. funebris*, *N. gilberti*, *N. insignis*, and *N. phaeus*. Taylor (1969) placed all these species in *Schilbeodes*; however, our results restrict this subgenus to *N. gyrinus* (type species), *N. lachneri*, *N. leptacanthus*, and *N. nocturnus.* As mentioned above, there is strong morphological and molecular support for a sister group relationship between *N. funebris* and *N. phaeus* (Taylor, 1969; Egge & Simons, 2009). Our molecular analysis places *N. funebris*, *N. phaeus*, and two potentially undescribed species in a clade (Clade 2) sister to one containing all other species of *Noturus* (Clade 1). According to our results, the first species to diverge in Clade 1 is *N. exilis*, a wide-ranging monophyletic species with geographically isolated populations in the Eastern and Interior American Highlands and the previously glaciated Central Lowlands (Blanton et al., 2013).

The remaining members of Clade 1 are divided among two subclades, one corresponding to the subgenus *Rabida* (Clade 1.1.1) and the other (Clade 1.1.2) comprising the subgenus

Schilbeodes (four species), *N. flavus* (monotypic subgenus *Noturus*), *N. gilberti*, and *N. insignis* (unassigned here). Although our analyses strongly support the monophyly of subgenus *Schilbeodes sensu stricto* in our fossil-calibrated phylogeny (1.0 PP), relationships involving *N. flavus* and *N. gilberti* + *N. insignis* remain poorly resolved. Similar to our results, previous studies provided weak support for a clade composed of *N. flavus*, *N. gilberti* and *N. insignis* (Hardman & Hardman, 2008; Egge & Simons, 2009). Our study independently corroborates these results because we used novel genetic sequence data for these species. The potential for a close relationship between *N. flavus* and *N. insignis* is biogeographically intriguing. The two species are mostly allopatric, with *N. flavus* widely distributed throughout the Mississippi and Great Lakes-St. Lawrence basins and *N. insignis* common to Atlantic slope drainages from New York to Georgia (Taylor, 1969). *Noturus gilberti*, on the other hand, is restricted to the upper Roanoke drainage in Virginia and North Carolina where it may co-occur with *N. insignis* (Jenkins & Burkhead, 1994), its sister species.

Topology of Ictalurus

In early molecular phylogenies, *Ictalurus* was limited to species distributed in the USA and Canada, including *I. furcatus*, *I. lupus*, and *I. punctatus* (Hardman, 2004; Wilcox et al., 2004; Hardman & Hardman, 2008). Arce H. et al. (2016) were the first to consider Mexican species in a phylogenic analysis that included genetic sequences for *I. balsanus*, *I. meridionalis*, and *I. pricei*. Their results provide evidence for a deep divergence within extant *Ictalurus* dividing *I. furcatus* + *I. meridionalis* from all other *Ictalurus* except *I. balsanus*. Rodiles-Hernández et al. (2010) previously supported the same relationship based on morphology. Our results support the same split except with *I. balsanus* sister to *I. furcatus* + *I. meridionalis* based on new genetic sequence data absent from Arce H. et al. (2016). Among the remaining *Ictalurus*, *I. punctatus*

was sister to a clade composed of *I. australis* + *I. mexicanus*, *I. lupus*, *I. dugesii* + *I. ochoterenai*, *I. pricei*, and a potentially new species from the Nazas River, Mexico.

Pérez-Rodríguez et al. (2022) constructed a molecular phylogeny of *Ictalurus*, the first to include specimens of all nominal species within the genus. Similar to our study, they found a deep divergence between the *I. balsanus*, *I. furcatus*, and *I. meridionalis* clade (the *furcatus* group) and all remaining extant *Ictalurus* species (the *punctatus* group). Pérez-Rodríguez et al. (2022) found very low genetic divergence between three pairs of species: *I. australis* + *I. mexicanus*, *I. dugesii* + *I. ochoterenai* and *I. furcatus* + *I. meridionalis*. Lundberg (1992) considered *I. mexicanus* distinct, but noted that *Ictalurus australis*, *I. ochoterenai*, and *I. meridionalis* may be conspecific with *I. punctatus*, *I. dugesii*, and *I. furcatus*, respectively. Rodiles-Hernández et al. (2010) alternatively supported the taxonomic distinctiveness of *I. furcatus* and *I. meridionalis* based on 12S/16S mitochondrial genes and morphological traits, such as pectoral spine ornamentation, anal-fin ray and vertebrae counts, and differences in the supraoccipital process. Our study corroborates the results of Pérez-Rodríguez et al. (2022), showing low genetic divergence between the species within each pair; however, we used the same sequence data for *I. australis* and *I. ochoterenai* downloaded from GenBank.

Pérez-Rodríguez et al. (2022) also found both *I. pricei* and *I. lupus* formed species complexes; each complex comprised distinct lineages that may represent potentially undescribed species. Three of these lineages were included within our phylogeny: *Ictalurus* sp. NAZA from the Nazas River, *Ictalurus* cf. *pricei* from the Mezquital River, and *I. lupus* from the Conchos River. Further study, including morphological analyses, are necessary to determine whether these lineages require formal species descriptions. Finally, Pérez-Rodríguez et al. (2022) estimated

Ictalurus began to diversify in the Oligocene, which overlaps with our somewhat older estimate between the Oligocene and Eocene.

Topology of Ameiurus

With respect to *Ameiurus*, our ML and time-calibrated phylogenies both placed *Ameiurus natalis* as sister to all other extant species within the genus based on novel genetic sequence data for all *Ameiurus* species. This result is consistent with the findings of Hardman & Page (2003), Hardman & Hardman (2008), and Arce H. et al. (2016). Our ML and time-calibrated phylogenies supported *A. catus* as sister to the remaining species of *Ameiurus*. This is consistent with Arce H. et al. (2016), but differs from Hardman & Page (2003) and Hardman & Hardman (2008) wherein *A. catus* is sister to *A. platycephalus.* Our study and previous ones based on morphology (Lundberg, 1992), molecules (Hardman & Hardman, 2008) or both (Arce H. et al., 2016) all support a close relationship between *A. melas* and *A. nebulosus*, but only the molecular phylogenies place these species in a crown clade with *A. brunneus* and *A. serracanthus*. Within this crown clade, *A. brunneus* was the first species to diverge in our analyses vs. *A. serracanthus* in Hardman & Hardman (2008). That said, our placement of *A. serracanthus* as sister to *A. melas* + *A. nebulosus* was poorly supported (65 BS, <0.5 PP). Alternatively, Arce H. et al. (2016) supported a clade composed of *A. serracanthus*, *A. brunneus*, and the extinct fossil species †*A. peregrinus.*

Surprisingly, we identified a potentially new species of *Ameiurus* from two Atlantic slope drainages, the Cape Fear and Santee of North and South Carolina, respectively. This species-level lineage was sister to a clade of three individuals of *A. platycephalus* from the Haw River (Cape Fear Basin), a Broad River tributary (Santee Basin), and Stevens Creek (Savannah Basin), respectively. *Ameiurus platycephalus* is native to Atlantic slope drainages and its range broadly

overlaps with that of *A. brunneus*, a similar looking species (Yerger & Relyea, 1968; Tracy et al., 2020). In our analysis, *A. brunneus* was represented by two individuals from separate tributaries to the Chattahoochee River (Apalachicola Basin), outside of the native range of *A. platycephalus*. Our results suggest that it is necessary to revisit relationships among the Atlantic and Gulf slope *Ameiurus* formerly known as "flat-headed" bullheads (Yerger & Relyea, 1968), namely *A. brunneus*, *A. platycephalus* and *A. serracanthus*.

Divergence-time estimations of Ictaluridae

We estimated that Ictaluridae originated sometime between the Late Cretaceous and Eocene, ~47-74 mya. This proposed origin time is consistent with the findings of Hardman & Hardman (2008), who proposed that Ictaluridae began to diversify ~59-72 mya in the Late Cretaceous to Paleocene. Kappas et al. (2016) similarly suggested that Ictaluridae originated ~63-72.5 mya. Larger phylogenies of Siluriformes have estimated younger origin times, albeit with the inclusion of only 1-3 representatives of Ictaluridae. For example, Lundberg et al. (2007) estimated that Ictaluridae originated ~37.9-42.7 mya. In their phylogeny of bony fishes (Osteichthyes), Betancur-R et al. (2017) estimated that Ictaluridae began to diverge ~30-35 mya. Arce H. et al. (2016) also proposed a relatively young origin for Ictaluridae during the Eocene, ~33.9-56 mya. We used the same ictalurid fossils as Arce H. et al. (2016) to calibrate our phylogeny with the notable exception of the extinct genus †*Astephus*, the oldest fossil to be considered an ictalurid (Buchheim & Surdam, 1977; Grande & Lundberg, 1988; Lundberg, 1992). In the phylogeny of Arce H. et al. (2016), †*Astephus* was nested within the outgroup lineages (vs. the sister lineage of extant ictalurids), prompting them to elevate this group from a subfamily of Ictaluridae to the rank family †Astephidae. Therefore, we did not include †*Astephus* in our analyses, which may partially account for our older estimation of Ictaluridae.

With respect to the troglobitic ictalurids, Arce H. et al. (2016) proposed that this monophyletic clade diverged from the surface-dwelling confamilials ~47 mya during the Eocene and began to diversify ~9 mya during the Miocene. Our time estimates for the divergence of cave species from surface-dwelling relatives overlapped with those of Arce H. et al. (2016); however, our results support two independent origins of cave-dwelling species within Ictaluridae. We propose that *P. phreatophila* + *T. pattersoni* diverged from *Ameiurus* during the Eocene (~34-48 mya) and that *P. lundbergi* diverged from *Ictalurus* during the Eocene to Oligocene (~33-54 mya).

Evolutionary history of troglobitic ictalurids

The hypothesis that cave-dwelling catfish species evolved in parallel within Ictaluridae is intuitive given the allopatric contemporary distribution of their insular habitats (Wilcox et al., 2004; Burr et al., 2020). The significant geological barriers separating these species, especially between the two *Prietella* species, suggests that subterranean radiation of a common troglobitic ancestor is unlikely (Hendrickson et al., 2001; Wilcox et al., 2004). That said, our evidence supported a sister relationship between *P. phreatophila* and *T. pattersoni*, which implies that subterranean dispersal events and subsequent speciation are possible. It is unsurprising that repeated cave-colonization events likely occurred within Ictaluridae. Many epigean ictalurids are preadapted to subterranean life (e.g., poor eyesight, nocturnal habits) and typically rely on other senses, such as touch, taste, and electroreception, to navigate and acquire food (Eigenmann, 1919; Langecker & Longley, 1993; Burr et al., 2020). Furthermore, some surface-dwelling species (*Ameiurus nebulosus*, *A. natalis*, and *I. punctatus*) partially live within caves and concentrate around cave entrances (Hale & Streever, 1994; Poly, 2001). The existence of these troglophyllic populations and the sister relationships of cave species with surface-dwelling

relatives further supports our hypothesis that ictalurids colonized subterranean habitats at least twice during their evolutionary history.

Our results indicate that *Prietella lundbergi* diverged from the common ancestor of *Ictalurus* sometime during the Paleocene-Eocene. The long distance and extensive geological barriers between *P. lundbergi* and *P. phreatophila* suggest that a subterranean divergence between these two species is unlikely (Hendrickson et al., 2001; Wilcox et al., 2004), whereas divergence from a surface-dwelling ancestor potentially resembling extant *Ictalurus* is more probable. This is further supported by the occurrence of epigean species of *Ictalurus* near *P. lundbergi* (Wilcox et al., 2004; Burr et al., 2020) and documented instances of *Ictalurus punctatus* living within caves (Hale & Streever, 1994). In contrast, the native distribution of *Ameiurus* (the closest relative of *P. phreatophila* + *T. pattersoni*) does not overlap with *P. lundbergi* (Wilcox et al., 2004; Burr et al., 2020). It is possible that during the Paleocene and/or Eocene, surface waters were connected with the subterranean springs in the Tamesí River drainage where *P. lundbergi* currently occurs (Walsh & Gilbert, 1995; Hendrickson et al., 2001). This may have allowed for the dispersal and subsequent selection of individuals better adapted for subterranean life. Magmatic activity as well as orogenesis in Mexico in the Late Cenozoic have been linked to the fragmentation of freshwater habitats and vicariant speciation (González-Rodríguez et al., 2013; Fitz-Díaz et al., 2018). Such activity may have disrupted connectivity between the subterranean springs and surface waters, further reinforcing the ancient reproductive isolation of the subterranean population. Alternatively, it is possible that parapatric speciation occurred as a result of *in situ* ecological specialization followed by reproductive isolation of the ancestral *P. lundbergi* population rather than vicariance from surface populations (Plath &

Tobler, 2010). Whichever the case, *P. lundbergi* appears to have been isolated from the ancestral stock of *Ictalurus* for at least 34 million years.

Our phylogeny suggests that the common ancestor of *Prietella phreatophila* + *Trogloglanis pattersoni* diverged from ancestral *Ameiurus* during the Eocene. A surface-dwelling ancestor similar to *Ameiurus* may have colonized subterranean waters somewhere near either the current distribution of *P. phreatophila* in northern Coahuila (Walsh & Gilbert, 1995; Hendrickson et al., 2001) or the Edwards Aquifer in Texas containing *T. pattersoni* (Langecker & Longley, 1993; Walsh & Gilbert, 1995). Similarly with *P. lundbergi* and *Ictalurus*, *Ameiurus* species currently occur in surface waters near both *P. phreatophila* and *T. pattersoni* (Wilcox et al., 2004; Burr et al., 2020), whereas contemporary *P. lundbergi* is geographically distant from the other cave species. In addition, populations of *A. natalis* and *A. nebulosus* have been documented living within caves (Hale & Streever, 1994; Poly, 2001). These occurrences, as well as our phylogenetic results, support the hypothesis that an *Ameiurus*-like ancestor invaded subterranean waters and subsequently diverged into *P. phreatophila* and *T. pattersoni*.

Prietella phreatophila split from *T. pattersoni* sometime between the Eocene and Miocene. Although the extent of connectivity is currently unknown between locations where *P. phreatophila* and *T. pattersoni* occur (Sanchez et al., 2016; Sanchez et al., 2018b), their shared common ancestor suggests that speciation may have resulted from a subterranean dispersal event between aquifers. The ancestral species may have travelled through the Knippa Gap, a hydrological restriction point east of the San Antonio Pool in Texas where *T. pattersoni* and *S. eurystomus* occur (Adkins, 2013; Green et al., 2019). Hydrological connectivity through the Knippa Gap is variable, depending on groundwater levels (Green et al., 2019). This transient barrier and others may have been sufficient to restrict frequent movement between the ancestral

Mexican and American populations, facilitating speciation. Additional evidence that supports the connectivity of these aquifers is the occurrence of *P. phreatophila* populations in northern Coahuila and the Amistad National Recreation Area, Texas (Walsh & Gilbert, 1995; Hendrickson et al., 2001; Hendrickson et al., 2017; Krejca & Reddell, 2019). The aquifer in northern Coahuila is separated from the Amistad Recreational Area by the Rio Grande, yet *P. phreatophila* is found both north and south of the river (Krejca & Reddell, 2019). The distribution of *P. phreatophila* and our results imply that the Edwards-Trinity Plateau and the aquifer in northern Coahuila were likely hydrologically connected during the Eocene-Miocene (Krejca & Reddell, 2019). Other troglobitic animals have demonstrated similar distribution patterns of closely related populations. Three isopod species (*Cirolanides texensis*, *Lirceolus cocytus*, and *Mexistenasellus coahuila*), as well as a species of amphipod (*Paraholsingerius smaragdinus*) occur both north and south of the Rio Grande in Mexican and American aquifers (Krejca, 2005; Krejca & Reddell, 2019). These populations are genetically similar to one another, which further supports the existence of hydrological connections between aquifers in Texas and Coahuila (Krejca, 2005; Krejca & Reddell, 2019).

Satan eurystomus

As previously indicated, we were unable to include *S. eurystomus* in our molecular phylogeny due to tissue samples being unavailable for sequencing. Therefore, we were unable to determine whether *S. eurystomus* is most closely related to *T. pattersoni* with which it co-occurs, or with an extant surface-dwelling relative. *Pylodictis olivaris* may be the closest living relative of *S. eurystomus* given the notable morphological traits both species share (Lundberg et al., 2017). Unlike for *Prietella* and *Trogloglanis*, early morphological studies agreed upon a sister relationship between *S. eurystomus* and *P. olivaris* (Hubbs & Bailey, 1947; Suttkus, 1961;

Taylor, 1969; Lundberg, 1970; Lundberg, 1982). Hubbs & Bailey (1947) mentioned that *P. olivaris* may be preadapted for subterranean life, being a light-averse species that commonly hides under rocks and logs. Similar to other ictalurid species, *P. olivaris* relies more on its senses of touch and taste to navigate and obtain food than its eyesight (Hubbs & Bailey, 1947; Burr et al., 2020). If *S. eurystomus* and *P. olivaris* are sister species, this would indicate that ictalurids have independently colonized underground habitats three times, evolving in parallel. Until tissue samples become available for *S. eurystomus*, however, this hypothesis is impossible to test with molecular data.

Conclusion

Our main goal was to investigate the phylogenetic relationships and evolutionary origins of Ictaluridae, with particular interest in the troglobitic species. We created a time-calibrated phylogeny of the family using first-occurrence fossil data and the largest molecular dataset representing all but two described extant species. We tested the hypothesis that troglobitic ictalurids evolved in parallel as a result of independent colonization events of subterranean habitats. We found that *P. lundbergi*, *P. phreatophila*, and *T. pattersoni* do not form a monophyletic group. This indicates that troglobitic ictalurids evolved at least twice following ancient cave colonization events. *Prietella phreatophila* and *Trogloglanis pattersoni* formed a sister pair, however, which suggests that these species diverged after a subterranean dispersal event between the Edwards Aquifer and the aquifer in northern Coahuila. Lastly, we found *P. lundbergi* was most closely related to *Ictalurus*, whereas *P. phreatophila* + *T. pattersoni* was most closely related to *Ameiurus*. Therefore, *P. lundbergi* should be reclassified as a new monotypic genus within Ictaluridae. With respect to epigean ictalurids, we found evidence for a potentially new *Ameiurus* species closely related to *A. platycephalus*. Within *Ictalurus*, three

species pairs (*I. dugesii* + *I. ochoterenai*, *I. australis* + *I. mexicanus*, and *I. meridionalis* + *I. furcatus*) displayed little genetic differentiation, which warrants further investigation. Finally, we proposed minor revisions to intrageneric classifications within *Noturus*.

Tables

Table 2-1 List of first-occurrence fossils used to time-calibrate Ictaluridae clades and siluriform outgroups for a divergence-time analysis using BEAST2 2.6.3. Extinct species are indicated with "†".

Fossil Species	Age (mya) [1]	Clade/Species Calibrated	Reference(s)
Ameiurus brunneus	1.0-1.5	*Ameiurus brunneus*	Lundberg, 1975, 1992
Ameiurus catus	0.0-0.11	*Ameiurus catus*	Lundberg, 1975, 1992
Ameiurus melas	0.5-2.5	*Ameiurus melas*	Lundberg, 1975, 1992
Ameiurus natalis	0.0-1.5	*Ameiurus natalis*	Lundberg, 1975, 1992
Ameiurus nebulosus	0.0-1.5	*Ameiurus nebulosus*	Lundberg, 1975, 1992
†***Ameiurus pectinatus***	34.0-34.2	*Ameiurus*	Lundberg, 1975, 1992; Evanoff et al., 2001
Ameiurus serracanthus	1.0-1.5	*Ameiurus serracanthus*	Lundberg, 1975, 1992
Ictalurus dugesii	1.0-1.5	*Ictalurus dugesii*	Lundberg, 1975, 1992
Ictalurus furcatus	1.0-1.5	*Ictalurus furcatus*	Lundberg, 1975, 1992
Ictalurus punctatus	15.9-18.9	*Ictalurus punctatus*	Tedford et al., 1987; Lundberg, 1975, 1992
†***Ictalurus rhaeas***	30.0-37.0	*Ictalurus*	Cope, 1891; Lundberg, 1975
Pylodictis olivaris	15.9-18.9	*Pylodictis olivaris*	Tedford et al., 1987; Lundberg, 1975, 1992
Clariidae sp.	34.0-56.0	Clariidae	Gayet & Meunier, 2003
†***Chrysichthys mahengeensis***	45.66-46.0	Claroteidae	Harrison et al., 2001; Murray & Budney, 2003
†***Eomacrones wilsoni***	56.0-59.2	Bagridae	Murray & Holmes, 2022
†***Pangasius indicus***	33.7-54.8	Pangasiidae	Fatimah & Ward 2009; Zonneveld et al., 2012; Murray et al., 2019
Synodontis sp.	~18	Mochokidae	Priem, 1920; Pinton et al., 2011

[1]mya = million years ago

Table 2-2 Comparison of *Noturus* subgenus and species group classifications proposed by Taylor (1969), Egge & Simons (2009), and the current study.

	Current Study		**Taylor 1969**		**Egge & Simons 2009**
Nominal Species (* denotes type species of respective subgenus)	Molecular Clade	Subgenus (Group)	Subgenera	Group	Clades (Subclades)
Noturus albater	Clade 1.1.1	*Rabida* (*albater*)	*Rabida*	—	*rabida* (*albater*)
Noturus maydeni	Clade 1.1.1	*Rabida* (*albater*)	*Rabida* [as *N. albater*]	—	*rabida* (*albater*)
Noturus eleutherus	Clade 1.1.1	*Rabida* (*furiosus*)	*Rabida*	—	*rabida* (*furiosus*)
Noturus flavater	Clade 1.1.1	*Rabida* (*furiosus*)	*Rabida*	*miurus*	*rabida* (*furiosus*)
*Noturus furiosus**	Clade 1.1.1	*Rabida* (*furiosus*)	*Rabida*	*furiosus*	*rabida* (*furiosus*)
Noturus gladiator	Clade 1.1.1	*Rabida* (*furiosus*)	*Rabida* [as *N. stigmosus*]	*furiosus* [as *N. stigmosus*]	*rabida* (*furiosus*)
Noturus munitus	Clade 1.1.1	*Rabida* (*furiosus*)	*Rabida*	*furiosus*	*rabida* (*furiosus*)
Noturus placidus	Clade 1.1.1	*Rabida* (*furiosus*)	*Rabida*	*furiosus*	*rabida* (*furiosus*)
Noturus stigmosus	Clade 1.1.1	*Rabida* (*furiosus*)	*Rabida*	*furiosus*	*rabida* (*furiosus*)
Noturus flavipinnis	Clade 1.1.1	*Rabida* (*furiosus*)	*Rabida*	*miurus*	*rabida* (*furiosus*)
Noturus miurus	Clade 1.1.1	*Rabida* (*miurus*)	*Rabida*	*miurus*	*rabida* (*furiosus*)
Noturus taylori	Clade 1.1.1	*Rabida* (*miurus*)	—	—	*rabida*
Noturus baileyi	Clade 1.1.1	*Rabida* (*elegans*)	*Rabida*	*hildebrandi*	*rabida* (*elegans*)
Noturus crypticus	Clade 1.1.1	*Rabida* (*elegans*)	*Rabida* [as *N. elegans*]	*elegans* [as *N. elegans*]	*rabida* (*elegans*)
Noturus elegans	Clade 1.1.1	*Rabida* (*elegans*)	*Rabida*	*elegans*	*rabida* (*elegans*)
Noturus fasciatus	Clade 1.1.1	*Rabida* (*elegans*)	*Rabida* [as *N. elegans*]	*elegans* [as *N. elegans*]	*rabida* (*elegans*)
Noturus hildebrandi	Clade 1.1.1	*Rabida* (*elegans*)	*Rabida*	*hildebrandi*	*rabida* (*elegans*)
Noturus stanauli	Clade 1.1.1	*Rabida* (*elegans*)	—	—	*rabida* (*elegans*)
Noturus trautmani	—	*Rabida* (*elegans*)	*Rabida*	*elegans*	*rabida* (*elegans*)
*Noturus gyrinus**	Clade 1.1.2	*Schilbeodes*	*Schilbeodes*	—	*gyrinus*

Noturus lachneri	Clade 1.1.2	*Schilbeodes*	*Schilbeodes*	—	*gyrinus*
Noturus leptacanthus	Clade 1.1.2	*Schilbeodes*	*Schilbeodes*	—	*funebris*
Noturus nocturnus	Clade 1.1.2	*Schilbeodes*	*Schilbeodes*	—	—
*Noturus flavus**	Clade 1.1.2	*Noturus*	*Noturus*	—	—
Noturus gilberti	Clade 1.1.2	—	*Schilbeodes*	—	—
Noturus insignis	Clade 1.1.2	—	*Schilbeodes*	—	—
Noturus exilis	Clade 1.2	—	*Schilbeodes*	—	—
Noturus funebris	Clade 2	— (*funebris*)	*Schilbeodes*	*funebris*	*funebris*
Noturus phaeus	Clade 2	— (*funebris*)	*Schilbeodes*	*funebris*	—

Figures

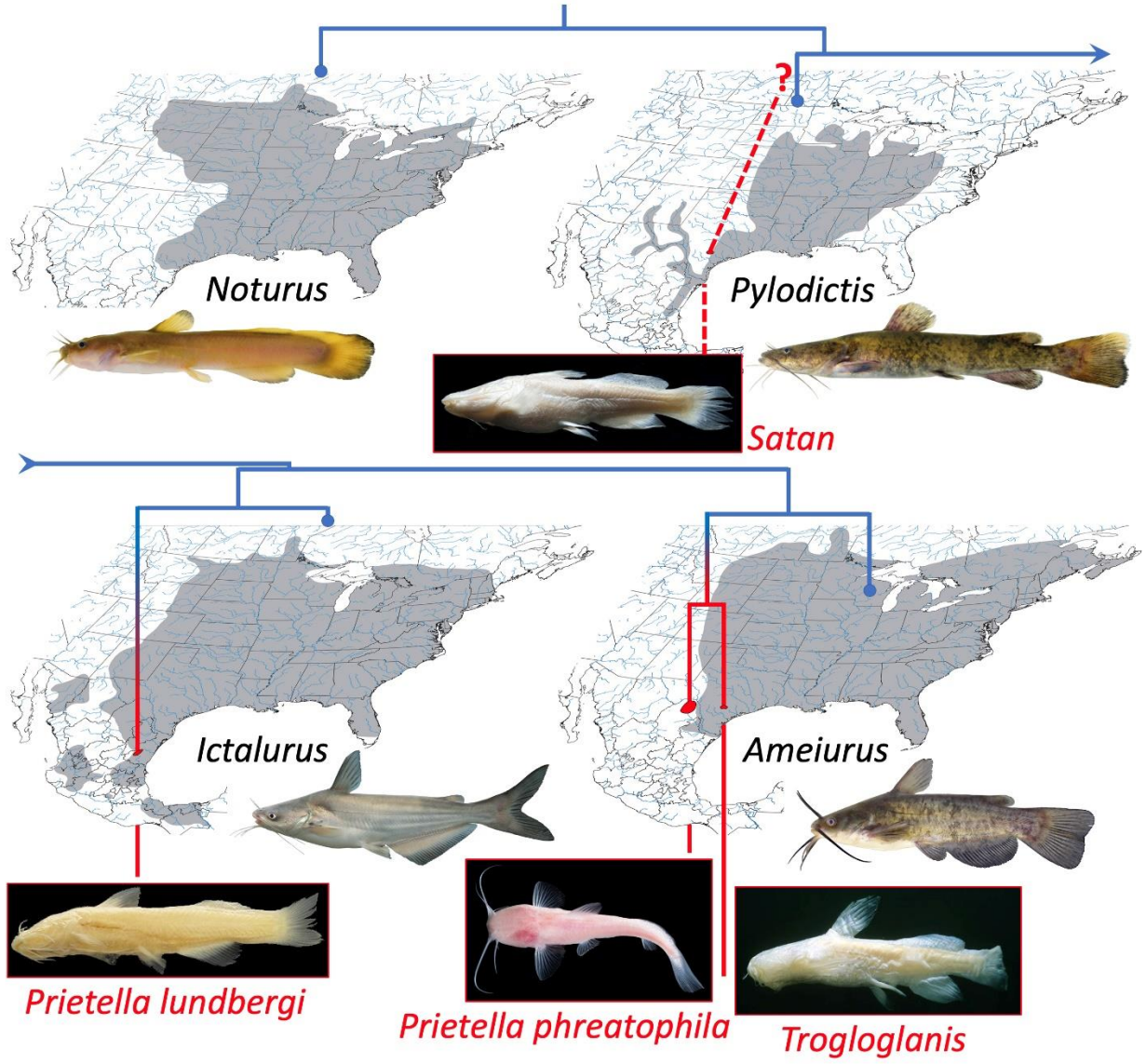

Figure 2-1 Phylogeographic sketch of extant Ictaluridae based on relationships supported in this study (solid lines) or inferred from previous ones (dashed line). Branch lengths proportional to those in Fig. 2; circles denote common ancestor of respective genus. Distribution maps of epigean genera (gray) and hypogean species (red) derived from Burr et al. (2020). Photos by D.A. Hendrickson (*P. lundbergi*), J. Krejca, Zara Environmental LLC. (*P. phreatophila*), M.H. Sabaj (*Noturus, Pylodictis*), G.W. Sneegas (*Satan, Trogloglanis*) and M.R. Thomas (*Ameiurus, Ictalurus*).

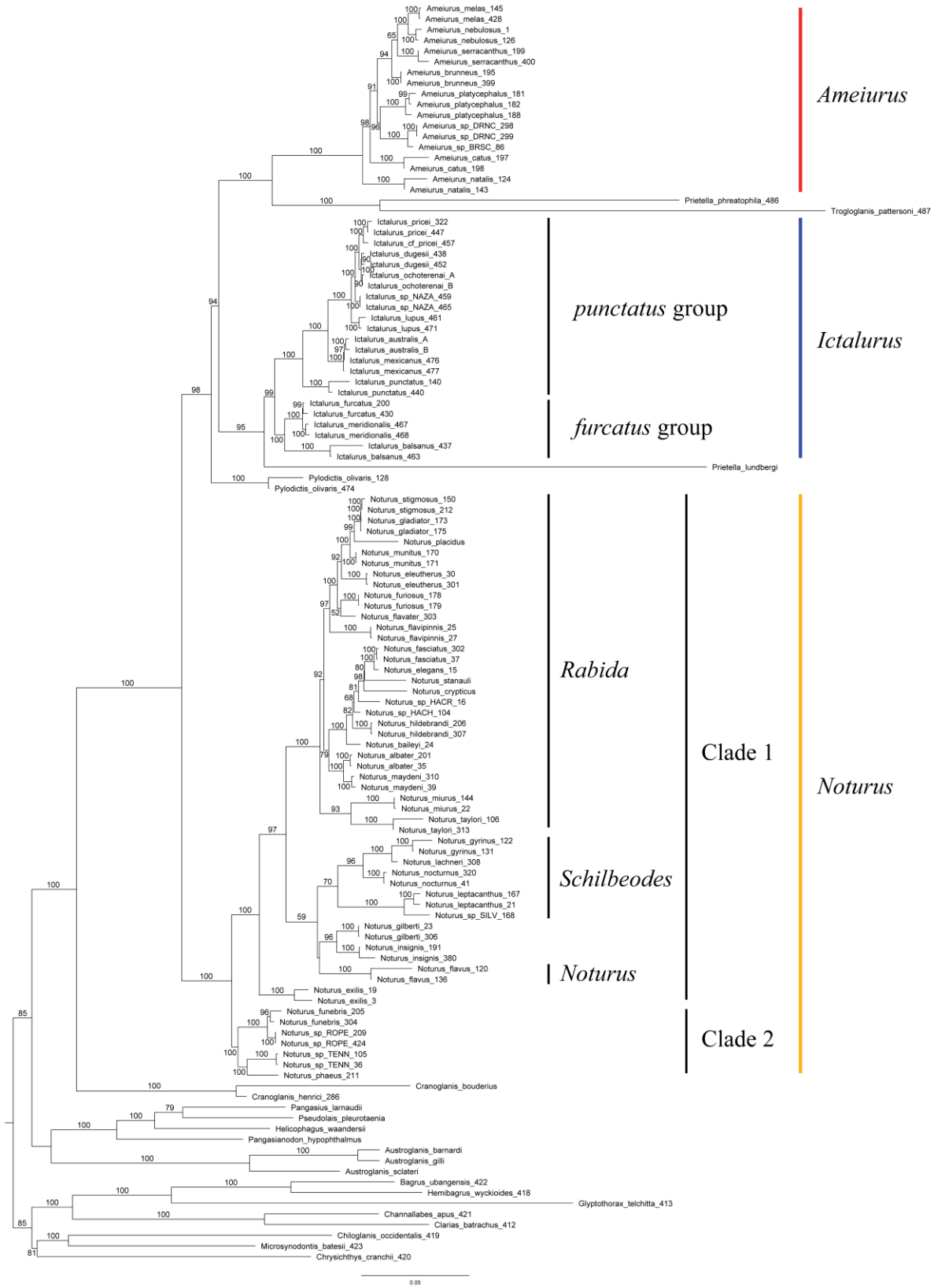

Figure 2-2 Maximum likelihood phylogeny of Ictaluridae based on an 11-region concatenated data matrix analyzed with IQ-TREE. Bootstrap values ≥ 50% are presented above each branch.

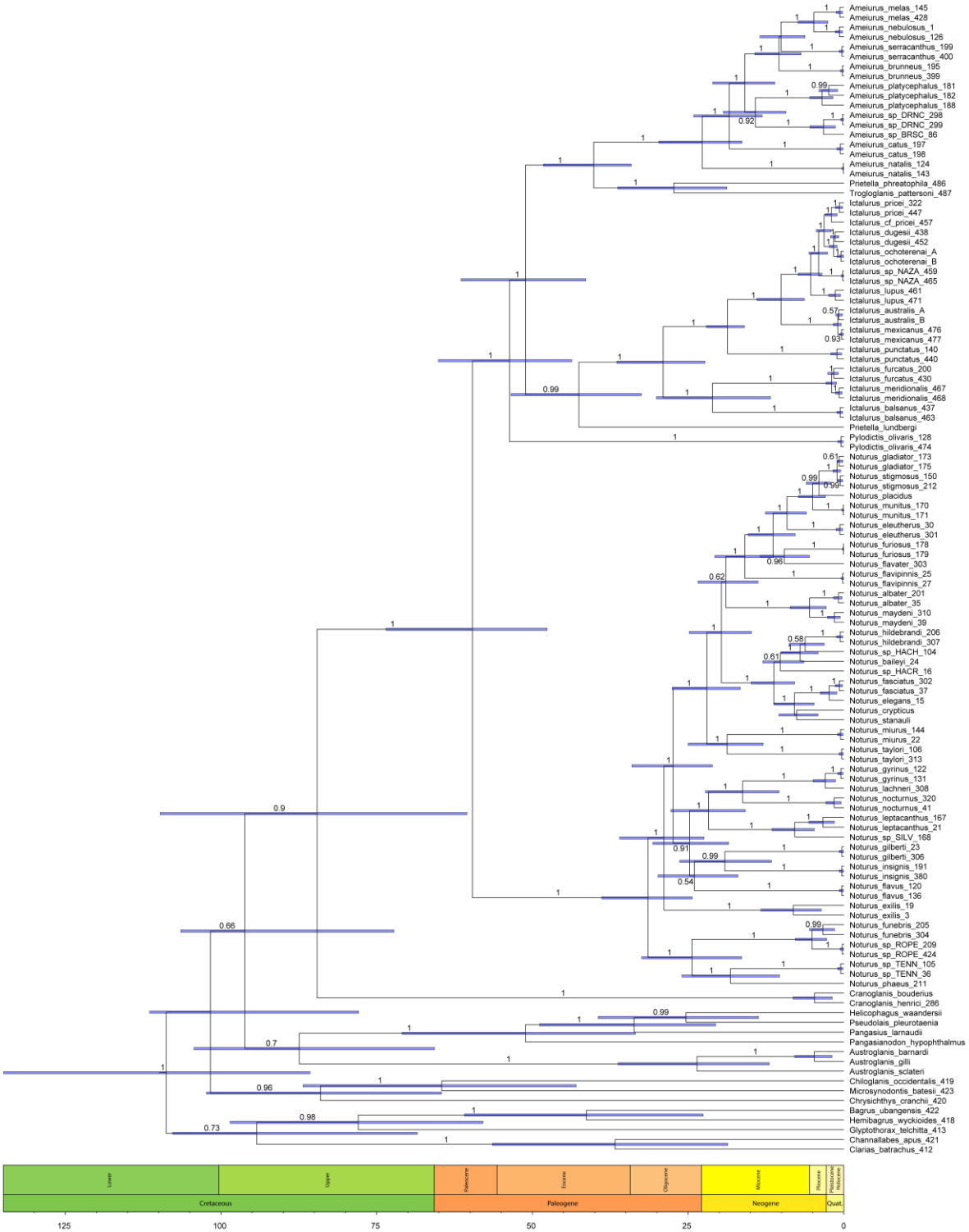

Figure 2-3 Fossil-calibrated phylogeny of Ictaluridae using the CladeAge package in BEAST2. Divergence-time estimates were calculated using 16 fossil specimens. Posterior probabilities ≥ 0.5 are presented above each branch. Blue node bars represent the 95% confidence interval of estimated origin times. Geological scale axis measured in million years before present.

Supplemental Material for Chapter 2

Table 2-S1 Museum voucher data for 101 ictalurid specimens and 17 siluriform outgroup species. GPS coordinates and GenBank accession numbers are available in the online publication at https://doi.org/10.1016/j.ympev.2023.107746.

Species	Specimen Label	Voucher museum and catalog no.	Locality
Ameiurus brunneus Jordan, 1877	F195	UF 165756	Hillabahatchee Creek, Georgia, USA
Ameiurus brunneus Jordan, 1877	F399	AUM 61306	Cedar Creek, Alabama, USA
Ameiurus catus (Linnaeus, 1758)	F197	UF 167624	Aucilla River, Florida, USA
Ameiurus catus (Linnaeus, 1758)	N/A	NEFC F16-261	South Carolina, USA
Ameiurus catus (Linnaeus, 1758)	F198	UF 174270	New River, Florida, USA
Ameiurus melas (Rafinesque, 1820)	F145	ROM 100161	Claireville Reservoir, Ontario, Canada
Ameiurus melas (Rafinesque, 1820)	F428	AUM 55552	Sturgeon River, Michigan, USA
Ameiurus natalis (Lesueur, 1819)	F124	ROM 71710	Tumblesons Pond, Ontario, Canada
Ameiurus natalis (Lesueur, 1819)	N/A	TNHCi 25769	Pin Oak Creek at CR 183, Texas, USA
Ameiurus natalis (Lesueur, 1819)	F143	ROM 95736	Lake Erie, Ontario, Canada
Ameiurus nebulosus (Lesueur, 1819)	F01	CMNFI 2018-0014.1	Aylmer, Quebec, Canada
Ameiurus nebulosus (Lesueur, 1819)	N/A	ANSP 182780	Uncertain location, Pennsylvania, USA
Ameiurus nebulosus (Lesueur, 1819)	F126	ROM 75638	Lake Simcoe, Ontario, Canada
Ameiurus platycephalus (Girard, 1859)	F181	NCSM 30412	Haw River, North Carolina, USA
Ameiurus platycephalus (Girard, 1859)	F182	NCSM 36753	Turkey Creek, South Carolina, USA
Ameiurus platycephalus (Girard, 1859)	F188	NCSM 43805	Hickory Creek, North Carolina, USA
Ameiurus serracanthus (Yerger & Relyea, 1968)	F199	UF 237833	Chipola River, Florida, USA
Ameiurus serracanthus (Yerger & Relyea, 1968)	F400	AUM 66262	Chattahoochee River, Georgia, USA
Ameiurus sp. BRSC	F86	ANSP 185091	Broad River, South Carolina, USA
Ameiurus sp. DRNC	F298	JFBM 42770	Deep River, North Carolina, USA
Ameiurus sp. DRNC	F299	JFBM 41862	Deep River, North Carolina, USA

Ictalurus australis (Meek, 1904)	A	MNCN 2901	Río Verde north of Río Verde town; Panuco Basin, San Luis Potosi, Mexico
Ictalurus australis (Meek, 1904)	B	CPUM 4800	Channel 800m northwest of Plazuela town; Panuco River, San Luis Potosi, Mexico
Ictalurus balsanus (Jordan & Snyder, 1899)	F437	UMSNH 4994	Río Balsas, Michoacán, Mexico
Ictalurus balsanus (Jordan & Snyder, 1899)	N/A	ECOSC 4264	Mexico
Ictalurus balsanus (Jordan & Snyder, 1899)	F463	UMSNH 41563	Río Tuxpan, Balsas, Michoacán, Mexico
Ictalurus dugesii (Bean, 1880)	F438	UMSNH 5012	Lago de Chapala, Mexico
Ictalurus dugesii (Bean, 1880)	F452	UMSNH 18723	Ayuquila-Armeria basin, Jalisco, Mexico
Ictalurus furcatus (Valenciennes, 1840)	F200	UF 238203	Apalachicola River, Florida, USA
Ictalurus furcatus (Valenciennes, 1840)	N/A	F1842	N/A
Ictalurus furcatus (Valenciennes, 1840)	F430	UMSNH 3232	Grijalva-Usumacinta River basin, Mexico
Ictalurus lupus (Girard, 1858)	F461	UMSNH 41562	Conchos alto, Durango, Mexico
Ictalurus lupus (Girard, 1858)	N/A	TNHCi 29350	San Felipe Creek in the vicinity of Del Rio, Texas, USA
Ictalurus lupus (Girard, 1858)	F471	UMSNH 57921	San Juan-Bravo, Nuevo León, Mexico
Ictalurus meridionalis (Günther, 1864)	F467	UMSNH 53454	Río Papaloapán, Oaxaca, Mexico
Ictalurus meridionalis (Günther, 1864)	N/A	ECOSC 4176	Mexico
Ictalurus meridionalis (Günther, 1864)	F468	UMSNH 53508	Río Papaloapán, Oaxaca, Mexico
Ictalurus mexicanus (Meek, 1904)	F476	MNCN 98771	Río Gallinas, San Luis de Potosi, Mexico
Ictalurus mexicanus (Meek, 1904)	F477	MNCN 98772	Río Gallinas, San Luis de Potosi, Mexico
Ictalurus ochoterenai (de Buen, 1946)	A	CPUM 5014	Lago de Chapala at Chapala town; Lerma-Chapala basin, Jalisco, Mexico
Ictalurus ochoterenai (de Buen, 1946)	B	CPUM-5018	Lago de Chapala at Chapala town; Lerma-Chapala basin, Jalisco, Mexico
Ictalurus pricei (Rutter, 1896)	F322	TNHCi 63142	Meade Fish Hatchery, Kansas, USA
Ictalurus pricei (Rutter, 1896)	N/A	TNHCi 21704	Madera, Chihuahua, Mexico
Ictalurus pricei (Rutter, 1896)	F447	UMSNH 7060	Río Fuerte, Chihuahua, Mexico
Ictalurus cf. *pricei* (Rutter, 1896)	F457	UMSNH 40871	Tunal - Mezquital, Durango, Mexico
Ictalurus punctatus (Rafinesque, 1818)	F140	ROM 86705	Lake St Clair, Ontario, Canada

Ictalurus punctatus (Rafinesque, 1818)	N/A	NEFC_F16-262	South Carolina, USA
Ictalurus punctatus (Rafinesque, 1818)	F440	UMSNH 5722	Bolaños-Santiago River basin (introduced), Mexico
Ictalurus sp. NAZA	F459	UMSNH 40907	Nazas, Durango, Mexico
Ictalurus sp. NAZA	F465	UMSNH 45533	Nazas, Durango, Mexico
Noturus albater Taylor, 1969	F35	YPM ICH.018748	White River Drainage, Arkansas, USA
Noturus albater Taylor, 1969	F201	UF 171997	Indian Creek, Missouri, USA
Noturus baileyi Taylor, 1969	F24	YPM ICH.015943	USA
Noturus crypticus Burr, Eisenhour & Grady, 2005	N/A	—	Little Chucky Creek, Tennessee, USA
Noturus elegans Taylor, 1969	F15	YPM ICH.021704	Duck River, Tennessee, USA
Noturus eleutherus Jordan, 1877	F30	YPM ICH.019824	Clinch Drainage, Tennessee, USA
Noturus eleutherus Jordan, 1877	F301	JFBM 43055	East Fork White River, Indiana, USA
Noturus exilis Nelson, 1876	F03	FMNH 118354	Praire Creek, Illinois, USA
Noturus exilis Nelson, 1876	F19	YPM ICH.018793	White River Drainage, Arkansas, USA
Noturus fasciatus Burr, Eisenhour & Grady, 2005	F37	YPM ICH.021908	Tennessee River, Tennessee, USA
Noturus fasciatus Burr, Eisenhour & Grady, 2005	F302	JFBM 45375	Buffalo River, Tennessee, USA
Noturus flavater Taylor, 1969	F303	JFBM 44589	North Fork White River, Missouri, USA
Noturus flavipinnis Taylor, 1969	F25	YPM ICH.015944	Tennessee River Drainage, Virginia, USA
Noturus flavipinnis Taylor, 1969	F27	YPM ICH.015946	Copper Creek, Virginia, USA
Noturus flavus Rafinesque, 1818	F120	ROM 62433	Fansher Creek, Ontario, Canada
Noturus flavus Rafinesque, 1819	N/A	TNHCi 25772	Beaver Cr abt 2500 ft S Hwy 53 bridge, Wisconsin, USA
Noturus flavus Rafinesque, 1818	F136	ROM 75305	Meux Creek, Ontario, Canada
Noturus funebris Gilbert & Swain, 1891	F205	UF 237655	Canoe Creek, Florida, USA
Noturus funebris Gilbert & Swain, 1891	F304	JFBM 43002	Blue Girth Creek, Alabama, USA
Noturus furiosus Jordan & Meek, 1889	F178	NCSM 30345	Swift Creek, North Carolina, USA
Noturus furiosus Jordan & Meek, 1889	F179	NCSM 46608	Contentnea Creek, North Carolina, USA

Noturus gilberti Jordan & Evermann, 1889	F23	YPM ICH.015878	Roanoke River, Virginia, USA
Noturus gilberti Jordan & Evermann, 1889	F306	JFBM 49747	USA
Noturus gladiator Thomas & Burr, 2004	F173	MMNS 67765	Hatchie River, Mississippi, USA
Noturus gladiator Thomas & Burr, 2004	F175	MMNS 67702	Wolf River, Mississippi, USA
Noturus gyrinus (Mitchill, 1817)	F122	ROM 63068	Twenty Mile Creek, Ontario, Canada
Noturus gyrinus (Mitchill, 1817)	N/A	TNHCi 25004	Cummins Creek at SH 109, Texas, USA
Noturus gyrinus (Mitchill, 1817)	F131	ROM 80082	Lac Saint-Paul, Quebec, Canada
Noturus hildebrandi (Bailey & Taylor, 1950)	F206	UF 172023	Terrapin Creek, Tennessee, USA
Noturus hildebrandi (Bailey & Taylor, 1950)	F307	JFBM 42700	Clarks Creek, Tennessee, USA
Noturus insignis (Richardson, 1836)	F191	CMNFI 2017-0086	Gatineau Park, Quebec, Canada
Noturus insignis (Richardson, 1836)	N/A	TNHCi 24985	Deep River, Moore Co., North Carolina, USA
Noturus insignis (Richardson, 1836)	F380	ANSP 202613	Cherry Creek, Pennsylvania, USA
Noturus lachneri Taylor, 1969	F308	JFBM 41077	Cypress Creek, Arkansas, USA
Noturus leptacanthus Jordan, 1877	F21	YPM ICH.016288	Talking Rock Creek, Georgia, USA
Noturus leptacanthus Jordan, 1877	F167	MMNS 51586	Williams Greer Road, Mississippi, USA
Noturus maydeni Egge, 2006	F39	UT 48.1412	Current River, Missouri, USA
Noturus maydeni Egge, 2006	F310	JFBM 42653	St. Francis River, Missouri, USA
Noturus miurus Jordan, 1877	F22	YPM ICH.015814	Kentucky River, Kentucky, USA
Noturus miurus Jordan, 1877	F144	ROM 97025	Lake St Clair, Ontario, Canada
Noturus munitus Suttkus & Taylor, 1965	F170	MMNS 66232	Upper Little Creek, Mississippi, USA
Noturus munitus Suttkus & Taylor, 1965	F171	MMNS 67619	Strong River, Mississippi, USA
Noturus nocturnus Jordan & Gilbert, 1886	F41	UT 48.1387	Big Crow Creek, Texas, USA
Noturus nocturnus Jordan & Gilbert, 1886	F320	TNHCi 61979	Rocky Creek, Texas, USA
Noturus phaeus Taylor, 1969	F211	UF 172020	Terrapin Creek, Tennessee, USA
Noturus placidus Taylor, 1969	N/A	INHS 96383	Neosho River, Kansas, USA
Noturus stanauli Etnier & Jenkins, 1980	N/A	UT 48.1238	Clinch River, Tennessee, USA
Noturus stigmosus Taylor, 1969	F150	ROM 102693	Thames River, Ontario, Canada
Noturus stigmosus Taylor, 1969	F212	UF 172694	French Creek, Pennsylvania, USA

Noturus taylori Douglas, 1972	F106	ANSP 194099	Caddo River, Arkansas, USA
Noturus taylori Douglas, 1973	N/A	N/A	USA
Noturus taylori Douglas, 1972	F313	JFBM 42285	USA
Noturus sp. HACH	F104	ANSP 194086	Spring Creek, Tennessee, USA
Noturus sp. HACR	F16	YPM ICH.018461	Hatters Creek, Kentucky, USA
Noturus sp. ROPE	F209	UF 165754	Hillabahatchee Creek, Georgia, USA
Noturus sp. ROPE	F424	AUM 52158	Ropes Creek, Alabama, USA
Noturus sp. SILV	F168	MMNS 61862	Silver Creek, Mississippi, USA
Noturus sp. TENN	F36	YPM ICH.020988	Indian Creek, Mississippi, USA
Noturus sp. TENN	F105	ANSP 194071	Spring Creek, Tennessee, USA
Prietella lundbergi Walsh & Gilbert, 1995	N/A	TNHCi 25767	Nacimiento del Río Frío, Tamaulipas, Mexico
Prietella phreatophila Carranza, 1954	F486	TNHCi 60415	Catfish Parlour Cave, Texas, USA
Prietella phreatophila Carranza, 1954	N/A	TNHCi 24986	Sotano de Amezcua, Cd. Acuña, Coahuila, Mexico
Prietella phreatophila Carranza, 1954	N/A	TNHCi 30820	Sotano de Amezcua, Cd. Acuña, Coahuila, Mexico
Pylodictis olivaris (Rafinesque, 1818)	F128	ROM 75465	Lake St Clair, Ontario, Canada
Pylodictis olivaris (Rafinesque, 1818)	N/A	TNHCi 25770	Pin Oak Creek at CR 183, Texas, USA
Pylodictis olivaris (Rafinesque, 1818)	F474	UMSNH 57621	San Luis Potosi, Pánuco, Mexico
Trogloglanis pattersoni Eigenmann, 1919	F487	TNHCi 42586	Aldridge Nursery, Texas, USA
Austroglanis barnardi (Skelton, 1981)	N/A	SAIAB 200084	Noordhoeks River, Western Cape, South Africa
Austroglanis gilli (Barnard, 1943)	N/A	SAIAB 200307	Upper Jan Dissels at footpath crossing, Clanwilliam, Western Cape, South Africa
Austroglanis sclateri (Boulenger, 1901)	N/A	SAIAB 78962	Near Three Rivers suburb of Vereeniging, Gauteng, South Africa
Bagrus ubangensis Boulenger, 1902	F422	AUM 51278	Lualaba River, Orientale, Democratic Republic of the Congo
Hemibagrus wyckioides (Fang & Chaux, 1949)	F418	AUM 55933	Mekong River, Ubon Ratchathani, Thailand
Channallabes apus (Günther, 1873)	F421	AUM 51306	Lindi River, Orientale, Democratic Republic of the Congo

Clarias batrachus (Linnaeus, 1758)	F412	AUM 55330	Padma River, Jessore, Bangladesh
Chrysichthys cranchii (Leach, 1818)	F420	AUM 51473	Lualaba River, Orientale, Democratic Republic of the Congo
Cranoglanis bouderius (Richardson, 1846)	N/A	IHB 0907767	China
Cranoglanis henrici (Vaillant, 1893)	F286	ANSP 203039	Red River basin, Ha Moi, Vietnam
Chiloglanis occidentalis Pellegrin, 1933	F419	AUM 59635	Bafing River, Mamou, Republic of Guinea
Microsynodontis batesii Boulenger, 1903	F423	AUM 58059	Mie River, Haut Nyong, Cameroon
Helicophagus waandersii Bleeker, 1858	N/A	N/A	N/A
Pangasianodon hypophthalmus (Sauvage, 1878)	N/A	N/A	N/A
Pangasius larnaudii Bocourt, 1866	N/A	N/A	N/A
Pseudolais pleurotaenia (Sauvage, 1878)	N/A	N/A	N/A
Glyptothorax telchitta (Hamilton, 1822)	F413	AUM 55306	Kangso River, Netrokona, Bangladesh

Table 2-S2 Primer sequences used for PCR amplification and sequencing reactions. An asterisk (*) denotes internal primers used only for sequencing reactions.

Gene	Primer name	Primer sequence (5'-3')	Primer reference
co1	*co1*fishF1	TCAACYAATCAYAAAGATATYGGCAC	Ward et al. 2009
	*co1*fishR1	ACTTCYGGGTGRCCRAARAATCA	
cyt b	GLUDGL	CGAAGCTTGACTTGAARAACCAYCGTTG	Palumbi et al. 1991
	*cyt b*R	CTCCGATCTTCGGATTACAAG	
egr1	*egr1* SilF	GCGGCTGCCCCCCATCTCCTACAC	This study
	egr1 SilR	CTGGATGGTGGTGGAGACYGAGGTG	
	egr1 SintF*	AGTGAGCCCAACCCCATTTATTC	
	egr1 SintR*	TCRCTGCGGCTGAAGTTGCG	
enc1	*enc1* SilFb	GATGCCTGTGCTGAGTTCCTGGAGA	This study
	enc1 SilR	CCTACTTTAGTCCACTGGTA	
	enc1 SintF*	AACTGGGTGAACTATGAYTTGG	
	enc1 SintR*	TCCTTGGACACACCGTTCTCTGAGCC	
glyt	*glyt* SilF	TATCAGTATGGCTTTGTACAGCC	This study
	glyt SilR	GTTCTCTCCCTGCTCCTGGATCCA	
	glyt SintF*	TAYAAAATGAGRACAGTCAC	
	glyt SintR*	ATGGTGTCTTGATAAATYC	
rag1	*rag1* SilF	CTCCGYAATGCTGARAAGGA	This study
	rag1 SilR	CCTAGCRTTCATYTTACGGAA	
	rag1 SintF*	GCAGAGCGTAAAGCTATGAA	
	rag1 SintR*	ATCTTRTAGAATTCRGTAGCA	
rag2	*rag2* SilF	CAGAAAGGATGGCCCAAACGTTCCTG	This study
	rag2 SilR	CCTCTGGAACAGAAGATCAT	
	rag2 SintF*	GGYCGAACACCCAACAAYGA	
	rag2 SintR*	CCCTCTCCATCACTGCTGWA	
rh1	*rh1* SilF	GCCTACATGTTCTTCYTMAT	This study
	rh1 SilR	TGGCGGAACTGCTTGTTCATGCA	
	rh1 SintF*	GTAGCATTYACYTGGGTCATGGC	
	rh1 SintR*	TGGGTGGTTTCAGACTCYTGCTG	
sreb2	*sreb2* SilF	AARCTAACCTCCYTGGGCTT	This study
	sreb2 SilR	ATGCAGATGAARGGRTTGAC	
	sreb2 SintF*	CGGCTGACCCTGTGGACGTGC	
	sreb2 SintR*	GCCAGGAGGATSAGGGCRAGCAGCA	
zic1	*zic1* SilF	GCGGGCTAAAGATGCTCTTGGACGC	This study
	zic1 SilRc	GAAACGGTTTCTCTCCGGTGTG	
	zic1 SintFnew*	GGACTGCACGAGCAAGCRGC	
	zic1 SintR*	AAAGTTTTGTTGCAGGACTT	

Table 2-S3 Best IQ-TREE nucleotide substitution models found using the Corrected Akaike Information Criterion in PartitionFinder2 2.2.1 for 30 gene partitions of the concatenated Ictaluridae alignment.

Nucleotide substitution model	**Gene partitions**
JC	*co1*_pos3, *enc1*_pos3, *glyt*_pos1, *rag2*_pos3, *zic1*_pos1, *zic1*_pos3
JC + I	*egr1*_pos2, *rh1*_pos1, *rh1*_pos3
K2P	*glyt*_pos2
K2P + G4	*co1*_pos1, *egr1*_pos1, *egr1*_pos3, *enc1*_pos1, *glyt*_pos3, *rag1*_pos3, *rh1*_pos2, *zic1*_pos2
K2P + I	*rag1*_pos2, *rag2*_pos1, *rag2*_pos2
K2P + I + G4	*cyt b*_pos3
TIM + F + I + G4	*cyt b*_pos1
TIM2 + F + I + G4	12S+16S_pos1, 12S+16S_pos2, 12S+16S_pos3
TNe + G4	*co1*_pos2
TNe + I	*enc1*_pos2
TPM2 + F + I + G4	*cyt b*_pos2
TPM2u + F + G4	*rag1*_pos1

Chapter 3

Restricted gene flow and paleohydrological events are associated with genetic diversification of a widespread Neotropical catfish, *Pimelodus ornatus* (Siluriformes: Actinopterygii)

Abstract

Heterogenous landscapes exert a variety of selective pressures on widespread species. Different selective pressures can eventually lead to speciation, either by separation of subpopulations (allopatry) or by local adaptations despite continued gene flow (parapatry). One example of a widespread species potentially subject to varied selection pressures is the ornate pim catfish (*Pimelodus ornatus*), which occurs in most major river basins in South America. *Pimelodus ornatus* populations are separated by impermeable and semi-permeable river basin boundaries, and individuals from different rivers are genetically distinct. We wished to examine how barriers to gene flow have shaped the genetic landscape of *Pimelodus ornatus*. We created a phylogeny of the species using 130 specimens to identify distinct lineages. We then fossil-calibrated this phylogeny to estimate origin times. Finally, we calculated uncorrected *p*-distances within and between each lineage, and compared these distances to published interspecific thresholds typically observed in fishes. We found evidence for seven distinct lineages strongly defined by geographic location, except for an Upper Amazon/Rupununi clade. The clades exhibited inter-lineage *p*-distances comparable to congeneric species of fishes, indicating a potential need for formal species description. We found that *P. ornatus* originated sometime between the Oligocene and Miocene, later than inferred in previous studies. The next steps will be to conduct an ancestral area state reconstruction to determine where the species likely evolved and differentiated, and to analyze morphological data to describe these potential new cryptic species formally.

Introduction

The physical environment has played an integral role in the evolution and speciation of organisms across the tree of life (Grinnell, 1924; Mayr, 1954; Skeels & Cardillo, 2019). Heterogeneous landscapes present a variety of selective pressures that promote genetic diversity between populations via local adaptation, especially in peripheral populations (Wade & Kalisz, 1990; Benton, 2009; Pearson et al., 2009). The physical environment may also affect gene flow by acting as a bridge or barrier between populations (Krewenka et al., 2011). Features such as deserts, oceans, mountain ranges, and human-made structures may reduce or eliminate gene flow between populations, counteracting the homogenizing effects of gene flow (Slatkin, 1985; Slatkin, 1987; Pearson et al., 2009; Sexton et al., 2014). Alternatively, these features may act as dispersal corridors between fragmented populations, increasing gene flow (Krewenka et al., 2011; Correa Ayram et al., 2016; Afiq-Rosli et al., 2021). For these reasons, we must account for environmental and geographical factors when elucidating the origins and evolutionary histories of species.

Given its role in promoting genetic differentiation between populations, the physical environment is an essential component of allopatric speciation (Mayr, 1954; Fitzpatrick et al., 2009; Dool et al., 2022). New species arise when physical barriers prevent gene flow between subgroups of a population, allowing for genetic differences to accrue in response to independent mutations, selective pressures, and stochastic events (Mayr, 1954; Lande, 1980; Hoskin et al., 2005). Two processes that result in allopatric speciation are vicariance and dispersal (Mayr, 1982; Zink et al., 2000). Vicariance occurs when barriers are imposed upon and then divide a population (Mayr, 1982; Wiley, 1988; Allmon, 1992). Barriers may be created following orogenesis, continental drift, creation or destruction of channels connecting bodies of water,

human construction of roads and cities, etc. (Allmon, 1992; Yoder & Nowak, 2006; Cowman & Bellwood, 2013). In contrast, dispersal occurs when a portion of the population migrates over existing barriers, resulting in subsequent isolation from the ancestral population (Ronquist, 1997; Bonte et al., 2012; Claramunt et al., 2012). These processes are not mutually exclusive; clades may diversify from a combination of vicariance and dispersal (Macey et al., 1998; Zink et al., 2000). For example, for modern freshwater fish clades, such as osteoglossomorphs (bony tongues and mooneyes) and percichthyids (temperate perches) both dispersal and vicariance were likely agents of speciation given their disjunct extant distributions (Ruzzante et al., 2006; Capobianco & Friedman, 2019; Peterson et al., 2022). Another example is South American *Dendrocincla* woodcreepers (Weir & Price, 2011). Speciation within this avian genus has been attributed to vicariance caused by Andean uplift and subsequent dispersal across this barrier (Weir & Price, 2011). Allopatric speciation is predicated on the presence of barriers interrupting gene flow (Allmon, 1992), but what happens when these barriers are spatially or temporally intermittently permeable?

When physical barriers are incomplete or porous, gene flow may reduce differentiation between adjacent subpopulations (Slatkin, 1973; Slatkin, 1987; Fitzpatrick et al., 2009; Barrera-Guzmán et al., 2022). Parapatric speciation, however, is still possible in the presence of gene flow (Bush, 1975; Slatkin, 1987; Gavrilets et al., 2000; Bank et al., 2012; Blanckaert et al., 2020). Widespread species with low vagility may display regional genetic variation due to random mutations and unique selective pressures from local environmental conditions despite continued gene flow (Bush, 1975; Gavrilets et al., 2000; Blanckaert & Hermisson, 2018). Clinal phenotypic traits reflect regional variation, displaying a gradient across the species distribution (Bush, 1975; Endler, 1977; Stankowski et al., 2017). Over time, these subpopulations continue to

accumulate differences and may become reproductively isolated, eventually resulting in parapatric speciation (Endler, 1977; Blanckaert et al., 2020). Parapatric speciation may also occur in species that display stepping-stone distributions, in which populations are dispersed among suitable, fragmented habitat patches (Gavrilets et al., 2000; Fitzpatrick et al., 2008; Descombes et al., 2018). Hybridization still occurs in areas of contact between the diverging species, but outbreeding depression may promote reproductive character displacement (Endler, 1977; Lande, 1982; Smadja & Ganem, 2005; Pfennig & Rice, 2014; Blanckaert et al., 2020). Parapatric speciation has been proposed as the predominant explanation for coral-reef fish diversity given the prevalence of porous, intermittent barriers between reef populations (Rocha & Bowens, 2008; Leprieur et al., 2016). Other examples of parapatric species pairs include *Triturus* newts (Arntzen, 2023), *Bombina* toads (Dufresnes et al., 2021), *Pipra* manakins (Barrera-Guzmán et al., 2022), *Rhagoletis* flies (Doellman et al., 2020), and *Drosophila* fruit flies (Wu & Ting, 2004).

One widespread species that could undergo allopatric and parapatric speciation is the ornate pim catfish, *Pimelodus ornatus* (Pimelodidae, Siluriformes). *Pimelodus ornatus* is a Neotropical freshwater fish that inhabits most major river basins in South America (Figure 3-1), including the Amazon, Orinoco, Paraná, Parnaíba, Corantijn, and Essequibo rivers (Ferraris Jr., 2007; Lundberg et al., 2011; Lima et al., 2021). These river basins are variably connected, possibly limiting or eliminating gene flow between *P. ornatus* populations (Albert et al., 2006; Wesselingh & Hoorn, 2011). The Amazon and Orinoco rivers currently drain eastward and northward, respectively, into the Atlantic Ocean (Meade et al., 1979; Meade, 1994). The only perennial connection between these two river basins is the Casiquiare River, a bifurcation of the Orinoco River headwaters flowing southward into the Rio Negro, a major tributary of the

Amazon River (Vari & Ferraris Jr., 2009; Willis et al., 2010; Wesselingh & Hoorn, 2011; Stokes et al., 2018). Connections between Paraná-Paraguay headwaters and Amazon River basin headwaters occur seasonally and sporadically, limiting dispersal between the basins (Iriondo & Paira, 2007; Torrico et al., 2009; Brea & Zucol, 2011). The Amazon River basin also connects annually with the Essequibo River basin of the Guiana Shield via the Rupununi Portal (de Souza et al., 2019; de Souza et al., 2020). The Rupununi Portal is composed of wetlands created by seasonal rains that flood the Rupununi savannah in south-central Guyana (Quinn & Woodward, 2015; de Souza et al., 2019; de Souza et al., 2020).

Major modern physical boundaries between South American river basins largely began to develop during the Eocene to Late Miocene, ~10-43 mya, such as Andean uplift and exposure of the Michicola Arch (Albert et al., 2006; Albert & Reis, 2011; Wesselingh & Hoorn, 2011; Tagliacollo et al., 2015; Abreu et al., 2020). The development of these barriers coincides with the origin of *P. ornatus*, estimated to have diverged from other pimelodids ~30-49 mya (Sullivan et al., 2013; Tagliacollo et al., 2015). It is important to note, however, that previous studies did not include the closest relative of *P. ornatus* currently recognized, *Pimelabditus moli* (Lundberg et al., 2012; Sullivan et al., 2013; Tagliacollo et al., 2015), and thus may have inaccurately estimated its origin time. Furthermore, Lundberg et al. (2011) constructed a phylogeny of Central and South American pimelodids including four *P. ornatus* specimens collected from four rivers: the Essequibo, Orinoco, Amazon, and Paraná. The representatives from the Essequibo and Orinoco Rivers displayed genetic divergence similar to that found between other congeneric species (Lundberg et al., 2011; Tagliacollo et al., 2015). The representatives from the Amazon and Paraná rivers did not demonstrate significant genetic differentiation, but were collectively distinct from the Orinoco and Essequibo representatives (Lundberg et al., 2011; Tagliacollo et

al., 2015). Therefore, three distinct, cryptic lineages were recovered: the Essequibo lineage, the Orinoco lineage, and the Amazon-Paraná lineage (Lundberg et al., 2011; Tagliacollo et al., 2015). Lundberg et al. (2011), however, indicated a need for increased genetic sampling and morphological data to confirm the taxonomic validity of these potentially new species. Given the evidence of distinct genetic lineages corresponding with isolated and semi-isolated river basin populations, *P. ornatus* provides an excellent opportunity to elucidate the possible influences of vicariance, dispersal, and gene flow on the genetic diversification of the species.

The purpose of our study was to determine how paleohydrological events throughout the geological history of South America have contributed to the genetic diversification and possible allopatric/parapatric speciation of *P. ornatus* populations. We tested the hypothesis that both permanent and intermittent barriers between major South American river basins have reduced or eliminated gene flow between subpopulations of *P. ornatus*, resulting in distinct subpopulations that may represent new species. We predicted the presence of at least three distinct lineages corresponding with the Essequibo, Orinoco, and Amazon-Paraná rivers, as observed in Lundberg et al. (2011) and Tagliacollo et al. (2015). To test our hypothesis, we generated a multi-gene phylogeny of *P. ornatus* using specimens collected throughout South America. We also calculated the mean uncorrected *p*-distance of *co1* sequences between all individuals to measure the genetic distances (genetic divergence) between subpopulations (Nei, 1972; Srivathsana & Meier, 2012; Fišer et al., 2018). Previous studies on vertebrates have indicated that individuals of the same species generally do not exceed 1% distance (Herbert et al., 2004; Ward et al., 2005; Li et al., 2018; Tsoupas et al., 2022).

Materials and methods

Specimen sampling and gene selection

To create our multi-gene phylogeny of *P. ornatus*, we combined sequence data we produced from 45 museum-deposited voucher specimens with sequence data from 85 specimens available from online DNA repositories (Table 3-S1), including GenBank and Barcode of Life Data (BOLD) Systems (Ratnasingham & Herbert, 2007; Benson et al., 2018). We selected 20 pimelodid species as outgroups (Table 3-S1), representing each of the major clades within Pimelodidae (Lundberg et al., 2011; Tagliacollo et al., 2015). This included *P. moli*, the closest known relative of *P. ornatus* (Lundberg et al., 2012). We selected four protein-coding genes to construct our *P. ornatus* phylogeny, two of which were mitochondrial barcoding genes (*co1* and *cyt b*) and two were nuclear genes (*enc1* and *rag2*). These single-copy genes were selected to (1) prevent gene paralog biases and (2) because they display variable evolutionary rates useful for providing both shallow- and deep-phylogenetic resolution (Lovejoy & Collette, 2001; Lovejoy et al., 2004; Sevilla et al., 2007; Chen et al., 2008; Hughes et al., 2018).

DNA sequencing and alignment

Using an adapted protocol from Ivanova et al. (2006), we extracted genomic DNA from muscle and fin tissues stored in 95% ethanol at -20°C. We amplified our four selected genes using PCR. We designed primers to amplify both nuclear genes, including separate internal primers for sequencing reactions to avoid non-specific products amplification (Table 2-S2). We amplified and sequenced *co1* and *cyt b* using primers published by Ward et al. (2009) and Palumbi et al. (1991), respectively. We used the following PCR recipe to amplify *cyt b*, *enc1*, and *rag2* for each reaction: 1X Dream buffer containing 2 mM $MgCl_2$, 0.2 mM of dNTPs, 0.25 μM of forward and reverse primers, 0.75 U of Dream *Taq*, ca. 20-30 ng of template DNA,

and nuclease-free water to adjust to the final reaction volume of 15 μL. Cycling conditions using a Mastercycler pro S were as follows: initial heating to 95°C for 3 minutes, 35 cycles of denaturation (95°C for 30 seconds), primer annealing (55°C for 30 seconds), and extension (72°C for 1 minute and 30 seconds) phases, and a final extension phase at 72°C for 10 minutes. We used the following PCR recipe to amplify *co1*: 1X Q5 buffer containing 2 mM $MgCl_2$, 0.2 mM of dNTPs, 0.5 μM of forward and reverse primers, 0.45 μL of DMSO, 0.3 U of Q5 polymerase, ca. 20-30 ng of template DNA, and nuclease-free water to adjust to the final reaction volume of 15 μL. Cycling conditions using a Mastercycler pro S were as follows: initial heating to 98°C for 30 seconds, 34 cycles of denaturation (98°C for 10 seconds), primer annealing (56°C for 30 seconds), and extension (72°C for 30 seconds) phases, and a final extension phase at 72°C for 5 minutes.

We visualized PCR products to confirm successful amplification using gel electrophoresis, followed by PCR products dilution with nuclease-free water according to band strength: 60 μL for strong bands, 30 μL for medium bands, and 15 μL for weak bands. Using a Mastercycler pro S, we performed sequencing reactions using the following recipe per sample: 0.9X ABI buffer, 0.5 μM of primer, 0.5 μL of BigDye containing ddNTPs, 1 μL of diluted PCR products, and nuclease-free water to adjust to the final reaction volume of 10 μL. The sequencing reaction cycling conditions were as follows: initial heating to 95°C for 3 minutes, 25 cycles of denaturation (96°C for 30 seconds), primer annealing (50°C for 20 seconds), and extension (60°C for 4 minutes) phases. Finally, we purified our sequencing reactions using an EDTA-NaOH-ethanol precipitation protocol provided by the manufacturer. The resulting DNA pellets were resuspended using HIDI formamide, followed by sequencing using a 3500 xL Genetic Analyzer (ThermoFisher Scientific). We aligned our sequences using MUSCLE 5.1 plugin

(Edgar, 2021) in Geneious Prime 2023.0.1 and concatenated each individual gene using SequenceMatrix 1.8 (Vaidya et al., 2011).

Phylogenetic analyses and genetic distances

We constructed our multi-gene phylogeny of *P. ornatus* using a ML analysis with IQ-TREE (Minh et al., 2020). We first partitioned our concatenated matrix by gene and by codon position, totaling 12 partitions. We used the IQ-TREE web server to identify the substitution model that best fit each partition with the AICc (Trifinopoulos et al., 2016; Kalyaanamoorthy et al., 2017). Using these unlinked substitution models of best fit (Table 3-S2; Chernomor et al., 2016) with our partitioned sequence matrix, we performed a ML analysis on the IQ-TREE web server (Trifinopoulos et al., 2016). We ran the analysis for 100 likelihood searches and calculated branch support using the ultrafast bootstrap approximation for 1000 replicates (Hoang et al., 2018). We visualized the resulting phylogeny using FigTree 1.4.4 (Rambaut, 2009).

We calculated the uncorrected *p*-distance between *co1* sequences of each *P. ornatus* individual (with the exception of three individuals due to unavailability from online repositories) using Geneious Prime 2023.0.1. We then calculated the mean uncorrected *p*-distance between lineages we observed in our ML phylogeny.

Results

Using a concatenated DNA matrix of four genes, totaling 3,849 nucleotide base pairs, we constructed a ML phylogeny of *P. ornatus*. *Pimelodus ornatus* specimens collected throughout South America clustered into seven distinct lineages: Lower Amazon-Xingu clade, Itapecuru clade, Marowijne clade, Essequibo-Berbice clade, Orinoco clade, Upper Amazon/Rupununi clade, and Paraná clade (Figure 3-2). Each lineage was strongly supported as monophyletic (96-100 BS; Figure 3-2) and was defined by geographic location (Figure 3-3), with the exception of

the Upper Amazon/Rupununi clade. The specimens that comprise this lineage include eight specimens collected from the Ucayali and Nanay rivers of the Peruvian Upper Amazon, two specimens from the Rupununi savannah, and one specimen from lowland Guyana (Table 3-S1). Within this lineage, Peruvian and Guyanese individuals were grouped into two separate monophyletic subclades (99 BS for Peruvian subclade, 78 BS for Guyanese subclade), and were reciprocally monophyletic (98 BS).

Each lineage exhibited low intra-lineage uncorrected *p*-distances <1.0%, ranging from 0.00 to 0.38% (Table 3-1). With respect to inter-lineage uncorrected *p*-distances, values ranged from 1.91 to 5.96% (Table 3-2). The shortest distance occurred between the Upper Amazon/Rupununi and Paraná clades (1.91%), whereas the longest distance occurred between the Upper Amazon-Rupununi and Lower Amazon-Xingu clades (5.96%). We also examined *p*-distances between the Upper Amazon/Rupununi subclades from Peru and Guyana; these subclades exhibited a distance of 0.85%.

We included two representatives of each *P. ornatus* lineage in our ten-gene fossil-calibrated BI phylogeny of Pimelodidae (see Chapter 4). The topology of both our ML and BI phylogenies were consistent (Figure 3-4): the Lower Amazon-Xingu clade was sister to all other lineages (99 BS, 1.0 PP), followed by the Itapecuru clade (69 BS, 0.58 PP) sister to two subclades composed of: 1) Essequibo-Berbice + Marowijne clades (89 BS, 0.96 PP) and 2) Orinoco (Paraná + Upper Amazon/Rupununi) clades (94 BS, 1.0 PP). The subclades were reciprocally monophyletic (77 BS, 0.92 PP). *Pimelodus ornatus* diverged from *P. moli* sometime between the Oligocene to Miocene ~19 mya, with a 95% CI of ~12-27 mya (Figure 3-4). *Pimelodus ornatus* began to diversify rapidly ~5 mya (3-8 mya 95% CI), with the divergence of

the Lower Amazon-Xingu clade between the Miocene and Pliocene. All remaining lineages diversified in the Late Miocene to Pleistocene ~2-5 mya (0.5-6 mya 95% CI).

Discussion

Cryptic lineage diversity of Pimelodus ornatus

We tested the hypothesis that both impermeable and semi-permeable barriers dividing major South American river basins have restricted gene flow between *P. ornatus* subpopulations using our ML phylogeny, fossil-calibrated BI phylogeny, and uncorrected p-distances within and between proposed lineages. We predicted the existence of at least three distinct lineages, corresponding with the Essequibo, Orinoco, and Amazon-Paraná rivers. Our inclusion of 130 *P. ornatus* specimens revealed a minimum of seven distinct lineages within the species, almost all defined by geographic area. In addition to the three lineages proposed by Lundberg et al. (2011) and Tagliacollo et al. (2015), we observed lineages from the Xingu, Itapecuru, and Marowijne rivers, and found evidence for distinct Upper Amazon/Rupununi and Paraná lineages. We included the four *P. ornatus* representatives used by Lundberg et al. (2011) and Tagliacollo et al. (2015) in our ML phylogeny, and found that: a) the Amazon representative grouped within our Upper Amazon/Rupununi clade, b) the Orinoco representative grouped within our Orinoco clade, c) the Paraná representative grouped within our Paraná clade, and d) the Essequibo representative grouped within our Essequibo-Berbice clade. These results support our hypothesis that inter-basin barriers have sufficiently reduced gene flow between subpopulations to allow for diversification within widespread *P. ornatus*, potentially representing undescribed cryptic species.

The uncorrected *p*-distances we calculated between *co1* sequences further support at least seven distinct lineages within *P. ornatus*. Using our ML phylogeny to define the lineages, we

calculated mean genetic distances within and between these clades. Mean intra-lineage genetic distances were <0.40%, with a maximum *p*-distance of 0.99% within the Upper-Amazon/Rupununi clade. In vertebrates, previous studies have indicated that individuals of the same species generally do not exceed 1.00% distance (Herbert et al., 2004; Ward et al., 2005; Li et al., 2018; Tsoupas et al., 2022). Tropical freshwater fishes from the Paraíba do Sul River (Pereira et al., 2011), freshwater fishes from the Lower Paraná River (Díaz et al., 2016), and African freshwater eels (Hanzen et al., 2020) all exhibit mean intraspecific genetic distances <1.00%. Ward et al. (2009) proposed that intraspecific distances >3.0% are likely due to misidentification or unrecognized cryptic species, and that genetic distances >2.00-3.00% likely represent individuals from different species.

Mean inter-lineage distances in our analyses ranged from 1.91 to 5.96%. All inter-lineage distances were >2.40% with the exception of 1.91% between the Upper Amazon/Rupununi and Paraná clades. This could reflect a recent splitting event, given that the *p*-distance between this pair of lineages was close to the 2.00% threshold proposed by Ward et al. (2009). These lineages may be in the process of differentiating, potentially because of limited seasonal dispersal between the Amazon and Paraná rivers. Alternatively, the seasonal connections between the Amazon and Paraná rivers may limit genetic differentiation of these clades through gene flow homogenizing the populations (Slatkin, 1973; Slatkin, 1987; Fitzpatrick et al., 2009; Barrera-Guzmán et al., 2022). Within the Upper Amazon/Rupununi clade, we observed a low mean inter-clade distance of 0.85%, below the 1.00% intraspecific threshold typical of other vertebrates (Herbert et al., 2004; Ward et al., 2005; Li et al., 2018; Tsoupas et al., 2022). Despite the disjunct distribution of these two subclades (Peruvian Amazon and Rupununi savannah), their low inter-

clade distance supports a monophyletic lineage. We discuss potential explanations for the distribution of this lineage below.

Lundberg et al. (2011) calculated the uncorrected *p*-distances between *P. ornatus* representatives included in their phylogeny of Pimelodidae using concatenated sequences combining *rag1*, *rag2*, 12S RNA, tRNA-val, 16S RNA, and *cyt b*, totaling 7,583 nucleotide bases. The *p*-distances between *P. ornatus* representatives estimated by Lundberg et al. (2011) ranged from 0.40 to 1.90%, lower than those we calculated. This is likely due to their inclusion of both mitochondrial and nuclear genes; mitochondrial genes generally evolve more quickly than nuclear genes, and provide better phylogenetic resolution of recently diverged populations and species (Brown et al., 1979; Saccone et al., 2000; Camus et al., 2022). Therefore, the presence of slowly-evolving nuclear genes with fewer nucleotide substitutions may have contributed to the underestimation of genetic distances between *P. ornatus* representatives in previous studies.

Topology of Pimelodus ornatus *species complex*

The evolutionary relationships of the *P. ornatus* lineages were consistent between our ML and fossil-calibrated BI phylogenies. Although we recovered the same topology in both trees, the support values in the BI phylogeny were higher than in the ML phylogeny. This is likely related to the number of genes and outgroups used to construct each tree. The ML phylogeny was built using four genes and 20 outgroup representatives of Pimelodidae, whereas the fossil-calibrated BI phylogeny of Pimelodidae was constructed using ten genes sequenced from 87 representatives of Pimelodidae and 29 additional outgroups selected from closely related catfish families (see Chapter 4). All inter-lineage relationships were strongly supported (0.92-1.0 PP), except the Itapecuru lineage. Both phylogenies placed this clade as sister to all remaining

lineages except the Lower Amazon-Xingu clade with low support (69 BS, 0.58 PP). This Northeast Atlantic lineage comprised eight individuals only represented by *co1* sequences downloaded from BOLD Systems (Ratnasingham & Herbert, 2007), whereas all other lineages contained individuals sequenced in this study. Using the same molecular dataset to create their phylogenies, Lundberg et al. (2011) and Tagliacollo et al. (2015) both found a close, sister pair relationship between *P. ornatus* individuals from the Paraná and Upper Amazon rivers. These individuals were, in turn, sister to the individual from the Orinoco River, corroborating our results. Both studies also placed the individual from the Essequibo River as sister to all remaining *P. ornatus* representatives. We found that the Essequibo-Berbice lineage formed a subclade with the Marowijne clade sister to the Orinoco (Upper Amazon/Rupununi + Paraná) subclade.

We propose that *P. ornatus* diverged from *P. moli* during the Oligocene to Miocene. Our origin estimation of *P. ornatus* is younger than those of Sullivan et al. (2013) and Tagliacollo et al. (2015), who proposed *P. ornatus* originated between the Eocene and Late Oligocene. We believe our younger age estimates more accurately reflect the origins of *P. ornatus* due to our inclusion of the most pimelodid taxa (87 of 116 valid species, Fricke et al., 2023), largest molecular dataset (ten genes, 9,734 nucleotide base pairs), and most comprehensive fossil calibrations (twelve constraints) of any study to date (see Chapter 4). Sullivan et al. (2013) constructed a multigene time-calibrated phylogeny of superfamily Pimelodoidea, including only eight pimelodid representatives (two representatives of *P. ornatus*), four genes (~6,000 nucleotide base pairs), and nine fossil constraints. Tagliacollo et al. (2015) constructed a time-calibrated multigene phylogeny of Pimelodidae using 57 pimelodid representatives (four *P. ornatus* representatives), six genes (7,362 nucleotide base pairs), and three fossil constraints.

Furthermore, neither study included *P. moli*, the closest known relative of *P. ornatus*. The common ancestor of these two species represents a node that was not accounted for in either of the previous studies, possibly contributing to their older age estimations. Both Sullivan et al. (2013) and Tagliacollo et al. (2015), however, proposed that *P. ornatus* began to diversify between the Miocene and Pliocene, corroborating our results.

Evolutionary origins of Pimelodus ornatus *lineages*

It is possible the *P. ornatus* species complex originated somewhere near the contemporary Lower Amazon or Guiana Shield regions. This is supported by two pieces of evidence: a) its sister relationship with *P. moli* and b) the current distributions of the two earliest diverging lineages. *Pimelabditus moli* is endemic to the Marowijne River basin in Suriname and French Guiana, north of the Lower Amazon River basin where the Xingu lineage occurs (Parisi & Lundberg, 2009; Lundberg et al., 2012). The other early diverging lineage within *P. ornatus*, the Itapecuru clade, occurs in Northeastern Brazil, a region that drains into the Atlantic Ocean via the São José Bay (Barros et al., 2011; Nascimento et al., 2016; Soares et al., 2017). The Itapecuru River is dominated by species shared with the Amazon River basin (Barros et al., 2011), implying these rivers were likely hydrologically connected during the Late Miocene to Pleistocene. Furthermore, the Amazon River was divided into easterly and westerly draining rivers separated by the Purús Arch during the Early to Mid-Miocene (Figueiredo et al., 2009; Wesselingh & Hoorn, 2011; Albert et al., 2018a). The Purús Arch maintained the division between these drainage basins until ~11 mya, when the easterly-flowing transcontinental Amazon River was established (Figueiredo et al., 2009; Wesselingh & Hoorn, 2011; Albert et al., 2018a; Abreu et al., 2020), occurring after the proposed split between *P. ornatus* and *P. moli* ~12-27 mya. The current distributions of *P. moli* and the two early *P. ornatus* lineages support

our hypothesis that *P. ornatus* originated near eastern river drainages of South America; however, a formal ancestral area state reconstruction will be required to test this hypothesis.

The ancestor of the first subclade within *P. ornatus*, composed of the Essequibo-Berbice and Marowijne lineages, split from the ancestor of the subclade containing the Orinoco (Upper Amazon/Rupununi + Paraná) lineages ~2.5-5 mya during the Pliocene. These Guiana Shield lineages are partially isolated from Amazonian lineages, with dispersal only possible through the Rupununi Portal during the rainy season (Lujan & Armbruster, 2011; de Souza et al., 2020; Henschel & Lujan, 2021). This semi-permeable barrier has significantly reduced gene flow between these lineages, resulting in mean intra-lineage *p*-distances >4.00%. Historical river-capture events may have provided dispersal opportunities between early Amazonian and Guiana Shield rivers (Lujan & Armbruster, 2011; Silva et al., 2014; Albert et al., 2018a). For example, the Proto-Berbice River paleo-drainage flowed northward into the Atlantic Ocean, connecting headwaters of the Orinoco River, the Branco River (a tributary of the Negro and Amazon rivers), the Essequibo River, and the Berbice River from the Paleocene to possibly the Pliocene or Pleistocene (Lujan & Armbruster, 2011; Lemopoulos & Covain, 2019; Henschel & Lujan, 2021). If this separation occurred during the Pliocene, vicariance via the division of modern rivers comprising the Proto-Berbice may have isolated ancestral populations of *P. ornatus*, resulting in Guiana Shield, Orinoco, and Amazonian lineages. Within the Guiana Shield, previous studies suggested two broad ecoregions based on faunal distributions: a) the western Essequibo region containing (but not limited to) the Essequibo, Berbice, Corantijn rivers and b) an eastern Guianas region containing major rivers of French Guiana, such as the Marowijne River (Fisch-Muller et al., 2018; Lemopoulos & Covain, 2019). The distinct fish assemblages observed in these ecoregions agree with the distinct Essequibo-Berbice and Marowijne *P. ornatus* lineages. Fishes

from the western ecoregion are closely associated with those of the Branco River, further supporting historic faunal exchange between Amazonian and Guianese rivers (Sidlauskas & Vari, 2012; Lemopoulos & Covain, 2019).

Differentiation of the lineages that comprise the Orinoco (Upper Amazon/Rupununi + Paraná) subclade may have coincided with the splitting of the constituent Proto-Berbice rivers. The Orinoco had largely been separated from the Amazon River by uplift of the Vaupés Arch during the Miocene ~8-10 mya (Winemiller & Willis, 2011; Albert et al., 2018a). The Proto-Berbice could have provided dispersal opportunities between river basins before its eventual separation during the Pliocene to Pleistocene (Lujan & Armbruster, 2011; Lemopoulos & Covain, 2019; Henschel & Lujan, 2021). The Orinoco lineage has mean inter-lineage *p*-distances >2.40%, despite the continued connection via the Casiquiare River (Winemiller et al., 2008; Winemiller & Willis, 2011; Stokes et al., 2018). Noteworthy, our analyses included a *P. ornatus* specimen collected from the Casiquiare River, nested within the Orinoco lineage and distinct from the Upper Amazon/Rupununi lineage (>3.00% *p*-distance). A possible explanation for this is the different water chemistries of the Orinoco and Negro rivers. The Orinoco is a clearwater river, characterized by neutral pH and limited quantities of dissolved solids and sediments, whereas the Negro River is a blackwater river, characterized by low pH, high tannin content, and a distinct tea colour (Winemiller et al., 2008; Ríos-Villamizar et al., 2013). Adaptations specific to each of these water types may impede *P. ornatus* populations from mixing and thus prevent gene flow (Winemiller et al., 2008).

Uplift of the Michicola Arch during the Oligocene divided the Upper Amazon River from the Paraná-Paraguay River basin (Carvalho & Albert, 2011; Albert et al., 2018a; Cassemiro et al., 2023). The divergence of the Upper Amazon/Rupununi lineage from the Paraná lineage

occurred well after the establishment of this barrier (Carvalho & Albert, 2011; Albert et al., 2018a; Cassemiro et al., 2023). Therefore, it is likely these lineages began to differentiate following dispersal of the ancestral population across seasonal connections between these basins (Carvalho & Albert, 2011). As previously mentioned, these lineages may be in the process of differentiating, or seasonal dispersal corridors may constrain differentiation.

The Upper Amazon/Rupununi lineage is the only clade not defined by geographic area, distributed in the Peruvian Amazon, Rupununi savannah, and lowland Guyana. We were unable to obtain *P. ornatus* specimens from most of the Amazon River basin, possibly explaining why this lineage exhibits a disjunct distribution. *Pimelodus ornatus* populations from the Middle Amazon and Branco River may belong to this lineage, bridging these subpopulations. Interestingly, other Guyanese fishes, *Skiotocharax meizon* and a subpopulation of *Gymnotus carapo*, are more closely related to Amazonian taxa than to other Guyanese taxa, similar to the Upper Amazon and Rupununi subclades (Presswell et al., 2000; Lehmberg et al., 2018). The two distinct lineages within Guyana (the Upper Amazon/Rupununi and Essequibo-Berbice lineages) have maintained a mean *p*-distance >4.00% despite the absence of physical barriers (documented to co-occur in the Konawaruk River). This indicates assortative mating maintains divisions between these lineages, and future studies should investigate what factors contribute to their reproductive isolation. Finally, the two Amazonian lineages display the highest mean inter-lineage *p*-distance (>5.90%) of any two lineages. Similar to the Orinoco and Upper Amazon/Rupununi lineages, it is possible that water chemistry impedes mixing of these populations. The Xingu is a clearwater river, whereas the Amazon is a whitewater river, characterized by high turbidity and dissolved nutrients (Wittmann et al., 2006; Ríos-Villamizar et al., 2013; Bertassoli Jr. et al., 2017). By collecting *P. ornatus* specimens from the Lower

Amazon near the mouth of the Xingu River, future studies can more accurately assess the distributions of *P. ornatus* lineages and whether water chemistry may act as a barrier to dispersal.

Our next step will be to analyze morphological and anatomical characters of museum-deposited *P. ornatus* voucher specimens. Physical character analyses combined with our molecular analyses will be used to describe each potentially new species formally, possibly resulting in up to six additional species. Furthermore, voucher specimens collected from additional regions may provide useful insights into species distributions and identify other cryptic species within the *P. ornatus* complex.

Conclusion

In this study, we investigated how paleohydrological events have shaped the genetic structure of the widespread ornate pim catfish. We tested the hypothesis that impermeable and semi-permeable barriers between subpopulations of *P. ornatus* have significantly reduced gene flow and resulted in genetic differentiation. We created a phylogeny of 130 *P. ornatus* specimens, fossil-calibrated this phylogeny, and calculated *p*-distances between individuals. We recovered seven distinct lineages strongly defined by geographic location, except for an Upper Amazon/Rupununi clade. These clades exhibited inter-lineage *p*-distances comparable to congeneric species of other vertebrates, indicating a potential need for formal species description. Our next steps will be to conduct an ancestral area state reconstruction to determine areas of origin within the species complex and to analyze morphological data to describe these potentially new species formally.

Tables

Table 3-1 Mean, median, minimum, and maximum intra-lineage uncorrected *co1 p*-distances (%) of seven observed clades within a maximum likelihood phylogeny of *Pimelodus ornatus*. P-distances were analyzed using 127 *co1* sequences, and sample sizes (n) of each lineage are provided below.

	Xingu	Itapecuru	Marowijne	Essequibo-Berbice	Orinoco	Upper Amazon/Rupununi	Paraná
Mean	0.04	0.00	0.00	0.02	0.15	0.38	0.08
Median	0.00	0.00	0.00	0.00	0.15	0.15	0.00
Minimum	0.00	0.00	0.00	0.00	0.00	0.00	0.00
Maximum	0.15	0.00	0.00	0.15	0.30	0.99	0.77
SD[1]	0.07	0.00	0.00	0.05	0.16	0.43	0.13
SE[2]	0.01	0.00	0.00	0.00	0.07	0.06	0.00
n	8	8	11	20	4	11	65

[1] SD = standard deviation

[2] SE = standard error

Table 3-2 Inter-lineage uncorrected *co1 p*-distances (%) between seven observed clades within a maximum likelihood phylogeny of *Pimelodus ornatus*. *P*-distances are presented above the diagonal and standard errors are presented below.

Lineage	Xingu	Itapecuru	Marowijne	Essequibo-Berbice	Orinoco	Upper Amazon/Rupununi	Paraná
Xingu	*	5.80	5.26	4.76	5.73	5.96	4.87
Itapecuru	0.01	*	4.17	4.83	5.54	5.89	4.68
Marowijne	0.01	0.00	*	2.83	4.41	4.11	2.70
Essequibo-Berbice	0.00	0.00	0.00	*	4.09	4.22	3.00
Orinoco	0.02	0.03	0.02	0.01	*	3.18	2.44
Upper Amazon/Rupununi	0.08	0.06	0.02	0.04	0.05	*	1.91
Paraná	0.00	0.00	0.00	0.00	0.01	0.01	*

Figures

Figure 3-1 Distribution map of *Pimelodus ornatus* within South America created using SimpleMappr (Shorthouse, 2010). Occurrence data was assembled from Ferraris, Jr. (2007), Fricke et al. (2023), and GBIF.org (2023a).

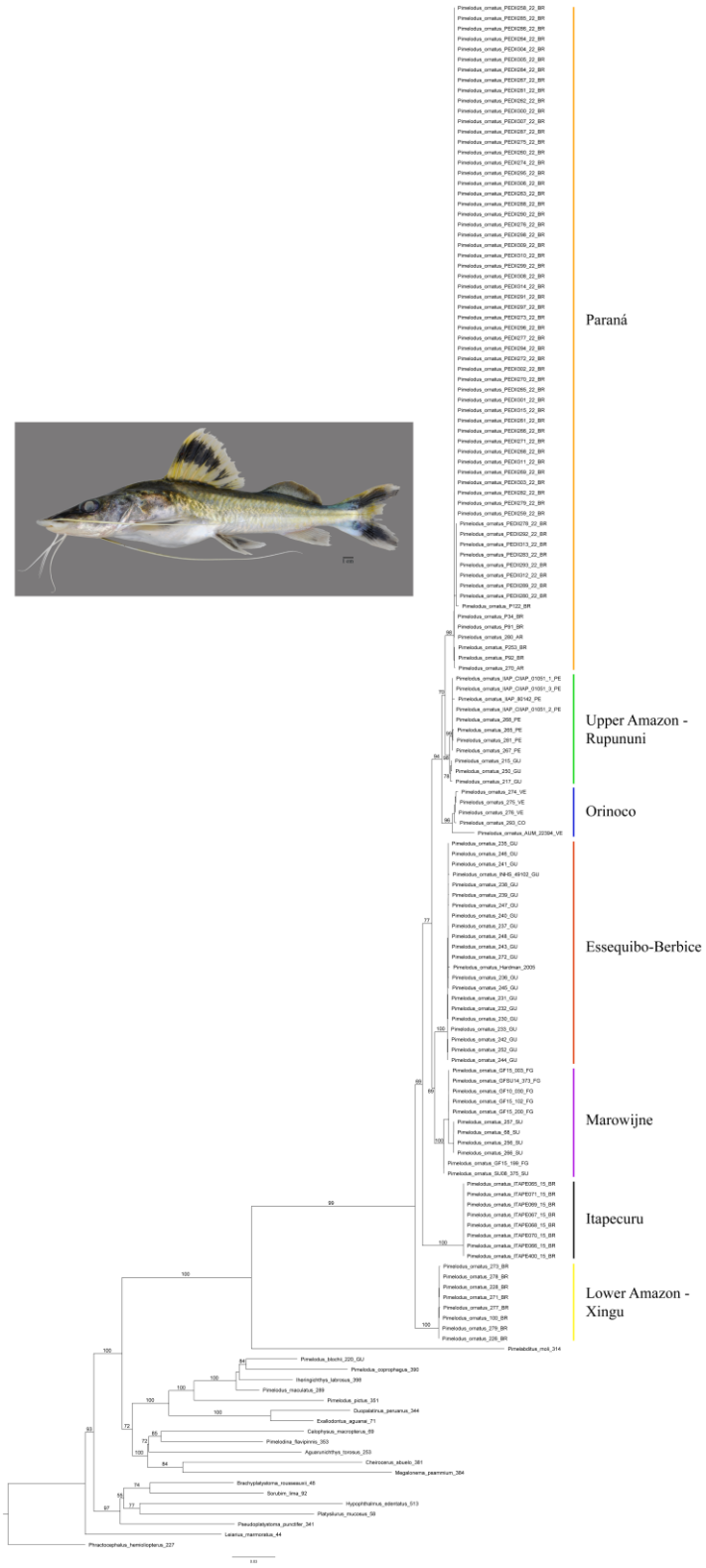

Figure 3-2 Maximum likelihood phylogeny of *Pimelodus ornatus* using a four-gene concatenated data matrix using IQ-TREE (Minh et al., 2020). Bootstrap values ≥ 50% are presented above each branch, and lineage names provided right of the specific epithets.

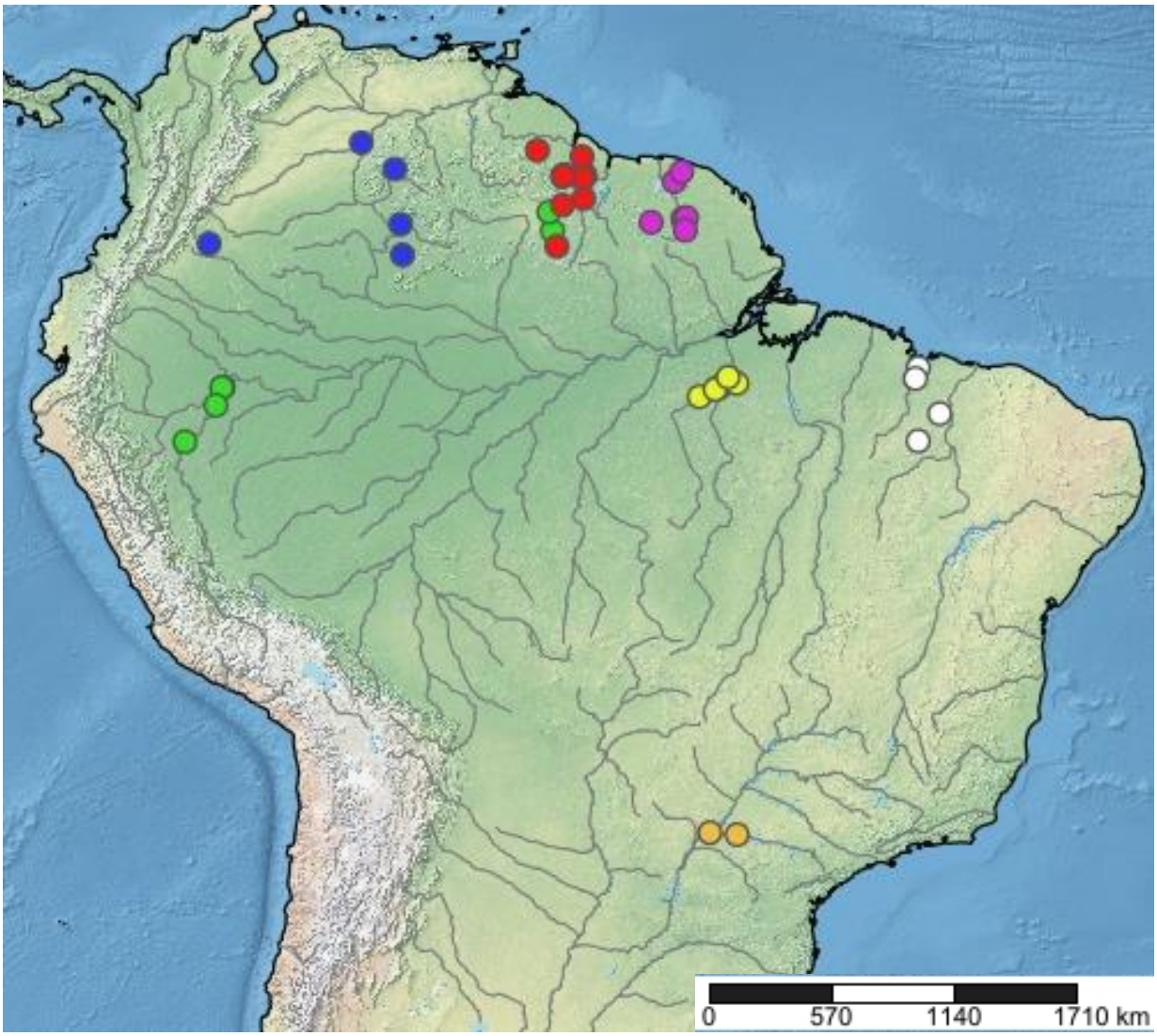

Figure 3-3 Distribution of *Pimelodus ornatus* sample sites in major river basins of South America. Seven major lineages observed within *P. ornatus* are distinguished by colour: yellow = Lower Amazon-Xingu, white = Itapecuru, purple = Marowijne, red = Essequibo-Berbice, blue = Orinoco, green = Upper Amazon/Rupununi, and orange = Paraná. Distribution map created using SimpleMappr (Shorthouse, 2010).

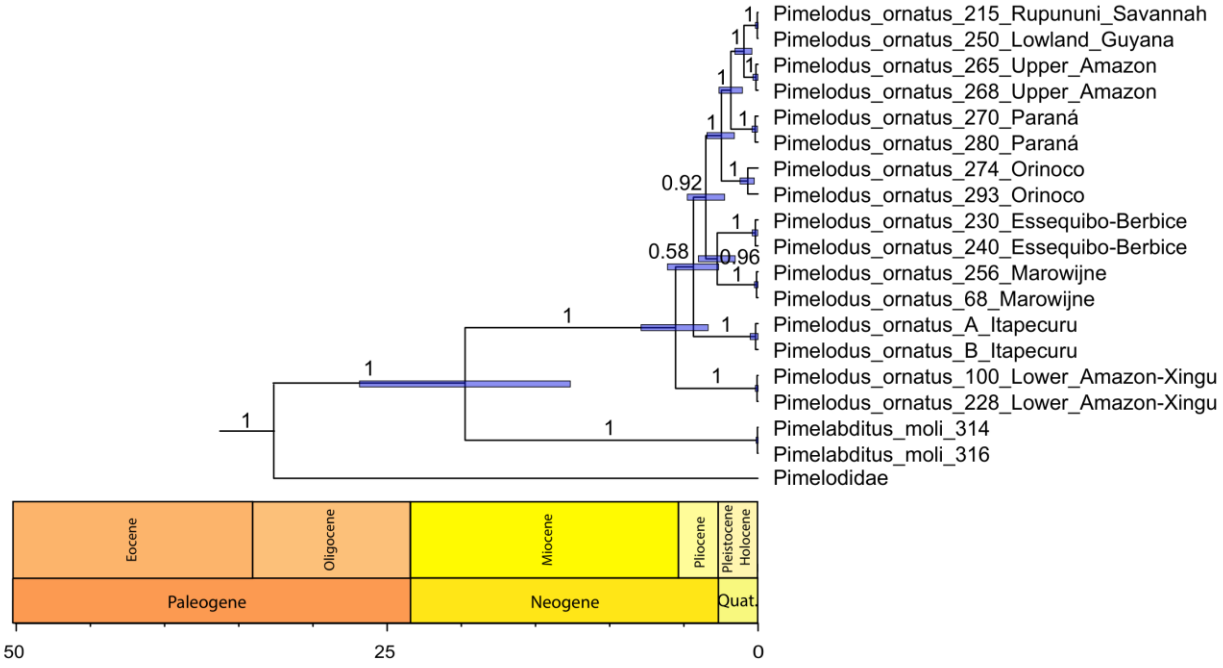

Figure 3-4 Fossil-calibrated Bayesian inference phylogeny of *Pimelodus ornatus* using a ten-gene concatenated data matrix. The phylogeny was created using the CladeAge package in BEAST2 (Matschiner et al., 2017), and divergence times were estimated using twelve fossil constraints. Posterior probabilities ≥ 0.5 are presented above each branch and blue node bars represent the 95% confidence interval of estimated origin times. Geological scale axis measured in million years before present.

Supplemental Material for Chapter 3

Table 3-S1 Museum voucher data for 130 Pimelodus ornatus specimens and 20 pimelodid outgroup species. Lineage abbreviations are as follows: XI = Lower Amazon – Xingu, IT = Itapecuru, MA = Marowijne, EB = Essequibo-Berbice, OR = Orinoco, AR = Upper Amazon/Rupununi, and PA = Paraná.

Species	Lineage	Specimen Label	Museum Voucher Number	Locality	Latitude/Longitude
Pimelodus ornatus Kner, 1858	XI	F100	ANSP 199580	Xingu River, Brazil	S03°36'29.3" W052°20'57.2"
Pimelodus ornatus Kner, 1858	XI	F226	ROM Tissue	Mouth of Iriri River, Brazil	S03°48'53.0" W052°37'09.0"
Pimelodus ornatus Kner, 1858	XI	F228	ROM Tissue	Rapids at Barinha, Brazil	S04°09'44.0" W053°23'04.0"
Pimelodus ornatus Kner, 1858	XI	F271	ANSP 193050	Xingu River, Brazil	S03°39'19.4" W052°23'30.1"
Pimelodus ornatus Kner, 1858	XI	F273	INPA 40000	Iriri River, Brazil	S03°49'24.5" W052°40'42.8"
Pimelodus ornatus Kner, 1858	XI	F277	INPA 43508	Xingu River, Brazil	S03°35'55.8" W051°49'57.4"
Pimelodus ornatus Kner, 1858	XI	F278	ANSP 196909	Iriri River, Brazil	S03°51'19.1" W052°43'43.5"
Pimelodus ornatus Kner, 1858	XI	F279	ANSP 198100	Xingu River, Brazil	S03°20'31.2" W052°11'09.8"
Pimelodus ornatus Kner, 1858	IT	ITAPE065-15	UEMA 104565	Itapecuru River, Brazil	S02°56'23.0" W044°14'26.0"
Pimelodus ornatus Kner, 1858	IT	ITAPE066-15	UEMA 104565	Itapecuru River, Brazil	S02°56'23.0" W044°14'26.0"
Pimelodus ornatus Kner, 1858	IT	ITAPE067-15	UEMA 104565	Itapecuru River, Brazil	S04°52'28.0" W043°20'48.0"
Pimelodus ornatus Kner, 1858	IT	ITAPE068-15	UEMA 104565	Itapecuru River, Brazil	S02°56'23.0" W044°14'26.0"
Pimelodus ornatus Kner, 1858	IT	ITAPE069-15	UEMA 104565	Itapecuru River, Brazil	S06°01'32.0" W044°14'57.0"

Pimelodus ornatus Kner, 1858	IT	ITAPE070-15	UEMA 104565	Itapecuru River, Brazil	S06°01'32.0" W044°14'57.0"
Pimelodus ornatus Kner, 1858	IT	ITAPE071-15	UEMA 104565	Itapecuru River, Brazil	S06°01'32.0" W044°14'57.0"
Pimelodus ornatus Kner, 1858	IT	ITAPE400-15	UEMA 104572	Itapecuru River, Brazil	S03°23'42.0" W044°21'35.0"
Pimelodus ornatus Kner, 1858	MA	F68	ANSP 187113	Lawa River, Suriname	N03°19'31.0" W054°03'48.0"
Pimelodus ornatus Kner, 1858	MA	F256	ROM 100852	Marowijne River, Suriname	N04°54'25.0" W054°26'22.0"
Pimelodus ornatus Kner, 1858	MA	F257	ROM 100852	Marowijne River, Suriname	N04°54'25.0" W054°26'22.0"
Pimelodus ornatus Kner, 1858	MA	F266	ANSP 187113	Lawa River, Suriname	N03°19'31.0" W054°03'48.0"
Pimelodus ornatus Kner, 1858	MA	GF10-030	MHNG 2721.079	Serpent Creek, Maroni River, French Guiana	N05°19'00.0" W054°07'59.0"
Pimelodus ornatus Kner, 1858	MA	GF15-003	MHNG Tissue	Lawa River, French Guiana	N03°22'59.0" W054°03'19.0"
Pimelodus ornatus Kner, 1858	MA	GF15-102	MHNG Tissue	Lawa River, French Guiana	N03°22'59.0" W054°03'19.0"
Pimelodus ornatus Kner, 1858	MA	GF15-199	MHNG Tissue	Tampok River, French Guiana	N03°23'24.0" W053°55'33.0"
Pimelodus ornatus Kner, 1858	MA	GF15-200	MHNG Tissue	Tampok River, French Guiana	N03°23'24.0" W053°55'33.0"
Pimelodus ornatus Kner, 1858	MA	GFSU14-373	MHNG Tissue	Marouini River, French Guiana	N02°51'30.0" W053°58'38.0"
Pimelodus ornatus Kner, 1858	MA	SU08-375	MHNG Tissue	Paloemeu River, Suriname	N03°11'53.0" W055°24'26.0"
Pimelodus ornatus Kner, 1858	EB	F230	ROM 87121	Mappa Lagoon camp, Guyana	N05°10'28.0" W058°09'48.0"
Pimelodus ornatus Kner, 1858	EB	F231	ROM 87208	Upper Demerara-Berbice, Guyana	N05°04'19.0" W058°15'19.0"

Pimelodus ornatus Kner, 1858	EB	F232	ROM 87208	Upper Demerara-Berbice, Guyana	N05°04'19.0" W058°15'19.0"
Pimelodus ornatus Kner, 1858	EB	F233	ROM 87151	East Berbice – Corentyne, Guyana	N04°11'12.0" W058°13'17.0"
Pimelodus ornatus Kner, 1858	EB	F235	ROM 96132	Stream mouth along Kuyuwini River, Guyana	N02°10'53.7" W059°20'51.3"
Pimelodus ornatus Kner, 1858	EB	F236	ROM 96132	Stream mouth along Kuyuwini River, Guyana	N02°10'53.7" W059°20'51.3"
Pimelodus ornatus Kner, 1858	EB	F237	ROM 96132	Stream mouth along Kuyuwini River, Guyana	N02°10'53.7" W059°20'51.3"
Pimelodus ornatus Kner, 1858	EB	F238	ROM 96132	Stream mouth along Kuyuwini River, Guyana	N02°10'53.7" W059°20'51.3"
Pimelodus ornatus Kner, 1858	EB	F239	ROM 96132	Stream mouth along Kuyuwini River, Guyana	N02°10'53.7" W059°20'51.3"
Pimelodus ornatus Kner, 1858	EB	F240	ROM 96132	Stream mouth along Kuyuwini River, Guyana	N02°10'53.7" W059°20'51.3"
Pimelodus ornatus Kner, 1858	EB	F241	ROM 96132	Stream mouth along Kuyuwini River, Guyana	N02°10'53.7" W059°20'51.3"
Pimelodus ornatus Kner, 1858	EB	F242	ROM 96132	Stream mouth along Kuyuwini River, Guyana	N02°10'53.7" W059°20'51.3"
Pimelodus ornatus Kner, 1858	EB	F243	ROM 96132	Stream mouth along Kuyuwini River, Guyana	N02°10'53.7" W059°20'51.3"
Pimelodus ornatus Kner, 1858	EB	F244	ROM 96257	Stream mouth along Kuyuwini River, Guyana	N02°10'53.7" W059°20'51.3"
Pimelodus ornatus Kner, 1858	EB	F245	ROM 81643	Konawaruk River, Guyana	N05°07'14.0" W059°06'38.0"
Pimelodus ornatus Kner, 1858	EB	F246	ROM 81643	Konawaruk River, Guyana	N05°07'14.0" W059°06'38.0"
Pimelodus ornatus Kner, 1858	EB	F247	ROM 81643	Konawaruk River, Guyana	N05°07'14.0" W059°06'38.0"
Pimelodus ornatus Kner, 1858	EB	F248	ROM 96885	Creek on road east of NARIL camp, Guyana	N05°08'26.0" W059°04'21.0"

Pimelodus ornatus Kner, 1858	EB	F252	ROM 97485	Mouth of Kurupung River, Guyana	N06°13'19.0" W060°09'04.0"
Pimelodus ornatus Kner, 1858	EB	F272	AUM 36051	Rupununi River, Guyana	N03°55'03.0" W059°06'01.0"
Pimelodus ornatus Kner, 1858	EB	Hardman 2005	INHS 49102	Demerara River, Guyana	N05°57'39.5" W058°17'43.2"
Pimelodus ornatus Kner, 1858	EB	INHS 49102	INHS 49102	Demerara River, Guyana	N05°57'39.5" W058°17'43.2"
Pimelodus ornatus Kner, 1858	OR	F274	AUM 41487	Manapiare River, Venezuela	N05°26'12.0" W066°06'45.0"
Pimelodus ornatus Kner, 1858	OR	F275	AUM 43632	Siapa River (Casiquiare drainage), Venezuela	N01°49'00.0" W065°47'41.0"
Pimelodus ornatus Kner, 1858	OR	F276	AUM 43339	Casiquiare River, Venezuela	N03°06'50.0" W065°52'38.0"
Pimelodus ornatus Kner, 1858	OR	F293	IAvHP Tissue	Guayabero River, Colombia	N02°17'35.6" W073°52'32.9"
Pimelodus ornatus Kner, 1858	OR	AUM 22394	AUM 22394	Cinaruco River, Orinoco drainage, Venezuela	N06°32'44.0" W067°30'24.0"
Pimelodus ornatus Kner, 1858	AR	F215	ROM 86203	Rupununi River at Dadanawa, Guyana	N02°49'54.0" W059°31'41.0"
Pimelodus ornatus Kner, 1858	AR	F217	ROM 86350	North of Lethem at Pirara, Guyana	N03°37'17.0" W059°40'29.0"
Pimelodus ornatus Kner, 1858	AR	F250	ROM 96990	Konawaruk River, Guyana	N05°12'05.0" W059°02'18.0"
Pimelodus ornatus Kner, 1858	AR	F265	ANSP 178452	Nanay River at Pampa Chica, Peru	S03°45'09.0" W073°17'00.0"
Pimelodus ornatus Kner, 1858	AR	F267	ANSP 181099	Nanay River, vicinity of Santa Clara, Peru	S03°46'56.0" W073°20'33.0"
Pimelodus ornatus Kner, 1858	AR	F268	ANSP 181099	Nanay River, vicinity of Santa Clara, Peru	S03°46'56.0" W073°20'33.0"
Pimelodus ornatus Kner, 1858	AR	F281	ANSP 178452	Nanay River at Pampa Chica, Peru	S03°45'09.0" W073°17'00.0"

Pimelodus ornatus Kner, 1858	AR	IIAP 80142	LBGM IIAP 80142	Marañón River, Amazon drainage, Peru	S04°31'18.9" W073°35'14.9"
Pimelodus ornatus Kner, 1858	AR	IIAP-CIIAP-01051-1	LBGM IIAP-CIIAP-01051-1	Ucayali River, Amazon drainage, Peru	S06°03'36.0" W074°52'48.0"
Pimelodus ornatus Kner, 1858	AR	IIAP-CIIAP-01051-2	LBGM IIAP-CIIAP-01051-2	Ucayali River, Amazon drainage, Peru	S06°03'36.0" W074°52'48.0"
Pimelodus ornatus Kner, 1858	AR	IIAP-CIIAP-01051-3	LBGM IIAP-CIIAP-01051-3	Ucayali River, Amazon drainage, Peru	S06°03'36.0" W074°52'48.0"
Pimelodus ornatus Kner, 1858	PA	F270	MLP Tissue	Purchased from aquarium in Corrientes, Argentina	N/A N/A
Pimelodus ornatus Kner, 1858	PA	F280	MLP 5131	Paraná River near town of Perichon, Argentina	N/A N/A
Pimelodus ornatus Kner, 1858	PA	P34	UEMS P34	Possibly near UEMS Aquidauana, Brazil	N/A N/A
Pimelodus ornatus Kner, 1858	PA	P91	UEMS P91	Possibly near UEMS Aquidauana, Brazil	N/A N/A
Pimelodus ornatus Kner, 1858	PA	P92	UEMS P92	Possibly near UEMS Aquidauana, Brazil	N/A N/A
Pimelodus ornatus Kner, 1858	PA	P122	UEMS P122	Possibly near UEMS Aquidauana, Brazil	N/A N/A
Pimelodus ornatus Kner, 1858	PA	P253	UEMS P253	Possibly near UEMS Aquidauana, Brazil	N/A N/A
Pimelodus ornatus Kner, 1858	PA	PEDII258-22	UEL Tissue	Paranapanema River in Rosana, Brazil	S22°31'49.8" W052°56'54.6"
Pimelodus ornatus Kner, 1858	PA	PEDII259-22	UEL Tissue	Paranapanema River in Rosana, Brazil	S22°31'49.8" W052°56'54.6"
Pimelodus ornatus Kner, 1858	PA	PEDII260-22	UEL Tissue	Paranapanema River in Rosana, Brazil	S22°31'49.8" W052°56'54.6"
Pimelodus ornatus Kner, 1858	PA	PEDII261-22	UEL Tissue	Paranapanema River in Rosana, Brazil	S22°31'49.8" W052°56'54.6"
Pimelodus ornatus Kner, 1858	PA	PEDII262-22	UEL Tissue	Paranapanema River in Rosana, Brazil	S22°31'49.8" W052°56'54.6"

Pimelodus ornatus Kner, 1858	PA	PEDII263-22	UEL Tissue	Paranapanema River in Rosana, Brazil	S22°31'49.8" W052°56'54.6"
Pimelodus ornatus Kner, 1858	PA	PEDII264-22	UEL Tissue	Paranapanema River in Rosana, Brazil	S22°31'49.8" W052°56'54.6"
Pimelodus ornatus Kner, 1858	PA	PEDII265-22	UEL Tissue	Paranapanema River in Rosana, Brazil	S22°31'49.8" W052°56'54.6"
Pimelodus ornatus Kner, 1858	PA	PEDII266-22	UEL Tissue	Paranapanema River in Rosana, Brazil	S22°31'49.8" W052°56'54.6"
Pimelodus ornatus Kner, 1858	PA	PEDII267-22	UEL Tissue	Paranapanema River in Rosana, Brazil	S22°31'49.8" W052°56'54.6"
Pimelodus ornatus Kner, 1858	PA	PEDII268-22	UEL Tissue	Paranapanema River in Rosana, Brazil	S22°31'49.8" W052°56'54.6"
Pimelodus ornatus Kner, 1858	PA	PEDII269-22	UEL Tissue	Paranapanema River in Rosana, Brazil	S22°31'49.8" W052°56'54.6"
Pimelodus ornatus Kner, 1858	PA	PEDII270-22	UEL Tissue	Paranapanema River in Rosana, Brazil	S22°31'49.8" W052°56'54.6"
Pimelodus ornatus Kner, 1858	PA	PEDII271-22	UEL Tissue	Paranapanema River in Rosana, Brazil	S22°31'49.8" W052°56'54.6"
Pimelodus ornatus Kner, 1858	PA	PEDII272-22	UEL Tissue	Paranapanema River in Rosana, Brazil	S22°31'49.8" W052°56'54.6"
Pimelodus ornatus Kner, 1858	PA	PEDII273-22	UEL Tissue	Paranapanema River in Rosana, Brazil	S22°31'49.8" W052°56'54.6"
Pimelodus ornatus Kner, 1858	PA	PEDII274-22	UEL Tissue	Paranapanema River in Rosana, Brazil	S22°31'49.8" W052°56'54.6"
Pimelodus ornatus Kner, 1858	PA	PEDII275-22	UEL Tissue	Paranapanema River in Rosana, Brazil	S22°31'49.8" W052°56'54.6"
Pimelodus ornatus Kner, 1858	PA	PEDII276-22	UEL Tissue	Paranapanema River in Rosana, Brazil	S22°31'49.8" W052°56'54.6"
Pimelodus ornatus Kner, 1858	PA	PEDII277-22	UEL Tissue	Paranapanema River in Rosana, Brazil	S22°31'49.8" W052°56'54.6"
Pimelodus ornatus Kner, 1858	PA	PEDII278-22	UEL Tissue	Paranapanema River in Rosana, Brazil	S22°31'49.8" W052°56'54.6"

Pimelodus ornatus Kner, 1858	PA	PEDII279-22	UEL Tissue	Paranapanema River in Rosana, Brazil	S22°31'49.8" W052°56'54.6"
Pimelodus ornatus Kner, 1858	PA	PEDII280-22	UEL Tissue	Paranapanema River in Rosana, Brazil	S22°31'49.8" W052°56'54.6"
Pimelodus ornatus Kner, 1858	PA	PEDII281-22	UEL Tissue	Paranapanema River in Rosana, Brazil	S22°31'49.8" W052°56'54.6"
Pimelodus ornatus Kner, 1858	PA	PEDII282-22	UEL Tissue	Paranapanema River in Rosana, Brazil	S22°31'49.8" W052°56'54.6"
Pimelodus ornatus Kner, 1858	PA	PEDII283-22	UEL Tissue	Paranapanema River in Rosana, Brazil	S22°31'49.8" W052°56'54.6"
Pimelodus ornatus Kner, 1858	PA	PEDII284-22	UEL Tissue	Paranapanema River in Rosana, Brazil	S22°31'49.8" W052°56'54.6"
Pimelodus ornatus Kner, 1858	PA	PEDII285-22	UEL Tissue	Paranapanema River in Rosana, Brazil	S22°31'49.8" W052°56'54.6"
Pimelodus ornatus Kner, 1858	PA	PEDII286-22	UEL Tissue	Paranapanema River in Rosana, Brazil	S22°31'49.8" W052°56'54.6"
Pimelodus ornatus Kner, 1858	PA	PEDII287-22	UEL Tissue	Paranapanema River in Rosana, Brazil	S22°31'49.8" W052°56'54.6"
Pimelodus ornatus Kner, 1858	PA	PEDII288-22	UEL Tissue	Paranapanema River in Rosana, Brazil	S22°31'49.8" W052°56'54.6"
Pimelodus ornatus Kner, 1858	PA	PEDII289-22	UEL Tissue	Paranapanema River in Rosana, Brazil	S22°31'49.8" W052°56'54.6"
Pimelodus ornatus Kner, 1858	PA	PEDII290-22	UEL Tissue	Paranapanema River in Rosana, Brazil	S22°31'49.8" W052°56'54.6"
Pimelodus ornatus Kner, 1858	PA	PEDII291-22	UEL Tissue	Paranapanema River near Taquaruçu River, Brazil	S22°36'57.8" W051°48'59.9"
Pimelodus ornatus Kner, 1858	PA	PEDII292-22	UEL Tissue	Paranapanema River near Taquaruçu River, Brazil	S22°36'57.8" W051°48'59.9"
Pimelodus ornatus Kner, 1858	PA	PEDII293-22	UEL Tissue	Paranapanema River near Taquaruçu River, Brazil	S22°36'57.8" W051°48'59.9"
Pimelodus ornatus Kner, 1858	PA	PEDII294-22	UEL Tissue	Paranapanema River near Taquaruçu River, Brazil	S22°36'57.8" W051°48'59.9"

Pimelodus ornatus Kner, 1858	PA	PEDII295-22	UEL Tissue	Paranapanema River near Taquaruçu River, Brazil	S22°36'57.8" W051°48'59.9"
Pimelodus ornatus Kner, 1858	PA	PEDII296-22	UEL Tissue	Paranapanema River near Taquaruçu River, Brazil	S22°36'57.8" W051°48'59.9"
Pimelodus ornatus Kner, 1858	PA	PEDII297-22	UEL Tissue	Paranapanema River near Taquaruçu River, Brazil	S22°36'57.8" W051°48'59.9"
Pimelodus ornatus Kner, 1858	PA	PEDII298-22	UEL Tissue	Paranapanema River near Taquaruçu River, Brazil	S22°36'57.8" W051°48'59.9"
Pimelodus ornatus Kner, 1858	PA	PEDII299-22	UEL Tissue	Paranapanema River near Taquaruçu River, Brazil	S22°36'57.8" W051°48'59.9"
Pimelodus ornatus Kner, 1858	PA	PEDII300-22	UEL Tissue	Paranapanema River near Taquaruçu River, Brazil	S22°36'57.8" W051°48'59.9"
Pimelodus ornatus Kner, 1858	PA	PEDII301-22	UEL Tissue	Paranapanema River in Rosana, Brazil	S22°31'49.8" W052°56'54.6"
Pimelodus ornatus Kner, 1858	PA	PEDII302-22	UEL Tissue	Paranapanema River in Rosana, Brazil	S22°31'49.8" W052°56'54.6"
Pimelodus ornatus Kner, 1858	PA	PEDII303-22	UEL Tissue	Paranapanema River in Rosana, Brazil	S22°31'49.8" W052°56'54.6"
Pimelodus ornatus Kner, 1858	PA	PEDII304-22	UEL Tissue	Paranapanema River in Rosana, Brazil	S22°31'49.8" W052°56'54.6"
Pimelodus ornatus Kner, 1858	PA	PEDII305-22	UEL Tissue	Paranapanema River in Rosana, Brazil	S22°31'49.8" W052°56'54.6"
Pimelodus ornatus Kner, 1858	PA	PEDII306-22	UEL Tissue	Paranapanema River in Rosana, Brazil	S22°31'49.8" W052°56'54.6"
Pimelodus ornatus Kner, 1858	PA	PEDII307-22	UEL Tissue	Paranapanema River in Rosana, Brazil	S22°31'49.8" W052°56'54.6"
Pimelodus ornatus Kner, 1858	PA	PEDII308-22	UEL Tissue	Paranapanema River in Rosana, Brazil	S22°31'49.8" W052°56'54.6"
Pimelodus ornatus Kner, 1858	PA	PEDII309-22	UEL Tissue	Paranapanema River in Rosana, Brazil	S22°31'49.8" W052°56'54.6"
Pimelodus ornatus Kner, 1858	PA	PEDII310-22	UEL Tissue	Paranapanema River in Rosana, Brazil	S22°31'49.8" W052°56'54.6"

Pimelodus ornatus Kner, 1858	PA	PEDII311-22	UEL Tissue	Paranapanema River in Rosana, Brazil	S22°31'49.8" W052°56'54.6"
Pimelodus ornatus Kner, 1858	PA	PEDII312-22	UEL Tissue	Paranapanema River near Taquaruçu River, Brazil	S22°36'57.8" W051°48'59.9"
Pimelodus ornatus Kner, 1858	PA	PEDII313-22	UEL Tissue	Paranapanema River near Taquaruçu River, Brazil	S22°36'57.8" W051°48'59.9"
Pimelodus ornatus Kner, 1858	PA	PEDII314-22	UEL Tissue	Paranapanema River near Taquaruçu River, Brazil	S22°36'57.8" W051°48'59.9"
Pimelodus ornatus Kner, 1858	PA	PEDII315-22	UEL Tissue	Paranapanema River near Taquaruçu River, Brazil	S22°36'57.8" W051°48'59.9"
Aguarunichthys torosus Stewart, 1986		F253	ROM 100218	Dué River, Amazon drainage, Ecuador	N00°00'12.0" W077°24'05.0"
Brachyplatystoma rousseauxii (Castelnau, 1855)		F48	ANSP 187109	Purchased from market in Paramaribo, Suriname	N/A N/A
Calophysus macropterus (Lichtenstein, 1819)		F69	ANSP 182754	Amazon River, vicinity of Iquitos, Peru	S03°40'36.0" W073°14'37.0"
Cheirocerus abuelo (Schultz, 1944)		F381	ANSP/CZUT	Sardinata River, Catutumbo, Colombia	N08°36'24.2" W072°37'45.8"
Duopalatinus peruanus Eigenmann & Allen, 1942		F344	ANSP 198892	Portuguesa River, Venezuela	N07°56'10.6" W067°32'20.4"
Exallodontus aguanai Lundberg, Mago-Leccia and Nass, 1991		F71	ANSP 180947	Amazon River, vicinity of Iquitos, Peru	S03°40'36.0" W073°14'37.0"
Hypophthalmus edentatus Spix & Agassiz, 1829		F513	MPEG Tissue	Tocantins River, Brazil	S05°20'11.9" W48°51'15.5"
Iheringichthys labrosus (Lütken, 1874)		F398	ANSP 203185	La Plata River, Uruguay	S34°26'17.8" W057°52'45.9"
Leiarius marmoratus (Gill, 1870)		F44	ANSP 178109	Purchased from fishermen in Iquitos, Peru	N/A N/A
Megalonema psammium Schultz, 1944		F384	ANSP/CZUT	Zulia River, Colombia	N/A N/A

Phractocephalus hemioliopterus (Bloch and Schneider, 1801)	F227	ROM Tissue	Curapé Island, Brazil	S04°06'52.0" W053°22'27.0"
Pimelabditus moli Parisi & Lundberg, 2009	F314	MHNG 2709.099	Paloemeu River, Suriname	N03°11'54.0" W055°24'24.0"
Pimelodina flavipinnis Steindachner, 1876	F353	ANSP 198936	Apure River, Venezuela	N07°53'55.3" W067°27'32.0"
Pimelodus blochii Valenciennes, 1840	F220	ROM 86545	Creek near Georgetown and Parika, Guyana	N/A N/A
Pimelodus coprophagus Schultz, 1944	F390	ANSP/CZUT	Quebrada Agualasal, Zulia River, Colombia	N08°13'24.9" W072°32'00.7"
Pimelodus maculatus Lacepède, 1803	F289	MZUSP 78460	Brazil	N/A N/A
Pimelodus pictus Steindachner, 1876	F351	ANSP 198956	Apure River, Venezuela	N07°54'02.3" W067°29'27.9"
Platysilurus mucosus (Vaillant, 1880)	F58	ANSP 178509	Purchased at Belem market, Iquitos, Peru	N/A N/A
Pseudoplatystoma punctifer (Castelnau, 1855)	F341	INPA 52557	Xingu River, Brazil	S03°33'44.8" W052°23'30.6"
Sorubim lima (Bloch & Schneider, 1801)	F92	ANSP 179842	Moena Cano & mouth of Ullpa Cano, Iquitos, Peru	S03°46'19.0" W073°14'16.0"

Table 3-S2 Best IQ-TREE nucleotide substitution models found using the Corrected Akaike Information Criterion for 30 gene partitions of the concatenated *Pimelodus ornatus* alignment.

Nucleotide substitution model	**Gene partitions**
HKY + F	*enc1*_pos3
HKY + F + G4	*co1*_pos3
JC	*co1*_pos2
K2P	*glyt*_pos2
K2P + G4	*rag2*_pos1
K2P + I	*rag2*_pos2, *rag2*_pos3
TIM2 + F + G4	*cyt b*_pos2
TN + F + I	*cyt b*_pos1, *enc1*_pos2
TNe + G4	*co1*_pos1, *cyt b*_pos3, *enc1*_pos1

Chapter 4

The influence of Andean uplift and river capture on the origins and evolution of Neotropical long-whiskered catfishes (Pimelodidae, Siluriformes)

Abstract

The Neotropical rainforest boasts the greatest biodiversity of any ecosystem on Earth. One defining geological process that contributed to this great diversity was the uplift of the Andean mountains, changing the South American landscape dramatically. The shifting landscape altered gene flow, presented unique selective pressures, and subjected organisms to stochastic events. Therefore, biologists seek to understand how these dramatic events influenced the genetic landscape of the hyper-diverse Neotropical species assemblage. Orogenesis and subsequent river capture resulting from migrating river boundaries have been proposed to elevate rates of speciation and extinction, but evolutionary changes are largely taxon-specific. Our goal was to investigate how Andean uplift influenced speciation and cladogenesis within the long-whiskered catfish family Pimelodidae. To do this, we created a time-calibrated phylogeny of Pimelodidae using ten genes and 87 of the 116 extant species within the family. We calibrated our phylogeny using twelve fossils and estimated divergence times. We proposed Pimelodidae originated between the Late Cretaceous and the Eocene. We recovered most pre-existing pimelodid clades with strong support; however, we found evidence for eight subclades within the "*Pimelodus*" *ornatus – Calophysus – Pimelodus* clade, splitting previous groups and creating a novel "*Pimelodus*" *grosskopfii* group comprised of trans-Andean species. Several genera, including *Leiarius*, *Brachyplatystoma*, *Propimelodus*, *Duopalatinus*, *Iheringichthys*, and *Pimelodus*, were paraphyletic or polyphyletic. We found evidence that Andean uplift may have contributed to speciation events within Pimelodidae following final separation of modern river basins. One trans-Andean clade, however, diverged from cis-Andean species prior to uplift of the Mérida Cordillera and the Eastern Cordillera, suggesting ecological factors and selective pressures may have influenced their evolution. Our next step will be to conduct an ancestral area state

reconstruction to determine where speciation events most likely occurred, and test which vicariance and dispersal models best fit the updated phylogeny.

Introduction

Evolutionary biology and biogeography are built upon the premise that the evolution and distribution of species are directly influenced by landscape and geography, among other factors (Grinnell, 1924; Humphries & Parenti, 1999; Kozak et al., 2008; Heads, 2015; Edwards et al., 2022). The physical environment may act as a bridge or barrier between populations, may provide unique selective pressures in different regions, and may subject organisms to stochastic events (Manel et al., 2003; Pearson et al., 2009; Krewenka et al., 2011; Kreyling et al., 2011; Rocha-Mendéz et al., 2019). Although landscape and geography appear relatively constant throughout the lifespan of most organisms, the Earth's surface is a dynamic system that has changed dramatically over the course of geological history (Murray et al., 2009; Flament et al., 2013; Duarte, 2022). Operating at a scale of thousands to millions of years, phenomena such as continental drift, orogenesis, and glaciation occur slowly (Grinnell, 1924; Brunsden & Thornes, 1979; Benton, 2009; Gingerich, 2021; Duarte, 2022). Nevertheless, these changes play a fundamental role in shaping biodiversity across the tree of life (Santucci, 2005; Hoorn et al., 2013; Li et al., 2015; Cauvy-Fraunié et al., 2019). Therefore, it is important to consider both contemporary and historical evidence when elucidating the evolutionary history of species (Harvey & Pagel, 1991; Davies et al., 2011; Li et al., 2015).

The well-documented geological and hydrological history of South America combined with the presence of the Neotropical rainforest, one of the most diverse ecosystems on Earth (Hoorn et al., 2010; Albert et al., 2018a; Antonelli et al., 2018; Rocha-Mendéz et al., 2019; Bedoya et al., 2021), provides an excellent opportunity to elucidate the influence of geomorphological changes on evolutionary processes. Following its split from Africa during the Cretaceous (Dietz & Holden, 1970; Lundberg et al., 1998; Hoorn et al., 2010; Wesselingh &

Hoorn, 2011; Hurtado et al., 2018; Cassemiro et al., 2023), South America's topography has changed dramatically (Hoorn et al., 2010; Dávila & Lithgow-Bertelloni, 2013; Rahbek et al., 2019). One of the most influential geological events was the uplift of the Andes (Hoorn et al., 2010; Hurtado et al., 2018; Rahbek et al., 2019; Cassemiro et al., 2023). The history of these mountains is intertwined with the formation of some of the world's largest modern rivers, such as the Amazon, Orinoco, and Paraná. (Antonelli et al., 2009; Anderson et al., 2016; Hurtado et al., 2018; Bedoya et al., 2021). Given the mega-diverse species assemblage found within South America, biologists have sought to understand how Andean orogenesis has contributed to the origins and evolution of Neotropical species (Antonelli et al., 2009; Hoorn et al., 2010; Albert et al., 2018b; Rincon-Sandoval et al., 2019; Hoorn et al., 2022). Orogenesis can either prevent or promote gene flow, depending on the biological and geomorphological context (Hoorn et al., 2013; Luebert & Weigend, 2014; Rahbek et al., 2019). Mountain uplift may separate previously continuous populations, preventing gene flow and promoting speciation via vicariance from distinct selective pressures and mutations (Macey et al., 1999; Sanmartín, 2003; Hoorn et al., 2013; Luebert & Weigend, 2014; Rahbek et al., 2019). Speciation resulting from orogenic vicariance has been proposed for *Aphanius* Eurasian killifishes (Hrbek & Meyer, 2003), *Drimys* tropical evergreens (Luebert & Weigend, 2014), *Dendrocincla* woodcreepers (Weir & Price, 2011), *Montivipera* mountain vipers (Ahmadi et al., 2021), etc. Alternatively, mountain uplift may connect previously isolated regions, providing dispersal opportunities and expanding the range of montane species (Hoorn et al., 2013; Luebert & Weigend, 2014; De-Silva et al., 2016; Sanín et al., 2022). Organisms, such as *Azorella* flowering plants (Luebert & Weigend, 2014), *Oleria* clearwing butterflies (De-Silva et al., 2016), and *Ceroxylon* montane palms (Sanín et al., 2022), were able to disperse and diversify following orogenesis.

Although the rise of the Andes established many barriers between modern South American rivers, it also created new connections via river capture events (Tagliacollo et al., 2015; Stokes et al., 2018; Albert et al., 2021; Bedoya et al., 2021). River or stream capture occurs when a river is diverted from its basin into a neighbouring basin (Tagliacollo et al., 2015; Albert et al., 2018b; Stokes et al., 2018; Albert et al., 2021). Capture events establish connections between previously isolated rivers, allowing aquatic species to disperse into new habitats (Burridge et al., 2006; Tagliacollo et al., 2015; Albert et al., 2021). River capture may also facilitate vicariance when individuals from the diverted river are isolated from the population in the original drainage basin (Burridge et al., 2006; Tagliacollo et al., 2015; Albert et al., 2018b; Albert et al., 2021). The evolution of several freshwater organisms, such as potamotrygonid freshwater stingrays (Albert et al., 2021), Galaxias fishes (Waters et al., 2020), and *Brotia* freshwater snails (Köhler et al., 2010), has been linked with historic river capture events.

Generally, orogenesis and river capture increase speciation and extinction rates; however, specific evolutionary responses are largely taxon-specific (Heard, 1996; Pigot et al., 2010; Albert et al., 2018b; Albert et al., 2021). Therefore, it is important to document differences between taxa to elucidate macroevolutionary patterns. One family of freshwater fishes that may provide insight into the connection between orogenesis and speciation is the long-whiskered catfishes, Pimelodidae. This Neotropical family inhabits cis- and trans-Andean drainage basins throughout South America, as well as the Tuira River basin on the Isthmus of Panama (Figure 4-1; Ribeiro et al., 2008; Lundberg et al., 2011; Lundberg et al., 2012; Sullivan et al., 2013; Nelson et al., 2016). Pimelodids are important food and sport fishes, and they exhibit a wide range of adult body size ranging from several centimeters to several meters (Buitrago–Suárez & Burr, 2007; García Vásquez et al., 2009; Lundberg et al., 2012). The goliath catfishes within

Brachyplatystoma undertake some of the longest freshwater migrations on Earth, spanning the length of the Amazon (García Vásquez et al., 2009; Van Damme et al., 2019). Pimelodidae is currently comprised of 116 extant species, divided into 31 genera (Lundberg et al., 2011; Lundberg et al., 2012; Nelson et al., 2016; Fricke et al., 2023).

Previous studies have proposed that Pimelodidae originated sometime between the Late Cretaceous and Eocene (Hardman & Lundberg, 2006; Sullivan et al., 2013; Tagliacollo et al., 2015; Betancur-R et al., 2017). This coincides with Andean uplift and the reorganization of large river basins. Andean uplift and exposure of the Purús Arch in Central Amazonia divided what is now the modern Amazon into eastern and western basins during the Early to Mid-Miocene (Figueiredo et al., 2009; Wesselingh & Hoorn, 2011; Albert et al., 2018a; Oberdorff et al., 2019; Cassemiro et al., 2023). As the Andes rose, subsidence increased in the sub-Andean foreland west of the Purús Arch, creating the Pebas mega-wetland (Wesselingh & Hoorn, 2011; Oberdorff et al., 2019; Hoorn et al., 2022). Over time, sedimentation and erosion from the rising Andes contributed to the establishment of the modern east-flowing Amazon, overcoming the Purús Arch sometime during the Late Miocene ~11 mya (Lundberg et al., 1998; Wesselingh & Hoorn, 2011; Hoorn et al., 2022; Cassemiro et al., 2023). In the north, the Eastern and Mérida cordilleras of the Andes divided trans-Andean drainages, such as the Magdalena and Maracaibo basins, from cis-Andean drainages, such as the Amazon, Orinoco, and Essequibo basins, during the Late Neogene (Lundberg et al., 1998; Albert et al., 2006; Hardman & Lundberg, 2006; Wesselingh & Hoorn, 2011; Anderson et al., 2016; Rincon-Sandoval et al., 2019). Uplift of other structural arches, such as the Michicola and Vaupés arches, created boundaries between neighbouring drainage basins, separating the Amazon basin from the Paraná-Paraguay and Orinoco basins,

respectively (Lundberg et al., 1998; Carvalho & Albert, 2011; Winemiller & Willis, 2011; Anderson et al., 2016; Caputo & Soares, 2016; Albert et al., 2018a; Cassemiro et al., 2023).

Owing to the widespread distribution and early origin of pimelodid species predating major Andean uplift and historical river capture events, the evolutionary history of Pimelodidae presents an excellent opportunity to investigate the relationship between geological/hydrological phenomena and patterns of diversification. The purpose of our study was to determine whether Andean uplift and changes to river drainage organization within South America coincided with cladogenesis within Pimelodidae. We hypothesized that speciation events within Pimelodidae increased following vicariance caused by Andean uplift and river capture events. Furthermore, we hypothesized that dispersal into new river basins via river capture also promoted speciation within the family as pimelodids colonized new habitats. We tested our hypotheses by constructing a time-calibrated phylogeny of Pimelodidae using the largest molecular dataset and most comprehensive taxon-sampling of any study to date. We used first-occurrence fossil data of both pimelodid ingroup and siluriform outgroups to estimate divergence times within the family. We then compared the timing of speciation events between allopatrically distributed species pairs with the timing of known orogenic and river capture events.

Materials and methods

Taxon and gene selection

To construct our multi-gene phylogeny of Pimelodidae, we sequenced DNA from muscle tissues and fin clippings collected from museum-deposited voucher specimens. We included 87 of the 116 nominal species within Pimelodidae, representing all but two monotypic genera (*Bagropsis* and *Zungaropsis*). We included two to four representatives per species when possible, accounting for geographic distribution of widespread species. We also included 21

potentially undescribed pimelodid species that warrant further taxonomic investigation. For outgroups, we selected 29 species, representing 1) closely related families within the superfamily Pimelodoidea (Pseudopimelodidae, Phreatobiidae, Heptapteridae, and *Conorhynchos conirostris*), and 2) more distantly related siluriform families within suborder Siluroidei (Aspredinidae, Auchenipteridae, Cetopsidae, Diplomystidae, Doradidae, and Ictaluridae) (Betancur-R et al., 2017; Schedel et al., 2022). In total, we constructed our multi-gene phylogeny of Pimelodidae using 233 specimens (Table 4-S1).

We selected two mitochondrial and eight nuclear protein-coding genes to construct our multi-gene phylogeny. The two mitochondrial genes were *co1* and *cyt b*. The eight nuclear genes we selected were *egr1*, *enc1*, *glyt*, *rag1*, *rag2*, *rh1*, super conserved receptor expressed in brain 2 (*sreb2*), and *zic1*. These genes were selected based on two criteria. First, they are single-copy genes to prevent biases from sequencing gene paralogs (Lovejoy & Collette, 2001; Li et al., 2007; Chen et al., 2008; Hughes et al., 2018). Second, these genes represent a mix of quickly-evolving and slowly-evolving genes, providing phylogenetic resolution at both deep and shallow nodes within the tree (Lovejoy, 2000; Springer et al., 2001; Le et al., 2006). In general, mitochondrial genes evolve more rapidly than nuclear genes (Brown et al., 1979; Saccone et al., 2000; Springer et al., 2001; Camus et al., 2022).

DNA sequencing and alignment

To sequence our selected genes for each individual, we adapted a DNA extraction protocol by Ivanova et al. (2006), creating a homemade DNA extraction kit. We extracted DNA from muscle or fin tissues stored in 95% ethanol at -20°C. We amplified our ten selected genes for each specimen using PCR with previously published primers provided by Ward et al. (2009) and Palumbi et al. (1991) to amplify *co1* and *cyt b*, respectively. To sequence our nuclear genes,

we created two sets of primers: external primers for PCR amplification and internal primers to avoid non-specific PCR product during the sequencing reaction (Table 2-S2).

We used two PCR recipes to sequence the ten genes we selected for our phylogenetic analyses. The Dream PCR recipe amplified *cyt b*, *enc1*, *rag2*, and *zic1*. The recipe for each reaction included: 1X Dream buffer containing 2 mM MgCl2, 0.2 mM of dNTPs, 0.25 μM of forward and reverse primers, 0.75 U of Dream *Taq*, ~20-30 ng of template DNA, and nuclease-free water to adjust to the final reaction volume of 15 μL. PCR cycling conditions were recreated using a Mastercycler pro S: initial heating to 95°C for 3 minutes, 35 cycles of denaturation (95°C for 30 seconds), primer annealing (55°C for 30 seconds), and extension (72°C for 1 minute and 30 seconds) phases, and a final extension phase at 72°C for 10 minutes. The Q5 PCR recipe amplified *co1*, *egr1*, *glyt*, *rag1*, *rh1*, and *sreb2*. This recipe included: 1X Q5 buffer containing 2 mM MgCl2, 0.2 mM of dNTPs, 0.5 μM of forward and reverse primers, 0.45 μL of dimethyl sulfoxide (DMSO), 0.3 U of Q5 polymerase, ~20-30 ng of template DNA, and nuclease-free water to adjust to the final reaction volume of 15 μL. We used a Mastercycler pro S to recreate the following cycling conditions: initial heating to 98°C for 30 seconds, 34 cycles of denaturation (98°C for 10 seconds), primer annealing (56°C for 30 seconds), and extension (72°C for 30 seconds) phases, and a final extension phase at 72°C for 5 minutes.

We used gel electrophoresis to visualize the results and assess whether we successfully amplified each PCR reaction. Then, we diluted each PCR product with a volume of nuclease-free water depending on the strength of the PCR bands: 60 μL for strong bands, 30 μL for medium bands, and 15 μL for weak bands. Following dilution, we prepared sequencing reactions using the following recipe per reaction: 0.9X ABI buffer, 0.5 μM of primer, 0.5 μL of BigDye containing ddNTPs, 1 μL of diluted PCR products, and nuclease-free water to adjust to the final

reaction volume of 10 μL. Sequencing reactions were then cycled using the following conditions in a Mastercycler pro S: initial heating to 95°C for 3 minutes, 25 cycles of denaturation (96°C for 30 seconds), primer annealing (50°C for 20 seconds), and extension (60°C for 4 minutes) phases. The final step involved purifying the sequencing reactions using an EDTA-NaOH-ethanol precipitation protocol provided by the manufacturer. DNA pellets were then resuspended with HIDI formamide and sequenced with a 3500 xL Genetic Analyzer. The resulting sequences were aligned for each individual gene using the MUSCLE 5.1 plugin (Edgar, 2021) in Geneious Prime 2023.0.1. Our ten gene alignments were then concatenated using SequenceMatrix 1.8 (Vaidya et al., 2011).

Divergence time estimation

To construct our fossil-calibrated phylogeny and estimate divergence times within Pimelodidae, we used a BI analysis in BEAST2 2.6.3 (Bouckaert et al., 2019). We specified our tree priors using the CladeAge package, which infers the optimal calibration density shapes for each clade, accounting for age estimation uncertainty (Matschiner et al., 2017). To do this, we specified rate parameters for net diversification (λ-μ; 0.041–0.081), turnover (μλ-1; 0.0011–0.37), and fossil sampling (ψ; 0.0066–0.01806) derived from previous studies of teleosts (Foote & Miller, 2007; Santini et al., 2009; Matschiner et al., 2017). We partitioned our concatenated alignment by gene and codon position (30 partitions), and then calculated the best substitution model for each partition using the bModelTest package in BEAST2 (Bouckaert & Drummond, 2017). We then selected two independent uncorrelated lognormal relaxed molecular clock models as priors for the mitochondrial and nuclear genes separately (Brown et al., 1979; Saccone et al., 2000; Springer et al., 2001; Drummond et al., 2006; Camus et al., 2022). For the tree prior, we selected a birth-death process model (Kendall, 1948). Twelve fossil constraints of both

ingroup pimelodids and outgroup siluriforms were specified as priors (see below). We ran two MCMC analyses for 100 million generations. Using Tracer 1.7.1, we assessed convergence and ESS for both runs (Rambaut et al., 2018). Then, we summarized the trees after discarding the first 10% as burn-in using TreeAnnotator 2.6.3 (Bouckaert et al., 2019) and visualized the tree using FigTree 1.4.4 (Rambaut, 2009).

As previously mentioned, we selected twelve first-occurrence fossils to time-calibrate our BI phylogeny of Pimelodidae. Six of these fossils belonged to Pimelodidae and six fossils represented outgroup siluriforms. We calibrated the genus *Steindachneridion* using the oldest known fossil species †*Steindachneridion silvasantosi* (Figueiredo & Costa Carvalho, 1999a; Figueiredo & Costa Carvalho, 1999b; Brito & Richter, 2016; Bogan & Agnolín, 2019). This late Oligocene-Early Miocene (~23.5-24.0 mya) fossil from the Taubaté basin near São Paulo, Brazil was classified as a *Steindachneridion* species based on skull morphology and dorsal spine ossification (Figueiredo & Costa Carvalho, 1999a; Bogan & Agnolín, 2019). We calibrated *Phractocephalus hemioliopterus* using fossils remains belonging to this genus from the La Victoria Formation dating back ~12.9-13.5 mya (Lundberg, 1997; Lundberg et al., 2010). Fossil remains identified as *Zungaro* sp. dating from the Late Miocene ~8.5-11.4 mya from the Solimões Formation were used to calibrate the genus *Zungaro* (Lundberg et al., 2010; Lacerda et al. 2021). We calibrated the genus *Platysilurus* using fossil records of *Platysilurus* sp. from the Urumaco Formation dating back to the Miocene ~7.4-9.0 mya (Sabaj et al., 2007; Lundberg et al., 2010). This fossil was classified as a *Platysilurus* species due to shared cranial morphology and dermal bone ornamentation (Sabaj et al., 2007; Lundberg et al., 2010). The fossil species †*Brachyplatystoma promagdalena* was used to calibrate the genus *Brachyplatystoma*. This Mid-Miocene fossil dating ~12.8-13.0 mya was found in the Villavieja Formation and was classified

as a *Brachyplatystoma* species based on the presence of a bony gas bladder platform and spongy textures of the first vertebra and fourth transverse process dorsal surface (Lundberg, 1997; Lundberg, 2005). Our last pimelodid fossil constraint calibrated the *Pimelodus ornatus*-*Calophysus*-*Pimelodus* (OCP) clade within Pimelodidae, comprising *Aguarunichthys*, *Bergiaria*, *Calophysus*, *Cheirocerus*, *Duopalatinus*, *Exallodontus*, *Iheringichthys*, *Luciopimelodus*, *Megalonema*, *Parapimelodus*, *Pimelabditus*, *Pimelodina*, *Pimelodus*, "*Pimelodus*" *ornatus*, *Pinirampus*, and *Propimelodus* (Lundberg et al., 2011; Tagliacollo et al., 2015). This fossil of uncertain classification occurred ~30.0-40.0 mya during the Eocene-Oligocene and was found in the Yahuarango Formation (Sullivan et al., 2013; Tagliacollo et al., 2015).

Our first outgroup calibration was also used by Sullivan et al. (2013) in their time-calibrated phylogeny of Pimelodoidea. Fossil remains from the Mid-Miocene (~11.5-15.9 mya) were classified within Pseudopimelodidae, belonging to either *Pseudopimelodus* or *Cephalosilurus* (Lundberg et al., 2010; Sullivan et al., 2013). Given the taxonomic uncertainty of this specimen, we applied this age constraint to our seven representatives of Pseudopimelodidae (*Batrochoglanis villosus*, *Cephalosilurus apurensis*, *Cruciglanis pacifici*, *Lophiosilurus alexandri*, *Microglanis* sp., *Rhyacoglanis annulatus*, and *Rhyacoglanis pulcher*). We used two fossil representatives of Heptapteridae to calibrate our phylogeny. Estimated ages of *Rhamdia* cf. *quelen* and *Pimelodella* cf. *laticeps* fossils were used to calibrate their respective genera, *Rhamdia quelen* and *Pimelodella cristata*. These fossils were deposited in the Luján Formation or rocks of a similar age, ~0.0355-0.0401 mya for *Rhamdia* cf. *quelen* and ~0.007-0.0075 mya for *Pimelodella* cf. *laticeps* (Thomas & Sabaj, 2020). We calibrated *Ictalurus punctatus*, our representative of Ictaluridae, with the oldest known extinct species †*Ictalurus rhaeas* based on similar pectoral spine morphology (Lundberg, 1975). †*Ictalurus rhaeas* was found in the Cypress

Hills Formation dating back to the Late Eocene ~30.0-37.0 mya (Cope, 1891; Lundberg, 1975; Hardman & Hardman, 2008; Arce H. et al., 2016). We used another fossil calibration from Sullivan et al. (2013), more specifically an unnamed fossil belonging to superfamily Doradoidea, comprising Doradidae and Auchenipteridae. We applied this age constraint of ~65.5-70.6 mya to the six representatives of Doradoidea (*Ageneiosus inermis*, *Auchenipterus nuchalis*, *Centromochlus reticulatus*, *Leptodoras acipenserinus*, *Leptodoras oyakawai*, and *Rhinodoras armbrusteri*) (Gayet & Meunier, 2003; Sullivan et al., 2013). Finally, we used an unclassified doradid fossil to calibrate the representatives of Doradidae within our phylogeny (*Leptodoras acipenserinus*, *Leptodoras oyakawai*, and *Rhinodoras armbrusteri*). This fossil was collected from the Castilletes Formation, estimated from the Early to Mid-Miocene, ~14.2-16.7 mya (Moreno et al., 2015). We list the first-occurrence fossils and specific age constraints in Table 4-1.

Results

Our time-calibrated phylogeny of Pimelodidae was estimated from a concatenated data matrix of 9,734 nucleotide base pairs. Both independent MCMC analyses achieved convergence with ESS values >450. Rooting the tree with representatives of Pimelodoidea and other distantly related catfishes, we found Pimelodidae to be strongly supported as a monophyletic family with a PP of 1.0 (Figure 4-2). *Steindachneridion*, *Phractocephalus*, and *Leiarius* + *Perrunichthys* were strongly supported (1.0 PP for each species) as sister to all remaining pimelodids (neopimelodines). The neopimelodines were divided into two clades: 1) the sorubimines (*Zungaro*, *Sorubim*, *Sorubimichthys*, *Pseudoplatystoma*, *Hemisorubim*, *Platystomatichthys*, *Platysilurus*, *Hypophthalmus*, *Brachyplatystoma*, and *Platynematichthys* (1.0 PP)) and 2) the OCP clade ("*Pimelodus*" *ornatus*, *Pimelabditus*, *Aguarunichthys*, *Pimelodina*, *Luciopimelodus*,

Calophysus, *Pinirampus*, *Cheirocerus*, *Megalonema*, *Propimelodus*, *Exallodontus*, *Duopalatinus*, *Iheringichthys*, *Bergiaria*, *Parapimelodus*, and *Pimelodus* (1.0 PP)). Within the sorubimines, genera were grouped into two subclades we designated as: 1) the *Pseudoplatystoma* group comprised of *Zungaro* (*Sorubim* (*Sorubimichthys* + *Pseudoplatystoma*)) (0.86 PP) and 2) the *Brachyplatystoma* group comprised of (*Hemisorubim* (*Platystomatichthys* + *Platysilurus*)) + *Hypophthalmus* (*Brachyplatystoma* + *Platynematichthys*) (1.0 PP). Within the OCP clade, we found evidence of eight subclades: 1) the "*Pimelodus*" *ornatus* – *Pimelabditus* group (1.0 PP), 2) the *Calophysus* group (*Aguarunichthys* + *Pimelodina* + *Luciopimelodus* + *Calophysus* + *Pinirampus*) (1.0 PP), 3) the *Cheirocerus* – *Megalonema* group (*Cheirocerus* + *Megalonema*) (1.0 PP), 4) the *Exallodontus* – "*Pimelodus*" *altissimus* group containing *Exallodontus*, "*Pimelodus*" *altissimus*, *Propimelodus*, *Duopalatinus peruanus*, and several potentially undescribed genera (1.0 PP), 5) the "*Pimelodus*" *pictus* (1.0 PP), 6) the "*Pimelodus*" *grosskopfii* group containing "*Pimelodus*" *crypticus*, "*Pimelodus*" *punctatus*, "*Pimelodus*" *grosskopfii*, and a potentially undescribed species (1.0 PP), 7) the "*Pimelodus*" *blochii* group (1.0 PP), and 8) the *Pimelodus sensu stricto* group containing *Duopalatinus emarginatus* ((*Iheringichthys* + *Bergiaria*) + (*Parapimelodus* + *Pimelodus sensu stricto*)) (1.0 PP).

Several genera within Pimelodidae were not monophyletic. *Perrunichthys perruno* was nested within *Leiarius*, causing the latter to be paraphyletic. *Brachyplatystoma* was also paraphyletic due to *Platynematichthys notatus* being nested within the genus as sister to *Brachyplatystoma vaillantii*. *Propimelodus* formed a paraphyletic genus within the *Exallodontus* – "*Pimelodus*" *altissimus* group, given the positions of *Exallodontus aguanai*, "*Pimelodus*" *altissimus*, and *Duopalatinus peruanus*. By extension, the two species of *Duopalatinus* formed a polyphyletic genus occurring in the *Exallodontus* – "*Pimelodus*" *altissimus* group (*D. peruanus*)

and the *Pimelodus sensu stricto* group (*D. emarginatus*). *Iheringichthys* was paraphyletic because *Bergiaria westermanni* was nested within the genus. Finally, *Pimelodus* was polyphyletic, occurring throughout the OCP clade. *Pimelodus* species were placed within the "*Pimelodus*" *ornatus* + *Pimelabditus*, *Exallodontus* – "*Pimelodus*" *altissimus*, "*Pimelodus*" *pictus*, "*Pimelodus*" *grosskopfii*, "*Pimelodus*" *blochii*, and *Pimelodus sensu stricto* groups (*Pimelodus sensu stricto* contained the type species *Pimelodus maculatus*).

Our divergence time estimations suggest that crown group Pimelodidae split from Pseudopimelodidae sometime between the Late Cretaceous and Eocene ~64 mya (51-78 mya 95% CI) (Figure 4-2). The family then began to diversify during the Eocene when the common ancestor of *Steindachneridion* split from the common ancestor of all remaining extant pimelodids ~ 44 mya (37-53 mya 95% CI). The common ancestor of the sorubimines split from the common ancestor of the OCP clade ~37 mya (31-43 mya 95% CI) between the Eocene and Oligocene, and subsequently diversified ~28 mya (23-36 mya 95% CI) between the Eocene and transition between the Oligocene and Miocene. The OCP clade began to diversify ~33 mya (27-43 mya 95% CI) between the Eocene and Oligocene, and the eight subclades comprising the OCP clade originated between the Eocene and Miocene.

Discussion

Phylogeny of Pimelodidae

Our multi-gene phylogeny of Pimelodidae was constructed using the largest molecular dataset, most comprehensive taxon-sampling, and most fossil calibration points of any study to date. The topology of our time-calibrated phylogeny was largely consistent with previous molecular phylogenies of Pimelodidae (Lundberg et al., 2011; Lundberg et al., 2012; Tagliacollo et al., 2015). Previous studies placed *Steindachneridion*, *Phractocephalus*, and *Leiarius* +

Perrunichthys perruno as three sister lineages to all remaining pimelodids (the neopimelodines) (Lundberg et al., 2011; Lundberg et al., 2012; Tagliacollo et al., 2015). Lundberg et al. (2011) organized the neopimelodines into clades based on their molecular analyses. These clades were recovered in each subsequent phylogeny of Pimelodidae, further supporting their validity (Lundberg et al., 2012; Tagliacollo et al., 2015). Our phylogeny was consistent with most of the clades within neopimelodines proposed by Lundberg et al. (2011); however, our phylogeny reorganized the genera within some of these groups and introduced novel groups within the OCP clade.

Our phylogeny supported the division of neopimelodines into the sorubimines and the OCP clade. Within the sorubimines, our phylogeny recovered two subclades, which we designate as the *Pseudoplatystoma* group and the *Brachyplatystoma* group. Lundberg et al. (2011) also observed these groups, but did not provide them with formal names. The first main difference between our phylogeny and those in previous studies was the placement of *Zungaro* within the *Pseudoplatystoma* group rather than sister to all sorubimines (Lundberg et al., 2011; Tagliacollo et al., 2015). Also, *Hypophthalmus*, a genus of pimelodids known as low-eye catfishes that used to be classified within their own family Hypophthalmidae (Nelson et al., 2016; Littmann et al., 2021), was sister to *Brachyplatystoma* (the goliath catfishes) within the *Brachyplatystoma* group. Lundberg et al. (2011) placed *Hypophthalmus* as sister to *Platysilurus* + *Platystomatichthys* with low support, whereas Tagliacollo et al. (2015) could not determine whether *Hypophthalmus* was sister to *Platysilurus* + *Platystomatichthys* or sister to all sorubimines except *Zungaro*.

Lundberg et al. (2011) defined the OCP clade as the "*Pimelodus*" *ornatus* species complex sister to the *Calophysus-Pimelodus* (CP) clade. The CP clade was then divided into the calophysines (C; *Calophysus* group and the *Cheirocerus-Megalonema* group) and the

pimelodines (P; *Exallodontus* - "*Pimelodus*" *altissimus* group and *Pimelodus* group). These clades within the OCP clade were further supported by Lundberg et al. (2012) and Tagliacollo et al. (2015). Our study supports the validity and phylogenetic placements of the "*Pimelodus*" *ornatus* – *Pimelabditus* group, calophysines with the *Calophysus* and *Cheirocerus* – *Megalonema* groups, and the *Exallodontus* – "*Pimelodus*" *altissimus* group within the pimelodines. We have reorganized the remaining groups within pimelodines and have introduced a new group comprised of trans-Andean species. Rather than lump "*Pimelodus*" *pictus* into the *Pimelodus* group, we propose this species forms a distinct, monotypic clade sister to three remaining groups within pimelodines. Our study was the first phylogeny of Pimelodidae to include "*Pimelodus*" *grosskopfii*, "*Pimelodus*" *punctatus*, "*Pimelodus*" *crypticus*, and a potentially undescribed species. These four species comprise the novel "*Pimelodus*" *grosskopfii* group, defined by occurring in trans-Andean river basins. We split the remaining members of the *Pimelodus* group into two groups ("*Pimelodus*" *blochii* group and *Pimelodus sensu stricto* group) to preserve the taxonomic validity of *Iheringichthys* and *Duopalatinus* (see below for our recommendation to reclassify *Bergiaria westermanni*).

We recommend the following taxonomic revisions to be formally examined in future studies. First, *Perrunichthys perruno* should be reclassified as *Leiarius perruno* to restore the monophyly of *Leiarius*. *Platynematichthys notatus* should also be reclassified as *Brachyplatystoma notatus*, again to restore the monophyly of *Brachyplatystoma*. Given that *Propimelodus* species are positioned throughout the *Exallodontus* – "*Pimelodus*" *altissimus* group, we recommend that *Exallodontus aguanai*, *Pimelodus altissimus*, and *Duopalatinus peruanus* be reclassified as *Propimelodus* species. By extension, this would solve the polyphyly of *Duopalatinus*, given that *Duopalatinus emarginatus* is the type species of its genus (Ferraris

Jr., 2007; Fricke et al., 2023). With respect to *Iheringichthys*, we propose that *Bergiaria westermanni* be reclassified as an *Iheringichthys* species. Since we were unable to include *Bergiaria platana* in our phylogeny, it is unclear as to whether *Bergiaria* is a valid monotypic genus, or if both *Bergiaria* species should be reclassified as *Iheringichthys* species. Finally, we propose extensive taxonomic changes to solve the polyphyly of *Pimelodus*. "*Pimelodus*" *ornatus*, "*Pimelodus*" *pictus*, the species comprising the "*Pimelodus*" *grosskopfii* group, and the species comprising the "*Pimelodus*" *blochii* group each require generic reclassifications, resulting in four new genera that accurately reflect their phylogenetic relationships. *Pimelodus* species within the *Pimelodus sensu stricto* clade should retain their genus because this clade contains the type species, *Pimelodus maculatus* (Ferraris Jr., 2007; Fricke et al., 2023).

Divergence time estimations of Pimelodidae

Using our time-calibrated phylogeny of Pimelodidae, we estimated the family originated between the Late Cretaceous and the Eocene. Previous studies generally corroborated our findings, also estimating a Late Cretaceous-Eocene origin time for Pimelodidae (Hardman & Lundberg, 2006; Sullivan et al., 2013; Tagliacollo et al., 2015; Betancur-R et al., 2017). Hardman & Lundberg (2006) proposed that Pimelodidae split from Pseudopimelodidae ~54 mya, falling within our 95% CI. Sullivan et al. (2013), Tagliacollo et al. (2015), and Betancur-R et al. (2017) hypothesized slightly older origin times for the family, ~70-90 mya; however, these origin times are still included within our 95% CI. We believe our time-calibrated phylogeny most accurately represents the historical origins of Pimelodidae based on three criteria: 1) inclusion of the most pimelodid taxa of any study to date (75%), 2) use of the largest molecular phylogeny of the family, and 3) use of twelve fossil constraints when constructing the tree, including six pimelodid fossils. Hardman & Lundberg (2006), Sullivan et al. (2013), and

Betancur-R et al. (2017) only included 5-8 representatives of Pimelodidae within their phylogenies, accounting for ~6% of all pimelodids, whereas Tagliacollo et al. (2015) included 57 species accounting for ~49%. Early multi-gene phylogenies only included between three and six genes, whereas we constructed our phylogeny using ten genes (Hardman & Lundberg, 2006; Sullivan et al., 2013; Taglicollo et al., 2015). Finally, the most ingroup pimelodid fossil constraints used in previous studies was three, whereas our study included six (Hardman & Lundberg, 2006; Sullivan et al., 2013; Taglicollo et al., 2015).

Orogenesis, river capture, and the evolution of Pimelodidae

The speciation events of several allopatric species pairs/clades within Pimelodidae coincided with orogenic events, supporting our hypothesis that orogenesis likely contributed to speciation within Pimelodidae. In our time-calibrated phylogeny, we found *Steindachneridion* species from the Paraná-Paraguay River basin (*S. melanodermatum* and *S. scriptum*) were sister to *S. parahybae*, a species endemic to the Paraíba do Sul River near the eastern Atlantic coast of Brazil (Ferraris Jr., 2007; Fricke et al., 2023). It is possible river capture of the Tietê River headwaters (tributary of the Paraná River) by the Paraíba do Sul River following erosion of headwater divisions provided a dispersal opportunity for the ancestor of *S. parahybae*, suggesting that river capture may have promoted speciation within the genus (Ihering, 1898; Ab'Saber, 1957; Buckup, 2011). The timing of this river capture event, however, is unclear (Buckup, 2011). Within *Leiarius* + *Perrunichthys perruno*, *Leiarius pictus* and *Perrunichthys perruno* likely diverged following Andean uplift. *Leiarius pictus* occurs throughout the Orinoco and Amazon rivers and *Perrunichthys perruno* occurs in the Maracaibo basin (Ferraris Jr., 2007; Fricke et al., 2023). These species split ~3-10 mya, possibly coinciding with the uplift of the

Mérida Cordillera of the Andes that separated the Maracaibo basin from the Orinoco River (Hardman & Lundberg, 2006; Rodríguez-Olarte et al., 2011; Albert et al., 2021).

Within the *Pseudoplatystoma* group, we found *Zungaro zungaro* from the Amazon and Essequibo basins were distinct from *Zungaro zungaro* from the Orinoco basin. This split occurred ~1-3 mya between the Pliocene and Pleistocene, potentially following the separation of modern rivers that comprised the Proto-Berbice (Lujan & Armbruster, 2011; Lemopoulos & Covain, 2019; Henschel & Lujan, 2021). The Proto-Berbice was a paleo-drainage that united headwaters of the Orinoco, Amazon, Essequibo, and Berbice rivers between the Paleocene and Pliocene/Pleistocene (Lujan & Armbruster, 2011; Lemopoulos & Covain, 2019; Henschel & Lujan, 2021). It is possible that separation of these modern rivers isolated ancestral *Zungaro zungaro* populations, promoting allopatric speciation. Alternatively, dispersal across the Casiquiare River, a contemporary river capture event occurring between the Orinoco and Negro rivers (Vari & Ferraris Jr., 2009; Willis et al., 2010; Wesselingh & Hoorn, 2011; Stokes et al., 2018), after the Proto-Berbice rivers is also possible. Two *Sorubim* species (*S. cuspicaudus* and a potentially undescribed species) from the Magdalena and Maracaibo basins diverged from all other cis-Andean *Sorubim* species ~6-12 mya, coinciding with the rise of the Mérida and Eastern cordilleras of the Andes (Hardman & Lundberg, 2006; Rodríguez-Olarte et al., 2011; Albert et al., 2021). With respect to *Pseudoplatystoma*, we observed the trans-Andean *P. magdaleniatum* diverged from cis-Andean species ~7-12 mya (Ferraris Jr., 2007; Fricke et al., 2023), which also coincided with the uplift of the Mérida and Eastern cordilleras (Hardman & Lundberg, 2006; Rodríguez-Olarte et al., 2011; Albert et al., 2021). *Pseudoplatystoma corruscans*, a Paraná-Paraguay and São Francisco species (Ferraris Jr., 2007; Fricke et al., 2023), split from all remaining *Pseudoplatystoma* species ~5-10 mya. This may have been linked with river capture

of Paraguay River headwaters by the Amazon River basin as the basin shifted southwards towards the Michicola Arch ~10 mya (Carvalho & Albert, 2011). Alternatively, seasonal connections between these river basins during the rainy seasons may have provided a dispersal opportunity for the ancestral population (Iriondo & Paira, 2007; Torrico et al., 2009; Brea & Zucol, 2011). Additionally, two other species of *Pseudoplatystoma* from the Orinoco River basin, *P. metaense* and *P. orinocoense* (Ferraris Jr., 2007; Fricke et al., 2023), diverged from Amazonian species ~3-9 mya. This may have occurred after uplift of the Vaupés Arch separated the Amazon and Orinoco basins (Winemiller & Willis, 2011; Albert et al., 2018a; Albert et al., 2021). Within the *Brachyplatystoma* group, trans-Andean *Platysilurus malarmo* from the Magdalena basin diverged from cis-Andean *Platysilurus mucosus* and a potentially undescribed species from the Orinoco basin ~7-14 mya (Ferraris Jr., 2007; Fricke et al., 2023). Similar to other trans-Andean species, this speciation event may have coincided with uplift of the Mérida Cordillera (Hardman & Lundberg, 2006; Rodríguez-Olarte et al., 2011; Albert et al., 2021).

Within the OCP clade, orogenesis and river capture have likely influenced the origins and speciation of several pimelodids. We discussed the evolutionary history of the "*Pimelodus*" *ornatus* – *Pimelabditus* group in Chapter 3, including the importance of vicariance and dispersal within this clade. Within the *Cheirocerus* – *Megalonema* group, trans-Andean *Cheirocerus abuelo* diverged from cis-Andean *C. eques* and *C. goeldii* before uplift of the Mérida Cordillera, suggesting that ecological pressures may have promoted genetic differentiation in the absence of known geological barriers (Hardman & Lundberg, 2006; Ferraris Jr., 2007; Rodríguez-Olarte et al., 2011; Albert et al., 2021; Fricke et al., 2023). *Megalonema* exhibited interesting distribution patterns in both cis- and trans-Andean drainages. *Megalonema orixanthum* from the Orinoco basin was sister to *M. amaxanthum* from the Amazon basin (Ferraris Jr., 2007; Fricke et al.,

2023). This split occurred ~5-12 mya, possibly coinciding with uplift of the Vaupés Arch (Winemiller & Willis, 2011; Albert et al., 2018a; Albert et al., 2021). The trans-Andean species *M. xanthum* and *M. psammium* diverged from a common ancestor around the same time as *M. amaxanthum* and *M. orixanthum*, again prior to Andean uplift isolating these basins (Ferraris Jr., 2007; Winemiller & Willis, 2011; Albert et al., 2018a; Albert et al., 2021; Fricke et al., 2023). Finally, two species from the Paraná-Paraguay basin, *M. argentina* and *M. platanum* diverged from Amazonian species ~2-6 mya (Ferraris Jr., 2007; Fricke et al., 2023). This may have been related to a dispersal event via the seasonal connections of Paraná-Paraguay and Amazon headwaters (Iriondo & Paira, 2007; Torrico et al., 2009; Brea & Zucol, 2011). Two potentially undescribed sister species within the *Exallodontus* – "*Pimelodus*" *altissimus* group, Gen. nov. sp. VENE and Gen. nov. sp. XIBE, are allopatrically distributed between the Orinoco and Amazon basins, respectively. They split ~2-5 mya, well after the uplift of the Vaupés Arch, indicating the possibility of speciation following dispersal through the Casiquiare River (Willis et al., 2010; Wesselingh & Hoorn, 2011; Winemiller & Willis, 2011; Albert et al., 2018a; Stokes et al., 2018; Albert et al., 2021). The "*Pimelodus*" *grosskopfii* group is restricted to trans-Andean species inhabiting the Magdalena, Maracaibo, Atrato, and Tuira rivers (Ferraris Jr., 2007; Fricke et al., 2023). This group diverged ~14-23 mya, predating major orogenic events in this region. It is possible that ecological pressures may have promoted differentiation from other pimelodids before geological barriers divided these clades. Furthermore, the only Central American species "*Pimelodus*" *punctatus* evolved ~2-7 mya, coinciding with the closure of the Isthmus of Panama that allowed faunal exchange between Central and South America (Coates et al., 1992; Haug & Tiedemann, 1998; O'Dea et al., 2016). Another group defined by geographic distribution is the *Pimelodus sensu stricto* clade. All genera and species here occur in the Paraná-Paraguay and/or

eastern Atlantic Brazilian drainage basins (Ferraris Jr., 2007; Fricke et al., 2023). Similar to *Steindachneridion*, it is possible river capture events resulting from erosion of headwaters provided opportunities for these species to disperse and evolve independently (Ihering, 1898; Ab'Saber, 1957; Buckup, 2011).

Although our phylogeny of Pimelodidae provides insight into the influence of orogenesis and river capture on gene flow and speciation of South American freshwater fishes, inclusion of missing pimelodid species in future studies could provide new insights into the evolutionary processes that led to the extant species. Approximately 25% of pimelodids are missing from our analyses, including two genera, *Bagropsis* and *Zungaropsis*. We plan to estimate ancestral area states across Pimelodidae. This analysis would provide valuable information regarding the origins of major clades within Pimelodidae, possibly improving our understanding of macroevolutionary patterns associated with orogenesis and river capture. Finally, the taxonomic revisions suggested here will require redescriptions and the creation of new genera to address widespread paraphyly and polyphyly within the family. Future studies should incorporate morphological and anatomical data to define the phylogenetic clades we identified in this study.

Conclusion

The physical environment plays an important role in the evolution of species. Orogenesis in particular dramatically transforms the landscape, dividing some populations, while providing dispersal opportunities for others. Our goal was to investigate how these phenomena have contributed to the diversification of the Neotropical fauna, specifically freshwater pimelodids. We created a time-calibrated phylogeny of Pimelodidae using fossil data to estimate divergence times within the family. We identified several species pairs and clades that may owe their origins to vicariance caused by Andean uplift and subsequent river capture as river boundaries shifted.

Notably, one trans-Andean clade diversified prior to uplift of the Mérida and Eastern cordilleras of the Andes, suggesting ecological pressures may have influenced their evolution in the absence of geological barriers. With respect to the taxonomy of Pimelodidae, we observed paraphyly and polyphyly in several genera, including the diverse genus *Pimelodus*. We proposed taxonomic revisions that future studies should formally address by analyzing morphological characters. Our next step will be to perform an ancestral area state reconstruction of Pimelodidae to identify potential origin sites of the major lineages within Pimelodidae.

Tables

Table 4-1 List of first-occurrence fossils used to time-calibrate Pimelodidae clades and siluriform outgroups for a divergence-time analysis using BEAST2 2.6.3. OCP stands for "*Pimelodus ornatus – Calophysus – Pimelodus* clade, comprised of "*Pimelodus*" *ornatus*, *Pimelabditus*, *Aguarunichthys*, *Pimelodina*, *Luciopimelodus*, *Calophysus*, *Pinirampus*, *Cheirocerus*, *Megalonema*, *Propimelodus*, *Exallodontus*, *Duopalatinus*, *Iheringichthys*, *Bergiaria*, *Parapimelodus*, and *Pimelodus.*

Fossil Species	**Age (mya)** [1]	**Clade/Species Calibrated**	**Reference(s)**
†***Brachyplatystoma promagdalena***	12.8-13.0	*Brachyplatystoma*	Lundberg, 1997; Lundberg, 2005
***Phractocephalus* sp.**	12.9-13.5	*Phractocephalus hemioliopterus*	Lundberg, 1997; Lundberg et al., 2010
***Platysilurus* sp.**	7.39-9.0	*Platysilurus*	Sabaj et al., 2007; Lundberg et al., 2010
cf. OCP clade	30.0-40.0	OCP clade	Lundberg et al., 2011; Tagliacollo et al., 2015
†***Steindachneridion silvasantosi***	23.5-24.0	*Steindachneridion*	Figueiredo & Costa Carvalho, 1999a; Figueiredo & Costa Carvalho, 1999b; Bogan & Agnolín, 2019
***Zungaro* sp.**	8.5-11.42	*Zungaro*	Lundberg et al., 2010; Lacerda et al. 2021
cf. Doradidae	14.2-16.7	Doradidae	Moreno et al., 2015
cf. Doradoidea	65.5-70.6	Doradoidea	Gayet & Meunier, 2003; Sullivan et al., 2013
†***Ictalurus rhaeas***	30.0-37.0	Ictaluridae	Cope, 1891; Lundberg, 1975
Pimelodella* cf. *laticeps	0.007-0.0075	*Pimelodella cristata*	Thomas & Sabaj, 2020
cf. Pseudopimelodidae	11.5-15.9	Pseudopimelodidae	Lundberg et al., 2010; Sullivan et al., 2013
Rhamdia* cf. *quelen	0.0355-0.0401	*Rhamdia quelen*	Thomas & Sabaj, 2020

[1]mya = million years ago

Figures

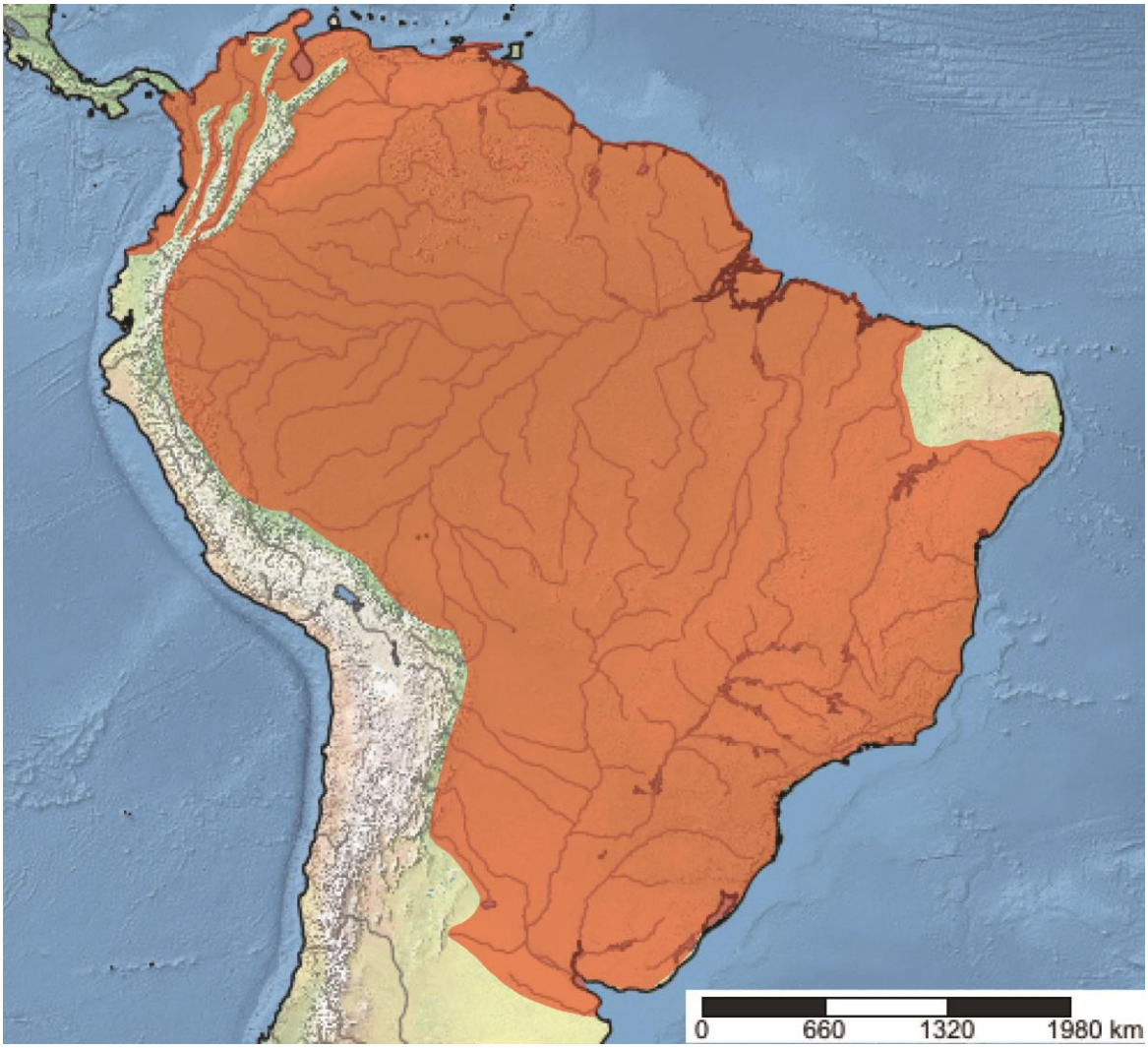

Figure 4-1 Distribution map of Pimelodidae within South America created using SimpleMappr (Shorthouse, 2010). Occurrence data was assembled from Ferraris, Jr. (2007), Fricke et al. (2023), and GBIF.org (2023b).

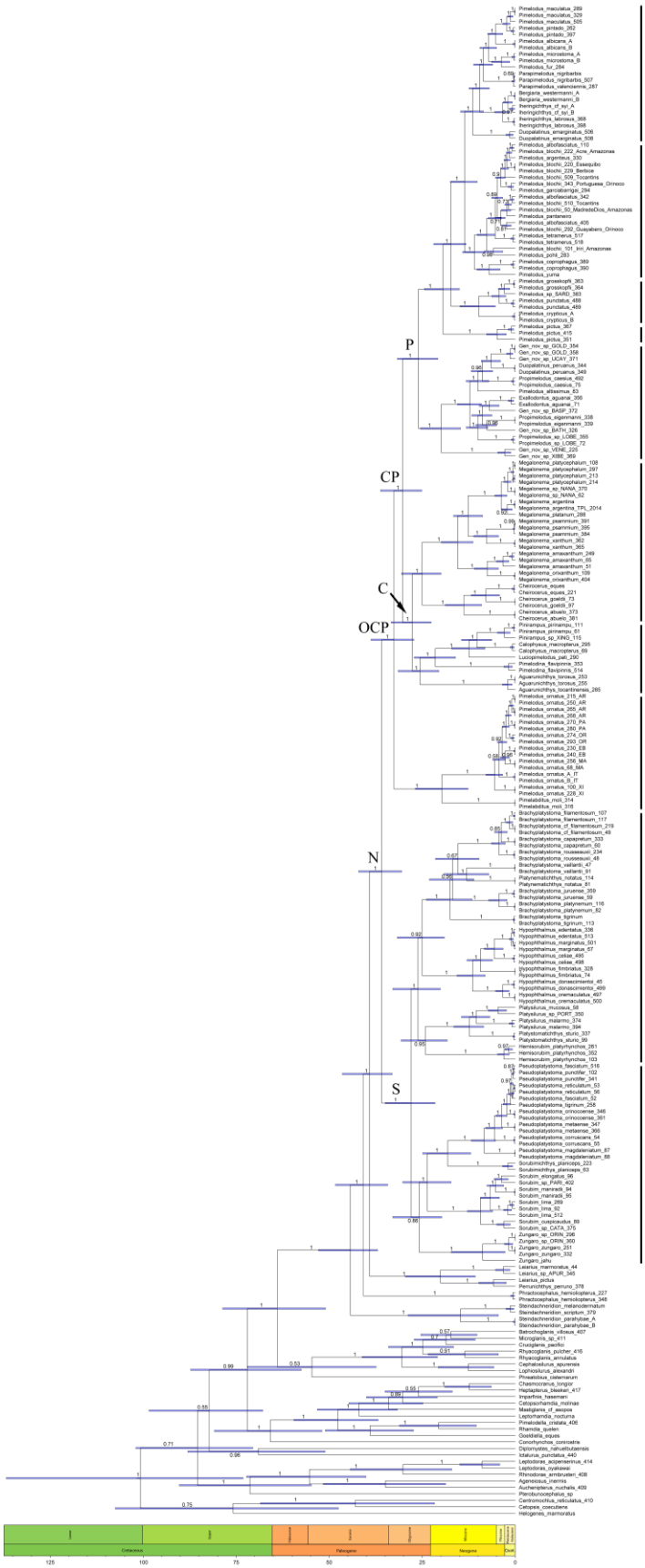
Pimelodus sensu stricto
"*Pimelodus*" *blochii*
"*Pimelodus*" *grosskopfii*
"*Pimelodus*" *pictus*
Exallodontus -
"*Pimelodus*" *altissimus*
Cheirocerus -
Megalonema
Calophysus
"*Pimelodus*" *ornatus* -
Pimelabditus
Brachyplatystoma
Pseudoplatystoma
P
CP
C
OCP
N
S
Cretaceous
Paleogene
Neogene
125
100
75
50
25
0

Figure 4-2 Time-calibrated multi-gene phylogeny of Pimelodidae constructed using the CladeAge package in BEAST2. The phylogeny was calibrated using twelve fossil constraints. Posterior probabilities >0.5 are presented above each node, and blue bars represent 95% confidence intervals of divergence-time estimations. Geological timescale provided below the phylogeny is measured in millions of years before present time. Group names provided to the right of specific epithets, and major clade designations proposed by Lundberg et al. (2011) are presented above the corresponding nodes: N = neopimelodines, S = sorubimines, OCP = "*Pimelodus*" *ornatus* – *Calophysus* – *Pimelodus* clade, CP = *Calophysus* – *Pimelodus* clade, C = calophysines, and P = pimelodines.

Supplemental Material for Chapter 4

Table 4-S1 Museum voucher data for 204 pimelodid specimens and 29 siluriform outgroup species.

Genus	Species	Isolate #	Field Collection #	Museum Voucher #	Country
Aguarunichthys	*tocantinsensis*	F285	N/A	INPA	Brazil
Aguarunichthys	*torosus*	F253	ECU14-02	ROM 100218	Ecuador
Aguarunichthys	*torosus*	F255	ECU14-21	ROM TISSUE	Ecuador
Bergiaria	*westermanni*	A	DCC 4195	UNESP Tissue	Brazil
Bergiaria	*westermanni*	B	DCC 4194	UNESP Tissue	Brazil
Brachyplatystoma	*capapretum*	F60	PERU 2001-11	ANSP 178524	Peru
Brachyplatystoma	*capapretum*	F333	Peru 99-17	INHS 52181	Peru
Brachyplatystoma	*filamentosum*	F107	VEN 05-18	ANSP 187070	Venezuela
Brachyplatystoma	*filamentosum*	F117	iXIN14-EXP2-33	ANSP 197504	Brazil
Brachyplatystoma	cf. *filamentosum*	F49	SUR 07-00A	ANSP 187105	Suriname
Brachyplatystoma	cf. *filamentosum*	F219	N/A	ROM TISSUE	Guyana
Brachyplatystoma	*juruense*	F59	PERU 2001-11	ANSP 178514	Peru
Brachyplatystoma	*juruense*	F359	VEN 15-10	ANSP 198480	Venezuela
Brachyplatystoma	*platynemum*	F82	PERU 2001-05	ANSP 178520	Peru
Brachyplatystoma	*platynemum*	F116	iXIN14-EXP2-33	ANSP 197503	Brazil
Brachyplatystoma	*rousseauxii*	F48	SUR 07-00A	ANSP 187109	Suriname
Brachyplatystoma	*rousseauxii*	F234	7848-10	ROM 93620	Peru
Brachyplatystoma	*tigrinum*	F113	iXIN14-EXP2-17	INPA 43226	Brazil
Brachyplatystoma	*tigrinum*	N/A	N/A	ANSP 179236	N/A
Brachyplatystoma	*vaillantii*	F47	SUR 07-00A	ANSP 187107	Suriname
Brachyplatystoma	*vaillantii*	F91	PERU 2003-00C	ANSP 187073	Peru
Calophysus	*macropterus*	F69	PERU 05-05	ANSP 182754	Peru
Calophysus	*macropterus*	F295	GUAYA18-P-6	IAvHP	Colombia
Cheirocerus	*abuelo*	F373	JGL-01-VE1	ANSP 197819	Venezuela
Cheirocerus	*abuelo*	F381	CO-2017-02	ANSP/CZUT	Colombia
Cheirocerus	*eques*	F221	PER10-31	AUM 51409	Peru

Cheirocerus	*eques*	N/A	N/A	INHS 52717	Peru
Cheirocerus	*goeldii*	F73	PERU 05-05	ANSP 181112	Peru
Cheirocerus	*goeldii*	F97	PERU 05-07	ANSP 181185	Peru
Duopalatinus	*emarginatus*	F506	tissue 14731	INPA	Brazil
Duopalatinus	*emarginatus*	F508	Z205714	ANSP 205714	Brazil
Duopalatinus	*peruanus*	F344	VEN 15-01	ANSP 198892	Venezuela
Duopalatinus	*peruanus*	F349	VEN 15-02	ANSP 198879	Venezuela
Exallodontus	*aguanai*	F71	PERU 05-05	ANSP 180947	Peru
Exallodontus	*aguanai*	F356	VEN 15-05	ANSP 198913	Venezuela
Hemisorubim	*platyrhynchos*	F103	BR12-07	ANSP 193032	Brazil
Hemisorubim	*platyrhynchos*	F261	MAZ16-04	ROM 101268	Guyana
Hemisorubim	*platyrhynchos*	F352	VEN 15-04	ANSP 198934	Venezuela
Hypophthalmus	*celiae*	F495	PERU 2001-11	ANSP 178517	Peru
Hypophthalmus	*celiae*	F498	PERU 05-07	ANSP 196764	Peru
Hypophthalmus	*donascimientoi*	F45	PERU 2001-02	ANSP 178457	Peru
Hypophthalmus	*donascimientoi*	F499	PERU 05-07	ANSP 180991	Peru
Hypophthalmus	*edentatus*	F336	iXIN14-EXP3-58	ANSP 197652	Brazil
Hypophthalmus	*edentatus*	F513	FDD2019110701	MPEG	Brazil
Hypophthalmus	*fimbriatus*	F74	PERU 05-05	ANSP 207015	Peru
Hypophthalmus	*fimbriatus*	F328	PERU 05-03	ANSP 182752	Peru
Hypophthalmus	*marginatus*	F67	SUR 07-00A	ANSP 187103	Suriname
Hypophthalmus	*marginatus*	F501	VEN 05-02	ANSP 180993	Venezuela
Hypophthalmus	*oremaculatus*	F497	PERU 2001-11	ANSP 178511	Peru
Hypophthalmus	*oremaculatus*	F500	PERU 05-03	ANSP 207016	Peru
Iheringichthys	*labrosus*	F368	ARG 05-01	ANSP 189660?	Argentina
Iheringichthys	*labrosus*	F398	CAT17-02	ANSP 203185	Uruguay
Iheringichthys	c.f. *syi*	A	491	SCG-2020	N/A
Iheringichthys	c.f. *syi*	B	492	SCG-2020	N/A
Leiarius	*marmoratus*	F44	PERU 2001-00A	ANSP 178109	Peru
Leiarius	*pictus*	N/A	N/A	ANSP 178108	Peru
Leiarius	sp. APUR	F345	VEN 15-00C	ANSP 198901	Venezuela

Luciopimelodus	*pati*	F290	N/A	MZUSP 78457	Brazil
Megalonema	*amaxanthum*	F51	TCEP 04-54	ANSP 180628	Peru
Megalonema	*amaxanthum*	F65	PERU 05-09	ANSP 182732	Peru
Megalonema	*amaxanthum*	F249	BAT14-25	ROM 97136	Guyana
Megalonema	*argentinum*	N/A	N/A	MG ZV-P 293	Argentina
Megalonema	*argentinum*	TPL_2014	P117	UEMS P117	Brazil
Megalonema	*orixanthum*	F109	VEN 05-04	ANSP 185144	Venezuela
Megalonema	*orixanthum*	F404	VEN 05-38	AUFT 3113	Venezuela
Megalonema	*platanum*	F288	N/A	MZUSP 78465	Brazil
Megalonema	*platycephalum*	F108	VEN 04-18	ANSP 182784	Venezuela
Megalonema	*platycephalum*	F213	HLF09-02	ROM 85941	Guyana
Megalonema	*platycephalum*	F214	HLF09-02	ROM 85941	Guyana
Megalonema	*platycephalum*	F297	GUAYA18-P-16	IAvHP	Colombia
Megalonema	*psammium*	F384	CO-2017-00A	ANSP/CZUT	Colombia
Megalonema	*psammium*	F391	CO-2017-10	ANSP/CZUT	Colombia
Megalonema	*psammium*	F395	CO-2017-04B	ANSP/CZUT	Colombia
Megalonema	*xanthum*	F362	2015-CO-02	CZUT	Colombia
Megalonema	*xanthum*	F365	2015-CO-06b	CZUT	Colombia
Megalonema	sp. NANA	F62	PERU 2001-02	ANSP 178450	Peru
Megalonema	sp. NANA	F370	PERU 2003-02	ANSP 185243	Peru
Parapimelodus	*nigribarbis*	N/A	N/A	MZUSP 78451	Brazil
Parapimelodus	*nigribarbis*	F507	ALA2002051901	ANSP 206298	Brazil
Parapimelodus	*valenciennes*	F287	N/A	MZUSP 78466	Brazil
Perrunichthys	*perruno*	F378	JGL-01-VE2	ANSP 200289	Venezuela
Phractocephalus	*hemioliopterus*	F227	HLF08-36	ROM TISSUE	Brazil
Phractocephalus	*hemioliopterus*	F348	VEN 15-00C	ANSP 198902	Venezuela
Pimelabditus	*moli*	F314	SU08-386	MHNG 2709.099	Suriname
Pimelabditus	*moli*	F316	SU08-824	MHNG 2709.100	Suriname
Pimelodina	*flavipinnis*	F353	VEN 15-04	ANSP 198936	Venezuela
Pimelodina	*flavipinnis*	F514	FDD2019110701	MPEG	Brazil
Pimelodus	*albicans*	A	N/A	ANSP 178802	Argentina

Pimelodus	*albicans*	B	UNMDP-T 0538	UNMDP T 538	Argentina
Pimelodus	*albofasciatus*	F110	VEN 05-03	AUM 43011	Venezuela
Pimelodus	*albofasciatus*	F342	iXIN14-EXP3-75	INPA 47829	Brazil
Pimelodus	*albofasciatus*	F405	GUY 05-16	AUFT 3145	Guyana
Pimelodus	*altissimus*	F83	PERU 2001-05	ANSP 178519	Peru
Pimelodus	*argenteus*	F330	ARG 05-01	ANSP 181017	Argentina
Pimelodus	*blochii*	F50	TCEP 04-52	ANSP 180564	Peru
Pimelodus	*blochii*	F101	BR12-05	ANSP 199658	Brazil
Pimelodus	*blochii*	F220	N/A	ROM 86545	Guyana
Pimelodus	*blochii*	F222	PER10-31	AUM	Peru
Pimelodus	*blochii*	F229	HLF10-01	ROM 86989	Guyana
Pimelodus	*blochii*	F292	GUAYA18-P-1	IAvHP	Colombia
Pimelodus	*blochii*	F343	VEN 15-01	ANSP 198893	Venezuela
Pimelodus	*blochii*	F509	FDD2019110701	MPEG	Brazil
Pimelodus	*blochii*	F510	FDD2019110701	MPEG	Brazil
Pimelodus	*coprophagus*	F389	CO-2017-04B	ANSP/CZUT	Colombia
Pimelodus	*coprophagus*	F390	CO-2017-04B	ANSP/CZUT	Colombia
Pimelodus	*crypticus*	A	Pcry08	N/A	Colombia
Pimelodus	*crypticus*	B	Pcry03	N/A	Colombia
Pimelodus	*fur*	F284	N/A	INPA	Brazil
Pimelodus	*garciabarrigai*	F294	GUAYA18-P-4	IAvHP	Colombia
Pimelodus	*grosskopfii*	F363	2015-CO-00	CZUT	Colombia
Pimelodus	*grosskopfii*	F364	2015-CO-00	CZUT	Colombia
Pimelodus	*maculatus*	F289	N/A	MZUSP 78460	Brazil
Pimelodus	*maculatus*	F329	ARG 05-01	ANSP 181019	Argentina
Pimelodus	*maculatus*	F505	tissue 14729	INPA ?	Brazil
Pimelodus	*microstoma*	A	12CAPV	UEL Tissue	Brazil
Pimelodus	*microstoma*	B	23CAPV	UEL Tissue	Brazil
Pimelodus	*ornatus* AR	F215	HLF09-02	ROM 86203	Guyana
Pimelodus	*ornatus* AR	F250	BAT14-22	ROM 96990	Guyana
Pimelodus	*ornatus* AR	F265	PERU 2001-02	ANSP 178452	Peru

Pimelodus	*ornatus* AR	F268	PERU 05-00D	ANSP 181099	Peru
Pimelodus	*ornatus* EB	F230	HLF10-02	ROM 87121	Guyana
Pimelodus	*ornatus* EB	F240	GUY13-21	ROM 96132	Guyana
Pimelodus	*ornatus* IT	A	MCB2006000003108	UEMA 104565	Brazil
Pimelodus	*ornatus* IT	B	MCB2006000003790	UEMA 104565	Brazil
Pimelodus	*ornatus* MA	F68	SUR 07-01	ANSP 187113	Suriname
Pimelodus	*ornatus* MA	F256	SES-15-004	ROM 100852	Suriname
Pimelodus	*ornatus* OR	F274	VEN 04-18	AUM 41487	Venezuela
Pimelodus	*ornatus* OR	F293	GUAYA18-P-4	IAvHP	Colombia
Pimelodus	*ornatus* PA	F270	ARG 05-02B	MLP	Argentina
Pimelodus	*ornatus* PA	F280	ARG 05-04	MLP	Argentina
Pimelodus	*ornatus* XI	F100	BR12-03	ANSP 199580	Brazil
Pimelodus	*ornatus* XI	F228	HLF08-37	ROM TISSUE	Brazil
Pimelodus	*pantaneiro*	N/A	185	N/A	Brazil
Pimelodus	*pictus*	F351	VEN 15-03	ANSP 198956	Venezuela
Pimelodus	*pictus*	F367	PERU 2001-04	ANSP 178168	Peru
Pimelodus	*pictus*	F415	PER06-18	AUFT 4017	Peru
Pimelodus	*pintado*	F262	HLF17-09	ROM 102967	Uruguay
Pimelodus	*pintado*	F397	CAT17-13	ANSP 203107	Uruguay
Pimelodus	*pohli*	F283	N/A	INPA	Brazil
Pimelodus	*punctatus*	F488	Pan-8-2016	LSU 7965	Panama
Pimelodus	*punctatus*	F489	Pan-8-2016	LSU 7966	Panama
Pimelodus	*tetramerus*	F517	JDBG-08-01-2015-008	UCF	Brazil
Pimelodus	*tetramerus*	F518	JDBG-08-01-2015-017	UCF	Brazil
Pimelodus	*yuma*	N/A	Py002	N/A	Colombia
Pimelodus	sp. SARD	F383	CO-2017-02	ANSP/CZUT	Colombia
Pinirampus	*pirinampu*	F61	PERU 2001-10	ANSP 178314	Peru
Pinirampus	*pirinampu*	F111	VEN 05-18	ANSP 187067	Venezuela
Pinirampus	sp. XING	F115	iXIN14-EXP2-33	ANSP 197502	Brazil
Platynematichthys	*notatus*	F81	PERU 2001-11	ANSP 178528	Peru
Platynematichthys	*notatus*	F114	iXIN14-EXP2-33	ANSP 197506	Brazil

Platysilurus	*malarmo*	F374	JGL-01-VE2	ANSP 187009	Venezuela
Platysilurus	*malarmo*	F394	CO-2017-00C	ANSP/CZUT	Colombia
Platysilurus	*mucosus*	F58	PERU 2001-11	ANSP 178509	Peru
Platysilurus	sp. PORT	F350	VEN 15-01	ANSP 198890	Venezuela
Platystomatichthys	*sturio*	F99	PERU 05-00C	ANSP 181048	Peru
Platystomatichthys	*sturio*	F337	iXIN14-EXP3-63	ANSP 197636	Brazil
Propimelodus	*caesius*	F75	PERU 05-05	ANSP 181192	Peru
Propimelodus	*caesius*	F492	BRA-4-2015	LSU 7521	Brazil
Propimelodus	*eigenmanni*	F338	iXIN14-EXP3-66	ANSP 197634	Brazil
Propimelodus	*eigenmanni*	F339	iXIN14-EXP3-66	INPA 47498	Brazil
Propimelodus	sp. LOBE	F72	PERU 05-05	ANSP 180939	Peru
Propimelodus	sp. LOBE	F355	VEN 15-04	ANSP 198943	Venezuela
Pseudoplatystoma	*corruscans*	F54	ARG 05-06	ANSP 188913	Argentina
Pseudoplatystoma	*corruscans*	F55	ARG 05-06	ANSP 188913	Argentina
Pseudoplatystoma	*fasciatum*	F52	SUR 07-00B	ANSP 187106	Suriname
Pseudoplatystoma	*fasciatum*	F516	OYA20191016-1	ANSP 207658	Brazil
Pseudoplatystoma	*magdaleniatum*	F87	CO-2006-01B	ANSP 188882	Colombia
Pseudoplatystoma	*magdaleniatum*	F88	CO-2006-01B	ANSP 192843	Colombia
Pseudoplatystoma	*metaense*	F347	VEN 15-00C	ANSP 198899	Venezuela
Pseudoplatystoma	*metaense*	F366	VEN 15-00C	ANSP 198899	Venezuela
Pseudoplatystoma	*orinocoense*	F346	VEN 15-00C	ANSP 198900	Venezuela
Pseudoplatystoma	*orinocoense*	F361	VEN 15-12	ANSP 198456	Venezuela
Pseudoplatystoma	*punctifer*	F102	BR12-05	ANSP 199584	Brazil
Pseudoplatystoma	*punctifer*	F341	iXIN14-EXP3-22	INPA 52557	Brazil
Pseudoplatystoma	*reticulatum*	F53	ARG 05-01	ANSP 188914	Argentina
Pseudoplatystoma	*reticulatum*	F56	ARG 05-06	ANSP 188912	Argentina
Pseudoplatystoma	*tigrinum*	F258	SES-15-005	ROM 100853	Suriname
Sorubim	*cuspicaudus*	F89	CO-2006-01B	ANSP 192844	Colombia
Sorubim	*elongatus*	F96	PERU 05-07	ANSP 182285	Peru
Sorubim	*lima*	F92	PERU 2003-03	ANSP 179842	Peru
Sorubim	*lima*	F269	ARG 05-01	ANSP 188824	Argentina

Sorubim	*lima*	F512	FDD2019110701	MPEG	Brazil
Sorubim	*maniradii*	F94	PERU 05-07	ANSP 182288	Peru
Sorubim	*maniradii*	F95	PERU 05-07	ANSP 182288	Peru
Sorubim	sp. CATA	F375	JGL-01-VE2	ANSP 200290	Venezuela
Sorubim	sp. PARI	F402	GUY07-40	AUFT 3107	Guyana
Sorubimichthys	*planiceps*	F63	N/A	INHS 54701	Peru
Sorubimichthys	*planiceps*	F223	VEN10-11	ROM TISSUE	Venezuela
Steindachneridion	*melanodermatum*	N/A	N/A	LGP 11105	Brazil
Steindachneridion	*parahybae*	A	LBP-42007	UNESP 42007	Brazil
Steindachneridion	*parahybae*	B	LBP2009	UNESP 42008	Brazil
Steindachneridion	*scriptum*	F379	N/A	MZUSP 78463	Brazil
Zungaro	*jahu*	N/A	LBP2170	UNESP Tissue	Brazil
Zungaro	*zungaro*	F251	BAT14-42	ROM Tissue	Guyana
Zungaro	*zungaro*	F332	Peru 99-03	SIUC	Peru
Zungaro	sp. ORIN	F296	GUAYA18-P-2	IAvHP	Colombia
Zungaro	sp. ORIN	F360	VEN 15-12	ANSP 198983	Venezuela
Gen. nov.	sp. BATH	F326	PERU 05-07	ANSP 181194	Peru
Gen. nov.	sp. BASP	F372	N/A	MUSM 36713	Peru
Gen. nov.	sp. VENE	F225	VEN10-33B	ROM TISSUE	Venezuela
Gen. nov.	sp. XIBE	F369	iXIN15-EXP4-06	ANSP 200081	Brazil
Gen. nov.	sp. GOLD	F354	VEN 15-04	ANSP 198939	Venezuela
Gen. nov.	sp. GOLD	F358	VEN 15-09	ANSP 198919	Venezuela
Gen. nov.	sp. UCAY	F371	N/A	MUSM 39439	Peru
Pterobunocephalus	sp.	N/A	N/A	ANSP 182774	Brazil
Ageneiosus	*inermis*	N/A	Aqua-BC-2015	N/A	N/A
Auchenipterus	*nuchalis*	F409	VEN 05-38	AUFT 3318	Venezuela
Centromochlus	*reticulatus*	F410	VEN 05-48	AUFT 3324	Venezuela
Cetopsis	*coecutiens*	N/A	N/A	INHS 52923	Peru
Helogenes	*marmoratus*	N/A	N/A	INHS 49125	Guyana
Diplomystes	*nahuelbutaensis*	N/A	N/A	N/A	N/A
Leptodoras	*acipenserinus*	F414	PER06-18	AUFT 4005	Peru

Leptodoras	*oyakawai*	N/A	N/A	ANSP 199567	Brazil
Rhinodoras	*armbrusteri*	F408	GUY07-18	AUFT 3307	Guyana
Cetopsorhamdia	*molinae*	N/A	N/A	T24588	Colombia
Chasmocranus	*longior*	N/A	N/A	AUFT 3167	Guyana
Goeldiella	*eques*	N/A	N/A	AUFT 3164	Guyana
Heptapterus	*bleekeri*	F417	SUR 09-08	AUFT 4771	Suriname
Imparfinis	*hasemani*	N/A	N/A	T14941	Guyana
Leptorhamdia	*nocturna*	N/A	N/A	T09452	N/A
Mastiglanis	c.f. *asopos*	N/A	N/A	T09911	N/A
Pimelodella	*cristata*	F406	GUY 05-16	AUFT 3147	Guyana
Rhamdia	*quelen*	N/A	N/A	LGEP 777	Argentina
Ictalurus	*punctatus*	F440	N/A	UMSNH 5722	Mexico
Conorhynchos	*conirostris*	N/A	N/A	MZUSP 53620	Brazil
Phreatobius	*cisternarum*	N/A	N/A	MZUSP 98804	Brazil
Batrochoglanis	*villosus*	F407	GUY07-41	AUFT 3172	Guyana
Cephalosilurus	*apurensis*	N/A	N/A	ANSP 179447	Venezuela
Cruciglanis	*pacifici*	N/A	AOL-023	N/A	Colombia
Lophiosilurus	*alexandri*	N/A	LBP 276	UNESP Tissue	Brazil
Microglanis	sp.	F411	PER06-27	AUFT 3739	Peru
Rhyacoglanis	*annulatus*	N/A	AOL-098	N/A	N/A
Rhyacoglanis	*pulcher*	F416	PER06-19	AUFT 4029	Peru

General Conclusion

Throughout my thesis, my research addressed how habitat and landscape have facilitated genetic diversification within catfishes. In each chapter, I used genetic data to test my hypotheses and discussed how both modern and historical geographic patterns have likely promoted diversification within catfishes by affecting gene flow. In my first chapter, I investigated whether habitat preferences and breeding site segregation have influenced the genetic structure of a sympatric population of channel catfish. Large channel catfish generally prefer deep river channels during the breeding season, returning to the same nests in successive years. Intermediate sized channel catfish, however, prefer shallower tributaries. I genotyped 162 channel catfish from the Ottawa River and its tributaries at Lac des Chats to determine whether these habitat preferences for lacustrine-like and fluvial breeding sites reduced gene flow between breeding populations. My microsatellite analyses revealed the population was panmictic, rejecting my hypothesis; however, previous studies have observed that genetic isolation by distance does influence channel catfish population genetics, at a greater spatial scale than the one at which I was working.

In my second chapter, I investigated the origins of cave-dwelling North American catfishes (*Prietella lundbergi*, *Prietella phreatophila*, *Satan eurystomus*, and *Trogloglanis pattersoni*) from the karst region surrounding the Gulf of Mexico. The origins of these species have been contentious, differing between previous morphological and molecular studies. The most recent study proposed that cave-dwelling ictalurids descended from a common ancestor. This hypothesis was unintuitive given the allopatric distribution of cave ictalurids divided by extensive mountain ranges. Therefore, I tested the alternative hypothesis that cave ictalurids

evolved in parallel, descending from common ancestors shared with surface-dwelling species. I constructed a time-calibrated phylogeny of Ictaluridae using the largest molecular dataset of any study to date, including all extant species except the troglobitic *Satan eurystomus*. I observed that *Prietella lundbergi* was sister to surface-dwelling *Ictalurus*, and *Prietella phreatophila* + *Trogloglanis pattersoni* were sister to surface-dwelling *Ameiurus*, suggesting two independent cave colonization events. Interestingly, the sister relationship between *Prietella phreatophila* and *Trogloglanis pattersoni* indicated that subterranean dispersal between American and Mexican aquifers was possible between the Eocene and Miocene.

In my third chapter, I shifted focus to South America, elucidating whether semi-permeable barriers between major river basins have sufficiently reduced gene flow between subpopulations of the widespread ornate pim catfish. Previous evidence suggested "*Pimelodus*" *ornatus* forms a species complex defined by river basin boundaries, but these conclusions were based on only four individuals. I constructed a multi-gene phylogeny of 130 "*Pimelodus*" *ornatus* specimens to test whether impermeable and semi-permeable barriers between river basins have sufficiently reduced or eliminated gene flow between populations, facilitating parapatric and allopatric speciation. I observed seven distinct lineages, six of which were strongly defined by geographic location. I then calculated uncorrected *p*-distances between each lineage and compared these values with generally accepted interspecific thresholds between vertebrate species. These distances were comparable to recognized species, indicating a need for formal species descriptions using morphological data.

Finally, in my fourth chapter, I investigated whether major orogenic and river capture events coincided with speciation and cladogenesis within Neotropical long-whiskered catfishes (Pimelodidae). Orogenesis and river capture generally increase speciation among organisms via

vicariance and new dispersal opportunities; however, speciation trends tend to be lineage-specific. Therefore, I elucidated how these natural phenomena may have influenced the evolution of pimelodids in response to widespread orogenesis throughout South America. I created a time-calibrated phylogeny of Pimelodidae using the largest molecular dataset and most comprehensive taxon-sampling (87 of the 116 extant species) of any study to date. I observed that well-documented uplift events, including the rise of the Mérida and Eastern Andean cordilleras and exposure of structural arches dividing major rivers, coincided with divergence times of allopatric species pairs within Pimelodidae. I also identified paraphyly and polyphyly in several genera, indicating a need for extensive taxonomic revisions.

The second, third, and four chapters within this thesis supported the hypothesis that geographic boundaries promote genetic differentiation within catfishes by reducing gene flow between populations. Furthermore, previous research indicates that isolation by distance may also affect the genetic structure of a sympatric population in the first chapter. My thesis has provided additional evidence to the growing body of research demonstrating the link between abiotic factors and genetic diversification within organisms.

Additional research is necessary to address further questions resulting from my findings. With respect to the first chapter, telemetry and additional genetic analyses may determine whether habitat preference changes over a channel catfish's lifespan resulting from improved ability to establish and defend high-quality nesting sites, or if sex-biased philopatry could explain the observed gene flow. For the second chapter, inclusion of *Satan eurystomus* may elucidate additional patterns of parallel evolution or subterranean diversification. Furthermore, taxonomic revisions are required to restore the monophyly of *Prietella* and to describe potentially new surface-dwelling species. With respect to the third chapter, an ancestral area state reconstruction

may determine areas of origin within the *Pimelodus ornatus* species complex. Additionally, morphological data should be analyzed to describe the potentially new species observed formally. For the fourth chapter, I proposed taxonomic revisions that future studies should formally address by analyzing morphological characters. An ancestral area state reconstruction of Pimelodidae may also identify potential origin sites of the major lineages within Pimelodidae. Future studies should make use of the large molecular datasets I produced to test their own biogeographical hypotheses. Ancestral area state reconstructions could elucidate where cladogenesis may have occurred, testing specific models of vicariance and dispersal within ictalurids and pimelodids. Furthermore, my research has indicated a need for extensive taxonomic revisions within these groups, providing a molecular roadmap that can guide the necessary morphological analyses required for these revisions.

Literature Cited

Ab'Saber, A.N. 1957. O problema das conexões antigas e da separação da drenagem do Paraiba e Tietê. *Boletim Paulista de Geografia* 26: 38–49.

Abreu, J.M.S., Saraiva, A.C.S., Albert, J.S., & Piorski, N.M. 2020. Paleogeographic influences on freshwater fish distributions in northeastern Brazil. *Journal of South American Earth Sciences* 102(2020): 102692.

Acosta, C.A. 1999. Benthic dispersal of Caribbean spiny lobsters among insular habitats: implications for the conservation of exploited marine species. *Conservation Biology* 13(3): 603-612.

Adams, C.E., Hamilton, D.J., McCarthy, I., Wilson, A.J., Grant, A., Alexander, G., Waldron, S., Snorasson, S.S., Ferguson, M.M., & Skúlason, S. 2006. Does breeding site fidelity drive phenotypic and genetic sub-structuring of a population of Arctic charr? *Evolutionary Ecology* 20(1): 11-26.

Adkins, J. 2013. Conceptualization of groundwater flow in the Edwards Aquifer through the Knippa Gap hydrogeologic constriction, Uvalde County, Texas. 13th Sinkhole Conference National Cave and Karst Research Institute- Symposium 2, May, 343-352, New Mexico.

Afiq-Rosli, L., Wainwright, B.J., Gajanur, A.R., Lee, A.C., Ooi, S.K., Chou, L.M., & Huang, D. 2021. Barriers and corridors of gene flow in an urbanized tropical reef system. *Evolutionary Applications* 14(10): 2502-2515.

Agashe, D., & Bolnick, D.I. 2010. Intraspecific genetic variation and competition interact to influence niche expansion. *Proceedings of the Royal Society B: Biological Sciences* 277(1696): 2915-2924.

Ahmadi, M., Hemami, M.R., Kaboli, M., Nazarizadeh, M., Malekian, M., Behrooz, R., Geniez, P., Alroy, J., & Zimmermann, N.E. 2021. The legacy of Eastern Mediterranean mountain uplifts: rapid disparity of phylogenetic niche conservatism and divergence in mountain vipers. BMC Ecology and Evolution 21(1): 1-13.

Albert, J.S., Bernt, M.J., Fronk, A.H., Fontenelle, J.P., Kuznar, S.L., & Lovejoy, N.R. 2021. Late Neogene megariver captures and the Great Amazonian biotic interchange. *Global and Planetary Change* 205: 103554.

Albert, J.S., Craig, J.M., Tagliacollo, V.A., & Petry, P. 2018b. Upland and lowland fishes: a test of the river capture hypothesis. In: Hoorn, C., Perrigo, A., & Antonelli, A. (Eds.), *Mountains, climate and biodiversity* pp. 273-294. John Wiley & Sons Ltd., New Jersey.

Albert, J.S., Lovejoy, N.R., & Crampton, W.G. 2006. Miocene tectonism and the separation of cis-and trans-Andean river basins: evidence from Neotropical fishes. *Journal of South American Earth Sciences* 21(1-2): 14-27.

Albert, J.S., & Reis, R.E. 2011. Introduction to Neotropical freshwaters. In: Albert, J.S. & Reis, R.E. (Eds.), Historical biogeography of Neotropical freshwater fishes, pp. 3-19. University of California Press, USA.

Albert, J.S., Val, P., & Hoorn, C. 2018a. The changing course of the Amazon River in the Neogene: center stage for Neotropical diversification. *Neotropical Ichthyology* 16(3): e180033.

Alcaide, M., Serrano, D., Tella, J.L., & Negro, J.J. 2009. Strong philopatry derived from capture–recapture records does not lead to fine-scale genetic differentiation in lesser kestrels. *Journal of Animal Ecology* 78(2): 468-475.

Allmon, W.D. 1992. A causal analysis of stages in allopatric speciation. *Oxford Surveys in Evolutionary Biology* 8: 219-219.

Anderson, V.J., Horton, B.K., Saylor, J.E., Mora, A., Tesón, E., Breecker, D.O., & Ketcham, R.A. 2016. Andean topographic growth and basement uplift in southern Colombia: implications for the evolution of the Magdalena, Orinoco, and Amazon river systems. *Geosphere* 12(4): 1235-1256.

Andrews, K.R., Good, J.M., Miller, M.R., Luikart, G., & Hohenlohe, P.A. 2016. Harnessing the power of RADseq for ecological and evolutionary genomics. *Nature Reviews Genetics* 17(2): 81-92.

Antonelli, A., Nylander, J.A., Persson, C., & Sanmartín, I. 2009. Tracing the impact of the Andean uplift on Neotropical plant evolution. *Proceedings of the National Academy of Sciences* 106(24): 9749-9754.

Antonelli, A., Zizka, A., Carvalho, F.A., Scharn, R., Bacon, C.D., Silvestro, D., & Condamine, F.L. 2018. Amazonia is the primary source of Neotropical biodiversity. *Proceedings of the National Academy of Sciences* 115(23): 6034-6039.

Arce-H, M., Lundberg, J.G., & O'Leary, M.A. 2016. Phylogeny of the North American catfish family Ictaluridae (Teleostei: Siluriformes) combining morphology, genes and fossils. *Cladistics* 33: 406-428.

Arntzen, J.W. 2023. A two-species distribution model for parapatric newts, with inferences on their history of spatial replacement. *Biological Journal of the Linnean Society* 138(1): 75-88.

Ayala, F.J. 1978. The mechanisms of evolution. *Scientific American* 239(3): 56-69.

Banerjee, M., Sarma, N., Biswas, R., Roy, J., Mukherjee, A., & Giri, A.K. 2008. DNA repair deficiency leads to susceptibility to develop arsenic-induced premalignant skin lesions. *International Journal of Cancer* 123: 283-287.

Bank, C., Bürger, R., & Hermisson, J. 2012. The limits to parapatric speciation: Dobzhansky–Muller incompatibilities in a continent–island model. *Genetics* 191(3): 845-863.

Barr Jr., T.C., & Holsinger, J.R. 1985. Speciation in cave faunas. *Annual Review of Ecology, Evolution, and Systematics* 16(1): 313-337.

Barrera-Guzmán, A.O., Aleixo, A., Faccio, M., Dantas, S.D.M., & Weir, J.T. 2022. Gene flow, genomic homogenization and the timeline to speciation in Amazonian manakins. *Molecular Ecology* 31(15): 4050-4066.

Barros, M.C., Fraga, E.C., & Birindelli, J.L.O. 2011. Fishes from the Itapecuru River basin, state of Maranhão, northeast Brazil. *Brazilian Journal of Biology* 71: 375-380.

Barton, N.H. 1986. The effects of linkage and density-dependent regulation on gene flow. *Heredity* 57: 415-426.

Barton, N.H. & Partridge, L. 2000. Limits to natural selection. *BioEssays* 22: 1075-1084.

Bedoya, A.M., Leache, A.D., & Olmstead, R.G. 2021. Andean uplift, drainage basin formation, and the evolution of plants living in fast-flowing aquatic ecosystems in northern South America. *New Phytologist* 232(5): 2175-2190.

Benjamini, Y., & Yekutieli, D. 2001. The control of the false discovery rate in multiple testing under dependency. *Annals of Statistics* 29(4): 1165-1188.

Benson, D.A., Cavanaugh, M., Clark, K., Karsch-Mizrachi, I., Ostell, J., Pruitt, K.D., & Sayers, E.W. 2018. GenBank. *Nucleic Acids Research* 46(Database issue): D41-D47.

Benton, M.J. 2009. The Red Queen and the Court Jester: species diversity and the role of biotic and abiotic factors through time. *Science* 323(5915): 728-732.

Bergsten, J. 2005. A review of long-branch attraction. *Cladistics* 21(2): 163-193.

Berner, D., & Thibert-Plante, X. 2015. How mechanisms of habitat preference evolve and promote divergence with gene flow. *Journal of Evolutionary Biology* 28(9): 1641-1655.

Bertassoli Jr., D.J., Sawakuchi, A.O., Sawakuchi, H.O., Pupim, F.N., Hartmann, G.A., McGlue, M.M., Chiessi, C.M., Zabel, M., Schefuß, E., Pereira, T.S., Santos, R.A., Faustino, S.B., Oliveira, P.E., & Bicudo, D.C. 2017. The fate of carbon in sediments of the Xingu and Tapajós clearwater rivers, Eastern Amazon. *Frontiers in Marine Science* 4(44): 1-14.

Betancur-R, R., Wiley, E.O., Arratia, G., Acero, A., Bailly, N., Miya, M., Lecointre, G., & Orti, G. 2017. Phylogenetic classification of bony fishes. *BMC Evolutionary Biology* 17(1): 1-40.

Beyer, H. L., Haydon, D. T., Morales, J. M., Frair, J. L., Hebblewhite, M., Mitchell, M., & Matthiopoulos, J. 2010. The interpretation of habitat preference metrics under use–availability designs. *Philosophical Transactions of the Royal Society B: Biological Sciences* 365(1550): 2245-2254.

Bidau, C.J., Miña, C.I., Castillo, E.R., & Martí, D.A. 2012. Effects of abiotic factors on the geographic distribution of body size variation and chromosomal polymorphisms in two Neotropical grasshopper species (Dichroplus: Melanoplinae: Acrididae). *Psyche* 2012: 1-11.

Blanckaert, A., Bank, C., & Hermisson, J. 2020. The limits to parapatric speciation 3: Evolution of strong reproductive isolation in presence of gene flow despite limited ecological differentiation. *Philosophical Transactions of the Royal Society B* 375(1806): 20190532.

Blanckaert, A., & Hermisson, J. 2018. The limits to parapatric speciation II: strengthening a preexisting genetic barrier to gene flow in parapatry. *Genetics* 209(1): 241-254.

Blanton, R.E., Page, L.M., & Hilber, S.A. 2013. Timing of clade divergence and discordant estimates of genetic and morphological diversity in the Slender Madtom, *Noturus exilis* (Ictaluridae). *Molecular Phylogenetics and Evolution* 66(3): 679-693.

Blundell, G.M., Ben-David, M., Groves, P., Bowyer, R.T., & Geffen, E. 2002. Characteristics of sex-biased dispersal and gene flow in coastal river otters: implications for natural recolonization of extirpated populations. *Molecular Ecology* 11(3): 289-303.

Bogan, S., & Agnolín, F.L. 2019. Phractocephaline catfishes from the late Miocene of Argentina, with the description of a new taxon. *Journal of Vertebrate Paleontology* 39(4): e1676254.

Boghici, R., Mace, R.E., Angle, E.S., & Mullican, W.F. 2004. Hydrogeology of Edwards-Trinity Aquifer of Texas and Coahuila in the border region. *Aquifers of the Edwards Plateau: Texas Water Development Board, Report* 360: 91-114.

Böhme, M., & Ilg, A. 2003. Database of vertebrates: fossil fishes, amphibians, reptiles, birds (fosFARbase). www.wahre-staerke.com/ (Accessed 21/07/2021).

Bolnick, D.I., Snowberg, L.K., Patenia, C., Stutz, W.E., Ingram, T., & Lau, O.L. 2009. Phenotype-dependent native habitat preference facilitates divergence between parapatric lake and stream stickleback. *Evolution* 63(8): 2004-2016.

Bolognesi, C. & Hayashi, M. 2011. Micronucleus assay in aquatic animals. *Mutagenesis* 26(1): 205-213.

Bonte, D., Van Dyck, H., Bullock, J.M., Coulon, A., Delgado, M., Gibbs, M., Lehouck, V., Matthysen, E., Mustin, K., Saastamoinen, M., Schtickzelle, N., Stevens, V.M., Vandewoestijne, S., Baguette, M., Barton, K., Benton, T.G., Chaput-Bardy, A., Clobert, J., Dytham, C., Hovestadt, T., Meier, C.M., Palmer, S.C.F., Turlure, C., & Travis, J.M.J. 2012. Costs of dispersal. *Biological Reviews* 87(2): 290-312.

Bornette, G. & Puijalon, S. 2011. Response of aquatic plants to abiotic factors: A review. *Aquatic Sciences* 73: 1-14.

Bouckaert, R.R., & Drummond, A.J. 2017. bModelTest: Bayesian phylogenetic site model averaging and model comparison. *BMC Evolutionary Biology* 17(1): 1-11.

Bouckaert, R.R., Vaughan, T.G., Barido-Sottani, J., Duchêne, S., Fourment, M., Gavryushkina, A., Heled, J., Jones, G., Kühnert, D., De Maio, N., Matschiner, M., Mendes, F.K., Müller, N.F., Ogilvie, H.A., du Plessis, L., Popinga, A., Rambaut, A., Rasmussen, D., Siveroni, I., Suchard, M.A., Wu, C-H., Xie, D., Zhang, C., Stadler, T., & Drummond, A.J. 2019. BEAST 2.5: An advanced software platform for Bayesian evolutionary analysis. *Public Library of Science Computational Biology* 15(4): e1006650.

Bowlin, M.S., Bisson, I-A., Shamoun-Baranes, J. Reichard, J.D., Sapir, N., Marra, P.P., Kunz, T.H., Wilcove, D.S., Hedenström, A., Guglielmo, C.G., Åkesson, S., Ramenofsky, M., & Wikelski, M. 2010. Grand challenges in migration biology. *Integrative and Comparative Biology* 50(3): 261–279.

Brante, A., Guzmán-Rendón, G., Barría, E.M., Guillemin, M., Vera-Escalona, I., & Hernández, C.E. 2019. Post-disturbance genetic changes: The impact of the 2010 mega-earthquake and tsunami on Chilean sandy beach fauna. *Scientific Reports* 9: 14239.

Brea, M. & Zucol, A.F. 2011. The Paraná-Paraguay Basin: Geology and paleoenvironments. In: Albert, J.S. & Reis, R.E. (Eds.), *Historical biogeography of Neotropical freshwater fishes*, pp. 69-87. University of California Press, USA.

Brito, P.M., & Richter, M. 2016. The contribution of Sir Arthur Smith Woodward to the palaeoichthyology of Brazil–Smith Woodward's types from Brazil. *Geological Society, London, Special Publications* 430(1): 201-217.

Brown, J.H. 1971. Mammals on mountaintops: nonequilibrium insular biogeography. *The American Naturalist* 105(945): 467-478.

Brown, J.H. 1978. The theory of insular biogeography and the distribution of boreal birds and mammals. *Great Basin Naturalist Memoirs* 2: 209-227.

Brown, W.M., George Jr., M., & Wilson, A.C. 1979. Rapid evolution of animal mitochondrial DNA. *Proceedings of the National Academy of Sciences* 76(4): 1967-1971.

Brunsden, D., & Thornes, J.B. 1979. Landscape sensitivity and change. *Transactions of the Institute of British Geographers* 4(4): 463-484.

Buchheim, H.P., & Surdam, R.C. 1977. Fossil catfish and the depositional environment of the Green River Formation, Wyoming. *Geology* 5(4): 196-198.

Buitrago–Suárez, U.A., & Burr, B.M. 2007. Taxonomy of the catfish genus *Pseudoplatystoma* Bleeker (Siluriformes: Pimelodidae) with recognition of eight species. *Zootaxa* 1512(1): 1-38.

Burr, B.M., Warren Jr., M.L., & Bennett, M.G. 2020. Ictaluridae: North American Catfishes, in: Warren Jr., M.L., Burr, B.M., Echelle, A.A., Kuhajda, B.R., Ross, S.T. (Eds.), *Freshwater fishes of North America*. Johns Hopkins University Press, Maryland, pp. 23-100.

Burridge, C.P., Craw, D., & Waters, J.M. 2006. River capture, range expansion, and cladogenesis: the genetic signature of freshwater vicariance. *Evolution* 60(5): 1038-1049.

Busack, C.A., & Currens, K.P. 1995. Genetic risks and hazards in hatchery operations: fundamental concepts and issues. *American Fisheries Society Symposium* 15(7): 71-80.

Bush, G.L. 1975. Modes of animal speciation. *Annual Review of Ecology and Systematics* 6: 339-364.

Bustaffa, E., Stoccoro, A., Bianchi, F., & Migliore, L. 2014. Genotoxic and epigenetic mechanisms in arsenic carcinogenicity. *Archives of Toxicology* 88(5): 1043-1067.

Cadet, J., Courdavault, S., Ravanat, J., & Douki, T. 2005. UVB and UVA radiation-mediated damage to isolated and cellular DNA. *Pure and Applied Chemistry* 77(6): 947-961.

Cahn, A.R. 1925. The migration of animals. *The American Naturalist* 59(665): 539-556.

Camacho, C., Canal, D., & Potti, J. 2015. Testing the matching habitat choice hypothesis in nature: phenotype-environment correlation and fitness in a songbird population. *Evolutionary Ecology* 29: 873-886.

Camus, M.F., Alexander-Lawrie, B., Sharbrough, J., & Hurst, G.D. 2022. Inheritance through the cytoplasm. *Heredity* 129(1): 31-43.

Capobianco, A., & Friedman, M. 2019. Vicariance and dispersal in southern hemisphere freshwater fish clades: a palaeontological perspective. *Biological Reviews* 94(2): 662-699.

Caputo, M.V., & Soares, E.A.A. 2016. Eustatic and tectonic change effects in the reversion of the transcontinental Amazon River drainage system. *Brazilian Journal of Geology* 46: 301-328.

Carvajal-Vallejos, F.M., Duponchelle, F., Desmarais, E., Cerqueira, F., Querouil, S., Nuñez, J., García, C., & Renno, J.-F. 2014. Genetic structure in Amazonian catfish *Brachyplatystoma rousseauxii*: influence of life history strategies. *Genetica* 142: 323-336.

Carvalho, T.P. & Albert, J.S. 2011. The Amazon-Paraguay divide. In: Albert, J.S. & Reis, R.E. (Eds.), *Historical biogeography of Neotropical freshwater fishes*, pp. 59-67. University of California Press, USA.

Cassemiro, F.A., Albert, J.S., Antonelli, A., Menegotto, A., Wüest, R.O., Coelho, M.T.P., Bailly, D., da Silva, V.F., Frota, A., da Graça, W.J. Ré, R., Ramos, T., Oliveira, A.G.D., Dias, M.S., Colwell, R.K., Rangel, T.F., & Graham, C.H. 2023. Landscape dynamics and diversification of the megadiverse South American freshwater fish fauna. *Proceedings of the National Academy of Sciences* 120(2): e2211974120.

Cauvy-Fraunié, S., & Dangles, O. 2019. A global synthesis of biodiversity responses to glacier retreat. *Nature Ecology & Evolution* 3(12): 1675-1685.

Chang, M.M., & Zhou, J.J. 1993. A brief survey of the Chinese Eocene ichthyofauna. *Kaupia Darmstädter Beiträge Naturgeschichte* 2: 157–162.

Chen, B., Cole, J.W., & Grond-Ginsbach, C. 2017. Departure from Hardy-Weinberg equilibrium and genotyping error. Frontiers in Genetics 8(167): 1-6.

Chen, G. & White, P.A. 2004. The mutagenic hazards of aquatic sediments: A review. *Mutation Research* 567: 151-225.

Chen, K.Y., Ludsin, S.A., Marcek, B.J., Olesik, J.W., & Marschall, E.A. 2020. Otolith microchemistry shows natal philopatry of walleye in western Lake Erie. *Journal of Great Lakes Research* 46(5): 1349-1357.

Chen, W.J., Miya, M., Saitoh, K., & Mayden, R.L. 2008. Phylogenetic utility of two existing and four novel nuclear gene loci in reconstructing Tree of Life of ray-finned fishes: the order Cypriniformes (Ostariophysi) as a case study. *Gene* 423(2): 125-134.

Chernomor, O., Von Haeseler, A., & Minh, B.Q. 2016. Terrace aware data structure for phylogenomic inference from supermatrices. *Systematic Biology* 65(6): 997-1008.

Christiansen, K. 1961. Convergence and parallelism in cave Entomobryinae. *Evolution* 15(3): 288-301

Christie, M.R., French, R.A., Marine, M.L., & Blouin, M.S. 2014. How much does inbreeding contribute to the reduced fitness of hatchery-born steelhead (*Oncorhynchus mykiss*) in the wild? *Journal of Heredity* 105(1): 111-119.

Christman, M.C., Culver, D.C., Madden, M.K., & White, D. 2005. Patterns of endemism of the eastern North American cave fauna. *Journal of Biogeography* 32(8): 1441-1452.

Claramunt, S., Derryberry, E.P., Remsen Jr, J.V., & Brumfield, R.T. 2012. High dispersal ability inhibits speciation in a continental radiation of passerine birds. *Proceedings of the Royal Society B: Biological Sciences* 279(1733): 1567-1574.

Clark, K., Karsch-Mizrachi, I., Lipman, D.J., Ostell, J., & Sayers, E.W. 2016. GenBank. *Nucleic Acids Research* 44(D1): D67-D72.

Cleaver, J.E. & Crowley, E. 2002. UV damage, DNA repair and skin carcinogenesis. *Frontiers in Bioscience* 7: d1024-1043.

Cloyed, C.S., & Eason, P.K. 2017. Niche partitioning and the role of intraspecific niche variation in structuring a guild of generalist anurans. *Royal Society Open Science* 4(3): 170060.

Coates, A.G., Jackson, J.B., Collins, L.S., Cronin, T.M., Dowsett, H.J., Bybell, L.M., Jung, P. & Obando, J.A. 1992. Closure of the Isthmus of Panama: the near-shore marine record of Costa Rica and western Panama. *Geological Society of America Bulletin* 104(7): 814-828.

Coates, B.S., Sumerford, D.V., Miller, N.J., Kim, K.S., Sappington, T.W., Siegfried, B.D., & Lewis, L.C. 2009. Comparative performance of single nucleotide polymorphism and microsatellite markers for population genetic analysis. *Journal of Heredity* 100(5): 556-564.

Cope, E.D. 1891. On Vertebrata from the Tertiary and Cretaceous rocks of the North West Territory, volume 3. WF Brown & Company, Massachusetts.

Correa Ayram, C.A., Mendoza, M.E., Etter, A., & Salicrup, D.R.P. 2016. Habitat connectivity in biodiversity conservation: A review of recent studies and applications. *Progress in Physical Geography* 40(1): 7-37.

Cowman, P.F., & Bellwood, D.R. 2013. Vicariance across major marine biogeographic barriers: temporal concordance and the relative intensity of hard versus soft barriers. *Proceedings of the Royal Society B: Biological Sciences* 280(1768): 20131541.

Crispo, E., Bentzen, P., Reznick, D.N., Kinnison, M.T., & Hendry, A.P. 2006. The relative influence of natural selection and geography on gene flow in guppies. *Molecular Ecology* 15: 49-62.

Culver, D.C. 1970. Cave life. Harvard University Press, Massachusetts.

Culver, D.C. 1976. The evolution of aquatic cave communities. *The American Naturalist* 110(976): 945-957.

Culver, D.C., & Pipan, T. 2010. Climate, abiotic factors, and the evolution of subterranean life. *Acta Carsologica* 39(3): 577-586.

Culver, D., & Pipan, T. 2015. Shifting paradigms of the evolution of cave life. *Acta Carsologica* 44(3): 415-425.

Dahlgren, C.P., & Eggleston, D.B. 2000. Ecological processes underlying ontogenetic habitat shifts in a coral reef fish. *Ecology* 81(8): 2227-2240.

Dames, H.R., & Coon, T.G. 1989. Movements of channel and flathead catfish between the Missouri River and a tributary, Perche Creek. Transactions of the American Fisheries Society 118: 670-679.

Darwin, C. 1859. On the origin of species by means of natural selection, or, The preservation of favoured races in the struggle for life. John Murray, United Kingdom.

Davies, T.J., Buckley, L.B., Grenyer, R., & Gittleman, J.L. 2011. The influence of past and present climate on the biogeography of modern mammal diversity. *Philosophical Transactions of the Royal Society B: Biological Sciences* 366(1577): 2526-2535.

Dávila, F.M., & Lithgow-Bertelloni, C. 2013. Dynamic topography in South America. *Journal of South American Earth Sciences* 43: 127-144.

De La Rosa-Reyna, X.F., Sifuentes-Rincón, A.M., Parra-Bracamonte, G.M., & Arellano-Vera, W. 2014. Identification of two Channel Catfish stocks, *Ictalurus punctatus*, cultivated in northeast Mexico. *Journal of the World Aquaculture Society* 45(2): 104-114.

De Meeûs, T. 2018. Revisiting F_{IS}, F_{ST}, Wahlund effects, and null alleles. *Journal of Heredity* 109(4): 446-456.

De Souza, L.S., Armbruster, J.W., & Willink, P.W. 2020. Connectivity of Neotropical river basins in the Central Guiana Shield based on fish distributions. *Frontiers in Forests and Global Change* 3(8): 1-15.

De Souza, L.S., Taphorn, D.C., & Armbruster, J.W. 2019. Review of *Ancistrus* (Siluriformes: Loricariidae) from the northwestern Guiana Shield, Orinoco Andes, and adjacent basins with description of six new species. *Zootaxa* 4552(1): 1-67.

De-Silva, D.L., Elias, M., Willmott, K., Mallet, J., & Day, J.J. 2016. Diversification of clearwing butterflies with the rise of the Andes. *Journal of Biogeography* 43(1): 44-58.

Dehnhard, N., Achurch, H., Clarke, J., Michel, L.N., Southwell, C., Sumner, M.D., Eens, M. & Emmerson, L. 2020. High inter-and intraspecific niche overlap among three sympatrically breeding, closely related seabird species: generalist foraging as an adaptation to a highly variable environment? *Journal of Animal Ecology* 89(1): 104-119.

Descombes, P., Gaboriau, T., Albouy, C., Heine, C., Leprieur, F., & Pellissier, L. 2018. Linking species diversification to palaeo-environmental changes: a process-based modelling approach. *Global Ecology and Biogeography* 27(2): 233-244.

DeWoody, J.A., Harder, A.M., Mathur, S., & Willoughby, J.R. 2021. The long-standing significance of genetic diversity in conservation. *Molecular Ecology* 30(17): 4147-4154.

Díaz, J., Villanova, G.V., Brancolini, F., Del Pazo, F., Posner, V.M., Grimberg, A., & Arranz, S.E. 2016. First DNA barcode reference library for the identification of South American freshwater fish from the lower Paraná River. *Public Library of Science One* 11(7): e0157419.

Dietz, R.S., & Holden, J.C. 1970. The breakup of Pangaea. *Scientific American* 223(4): 30-41.

Dionne, M., Caron, F., Dodson, J.J., & Bernatchez, L. 2008. Landscape genetics and hierarchical genetic structure in Atlantic salmon: the interaction of gene flow and local adaptation. *Molecular Ecology* 17(10): 2382-2396.

Divay, J.D., & Murray, A.M. 2015. The late Eocene–early Oligocene ichthyofauna from the Eastend area of the Cypress Hills Formation, Saskatchewan, Canada. *Journal of Vertebrate Paleontology* 35(4): e956877 [1–25].

Do, C., Waples, R.S., Peel, D., Macbeth, G.M., Tillett, B.J., & Ovenden, J.R. 2014. NeEstimator v2: re-implementation of software for the estimation of contemporary effective population size (Ne) from genetic data. *Molecular Ecology Resources* 14(1): 209-214.

Doellman, M.M., Saint Jean, G., Egan, S.P., Powell, T.H., Hood, G.R., Schuler, H., Bruzzese, D.J., Glover, M.M., Smith, J.J., Yee, W.L., Goughnour, R., Rull, J., Aluja, M., & Feder, J.L. 2020. Evidence for spatial clines and mixed geographic modes of speciation for North American cherry-infesting *Rhagoletis* (Diptera: Tephritidae) flies. *Ecology and Evolution* 10(23): 12727-12744.

Dool, S.E., Picker, M.D., & Eberhard, M.J. 2022. Limited dispersal and local adaptation promote allopatric speciation in a biodiversity hotspot. *Molecular Ecology* 31(1): 279-295.

Drummond, A.J., Ho, S.Y., Phillips, M.J., & Rambaut, A. 2006. Relaxed phylogenetics and dating with confidence. *Public Library of Science Biology* 4(5): e88

Duarte, J.C. 2022. A timeline of Earth's history. In: Green, M., & Duarte, J.C. (Eds.), *A Journey Through Tides*, pp. 117-131. Elsevier, Amsterdam.

Dufresnes, C., Suchan, T., Smirnov, N.A., Denoël, M., Rosanov, J.M., & Litvinchuk, S.N. 2021. Revisiting a speciation classic: comparative analyses support sharp but leaky transitions between *Bombina* toads. *Journal of Biogeography* 48(3): 548-560.

Earl, D.A., & VonHoldt, B.M. 2012. STRUCTURE HARVESTER: a website and program for visualizing STRUCTURE output and implementing the Evanno method. *Conservation Genetics Resources* 4(2): 359-361.

Edgar, R.C. 2021. MUSCLE v5 enables improved estimates of phylogenetic tree confidence by ensemble bootstrapping. *BioRxiv* 2021-06.

Edwards, S.V., Robin, V.V., Ferrand, N., & Moritz, C. 2022. The evolution of comparative phylogeography: putting the geography (and more) into comparative population genomics. *Genome Biology and Evolution* 14(1): evab176.

Egge, J.J., & Simons, A.M. 2009. Molecules, morphology, missing data and the phylogenetic position of a recently extinct madtom catfish (Actinopterygii: Ictaluridae). *Zoological Journal of the Linnean Society* 155(1): 60-75.

Eigenmann, C.H. 1919. *Trogloglanis pattersoni* a new blind fish from San Antonio, Texas. *Proceedings of the American Philosophical Society* 58(6): 397-400.

Emerson, B.C., & Kolm, N. 2005. Species diversity can drive speciation. *Nature* 434(7036): 1015-1017.

Endler, J.A. 1977. Geographic variation, speciation and clines. (MPB-10), Volume 10. Princeton University Press, New Jersey.

Espinasa-Pereña, R. 2007. El Karst de México (Mapa NA III 3), in: Coll-Hurtado, A., (Ed.), *Nuevo Atlas Nacional de México*, Instituto de Geografía, Universidad Nacional Autónoma de México.

Evanoff, E., McIntosh, W.C., & Murphey, P.C. 2001. Stratigraphic summary and 40Ar/39Ar geochronology of the Florissant Formation, Colorado, in: Evanoff, E., Gregory-Wodzicki, K.M., Johnson, K.R. (Eds.), *Fossil flora and stratigraphy of the Florissant Formation, Colorado*. Proceedings of the Denver Museum of Natural History, Colorado, pp. 1–16.

Excoffier, L., & Lischer, H.E.L. 2010. Arlequin suite ver 3.5: A new series of programs to perform population genetics analyses under Linux and Windows. *Molecular Ecology Resources* 10(3): 564-567.

Exposito-Alonso, M., Booker, T.R., Czech, L., Gillespie, L., Hateley, S., Kyriazis, C.C., Lang, P.L.M., Leventhal, L., Nogues-Bravo, D., Pagowski, V., Ruffley, M., Spence, J.P., Toro Arana, S.E., Weiß, C.L., & Zess, E. 2022. Genetic diversity loss in the Anthropocene. *Science* 377(6613): 1431-1435.

Falush, D., Stephens, M., & Pritchard, J.K. 2003. Inference of population structure using multilocus genotype data: linked loci and correlated allele frequencies. *Genetics* 164(4): 1567-1587.

Fatimah, Ward, C.R. 2009. Mineralogy and organic petrology of oil shales in the Sangkarewang Formation, Ombilin Basin, West Sumatra. International Journal of Coal Geology 77: 424–435.

Ferraris Jr., C.J. 2007. Checklist of catfishes, recent and fossil (Osteichthyes: Siluriformes), and catalogue of siluriform primary types. *Zootaxa* 1418(1): 1-628.

Ferreira, R.L., & Pellegrini, T.G. 2019. Species-area model predicting diversity loss in an artificially flooded cave in Brazil. *International Journal of Speleology* 48(2): 155-165.

Fieberg, J., Signer, J., Smith, B., & Avgar, T. 2021. A 'How to' guide for interpreting parameters in habitat-selection analyses. *Journal of Animal Ecology* 90(5): 1027-1043.

Figueiredo, F.J., & Costa Carvalho, B. 1999a. *Steindachneridion silvasantosi* n. sp. (Teleostei, Siluriformes, Pimelodidae) from the Tertiary of Taubaté Basin, São Paulo, Brazil. *Anais da Academia Brasileira de Ciências* 71: 683-695.

Figueiredo, F.J., & Costa Carvalho, B. 1999b. Redescription of *Steindachneridion iheringi* (Woodward, 1898) (Teleostei, Siluriformes, Pimelodidae) from the Tertiary of Taubaté Basin, São Paulo State, Brazil. *Anais da Academia Brasileira de Ciências* 7: 869-884.

Figueiredo, J.J.J.P., Hoorn, C., Van der Ven, P., & Soares, E. 2009. Late Miocene onset of the Amazon River and the Amazon deep-sea fan: evidence from the Foz do Amazonas Basin. *Geology* 37(7): 619-622.

Fisch-Muller, S., Mol, J.H., & Covain, R. 2018. An integrative framework to reevaluate the Neotropical catfish genus *Guyanancistrus* (Siluriformes: Loricariidae) with particular emphasis on the *Guyanancistrus brevispinis* complex. *Public Library of Science One* 13(1) : e0189789.

Fišer, C., Robinson, C.T., & Malard, F. 2018. Cryptic species as a window into the paradigm shift of the species concept. *Molecular Ecology* 27(3): 613-635.

Fitz-Díaz, E., Lawton, T.F., Juárez-Arriaga, E., & Chávez-Cabello, G. 2018. The Cretaceous-Paleogene Mexican orogen: Structure, basin development, magmatism and tectonics. *Earth-Science Reviews* 183: 56-84.

Fitzpatrick, B.M., Fordyce, J.A., & Gavrilets, S. 2008. What, if anything, is sympatric speciation? *Journal of Evolutionary Biology* 21(6): 1452-1459.

Fitzpatrick, B.M., Fordyce, J.A., & Gavrilets, S. 2009. Pattern, process and geographic modes of speciation. *Journal of Evolutionary Biology* 22: 2342-2347.

Flament, N., Gurnis, M., & Müller, R.D. 2013. A review of observations and models of dynamic topography. *Lithosphere* 5(2): 189-210.

Foote, M., & Miller, A.I., 2007. Principles of paleontology, 3rd ed. W.H. Freeman and Company, New York.

Freeman, B.G., & Pennell, M.W. 2021. The latitudinal taxonomy gradient. *Trends in Ecology & Evolution* 36(9): 778-786.

Fricke, R., Eschmeyer, W.N., & Van der Laan, R. (Eds). 2023. Eschmeyer's catalog of fishes: genera, species, references. http://researcharchive.calacademy.org/research/ichthyology/catalog/fishcatmain.asp. Electronic version accessed 15 April 2023.

Frost, L.A., Evans, B.S., & Jerry, D.R. 2006. Loss of genetic diversity due to hatchery culture practices in barramundi (*Lates calcarifer*). *Aquaculture* 261(3): 1056-1064.

García Vásquez, A., Alonso, J.C., Carvajal, F., Moreau, J., Nunez, J., Renno, J.F., Tello, S., Montreuil, V., & Duponchelle, F. 2009. Life-history characteristics of the large Amazonian migratory catfish *Brachyplatystoma rousseauxii* in the Iquitos region, Peru. *Journal of Fish Biology* 75(10): 2527-2551.

Gavrilets, S., Li, H., & Vose, M.D. 2000. Patterns of parapatric speciation. *Evolution* 54(4): 1126-1134.

Gayet, M., & Meunier, F.J. 2003. Paleontology and palaeobiogeography of catfishes. In: Arratia, G., Kapoor, B.G., Chardon, M., Diogo, R. (Eds.), *Catfishes*, vol. 2. Science Publishers, Inc., EnWeld, pp. 291–522.

GBIF.org, 2022. GBIF Occurrence Download Ictaluridae https://doi.org/10.15468/dl.2qk495.

GBIF.org. 2023a. GBIF Occurrence Download *Pimelodus ornatus* https://doi.org/10.15468/dl.vhnyve.

GBIF.org 2023b GBIF Occurrence Download Pimelodidae https://doi.org/10.15468/dl.p8gwd9

Geneious Prime 2023.0.1. https://www.geneious.com.

González-Rodríguez, K.A., Espinosa-Arrubarrena, L., & González-Barba, G. 2013. An overview of the Mexican fossil fish record. In: Arratia, G., Schultze, H.-P., Wilson, M.V.H. (Eds.), *Mesozoic Fishes 5 – Global Diversity and Evolution*, Verlag Dr. Friedrich Pfeil, München, Germany, pp. 9-34.

Goudet, J.F. 1995. FSTAT (version 1.2): a computer program to calculate F-statistics. *Journal of Heredity* 86(6): 485-486.

Goudet, J.F. 2002. FSTAT (version 2.9. 3.2): a program to estimate and test gene diversities and fixation indices. Available at: http://www.unil.ch/izea/software/fstat.html.

Grande, L., & Lundberg, J.G. 1988. Revision and redescription of the genus *Astephus* (Siluriformes: Ictaluridae) with a discussion of its phylogenetic relationships. *Journal of Vertebrate Paleontology* 8(2): 139-171.

Green, R.T., Bertetti, F.P., Fratesi, B., & McGinnis, R.N. 2019. Uvalde Pool of the Edwards (Balcones Fault Zone) Aquifer. In: Sharp, J.M., Jr., Green, R.T., Schindel, G.M., (Eds.), *The Edwards Aquifer: The Past, Present, and Future of a Vital Water Resource*. Geological Society of America Memoir 215, pp. 47–60.

Greenwood, P.J. 1980. Mating systems, philopatry and dispersal in birds and mammals. *Animal Behaviour*, *28*(4): 1140-1162.

Grinnell, J. 1924. Geography and evolution. *Ecology* 5(3): 225-229.

Hale, J.A., & Streever, W.J. 1994. Cave fauna distribution within fully-flooded cave systems in Florida. *Journal of Freshwater Ecology* 9(3): 171-174.

Hanzen, C., Lucas, M.C., O'Brien, G., Downs, C.T., & Willows-Munro, S. 2020. African freshwater eel species (*Anguilla* spp.) identification through DNA barcoding. *Marine and Freshwater Research* 71(11): 1543-1548.

Hardman, M. 2004. The phylogenetic relationships among *Noturus* catfishes (Siluriformes: Ictaluridae) as inferred from mitochondrial gene cytochrome b and nuclear recombination activating gene 2. *Molecular Phylogenetics and Evolution* 30(2): 395-408.

Hardman, M., & Hardman, L.M. 2008. The relative importance of body size and paleoclimatic change as explanatory variables influencing lineage diversification rate: an evolutionary analysis of bullhead catfishes (Siluriformes: Ictaluridae). *Systematic Biology* 57(1): 116-130.

Hardman, M., & Lundberg, J. G. 2006. Molecular phylogeny and a chronology of diversification for "phractocephaline" catfishes (Siluriformes: Pimelodidae) based on mitochondrial DNA and nuclear recombination activating gene 2 sequences. *Molecular Phylogenetics and Evolution* 40(2): 410-418.

Hardman, M., & Page, L.M. 2003. Phylogenetic relationships among bullhead catfishes of the genus *Ameiurus* (Siluriformes: Ictaluridae). *Copeia* 2003(1): 20-33.

Harrison, T., Msuya, C.P., Murray, A.M., Fine Jacobs, B., Báez, A.M., Mundil, R., & Ludwig, K.R. 2001. Paleontological investigations at the Eocene locality of Mahenge in north-central Tanzania, East Africa. In: Gunnel, G.F. (Ed.), *Eocene biodiversity: unusual occurrences and rarely sampled habitats*. Topics in Geobiology. Kluwar Academic–Plenum Publishers, New York, pp. 39–74.

Harvey, P.H., & Pagel, M.D. 1991. The comparative method in evolutionary biology (Vol. 239). Oxford University Press, Oxford.

Hastings, K.K., Jemison, L.A., Pendleton, G.W., Raum-Suryan, K.L., & Pitcher, K.W. 2017. Natal and breeding philopatry of female Steller sea lions in southeastern Alaska. *PLoS One* 12(6): e0176840.

Haug, G.H., & Tiedemann, R. 1998. Effect of the formation of the Isthmus of Panama on Atlantic Ocean thermohaline circulation. *Nature* 393(6686): 673-676.

Haxton, T., & Chubbuck, D. 2002. Review of the historical and existing natural environment and resource uses on the Ottawa River. Ontario Ministry of Natural Resources, Science and Information Branch, Southcentral Science and Information Section Technical Report #119. 76 p.

Heads, M. 2015. The relationship between biogeography and ecology: envelopes, models, predictions: biogeography and ecology. *Biological Journal of the Linnean Society* 115(2): 456-468.

Heard, S.B. 1996. Patterns in phylogenetic tree balance with variable and evolving speciation rates. *Evolution* 50(6): 2141-2148.

Hellberg, M.E. 1994. Relationships between inferred levels of gene flow and geographic distance in a philopatric coral, *Balanophyllia elegans*. *Evolution* 48(6): 1829-1854.

Hendrickson, D.A., Johnson, J., Sprouse, P., Howard, S., Garrett, G.P., Krejca, J.K., Gluesenkamp, A., Paulín, J.A.D., Dugan, L., Cohen, A.E., Espriú, A.H., Sullivan, J.P., Fenolio, D.B., Karges, J., Smith, R., García De León, F.J., Wolaver, B., & Reddell, J. 2017. Discovery of the Mexican Blindcat, *Prietella phreatophila*, in the US, and an update on its rangewide conservation status. UT Faculty/Researcher Works, Texas.

Hendrickson, D.A., Krejca, J.K., & Martinez, J.M.R. 2001. Mexican blindcats genus *Prietella* (Siluriformes: Ictaluridae): an overview of recent explorations. *Environmental Biology of Fishes* 62(1): 315-337.

Henschel, E., & Lujan, N.K. 2021. Range extension of the miniature pencil-catfish *Potamoglanis wapixana* (Siluriformes: Trichomycteridae) into the Essequibo River basin, Guyana. *Journal of Fish Biology* 99(5): 1741-1745.

Herberstein, M.E. & Fleisch, A.F. 2003. Effect of abiotic factors on the foraging strategy of the orb-web spider *Argiope keyserlingi* (Araneae: Araneidae). *Austral Ecology* 28: 622-628.

Herbert, P.D.N., Stoeckle, M.Y., Zemlak, T.S., & Francis, C.M. 2004. Identification of birds through DNA barcodes. *Public Library of Science Biology* 2(10): e312.

Hernández Cordero, A.L., & Seitz, R.D. 2014. Structured habitat provides a refuge from blue crab, *Callinectes sapidus*, predation for the bay scallop, *Argopecten irradians concentricus* (Say 1822). *Journal of Experimental Marine Biology and Ecology* 460: 100-108.

Hessen, D.O. 2008. Solar radiation and the evolution of life. In: [Bjertness, E. (ed.)] Solar Radiation and Human Health, pp. 123-136. The Norwegian Academy of Science and Letters, Norway.

Hoang, D.T., Chernomor, O., Von Haeseler, A., Minh, B.Q., & Vinh, L.S. 2018. UFBoot2: improving the ultrafast bootstrap approximation. *Molecular Biology and Evolution* 35(2): 518-522.

Holm, S. 1979. A simple sequentially rejective multiple test procedure. Scandinavian Journal of Statistics 6: 65-70.

Homola, J.J., Scribner, K.T., Baker, E.A., & Auer, N.A. 2010. Genetic assessment of straying rates of wild and hatchery reared lake sturgeon (Acipenser fulvescens) in Lake Superior tributaries. Journal of Great Lakes Research 36(4): 798-802.

Homola, J.J., Scribner, K.T., Elliott, R.F., Donofrio, M.C., Kanefsky, J., Smith, K.M., & McNair, J.N. 2012. Genetically derived estimates of contemporary natural straying rates and historical gene flow among Lake Michigan lake sturgeon populations. Transactions of the American Fisheries Society 141(5): 1374-1388.

Hoorn, C., Boschman, L.M., Kukla, T., Sciumbata, M., & Val, P. 2022. The Miocene wetland of western Amazonia and its role in Neotropical biogeography. *Botanical Journal of the Linnean Society* 199(1): 25-35.

Hoorn, C., Mosbrugger, V., Mulch, A., & Antonelli, A. 2013. Biodiversity from mountain building. *Nature Geoscience* 6(3): 154-154.

Hoorn, C., Wesselingh, F.P., Ter Steege, H., Bermudez, M.A., Mora, A., Sevink, J., Sanmartín, I., Sanchez-Meseguer, A., Anderson, C.L., Figueiredo, J.P., Jaramillo, C., Riff, D., Negri, F.R., Hooghiemstra, H., Lundberg, J.G., Stadler, T., Särkinen, T., & Antonelli, A. 2010. Amazonia through time: Andean uplift, climate change, landscape evolution, and biodiversity. *Science* 330(6006): 927-931.

Hoskin, C.J., Higgie, M., McDonald, K.R., & Moritz, C. 2005. Reinforcement drives rapid allopatric speciation. *Nature* 437 :1353-1356.

Howe, G.E. 1976. The evolutionary role of wildfire in the Northern Rockies and implications for resource managers. *Proceedings of the Tall Timbers Fire Ecology Conference* 14: 257-265.

Hrbek, T., & Meyer, A. 2003. Closing of the Tethys Sea and the phylogeny of Eurasian killifishes (Cyprinodontiformes: Cyprinodontidae). *Journal of Evolutionary Biology* 16(1), 17-36.

Hubbs, C.L., & Bailey, R.M. 1947. Blind catfishes from artesian waters of Texas. *Occasional Papers of the Museum of Zoology, University of Michigan* 499: 1–15.

Hubert, W.A. 1999. Biology and management of Channel Catfish. In: Catfish 2000: Proceedings of the International Ictalurid Symposium, pp. 3-22. American Fisheries Society, Symposium 24, USA.

Hubert, W.A., & O'Shea, D.T. 1991. Reproduction by fishes in a headwater stream flowing into Grayrocks Reservoir, Wyoming. *Prairie Naturalist* 23: 61-68.

Huey, R.B. 1991. Physiological consequences of habitat selection. *The American Naturalist* 137: S91-S115.

Hughes, A.R., Inouye, B.D., Johnson, M.T.J., Underwood, N., & Vellend, M. 2008. Ecological consequences of genetic diversity. *Ecology Letters* 11: 609-623.

Hughes, L.C., Ortí, G., Huang, Y., Sun, Y., Baldwin, C.C., Thompson, A.W., Arcila, D., Betancur-R, R., Li C., Becker, L., Bellora, N., Zhao, X., Li, X., Wang, M., Fang, C., Xie, B., Zhou, Z., Huang, H., Chen, S. Venkatesh, B., & Shi, Q. 2018. Comprehensive phylogeny of ray-finned fishes (Actinopterygii) based on transcriptomic and genomic data. *Proceedings of the National Academy of Sciences* 115(24): 6249-6254

Hulce, D., Li, X., Snyder-Leiby, T., & Liu, C.J. 2011. GeneMarker® genotyping software: tools to increase the statistical power of DNA fragment analysis. *Journal of Biomolecular Techniques* 22(Suppl): S35.

Humphries, C.J., & Parenti, L.R. 1999. Cladistic biogeography. Oxford University Press, Oxford.

Hurtado, C., Roddaz, M., Santos, R.V., Baby, P., Antoine, P.O., & Dantas, E.L. 2018. Cretaceous-early Paleocene drainage shift of Amazonian rivers driven by Equatorial Atlantic Ocean opening and Andean uplift as deduced from the provenance of northern Peruvian sedimentary rocks (Huallaga basin). *Gondwana Research* 63: 152-168.

Hutto, R.L. 1985. In: [Cody, M.L. (ed.)] Habitat Selection in Birds, pp. 455-472. Academic Press, Inc., USA.

Igarashi, Y., Zhang, H., Tan, E., Sekino, M., Yoshitake, K., Kinoshita, S., Mitsuyama, S., Yoshinaga, T., Chow, S., Kurogi, H., Shinoda, A., Han, Y.-S., Wakiya, R., Mochioka, N., Yamamoto, T., Kuwada, H., Kaji, Y., Suzuki, Y., Gojobori, T., Kobayashi, T., Saitoh, K., Watabe, S., & Asakawa, S. 2018. Whole-genome sequencing of 84 Japanese eels reveals evidence against panmixia and support for sympatric speciation. *Genes* 9(10): 474.

Ihering, H. von. 1898. Observações sobre os peixes fósseis de Taubaté. *Revista do Museu Paulista* 3: 71–75.

Iriondo, M.H., & Paira, A.R. 2007. Physical geography of the basin. In: Iriondo, M.H., Paggi, J.C., & Parma, M.J. (Eds.), *The middle Paraná River: limnology of a subtropical wetland*. 7-31. Huxley, A.C.H.J., & Ford, E.B. (Eds.), pp. 7-31. Springer, USA.

Ivanova, N.V., Dewaard, J.R., & Hebert, P.D. 2006. An inexpensive, automation-friendly protocol for recovering high-quality DNA. *Molecular Ecology Notes* 6(4): 998-1002.

Jaenike, J., & Holt, R.D. 1991. Genetic variation for habitat preference: evidence and explanations. *The American Naturalist* 137: S67-S90.

Jansen, G., Devaere, S., Weekers, P.H.H., & Adriaens, D. 2006. Phylogenetic relationships and divergence time estimate of African anguilliform catfish (Siluriformes: Clariidae) inferred from ribosomal gene and spacer sequences. Molecular Phylogenetics and Evolution 38(1): 65-78.

Jenkins, R.E., & Burkhead, N.M. 1994. Freshwater fishes of Virginia. American Fisheries Society, Bethesda, Maryland. 1079 p.

Johnson, D. H. 1980. The comparison of usage and availability measurements for evaluating resource preference. *Ecology* 61(1): 65-71.

Johnson, F.M. 1998. The genetic effects of environmental lead. *Mutation Research* 410: 123-140.

Johnson, K.P., Adler, F.R., & Cherry, J.L. 2000. Genetic and phylogenetic consequences of island biogeography. *Evolution* 54(2): 387-396.

Jones, K.A., Ratcliffe, N., Votier, S.C., Newton, J., Forcada, J., Dickens, J., Stowasser, G., & Staniland, I.J. 2020. Intra-specific niche partitioning in Antarctic fur seals, *Arctocephalus gazella*. *Scientific Reports* 10(1): 1-15.

Jones, K.E., Bininda-Emonds, O.R., & Gittleman, J.L. 2005. Bats, clocks, and rocks: diversification patterns in Chiroptera. *Evolution* 59(10): 2243-2255.

Jorgensen, S.J., Reeb, C.A., Chapple, T.K., Anderson, S., Perle, C., Van Sommeran, S.R., Fritz-Cope, C., Brown, A.C., Klimley, A.P., & Block, B.A. 2010. Philopatry and migration of Pacific white sharks. *Proceedings of the Royal Society B: Biological Sciences* 277(1682): 679-688.

June, F.C. 1977. Reproductive patterns in seventeen species of warmwater fishes in a Missouri River reservoir. *Environmental Biology of Fishes* 2: 285-296.

Kalinowski, S.T. 2005. hp-rare 1.0: a computer program for performing rarefaction on measures of allelic richness. *Molecular Ecology Notes* 5(1): 187-189.

Kalyaanamoorthy, S., Minh, B.Q., Wong, T.K., Von Haeseler, A., & Jermiin, L.S. 2017. ModelFinder: fast model selection for accurate phylogenetic estimates. *Nature Methods* 14(6): 587-589.

Kappas, I., Vittas, S., Pantzartzi, C.N., Drosopoulou, E., & Scouras, Z.G. 2016. A time-calibrated mitogenome phylogeny of catfish (Teleostei: Siluriformes). *Public Library of Science ONE* 11(12): e0166988 doi: 10.1371/journal.pone.0166988.

Kapralova, K.H., Jónsson, Z.O., Palsson, A., Franzdóttir, S.R., le Deuff, S., Kristjánsson, B. K., & Snorrason, S.S. 2015. Bones in motion: Ontogeny of craniofacial development in sympatric arctic charr morphs. *Developmental Dynamics* 244(9): 1168-1178.

Keeney, D.B., Heupel, M.R., Hueter, R.E., & Heist, E.J. 2005. Microsatellite and mitochondrial DNA analyses of the genetic structure of blacktip shark (*Carcharhinus limbatus*)

nurseries in the northwestern Atlantic, Gulf of Mexico, and Caribbean Sea. *Molecular Ecology* 14(7): 1911-1923.

Kendall, D.G. 1948. On the generalized" birth-and-death" process. *Annals of Mathematical Statistics* 19(1): 1-15.

Keren-Rotem, T., Bouskila, A., & Geffen, E. 2006. Ontogenetic habitat shift and risk of cannibalism in the common chameleon (*Chamaeleo chamaeleon*). *Behavioral Ecology and Sociobiology* 59: 723-731.

Kernaléguen, L., Arnould, J.P.Y., Guinet, C., Cazelles, B., Richard, P., & Cherel, Y. 2016. Early-life sexual segregation: ontogeny of isotopic niche differentiation in the Antarctic fur seal. *Scientific Reports* 6(1): 33211.

Khan, M.K., & Herberstein, M.E. 2020. Ontogenetic habitat shifts reduce costly male–male interactions. *Evolutionary Ecology* 34(5): 735-743.

Kimura, M. 1962. On the probability of fixation of mutant genes in a population. *Genetics* 47: 713-719.

Köhler, F., Panha, S., & Glaubrecht, M. 2010. Speciation and radiation in a river: assessing the morphological and genetic differentiation in a species flock of viviparous gastropods (Cerithioidea: Pachychilidae). *Evolution in Action: Case studies in Adaptive Radiation, Speciation and the Origin of Biodiversity* 2010: 513-550.

Kozak, K.H., Graham, C.H., & Wiens, J.J. 2008. Integrating GIS-based environmental data into evolutionary biology. *Trends in Ecology & Evolution* 23(3): 141-148.

Krejca, J.K. 2005. Stygobite phylogenetics as a tool for determining aquifer evolution. Ph.D. dissertation, The University of Texas at Austin.

Krejca, J.K., & Reddell, J. 2019. Biology and ecology of the Edwards Aquifer. In: Sharp Jr., J.M., Green, R.T., Schindel, G.M. (Eds.), *The Edwards Aquifer: the past, present, and future of a vital water resource*. Geological Society of America, Colorado, pp. 159-169.

Krewenka, K.M., Holzschuh, A., Tscharntke, T., & Dormann, C.F. 2011. Landscape elements as potential barriers and corridors for bees, wasps and parasitoids. *Biological Conservation* 144(6): 1816-1825.

Kreyling, J., Jentsch, A., & Beierkuhnlein, C. 2011. Stochastic trajectories of succession initiated by extreme climatic events. *Ecology Letters* 14(8): 758-764.

Lacerda, M., Romano, P.S., Bandeira, K.L., & Souza, L.G. 2021. Georeferencing fossiliferous localities from Solimões and Acre Basins (Brazil)-what we know so far about Solimões Formation and future perspectives. Anais da Academia Brasileira de Ciências 93(2).

Lamkom, T., Kucuktas, H., Liu, Z., Li, P., Na-Nakorn, U., Klinbunga, S., Hutson, A., Chaimongkol, A., Ballenger, J., Umali, G., & Dunham, R.A. 2008. Microsatellite variation among domesticated populations of Channel Catfish (*Ictalurus punctatus*) and blue catfish (*I. furcatus*). *Kasetsart University Fisheries Research Bulletin* 32(2): 37-47.

Lande, R. 1980. Genetic variation and phenotypic evolution during allopatric speciation. *The American Naturalist* 116(4): 463-479.

Lande, R. 1982. Rapid origin of sexual isolation and character divergence in a cline. *Evolution* 36(2): 213-223.

Lanfear, R., Frandsen, P.B., Wright, A.M., Senfeld, T., & Calcott, B. 2017. PartitionFinder 2: new methods for selecting partitioned models of evolution for molecular and morphological phylogenetic analyses. *Molecular Biology and Evolution* 34(3): 772-773.

Langecker, T.G., & Longley, G. 1993. Morphological adaptations of the Texas blind catfishes *Trogloglanis pattersoni* and *Satan eurystomus* (Siluriformes: Ictaluridae) to their underground environment. *Copeia* 4: 976-986.

Lara-Rivera, A.L., Parra-Bracamonte, G.M., Sifuentes-Rincón, A.M., & De la Rosa-Reyna, X.F. 2019. Genetic diversity and structure of Channel Catfish from continental waters of Mexico. *North American Journal of Aquaculture* 81(1): 74-80.

Lashin, S.A., Suslov, V.V., & Matushkin, Y.G. 2012. Theories of biological evolution from the viewpoint of the modern systemic biology. *Russian Journal of Genetics* 48(5): 481-496.

Lawson Handley, L.J., & Perrin, N. 2007. Advances in our understanding of mammalian sex-biased dispersal. *Molecular Ecology* 16(8): 1559-1578.

Le, M., Raxworthy, C.J., McCord, W.P., & Mertz, L. 2006. A molecular phylogeny of tortoises (Testudines: Testudinidae) based on mitochondrial and nuclear genes. *Molecular Phylogenetics and Evolution* 40(2): 517-531.

Lehmberg, E.S., Elbassiouny, A.A., Bloom, D.D., López-Fernández, H., Crampton, W.G., & Lovejoy, N.R. 2018. Fish biogeography in the "Lost World" of the Guiana Shield: phylogeography of the weakly electric knifefish *Gymnotus carapo* (Teleostei: Gymnotidae). *Journal of Biogeography* 45(4): 815-825.

Lemopoulos, A., & Covain, R. 2019. Biogeography of the freshwater fishes of the Guianas using a partitioned parsimony analysis of endemicity with reappraisal of ecoregional boundaries. *Cladistics* 35(1): 106-124.

Lemopoulos, A., Prokkola, J.M., Uusi-Heikkilä, S., Vasemägi, A., Huusko, A., Hyvärinen, P., Koljonen, M.L., Koskiniemi, J. & Vainikka, A. 2019. Comparing RADseq and microsatellites for estimating genetic diversity and relatedness—implications for brown trout conservation. *Ecology and Evolution* 9(4): 2106-2120.

Leprieur, F., Descombes, P., Gaboriau, T., Cowman, P.F., Parravicini, V., Kulbicki, M., Melián, C.J., De Santana, C.N., Heine, C., Mouillot, D., Bellwood, D.R., & Pellissier, L. 2016. Plate tectonics drive tropical reef biodiversity dynamics. *Nature Communications* 7(1): 1-8.

Lescak, E.A., Bassham, S.L., Catchen, J., Gelmond, O., Sherbick, M.L., von Hippel, F.A., & Cresko, W.A. 2015. Evolution of stickleback in 50 years on earthquake-uplifted islands. *Proceedings of the National Academy of Sciences* 112(52): E7204-E7212.

Li, C., Ortí, G., Zhang, G., & Lu, G. 2007. A practical approach to phylogenomics: the phylogeny of ray-finned fish (Actinopterygii) as a case study. *BMC Evolutionary Biology* 7(1): 1-11.

Li, F., Tierno de Figueroa, J.M., Lek, S., & Park, Y.S. 2015. Continental drift and climate change drive instability in insect assemblages. *Scientific Reports* 5(1): 11343.

Li, X., Shen, X., Chen, X., Xiang, D., Murphy, R.W., & Shen, Y. 2018. Detection of potential problematic Cytb gene sequences of fishes in GenBank. *Frontiers in Genetics* 9(30): 1-5.

Lima, E.S., Oliveira, M.S.B., & Tavares-Dias, M. 2021. Diversity and community ecology of metazoan parasites in *Pimelodus ornatus* (Siluriformes: Pimelodidae) from the Amazonas River in Brazil. *Revista Brasileira de Parasitologia Veterinária* 30(3): e006021.

Littmann, M.W., Lundberg, J.G., & Rocha, M.S. 2021. Revision of the South American catfish genus *Hypophthalmus* (Siluriformes, Pimelodidae) with descriptions of two new species from the Amazon and Orinoco Basins. *Proceedings of the Academy of Natural Sciences of Philadelphia* 167(1): 171-223.

Losos, J.B., & Ricklefs, R.E. 2009. Adaptation and diversification on islands. *Nature* 457(7231): 830-836.

Lovejoy, N.R. 2000. Reinterpreting recapitulation: systematics of needlefishes and their allies (Teleostei: Beloniformes). *Evolution* 54(4): 1349-1362.

Lovejoy, N.R., & Collette, B.B. 2001. Phylogenetic relationships of New World needlefishes (Teleostei: Belonidae) and the biogeography of transitions between marine and freshwater habitats. *Copeia* 2001(2): 324-338.

Lovejoy, N.R., Iranpour, M., & Collette, B.B. 2004. Phylogeny and jaw ontogeny of Beloniform fishes. *Integrative and Comparative Biology* 44(5): 366-377.

Luebert, F., & Weigend, M. 2014. Phylogenetic insights into Andean plant diversification. *Frontiers in Ecology and Evolution*, 2(27): 1-17.

Lujan, N.K., & Armbruster, J.W. 2011. The Guiana Shield. In: Albert, J.S. & Reis, R.E. (Eds.), *Historical biogeography of Neotropical freshwater fishes*, pp. 59-67. University of California Press, USA.

Lundberg, J.G. 1970. The evolutionary history of North American catfishes, family Ictaluridae. University of Michigan, Michigan.

Lundberg, J.G., 1975. The fossil catfishes of North America. *University of Michigan Papers on Paleontology* 11(2): 1-58.

Lundberg, J.G. 1982. The comparative anatomy of the toothless blindcat, *Trogloglanis pattersoni* Eigenmann, with a phylogenetic analysis of the ictalurid catfishes. *Miscellaneous publications (University of Michigan. Museum of Zoology* 163: 1–85.

Lundberg, J.G. 1992. The phylogeny of ictalurid catfishes: a synthesis of recent work. In: Mayden, R.L. (Ed.), *Systematics, historical ecology, and North American freshwater fishes.* Stanford University Press, Stanford, pp. 392–420.

Lundberg, J.G. 1997. Freshwater fishes and their paleobiotic implications. In: R.F. Kay, R.H. Madden, R.L. Cifelli, & J.J. Flynn (Eds.), *Vertebrate Paleontology in the Neotropics: The Miocene Fauna of La Venta, Colombia*, pp. 67-91. Smithsonian Institution Press, Washington DC.

Lundberg, J.G. 2005. *Brachyplatystoma promagdalena*, new species, a fossil goliath catfish (Siluriformes: Pimelodidae) from the Miocene of Colombia, South America. *Neotropical Ichthyology* 3: 597-605.

Lundberg, J.G., Covain, R., Sullivan, J.P., & Fisch-Muller, S. 2012. Phylogenetic position and notes on the natural history of *Pimelabditus moli* Parisi & Lundberg, 2009 (Teleostei: Siluriformes), a recently discovered pimelodid catfish from the Maroni River basin. *Cybium* 36(1): 105-114.

Lundberg, J.G., Hendrickson, D.A., Luckenbill, K.R., & Mariangeles, A.H., 2017. Satan's skeleton revealed: a tomographic and comparative osteology of *Satan eurystomus*, the subterranean Widemouth Blindcat (Siluriformes, Ictaluridae). *Proceedings of the Academy of Natural Sciences of Philadelphia* 165(1): 117-173.

Lundberg, J.G., Marshall, L.G., Guerrero, J., Horton, B., Malabarba, M.C.S.L., & Wesselingh, F. 1998. The stage for Neotropical fish diversification: a history of tropical South American rivers. *Phylogeny and Classification of Neotropical Fishes* 27: 13-48.

Lundberg, J.G., Sabaj Pérez, M.H., Dahdul, W.M., & Aguilera, O.A. 2010. The Amazonian Neogene fish fauna. In: C. Hoorn, & F.P. Wesselingh (Eds.) *Amazonia: Landscape and Species Evolution*, pp. 281-301. Wiley-Blackwell Publishing, Oxford.

Lundberg, J.G., Sullivan, J.P., & Hardman, M. 2011. Phylogenetics of the South American catfish family Pimelodidae (Teleostei: Siluriformes) using nuclear and mitochondrial gene sequences. *Proceedings of the Academy of Natural Sciences of Philadelphia* 161: 153-189.

Lundberg, J.G., Sullivan, J.P., Rodiles-Hernández, R., & Hendrickson, D.A. 2007. Discovery of African roots for the Mesoamerican Chiapas catfish, *Lacantunia enigmatica*, requires an ancient intercontinental passage. *Proceedings of the Academy of Natural Sciences of Philadelphia* 156(1): 39-53.

MacArthur, R.H., & Wilson, E.O. 1963. An equilibrium theory of insular zoogeography. *Evolution* 17(4): 373-387.

MacArthur, R.H., & Wilson, E.O. 1967. The theory of island biogeography, Princeton University Press, New Jersey.

Macey, J.R., Schulte II, J.A., Larson, A., Fang, Z., Wang, Y., Tuniyev, B.S., & Papenfuss, T.J. 1998. Phylogenetic relationships of toads in the *Bufo bufo* species group from the eastern escarpment of the Tibetan Plateau: a case of vicariance and dispersal. *Molecular Phylogenetics and Evolution* 9(1): 80-87.

Mammola, S., & Isaia, M. 2017. Spiders in caves. *Proceedings of the Royal Society B: Biological Sciences* 284(1853): 20170193.

Manel, S., Schwartz, M.K., Luikart, G., & Taberlet, P. 2003. Landscape genetics: combining landscape ecology and population genetics. *Trends in Ecology & Evolution* 18(4): 189-197.

Marra, P.P., & Holmes, R.T. 2001. Consequences of dominance-mediated habitat segregation in American Redstarts during the nonbreeding season. *The Auk* 118(1): 92-104.

Markert, J.A., Arnegard, M.E., Danley, P.D., & Kocher, T.D. 1999. Biogeography and population genetics of the Lake Malawi cichlid *Melanochromis auratus*: habitat transience, philopatry and speciation. *Molecular Ecology* 8(6): 1013-1026.

Matschiner, M., Musilová, Z., Barth, J.M., Starostová, Z., Salzburger, W., Steel, M., & Bouckaert, R. 2017. Bayesian phylogenetic estimation of clade ages supports trans-Atlantic dispersal of cichlid fishes. *Systematic Biology* 66(1): 3-22.

Mayo, O. 2008. A century of Hardy–Weinberg equilibrium. *Twin Research and Human Genetics* 11(3): 249-256.

Mayr, E. 1954. Change of genetic environment and evolution. 157-180. In: Huxley, J., Hardy, A.C., & Ford, E.B. (Eds.), *Evolution as a Process*, pp. 157-180. Allen and Unwin, United Kingdom.

Mayr, E. 1982. Speciation and macroevolution. *Evolution* 36(6): 1119-1132.

McGarigal, K., Wan, H.Y., Zeller, K.A., Timm, B.C., & Cushman, S.A. 2016. Multi-scale habitat selection modeling: a review and outlook. *Landscape Ecology* 31: 1161-1175.

Meade, R.H. 1994. Suspended sediments of the modern Amazon and Orinoco rivers. *Quaternary International* 21: 29-39.

Meade, R.H., Nordin Jr, C.F., Curtis, W.F., Costa Rodrigues, F.M., Do Vale, C.M., & Edmond, J.M. 1979. Sediment loads in the Amazon River. *Nature* 278(5700): 161-163.

Menotti-Raymond, M. & O'Brien, S.J. 1993. Dating the genetic bottleneck of the African cheetah. *Proceedings of the National Academy of Sciences of the United States of America* 90: 3172-3176.

Mickett, K., Morton, C., Feng, J., Li, P., Simmons, M., Cao, D., Dunham, R.A., & Liu, Z. 2003. Assessing genetic diversity of domestic populations of channel catfish (*Ictalurus punctatus*) in Alabama using AFLP markers. *Aquaculture* 228(2003): 91-105.

Miller, M.A., Pfeiffer, W., & Schwartz, T. 2011. The CIPRES science gateway: a community resource for phylogenetic analyses. In: Proceedings of the 2011 TeraGrid Conference: extreme digital discovery, pp. 1-8.

Mills, W.F., McGill, R.A., Cherel, Y., Votier, S.C., & Phillips, R.A. 2021. Stable isotopes demonstrate intraspecific variation in habitat use and trophic level of non-breeding albatrosses. *Ibis* 163(2): 463-472.

Minh, B.Q., Nguyen, M.A.T., & von Haeseler, A. 2013. Ultrafast approximation for phylogenetic bootstrap. *Molecular Biology and Evolution* 30(5): 1188-1195

Minh, B.Q., Schmidt, H.A., Chernomor, O., Schrempf, D., Woodhams, M.D., Von Haeseler, A., & Lanfear, R. 2020. IQ-TREE 2: new models and efficient methods for phylogenetic inference in the genomic era. *Molecular Biology and Evolution* 37(5): 1530-1534.

Mittelbach, G.G., Schemske, D.W., Cornell, H.V., Allen, A.P., Brown, J.M., Bush, M.B., Harrison, S.P., Hurlbert, A.H., Knowlton, N., Lessios, H.A., McCain, C.M., McCune, A.R., McDade, L.A., McPeek, M.A., Near, T.J., Price, T.D., Ricklefs, R.E., Roy, K., Sax, D.F., Schluter, D., Sobel, J.M., & Turelli, M. 2007. Evolution and the latitudinal diversity gradient: speciation, extinction and biogeography. *Ecology Letters* 10(4): 315-331.

Moreno, F., Hendy, A.J.W., Quiroz, L., Hoyos, N., Jones, D.S., Zapata, V., Zapata, S., Ballen, G.A., Cadena, E., Cárdenas, A.L., Carrillo-Briceño, J.D., Carrillo, J.D., Delgado-Sierra, D., Escobar, J., Martínez, J.I., Martínez, C., Montes, C., Moreno, J., Pérez, N., Sánchez, R., Suárez, C., Vallejo-Pareja, M.C., & Jaramillo, C. 2015. Revised stratigraphy of Neogene strata in the Cocinetas basin, La Guajira, Colombia. *Swiss Journal of Palaeontology* 134(1): 5-43.

Morris, D.W. 2003. Toward an ecological synthesis: A case for habitat selection. *Oecologia* 136: 1-13.

Murray, A.B., Lazarus, E., Ashton, A., Baas, A., Coco, G., Coulthard, T., Fonstad, M., Haff, P., McNamara, D., Paola, C., Pelletier, J., & Reinhardt, L. 2009. Geomorphology, complexity, and the emerging science of the Earth's surface. *Geomorphology* 103(3): 496-505.

Murray, A.M. 2019. Redescription of *Barbus megacephalus* G€unther, 1876 and *Thynnichthys amblyostoma* von der Marck, 1876 (Cypriniformes: Cyprinidae) from probable Eocene deposits of Southeast Asia, and an assessment of their taxonomic positions. *Journal of Systematic Palaeontology* 17(17): 1213–1235.

Murray, A.M., & Budney, L.A. 2003. A new species of catfish (Claroteidae, *Chrysichthys*) from an Eocene crater lake in East Africa. *The Canadian Journal of Earth Sciences* 40(7): 983-993.

Murray, A.M., & Holmes, R. 2021. Osteology of the cranium and Weberian apparatus of African catfish families (Teleostei: Ostariophysi: Siluriformes) with an assessment of Palaeogene genera. *Vertebrate Anatomy Morphology Palaeontology* 9(1): 156-191.

Nakazawa, T. 2015. Ontogenetic niche shifts matter in community ecology: a review and future perspectives. *Population Ecology* 57(2): 347-354.

Nascimento, M.H.S., Almeida, M.S., Veira, M.N.S., Limeira Filho, D., Lima, R.C., Barros, M.C., & Fraga, E.C. 2016. DNA barcoding reveals high levels of genetic diversity in the fishes of the Itapecuru Basin in Maranhão, Brazil. *Genetics and Molecular Research* 15(3): 1-11.

Near, T.J., & Hardman, M. 2006. Phylogenetic relationships of *Noturus stanauli* and *N. crypticus* (Siluriformes: Ictaluridae), two imperiled freshwater fish species from the southeastern United States. *Copeia* 2006(3): 378-383

Nei, M. 1972. Genetic distance between populations. *The American Naturalist* 106(949): 283-292.

Nelson, J.S., Grande, T.C., & Wilson, M.V. 2016. *Fishes of the World* (5th ed.). John Wiley & Sons, New Jersey.

Nguyen, L.T., Schmidt, H.A., Von Haeseler, A., & Minh, B.Q. 2015. IQ-TREE: a fast and effective stochastic algorithm for estimating maximum-likelihood phylogenies. *Molecular Biology and Evolution* 32(1) : 268-274.

Ni, L., Li, Q., & Kong, L. 2011. Microsatellites reveal fine-scale genetic structure of the Chinese surf clam *Mactra chinensis* (Mollusca, Bivalvia, Mactridae) in Northern China. *Marine Ecology* 32: 488-497.

O'Dea, A., Lessios, H.A., Coates, A.G., Eytan, R.I., Restrepo-Moreno, S.A., Cione, A. L., ... & Jackson, J.B. 2016. Formation of the Isthmus of Panama. *Science Advances* 2(8): e1600883.

Oberdorff, T., Dias, M.S., Jézéquel, C., Albert, J.S., Arantes, C.C., Bigorne, R., Carvajal-Valleros, F.M., De Wever, A., Frederico, R.G., Hidalgo, M., Hugueny, B., Leprieur, F., Maldonado, M., Maldonado Ocampo, J., Martens, K., Ortega, H., Sarmiento, J., Tedesco, P.A., Torrente-Vilara, G., Winemiller, K.O., Zuanon, J. 2019. Unexpected fish diversity gradients in the Amazon basin. *Science Advances* 5(9): p.eaav8681.

Paleobiology Database. 2018. The Paleobiology Database. Checklist dataset https://doi.org/10.15468/zzoyxi (21/07/2021).

Palumbi, S.R., Martin, A., Romano, S., McMillan, W.O., Stice, L., & Grabowski, G. 1991. The Simple Fool's Guide to PCR. University of Hawaii Press, Honolulu.

Parisi, B.M., & Lundberg, J.G. 2009. *Pimelabditus moli*, a new genus and new species of pimelodid catfish (Teleostei: Siluriformes) from the Maroni River basin of northeastern South America. *Academy of Natural Sciences* 2009.

Park, T. & Lloyd, M. 1955. Natural selection and the outcome of competition. The American Naturalist 89(847): 235-240.

Parmesan, C. 2006. Ecological and evolutionary responses to recent climate change. *Annual Review of Ecology, Evolution, and Systematics* 37: 637-669.

Parra-Bracamonte, G.M., Sifuentes-Rincón, A.M., Rosa-Reyna, X.F.D.L., Arellano-Vera, W., & Sosa-Reyes, B. 2011. Inbreeding evidence in a traditional Channel Catfish (*Ictalurus punctatus*) hatchery in Mexico. *Electronic Journal of Biotechnology* 14(6): 1-6.

Patiño, J., Whittaker, R.J., Borges, P.A., Fernández-Palacios, J.M., Ah-Peng, C., Araújo, M.B., Ávila, S.P., Cardoso, P., Cornuault, J., de Boer, E.J., de Nascimento, L., Gil, A., González-Castro, A., Gruner, D.S., Heleno, R., Hortal, J., Illera, J.C., Kaiser-Bunbury, C., Matthews, T.J., Papadopoulou, A., Pettorelli, N., Price, J.P., Santos, A.M.C., Steinbauer, M.J., Triantis, K.A., Valente, L., Vargas, P., Weigelt, P., & Emerson, B.C. 2017. A roadmap for island biology: 50 fundamental questions after 50 years of The Theory of Island Biogeography. *Journal of Biogeography* 44(5): 963-983.

Pearce, J.M. 2007. Philopatry: a return to origins. *The Auk* 124(3): 1085-1087.

Pearson, G.A., Lago-Leston, A., & Mota, C. 2009. Frayed at the edges: selective pressure and adaptive response to abiotic stressors are mismatched in low diversity edge populations. *Journal of Ecology* 97(3): 450-462.

Peery, M.Z., Kirby, R., Reid, B.N., Stoelting, R., Doucet-Bëer, E., Robinson, S., Vásquez-Carrillo, C., Pauli, J.N., & Palsbøll, P.J. 2012. Reliability of genetic bottleneck tests for detecting recent population declines. *Molecular Ecology* 21: 3403-3418.

Pellett, T.D., Van Dyck, G.J., & Adams, J.V. 1998. Seasonal migration and homing of Channel Catfish in the Lower Wisconsin River, Wisconsin. *North American Journal of Fisheries Management* 18: 85-95.

Perales-Flores, L.E., Sifuentes-Rincón, A.M., & León, F.J. 2007. Microsatellite variability analysis in farmed catfish (*Ictalurus punctatus*) from Tamaulipas, Mexico. *Genetics and Molecular Biology* 30(3): 570-574.

Pereira, L.H., Maia, G.M., Hanner, R., Foresti, F., & Oliveira, C. 2011. DNA barcodes discriminate freshwater fishes from the Paraíba do Sul River Basin, São Paulo, Brazil. *Mitochondrial DNA* 22(S1): 71-79.

Pérez-Rodríguez, R., Domínguez-Domínguez, O., Pedraza-Lara, C.C., Rosas-Valdez, R., de León, G.P.P., García-Andrade, A.B., & Doadrio, I. 2022. Multi-locus phylogeny and species delimitation in the catfish genus *Ictalurus* Rafinesque, 1820 (Actinopterygii, Siluriformes). Research Square Preprint.

Peterson, R.D., Sullivan, J.P., Hopkins, C.D., Santaquiteria, A., Dillman, C.B., Pirro, S., Betancur-R, R., Arcila, D., Hughes, L.C. & Ortí, G. 2022. Phylogenomics of bony-tongue fishes (Osteoglossomorpha) shed light on the craniofacial evolution and biogeography of the weakly electric clade (Mormyridae). *Systematic Biology* 71(5): 1032–1044.

Pfennig, K.S., & Rice, A.M. 2014. Reinforcement generates reproductive isolation between neighbouring conspecific populations of spadefoot toads. *Proceedings of the Royal Society B: Biological Sciences* 281(1789): 20140949.

Pigot, A.L., Phillimore, A.B., Owens, I.P., & Orme, C.D.L. 2010. The shape and temporal dynamics of phylogenetic trees arising from geographic speciation. *Systematic Biology* 59(6): 660-673.

Pinton, A., Otero, O., Likius, A., Mackaye, H.T., Vignaud, P., & Brunet, M. 2011. Giants in a minute catfish genus: first description of fossil *Mochokus* (Siluriformes, Mochokidae) in the Late Miocene of Chad, including *M. gigas*, sp. nov. *Journal of Vertebrate Paleontology* 31(1): 22-31.

Plath, M., & Tobler, M. 2010. Subterranean fishes of Mexico (*Poecilia mexicana*, Poeciliidae). In: Trajano, E., Bichuette, M.E., Kapoor, B.G. (Eds.), *The biology of subterranean fishes*. Science Publishers, New Hampshire, pp. 283-332.

Poly, W.J. 2001. Nontroglobitic fishes in Bruffey-Hills Creek Cave, West Virginia, and other caves worldwide. *Environmental Biology of Fishes* 62(1): 73-83.

Presswell, B., Weitzman, S.H., & Bergquist, T. *Skiotocharax meizon*, a new genus and species offish from Guyana with a discussion of its relationships (Characiformes: Crenuchidae). *Ichthyological Exploration of Freshwaters* 11(2): 175-192.

Priem R., 1920. Poissons fossiles du Miocène d'Egypte (Burdingalien de Moghara, "Désert lybique"). In: Fourtau R., (Ed.), *Contribution à l'étude des vertébrés Miocènes de l'Egypte*. Government Press, Cairo, pp. 8–15.

Pritchard, J.K., Stephens, M., & Donnelly, P. 2000. Inference of population structure using multilocus genotype data. *Genetics* 155(2): 945-959.

Pujolar, J.M., Vincenzi, S., Zane, L., Jesensek, D., De Leo, G.A., & Crivelli, A.J. 2011. The effect of recurrent floods on genetic composition of marble trout populations. *Public Library of Science One* 6(9): 1-11.

Pulliam, H.R., & Danielson, B.J. 1991. Sources, sinks, and habitat selection: A landscape perspective on population dynamics. *The American Naturalist* 137: S50-S66.

Quinn, J.A., & Woodward, S.L. (Eds.). 2015. Earth's Landscape: An Encyclopedia of the World's Geographic Features [2 volumes]: An Encyclopedia of the World's Geographic Features. ABC-CLIO.

Rahbek, C., Borregaard, M.K., Antonelli, A., Colwell, R.K., Holt, B.G., Nogues-Bravo, D., Rasmussen, C.M., Richardson, K., Rosing, M.T., Whittaker, R.J. and Fjeldså, J. 2019. Building mountain biodiversity: geological and evolutionary processes. *Science* 365(6458): 1114-1119.

Ramasamy, R.K., Ramasamy, S., Bindroo, B.B., & Naik, V.G. 2014. STRUCTURE PLOT: a program for drawing elegant STRUCTURE bar plots in user friendly interface. *Springer Plus* 3(1): 1-3.

Rambaut, A. 2009. FigTree. Tree figure drawing tool. http://tree. bio. ed. ac. uk/software/figtree/.

Rambaut, A., Drummond, A.J., Xie, D., Baele, G., & Suchard, M.A. 2018. Posterior summarization in Bayesian phylogenetics using Tracer 1.7. *Systematic Biology* 67(5): 901-904.

Ratnasingham, S., & Herbert, P.D.N. 2007. BOLD: The Barcode of Life Data System (www.barcodinglife.org). *Molecular Ecology Notes* 7: 355-364.

Rausher, M.D. 1984. The evolution of habitat preference in subdivided populations. *Evolution* 38(3): 596-608.

Reed, D.H., & Frankham, R. 2003. Correlation between fitness and genetic diversity. *Conservation Biology* 17(1): 230-237.

Ribeiro, F.R., Lucena, C.A., & Lucinda, P.H. 2008. Three new *Pimelodus* species (Siluriformes: Pimelodidae) from the Rio Tocantins drainage, Brazil. *Neotropical Ichthyology* 6: 455-464.

Rincon-Sandoval, M., Betancur-R, R., & Maldonado-Ocampo, J.A. 2019. Comparative phylogeography of trans-Andean freshwater fishes based on genome-wide nuclear and mitochondrial markers. *Molecular Ecology* 28(5): 1096-1115.

Ríos-Villamizar, E.A., Piedade, M.T.F., Da Costa, J.G., Adeney, J.M., & Junk, W.J. 2013. Chemistry of different Amazonian water types for river classification: a preliminary review. *Water and Society II* 178: 17-28.

Robinson, B.W., Wilson, D.S., & Shea, G.O. 1996. Trade-offs of ecological specialization: an intraspecific comparison of pumpkinseed sunfish phenotypes. *Ecology* 77(1): 170-178.

Rocha, L.A., & Bowen, B.W. 2008. Speciation in coral-reef fishes. *Journal of Fish Biology* 72(5): 1101-1121.

Rocha-Méndez, A., Sánchez-González, L.A., González, C., & Navarro-Sigüenza, A.G. 2019. The geography of evolutionary divergence in the highly endemic avifauna from the Sierra Madre del Sur, Mexico. *BMC Evolutionary Biology* 19: 1-21.

Rodríguez-Olarte, D., Mojica Corzo, J.I., & Taphorn Baechle, D.C. 2011. Northern South America, Magdalena and Maracaibo basins. In: Albert, J.S. & Reis, R.E. (Eds.), *Historical biogeography of Neotropical freshwater fishes*, pp. 59-67. University of California Press, USA.

Ronquist, F. 1997. Dispersal-vicariance analysis: a new approach to the quantification of historical biogeography. *Systematic Biology* 46(1): 195-203.

Rodiles-Hernández, R., Lundberg, J.G., & Sullivan, J.P. 2010. Taxonomic discrimination and identification of extant blue catfishes (Siluriformes: Ictaluridae: *Ictalurus furcatus* Group). *Proceedings of the Academy of Natural Sciences of Philadelphia* 159(1): 67-82.

Rosenzweig, M.L. 1981. A theory of habitat selection. *Ecology* 62(2): 327-335.

Ruzzante, D.E., Walde, S.J., Cussac, V.E., Dalebout, M.L., Seibert, J., Ortubay, S., & Habit, E. 2006. Phylogeography of the Percichthyidae (Pisces) in Patagonia: roles of orogeny, glaciation, and volcanism. *Molecular Ecology* 15(10): 2949-2968.

Ryman, N., & Palm, S. 2006 POWSIM: a computer program for assessing statistical power when testing for genetic differentiation. *Molecular Ecology Notes* 6: 600-602.

Sabaj, M.H., & Lundberg, J.G. 2007. Fossil catfishes of the families Doradidae and Pimelodidae (Teleostei: Siluriformes) from the Miocene Urumaco Formation of Venezuela. *Proceedings of the Academy of Natural Sciences of Philadelphia* 156(1): 157-194.

Saccone, C., Gissi, C., Lanave, C., Larizza, A., Pesole, G., & Reyes, A. 2000. Evolution of the mitochondrial genetic system: an overview. *Gene* 261(1): 153-159.

Salin, K., Voituron, Y., Mourin, J., & Hervant, F. 2010. Cave colonization without fasting capacities: an example with the fish *Astyanax fasciatus mexicanus*. *Comparative Biochemistry & Physiology Part A: Molecular and Integrative Physiology* 156(4): 451-457.

Sanchez, R., Lopez, V., & Eckstein, G. 2016. Identifying and characterizing transboundary aquifers along the Mexico–US border: an initial assessment. *Journal of Hydrology* 535: 101-119.

Sanchez, R., Rodriguez, L., & Tortajada, C. 2018a. The transboundariness approach and prioritization of transboundary aquifers between Mexico and Texas. *Ambio* 47(7): 760-770.

Sanchez, R., Rodriguez, L., & Tortajada, C. 2018b. Transboundary aquifers between Chihuahua, Coahuila, Nuevo Leon and Tamaulipas, Mexico, and Texas, USA: identification and categorization. *Journal of Hydrology Regional Studies* 20: 74-102.

Sanín, M.J., Cardona, A., Valencia-Montoya, W.A., Jiménez, M.F.T., Carvalho-Madrigal, S., Gómez, A.C., Bacon, C.D., Tangarife, T.R., Jaramillo, J.S., Zapata, S., Valencia, V., Valencia, J.W.A., Vargas, V., & Paris, M. 2022. Volcanic events coincide with plant dispersal across the Northern Andes. *Global and Planetary Change* 210: 103757.

Sanmartín, I. 2003. Dispersal vs. vicariance in the Mediterranean: historical biogeography of the Palearctic Pachydeminae (Coleoptera, Scarabaeoidea). *Journal of Biogeography* 30(12): 1883-1897.

Santini, F., Harmon, L.J., Carnevale, G., & Alfaro, M.E. 2009. Did genome duplication drive the origin of teleosts? A comparative study of diversification in ray-finned fishes. *BMC Evolutionary Biology* 9(1): 1-15.

Santucci, V.L. 2005. Historical perspectives on biodiversity and geodiversity. *The George Wright Forum* 22(3): 29-34.

Schedel, F.D., Chakona, A., Sidlauskas, B.L., Popoola, M.O., Usimesa Wingi, N., Neumann, D., Vreven, E.J.W.M.N., & Schliewen, U.K. 2022. New phylogenetic insights into the African catfish families Mochokidae and Austroglanididae. *Journal of Fish Biology* 100(5): 1171-1186.

Schluter, D. 1988. Character displacement and the adaptive divergence of finches on islands and continents. *The American Naturalist* 131(6): 799-824.

Schultz, E.T., Conover, D.O., & Ehtisham, A. 1998. The dead of winter: size-dependent variation and genetic differences in seasonal mortality among Atlantic silverside (Atherinidae: *Menidia menidia*) from different latitudes. *Canadian Journal of Fisheries and Aquatic Sciences* 55: 1149-1157.

Sevilla, R.G., Diez, A., Norén, M., Mouchel, O., Jérôme, M., Verrez-Bagnis, V., Van Pelt, H., Favre-Krey, L., Krey, G., & Bautista, J.M. 2007. Primers and polymerase chain reaction conditions for DNA barcoding teleost fish based on the mitochondrial cytochrome b and nuclear rhodopsin genes. *Molecular Ecology Notes* 7(5): 730-734.

Sexton, J.P., Hangartner, S.B., & Hoffmann, A.A. 2014. Genetic isolation by environment or distance: which pattern of gene flow is most common? *Evolution* 68(1): 1-15.

Sharp Jr., J.M., Green, R.T., & Schindel, G.M. 2019. The Edwards Aquifer: the past, present, and future of a vital water resource, vol. 215, Geological Society of America, Colorado.

Shorthouse, D.P. 2010. SimpleMappr, an online tool to produce publication-quality point maps. [Retrieved from https://www.simplemappr.net. Accessed May 02, 2023].

Sidlauskas, B.L., & Vari, R.P. 2012. Diversity and distribution of anostomoid fishes (Teleostei: Characiformes) throughout the Guianas. *Cybium* 36(1): 71-103.

Sievers, F., Wilm, A., Dineen, D.G., Gibson, T.J., Karplus, K., Li, W., Lopez, R., McWilliam, H., Remmert, M., Söding, J., Thompson, J.D., & Higgins, D.G. 2011. Fast, scalable generation of high-quality protein multiple sequence alignments using Clustal Omega. *Molecular Systems Biology* 7(1): 539.

Silva, G.D.S.D.C.E., Roxo, F.F., Britzke, R., & Oliveira, C. 2014. New species of the *Pseudancistrus barbatus* group (Siluriformes, Loricariidae) with comments on its biogeography and dispersal routes. ZooKeys 406: 1-23.

Simmons, M., Mickett, K., Kucuktas, H., Li, P., Dunham, R., & Liu, Z. 2006. Comparison of domestic and wild channel catfish (*Ictalurus punctatus*) populations provides no evidence for genetic impact. *Aquaculture* 252(2-4): 133-146.

Skeels, A., & Cardillo, M. 2019. Reconstructing the geography of speciation from contemporary biodiversity data. *The American Naturalist* 193(2): 240-255.

Slatkin, M. 1973. Gene flow and selection in a cline. *Genetics* 75(4): 733-756.

Slatkin, M. 1985. Gene flow in natural populations. *Annual Review of Ecology and Systematics* 16: 393-430.

Slatkin, M. 1987. Gene flow and the geographic structure of natural populations. *Science* 236(4803): 787-792.

Smadja, C., & Ganem, G. 2005. Asymmetrical reproductive character displacement in the house mouse. *Journal of Evolutionary Biology* 18(6): 1485-1493.

Smadja, C.M., & Butlin, R.K. 2011. A framework for comparing processes of speciation in the presence of gene flow. *Molecular Ecology* 20(24): 5123-5140.

Smith, J.M. 1966. Sympatric speciation. *The American Naturalist* 100(916): 637-650.

Snorrason, S.S., Skúlason, S., Jonsson, B., Malmquist, H.J., Jónasson, P.M., Sandlund, O.T., & Lindem, T. 1994. Trophic specialization in Arctic charr *Salvelinus alpinus* (Pisces; Salmonidae): morphological divergence and ontogenetic niche shifts. *Biological Journal of the Linnean Society* 52(1): 1-18.

Soares, LS., Lopes, W.G.R.G.R., de Castro, A.C.L., da Silva, E.V., de Araújo, G.C., dos Santos Moreira, M., de França, V.L., & Mendes, K.C. 2017. Analysis of spatiotemporal changes in land use and land cover in sub-watersheds of the lower Itapecuru River in the state of Maranhão, Brazil. *Revista do Departamento de Geografia* 34: 55-67.

Soares, M.G.M., Menezes, N.A., & Junk, W.J. 2006. Adaptations of fish species to oxygen depletion in a central Amazonian floodplain lake. *Hydrobiologia* 568: 353-367.

Sotola, V.A., Schrey, A.W., Ragsdale, A.K., Whitledge, G.W., Frankland, L., Bollinger, E.K., and Colombo, R.E. 2017. Genetic evidence of isolation by distance and impact of impoundments on genetic diversity of riverine Channel Catfish. Transactions of the American Fisheries Society 146(6): 1204-1211.

Springer, M.S., DeBry, R.W., Douady, C., Amrine, H.M., Madsen, O., de Jong, W.W., & Stanhope, M.J. 2001. Mitochondrial versus nuclear gene sequences in deep-level mammalian phylogeny reconstruction. *Molecular Biology and Evolution* 18(2): 132-143.

Srivathsan, A., & Meier, R. 2012. On the inappropriate use of Kimura-2-parameter (K2P) divergences in the DNA-barcoding literature. *Cladistics* 28(2): 190-194.

Stankowski, S., Sobel, J.M., & Streisfeld, M.A. 2017. Geographic cline analysis as a tool for studying genome-wide variation: a case study of pollinator-mediated divergence in a monkeyflower. *Molecular Ecology* 26(1): 107-122.

Steeves, T.E., Anderson, D.J., McNally, H., Kim, M.H., Friesen, V.L. 2003. Phylogeography of *Sula*: The role of physical barriers to gene flow in the diversification of tropical seabirds. *Journal of Avian Biology* 34(2): 217-223.

Stepien, C.A., Murphy, D.J., Lohner, R.N., Sepulveda-Villet, O.J., & Haponski, A.E. 2009. Signatures of vicariance, postglacial dispersal and spawning philopatry: population genetics of the walleye *Sander vitreus*. *Molecular Ecology* 18(16): 3411-3428.

Stokes, M.F., Goldberg, S.L., & Perron, J.T. 2018. Ongoing river capture in the Amazon. *Geophysical Research Letters* 45(11): 5545-5552.

Strecker, U., Hausdorf, B., & Wilkens, H. 2012. Parallel speciation in *Astyanax* cave fish (Teleostei) in Northern Mexico. *Molecular Phylogenetics and Evolution* 62(1): 62-70.

Sullivan, J.P., Friel, J.P., Hardman, M., Iyaba, R.M., & Stiassny, M.L.J. 2008. A time tree for the Claroteinae (Claroteidae: Siluriformes) and affinities of the Tanganyikan claroteine species flock. *Copeia* 1: 43-56.

Sullivan, J.P., Lundberg, J.G., & Hardman, M. 2006. A phylogenetic analysis of the major groups of catfishes (Teleostei: Siluriformes) using *rag1* and *rag2* nuclear gene sequences. *Molecular Phylogenetics and Evolution* 41: 636-662.

Sullivan, J.P., Muriel-Cunha, J., & Lundberg, J.G. 2013. Phylogenetic relationships and molecular dating of the major groups of catfishes of the Neotropical superfamily Pimelodoidea (Teleostei, Siluriformes). *Proceedings of the Academy of Natural Sciences of Philadelphia* 162: 89-110.

Sunde, J., Yıldırım, Y., Tibblin, P., & Forsman, A. 2020. Comparing the performance of microsatellites and RADseq in population genetic studies: analysis of data for pike (*Esox lucius*) and a synthesis of previous studies. *Frontiers in Genetics* 11(218): 1-17.

Susko, E., & Roger, A.J. 2021. Long branch attraction biases in phylogenetics. *Systematic Biology* 70(4): 838-843.

Suttkus, R.D. 1961. Additional information about blind catfishes from Texas. *The Southwestern Naturalist* 6(2): 55-64.

Svanbäck, R., Eklöv, P., Fransson, R., & Holmgren, K. 2008. Intraspecific competition drives multiple species resource polymorphism in fish communities. *Oikos* 117(1): 114-124.

Tagliacollo, V.A., Roxo, F.F., Duke-Sylvester, S.M., Oliveira, C., & Albert, J.S. 2015. Biogeographical signature of river capture events in Amazonian lowlands. *Journal of Biogeography* 42(12): 2349-2362.

Tatarenkov, A., Barreto, F., Winkelman, D.L., & Avise, J.C. 2006. Genetic monogamy in the Channel Catfish, *Ictalurus punctatus*, a species with uniparental nest guarding. *Copeia* 2006(4): 735-741.

Tauber, C.A. & Tauber, M.J. 1981. Insect seasonal cycles: Genetics and evolution. *Annual Review of Ecology and Systematics* 12: 281-308.

Taylor, W.R. 1969. A revision of the catfish genus *Noturus* Rafinesque with an analysis of higher groups in the Ictaluridae. *Bulletin of the United States National Museum* 1-315.

Tedford, R.H., Skinner, M.F., Fields, R.W., Rensberger, J.M., Whistler, D.P., Galusha, T., Taylor, B.E., Macdonald, J.R., & Webb, S.D. 1987. Faunal succession and biochronology of the Arikareean through Hemphillian interval (Late Oligocene through Earliest Pliocene Epochs) in North America. In: Woodburne, M.O. (Ed.), *Cenozoic Mammals of North America*. University of California Press, Berkeley. pp. 153–210.

Templeton, A.R. 1980. Modes of speciation and inferences based on genetic distances. *Evolution* 34(4): 719-729.

Thomas, M.R., & Sabaj, M.H. 2020. Heptapteridae: seven-finned catfishes. In: Warren, M.L., Burr, B.M., Echelle, A.A., Kuhajda, B.R., & Ross, S.T. (Eds.), *Freshwater fishes of North America: Characidae to Poeciliidae* 2: 123-148.

Torrico, J.P., Hubert, N., Desmarais, E., Duponchelle, F., Nuñez Rodriguez, J., Montoya-Burgos, J., Garcia Davila, C., Carvajal-Vallejos, F.M., Grajales, A.A., Bonhomme, F. & Renno, J.F. 2009. Molecular phylogeny of the genus *Pseudoplatystoma* (Bleeker, 1862): biogeographic and evolutionary implications. *Molecular Phylogenetics and Evolution* 51(3): 588-594.

Tracy, B.H., Rohde, F.C., & Hogue, G.M. 2020. An Annotated Atlas of the Freshwater Fishes of North Carolina. *Southeastern Fishes Council Proceedings* No. 60.

Trifinopoulos, J., Nguyen, L.T., von Haeseler, A., & Minh, B.Q. 2016. W-IQ-TREE: a fast online phylogenetic tool for maximum likelihood analysis. *Nucleic Acids Research* 44(W1): W232-W235.

Tsoupas, A., Papavasileiou, S., Minoudi, S., Gkagkavouzis, K., Petriki, O., Bobori, D., Sapounidis, A., Koutrakis, E., Leonardos, I., Karaiskou, N., & Triantafyllidis, A. 2022.

DNA barcoding identification of Greek freshwater fishes. *Public Library of Science One* 17(1): p.e0263118.

Turner Tomaszewicz, C.N., Seminoff, J.A., Peckham, S.H., Avens, L., & Kurle, C.M. 2017. Intrapopulation variability in the timing of ontogenetic habitat shifts in sea turtles revealed using δ15N values from bone growth rings. *Journal of Animal Ecology* 86(3): 694-704.

Vaidya, G., Lohman, D.J., & Meier, R. 2011. SequenceMatrix: concatenation software for the fast assembly of multi-gene datasets with character set and codon information. *Cladistics* 27(2): 171-180.

Van Damme, P.A., Córdova-Clavijo, L., Baigún, C., Hauser, M., Doria, C.R., & Duponchelle, F. 2019. Upstream dam impacts on gilded catfish *Brachyplatystoma rousseauxii* (Siluriformes: Pimelodidae) in the Bolivian Amazon. *Neotropical Ichthyology* 17(4): e190118.

Van den Berghe, E.P. & Gross, M.R. 1989. Natural selection resulting from female breeding competition in a Pacific salmon (Coho: *Oncorhynchus kisutch*). *Evolution* 43(1): 125-140.

Van Oosterhout, C., Hutchinson, W.F., Wills, D.P., & Shipley, P. 2004. MICRO-CHECKER: software for identifying and correcting genotyping errors in microsatellite data. *Molecular Ecology Notes* 4(3): 535-538.

Van Oosterhout, C., Weetman, D., & Hutchinson, W.F. 2006. Estimation and adjustment of microsatellite null alleles in nonequilibrium populations. *Molecular Ecology Notes* 6(1): 255-256.

Vari, R.P., & Ferraris Jr., C.J. 2009. Fishes of the Guiana Shield. *Bulletin of the Biological Society of Washington* 17(1), 8-18.

Via, S. 2001. Sympatric speciation in animals: the ugly duckling grows up. *Trends in Ecology & Evolution* 16(7): 381-390.

Vieira, M.L.C., Santini, L., Diniz, A.L., & Munhoz, C.D.F. 2016. Microsatellite markers: what they mean and why they are so useful. *Genetics and Molecular Biology* 39: 312-328.

Violle, C., Enquist, B.J., McGill, B.J., Jiang, L.I.N., Albert, C.H., Hulshof, C., Jung, V., & Messier, J. 2012. The return of the variance: intraspecific variability in community ecology. *Trends in Ecology & Evolution* 27(4): 244-252.

Wade, M. J., & Kalisz, S. 1990. The causes of natural selection. *Evolution* 44(8): 1947-1955.

Waldbieser, G.C., & Bosworth, B.G. 1997. Cloning and characterization of microsatellite loci in Channel Catfish, *Ictalurus punctatus*. *Animal Genetics* 28(4): 295-298.

Waldbieser, G.C., & Bosworth, B.G. 2013. A standardized microsatellite marker panel for parentage and kinship analyses in channel catfish, *Ictalurus punctatus*. *Animal Genetics* 44(4): 476-479.

Waldbieser, G.C., & Wolters, W.R. 1999. Application of polymorphic microsatellite loci in a Channel Catfish *Ictalurus punctatus* breeding program. *Journal of The World Aquaculture Society* 30(2): 256-262.

Walsh, S.J., & Gilbert, C.R. 1995. New species of troglobitic catfish of the genus *Prietella* (Siluriformes: Ictaluridae) from northeastern México. *Copeia* 4: 850-861.

Wang, J., Li, G., & Wang, J. 1981. The early Tertiary fossil fishes from Sanshui and its adjacent basin, Guangdong. *Palaeontologia Sinica* 160(22): 1–90.

Ward, A.J., Webster, M.M., & Hart, P.J. 2006. Intraspecific food competition in fishes. *Fish and Fisheries* 7(4): 231-261.

Ward, R.D., Hanner, R., & Hebert, P.D. 2009. The campaign to DNA barcode all fishes, FISH-BOL. *Journal of Fish Biology* 74(2): 329-356.

Ward, R.D., Zemlak, T.S., Innes, B.H., Last, P.R., & Hebert, P.D. 2005. DNA barcoding Australia's fish species. *Philosophical Transactions of the Royal Society B: Biological Sciences* 360(1462): 1847-1857.

Waters, C.D., Hard, J.J., Fast, D.E., Knudsen, C.M., Bosch, W.J., & Naish, K.A. 2020. Genomic and phenotypic effects of inbreeding across two different hatchery management regimes in Chinook salmon. *Molecular Ecology* 29(4): 658-672.

Waters, J.M., Burridge, C.P., & Craw, D. 2020. River capture and freshwater biological evolution: a review of galaxiid fish vicariance. *Diversity* 12(6): 216.

Weir, J.T. & Price, M. 2011. Andean uplift promotes lowland speciation through vicariance and dispersal in *Dendrocincla* woodcreepers. *Molecular Ecology* 20: 4550-4563.

Wellborn, T.L. 1988. Channel Catfish: life history and biology. *Southern Regional Aquaculture Center*, Publication 180, Mississippi State University, USA.

Werner, E.E., & Hall, D.J. 1988. Ontogenetic habitat shifts in bluegill: the foraging rate-predation risk trade-off. *Ecology* 69(5): 1352-1366.

Wesselingh, F.P. & Hoorn, C. 2011. Geological development of Amazon and Orinoco Basins. In: Albert, J.S. & Reis, R.E. (Eds.), *Historical biogeography of Neotropical freshwater fishes*, pp. 59-67. University of California Press, USA.

Whitlock, M.C. 2003. Fixation probability and time in subdivided populations. *Genetics* 164: 767-779.

Whittaker, R.J., Triantis, K.A., & Ladle, R.J. 2008. A general dynamic theory of oceanic island biogeography. *Journal of Biogeography* 35(6): 977-994.

Wilcox, T.P., García de León, F.J., Hendrickson, D.A., & Hillis, D.M. 2004. Convergence among cave catfishes: long-branch attraction and a Bayesian relative rates test. *Molecular Phylogenetics and Evolution* 31(3): 1101-1113.

Wilkens, H. 2001. Convergent adaptations to cave life in the *Rhamdia laticauda* catfish group (Pimelodidae, Teleostei). *Environmental Biology of Fishes* 62(1): 251-261.

Williams, S.T., Elbers, J.P., & Taylor, S.S. 2021. Population structure, gene flow, and sex-biased dispersal in the reticulated flatwoods salamander (*Ambystoma bishopi*): implications for translocations. *Evolutionary Applications* 14(9): 2231-2243.

Willis, S.C., Nunes, M., Montaña, C.G., Farias, I.P., Ortí, G., & Lovejoy, N.R. 2010. The Casiquiare River acts as a corridor between the Amazonas and Orinoco river basins: biogeographic analysis of the genus *Cichla*. *Molecular Ecology* 19(5):1014-1030.

Winemiller, K.O., López-Fernández, H., Taphorn, D.C., Nico, L.G., & Duque, A.B. 2008. Fish assemblages of the Casiquiare River, a corridor and zoogeographical filter for dispersal between the Orinoco and Amazon basins. *Journal of Biogeography* 35(9): 1551-1563.

Winemiller, K.O., & Willis, S.C. 2011. The Vaupes Arch and Casiquiare Canal. In: Albert, J.S. & Reis, R.E. (Eds.), *Historical biogeography of Neotropical freshwater fishes*, pp. 59-67. University of California Press, USA.

Winger, B.M., Auteri, G.G., Pegan, T.M., & Weeks, B.C. 2019. A long winter for the Red Queen: rethinking the evolution of seasonal migration. *Biological Reviews* 94(3): 737-752.

Wittke-Thompson, J.K., Pluzhnikov, A., & Cox, N.J. 2005. Rational inferences about departures from Hardy-Weinberg equilibrium. *The American Journal of Human Genetics* 76(6): 967-986.

Wittmann, F., Schöngart, J., Montero, J.C., Motzer, T., Junk, W.J., Piedade, M.T., Queiroz, H.L., & Worbes, M. 2006. Tree species composition and diversity gradients in white-water forests across the Amazon Basin. *Journal of Biogeography* 33(8): 1334-1347.

Wózniak, K. & Blasiak, J. 2003. In vitro genotoxicity of lead acetate: Induction of single and double DNA strand breaks and DNA–protein cross-links. *Mutation Research* 535: 127-139.

Wu, C.I., & Ting, C.T. 2004. Genes and speciation. *Nature Reviews Genetics* 5(2): 114-122.

Yamaguchi, R. & Iwasa, Y. 2017. Parapatric speciation in three islands: Dynamics of geographical configuration of allele sharing. *Royal Society Open Science* 4(2): 160819.

Yerger, R.W., & Relyea, K. 1968. The flat-headed bullheads (Pisces: Ictaluridae) of the southeastern United States, and a new species of *Ictalurus* from the Gulf Coast. *Copeia* 1968(2): 361-384.

Yoder, A.D., & Nowak, M.D. 2006. Has vicariance or dispersal been the predominant biogeographic force in Madagascar? Only time will tell. *Annual Review of Ecology, Evolution, and Systematics* 37: 405-431.

Zink, R.M., Blackwell-Rago, R.C., & Ronquist, F. 2000. The shifting roles of dispersal and vicariance in biogeography. *Proceedings of the Royal Society of London. Series B: Biological Sciences* 267(1442): 497-503.

Zonneveld, J.-P., Zaim, Y., Rizal, Y., Ciochon, R.L., Bettis III, E.A., Aswan, Gunnell, G.F. 2012. Ichnological constraints on the depositional environment of the Sawahlunto

Formation, Kandi, Northwest Ombilin Basin, West Sumatra, Indonesia. *Journal of Asian Earth Sciences* 45: 106–113.

Zúñiga, D., Gager, Y., Kokko, H., Fudickar, A.D., Schmidt, A., Naef-Daenzer, B., Wikelski, M., & Partecke, J. 2017. Migration confers winter survival benefits in a partially migratory songbird. *Elife* 6: e28123.